THE RELEVANCE OF HYDROGEN SULFIDE (H2S) IN OBESITY AND ADIPOSE TISSUE PHYSIOLOGY

Ferran Comas Vila

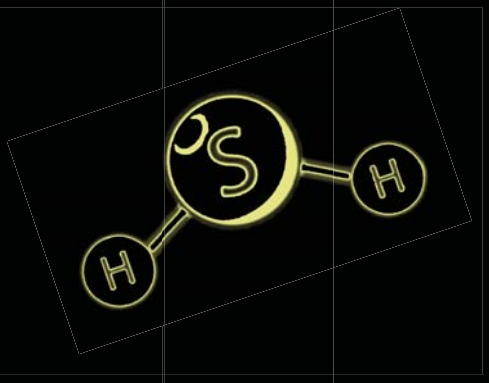

THE RELEVANCE OF HYDROGEN SULFIDE (H_2S) IN OBESITY AND ADIPOSE TISSUE PHYSIOLOGY

Ferran Comas Vila

Universitat de Girona

DOCTORAL THESIS

THE RELEVANCE OF HYDROGEN SULFIDE (H_2S) IN OBESITY AND ADIPOSE TISSUE PHYSIOLOGY

FERRAN COMAS VILA

2021

DOCTORAL THESIS

THE RELEVANCE OF HYDROGEN SULFIDE (H_2S) IN OBESITY AND ADIPOSE TISSUE PHYSIOLOGY

FERRAN COMAS VILA

2021

Universitat de Girona

DOCTORAL THESIS

THE RELEVANCE OF HYDROGEN SULFIDE (H_2S) IN OBESITY AND ADIPOSE TISSUE PHYSIOLOGY

Ferran Comas Vila

2021

Doctoral Programme in Molecular Biology, Biomedicine and Health

Supervised by:
José María Moreno Navarrete, PhD

Tutor:
Prof. José Manuel Fernández-Real Lemos

Presented to obtain the degree of PhD at the University of Girona

Universitat de Girona

Dr. **José María Moreno Navarrete**, principal investigator of the *Biomedical Research Institute of Girona (IDIBGI), Endocrinology, Diabetes and Nutrition Research Unit (UDEN)*. Researcher ascribed to the CIBER *de la Fisiopatología de la Obesidad y la Nutrición (CIBEROBN, ISCIII)*.

I DECLARE:

That the thesis entitled "THE RELEVANCE OF HYDROGEN SULFIDE (H_2S) IN OBESITY AND ADIPOSE TISSUE PHYSIOLOGY", presented by Ferran Comas Vila to obtain the doctoral degree in Molecular Biology, Biomedicine and Health by the UdG, has been completed under my supervision.

For all intents and purposes, we hereby sign this document.

Dr. José María Moreno Navarrete

Dr. José-Manuel Fernández-Real Lemos

Ferran Comas Vila

Girona, 2021

El plaer més noble és
el goig de comprendre

Leonardo da Vinci

ACKNOWLEDGEMENTS

Encara recordo fa uns 4 anys quan començava el treball final de màster a l'IDIBGI, com tot estudiant al principi llegint articles i anar observant com treballaven els del grup, i qui m'havia de dir en aquell moment que ara em trobaria aquí escrivint els agraïments de la tesi. Tot això ha estat possible gràcies a la contribució de moltes persones que d'una manera o altre m'han ajudat i acompanyant en aquest repte tant meravellós i emocionant que ha sigut aquesta etapa de la meva vida. Per tant m'agradaria agrair-vos-ho amb unes línies, ja que una part d'aquesta tesi es vostre.

Primer de tot m'agradaria donar les gràcies al Dr. José Manuel Fernández-Real i al Dr. José María Moreno Navarrete, per l'oportunitat i confiança dipositada en mi per a dur a terme el doctorat i per ajudar-me a créixer com a investigador.

José, gràcies també per haver-me transmès la teva passió i coneixements per la recerca des del primer dia invertint una gran part del teu temps instruint-me, he aprés moltissím en tots els sentits al teu costat. Com vas dir un dia, ha estat un plaer tenir-te de company de batalla. Gràcies per tot.

Paco, gràcies per donar-me un cop de mà sempre que ho necessitava, pels teus consells i advertències, per les converses fent el cafè, per la teva música chill-out que portava sempre bon ambient al lab.

Moni, encara recordo la d'hores que haviém arribat a estar al Trueta esperant les mostres i processant-les fins tard, moltes gràcies per fer que aquests moments passesin amb riures i bones converses, per tot el que em vas ensenyar, i per fer que les coses fossin més fàcils sempre.

A la Jess i l'Aina, em considero un afortunat d'haver pogut compartir moltes hores dins i fora de la feina al vostre costat. Jess gràcies per fer la funció de "germana gran". Gràcies per estar sempre allà disposades a ajudar-me i escoltar-me, quan ho necessitava. Escrivint aquestes línies em venen a la ment molts moments que hem viscut junts, nits de festa, quan deixava anar alguna frase o paraula de les meves i no paraveu de riure, el dia que vam plorar de riure per la traducció al finés del google translator, etc.

A la Núria i Anna, vau arribar més tard al grup i amb poc temps ja heu posat el vostre granet de sorra en aquesta tesi. Núria, conec poques persones tant treballadores com tu, gràcies per ajudar-me sempre que em veies enfeinat, encara que jo no t'ho demanes. Anna, des dels primers dies que vas arribar cooperant amb el tema de l'intestí vam tenir temps de tenir moltes converses al Trueta que no oblidaré, gràcies per tots els consells referits als temes post-doc que em vas donar els últims dies.

A la resta d'UDENs que m'han acompanyat en aquesta etapa en un moment o altre, Òscar, Emili, María, Estefanía, Isma, Ylenia, ... i a tots el que en un moment o altre han realitzat una estada al grup, moltes gràcies.

Agraïr a tots els col·laboradors del grup, en especial als de Lleida i Sevilla, que han participat directament en aquesta tesi.

A al resta de "família" IDIBGI, gràcies per compartir aquest camí amb mi. Als de Rep. Chrom., Marini i Adrian, hem compartit bastantes hores junts sobretot de tarda quan quedava poca gent al lab. Marini, fent conya sempre que et venia a demanar si podia fer servir l'incubador dient que et posaria simplement per això al agraïments de la tesi, aquí ho tens, gràcies per alegrar el lab. Adrian, en poco tiempo entablamos una gran amistad, gran persona y mejor surfero. María, aún recuerdo que fuiste la primera en recibirme con una sonrisa cuando regresé al lab después de las prácticas en PEDI el anterior verano. Por todos los audios de whatsapp cuando ponían "Avicii", por todas las cerves y partidos de futbol que hemos ido a ver juntos, se te perdona que seas del Madrid!. Rocío, sempre que em veies m'apodaves com a "niño", espero que m'ho puguis dir per molt temps. A les Pedis, Berta i Ari, gràcies per aguantar-me quan tenia revelats del Western i venia a la vostre poiata a passar el temps de revelat i sobretot els nervis. Gràcies per ser més que companys de feina, us trobo a faltar!

Voldria donar també les gràcies a la Carme, Sílvia, Ester, Laia, Gerard, Sara, Bet, i a l'Esther que malauradament ens va deixar massa aviat.

No vull oblidar-me dels que han estat presents en aquesta tesi donant-me suport fora del lab. Primer de tot donar gràcies al millor que m'ha pogut donar la Uni, vosaltres Andrea, Guillem, Martí, Miquel, Neus, Pol, Sheila, Xevi i Yentel. Gràcies per el suport, per escoltar i aguantar les meves rallades, pels vostres consells, per totes les birres i moments de desconnexió unics que hem viscut i ens queden per viure, per la vostre amistat sincera, i sobretot als que us ha tocat compartir pis amb mi. Donar ànims als futurs doctors que hi ha al grup, que van molt ben encaminats. Per cert encara em sona bé la lletra grega carro que em vaig inventar. Dins de la mateixa categoria incloure al grup de "Los de para siempre" de la Uni, encara que últimament no ens haguem vist tant, gràcies per tot.

Als que em coneixen de tota la vida, Roger, Xevi, Ferran, Guillem. Gràcies per les nits de festa, per tots els dies de piscina, per tots els viatges, per les sortides amb bici el diumenge el matí, per estar orgullosos de mi quan dèieu que tindríeu un amic doctor, per tot.

Finalment els més importants, els meus pares (Jordi i Silvia) i al meu germà (Ernest), gràcies de tot cor. Aquesta tesi no seria possible sense vosaltres, m'heu permés centrar-me en el que més m'agradava sense demanar-me res a canvi. Pares, gràcies per ser els millors exemples que un pot tenir, vosaltres m'heu ensenyat el valor de les coses, el sacrifici, a lluitar per el que t'agrada... Hauria de fer una llista massa llarga per agrair-vos tot el que heu fet per mi, gràcies per tot!

Moltes gràcies a tothom!

LISTS OF MANUSCRIPTS

This thesis is presented as a compendium of four manuscripts:

Manuscript 1:

Ferran Comas, Jèssica Latorre, Francisco Ortega, María Arnoriaga Rodríguez, Aina Lluch, Mònica Sabater, Ferran Rius, Xavier Ribas, Miquel Costas, Wifredo Ricart, Albert Lecube, José Manuel Fernández-Real, José María Moreno-Navarrete. **Morbidly obese subjects show increased serum hydrogen sulfide in proportion to fat mass.** *Int J Obes (London).* 2020 Oct; doi: 10.1038/s41366-020-00696-z.

Impact factor (2019): 4.419 (Q1, Nutrition & Dietetics)

Manuscript 2:

Ferran Comas, Jèssica Latorre, Olaf Cussó, Francisco Ortega, Aina Lluch, Mònica Sabater, Anna Castells-Nobau, Wifredo Ricart, Xavier Ribas, Miquel Costas, José Manuel Fernández-Real, José María Moreno-Navarrete. **Hydrogen sulfide impacts on inflammation-induced adipocyte dysfunction.** *Food Chem Toxicol*. 2019 Sep; doi: 10.1016/j.fct.2019.05.051.

Impact factor (2019): 4.679 (D1, Food Science & Technology)

Manuscript 3:

Ferran Comas, Jèssica Latorre, Francisco Ortega, Núria Oliveras, Aina Lluch, Wifredo Ricart, José Manuel Fernandez-Real, José Maria Moreno-Navarrete. **Permanent cystathionine-β-Synthase gene knockdown promotes inflammation and oxidative stress in immortalized human adipose-derived mesenchymal stem cells, enhancing their adipogenic capacity.** *Redox Biol.* 2020 Aug; doi: 10.1016/j.redox.2020.101668.

Impact factor (2019): 9.986 (D1, Biochemistry & Molecular biology)

Manuscript 4:

Ferran Comas, Jèssica Latorre, Francisco Ortega, María Arnoriaga Rodríguez, Matthias Kern, Aina Lluch, Wifredo Ricart, Matthias Blüher, Cecilia Gotor, Luis C. Romero, José Manuel Fernández-Real, José María Moreno-Navarrete. **Activation of endogenous H_2S biosynthesis or supplementation with exogenous H_2S enhances adipose tissue adipogenesis and preserves adipocyte physiology in humans.** *Antioxid Redox Signal.* 2021 Feb; doi: 10.1089/ars.2020.8206

Impact factor (2019): 7.040 (D1, Endocrinology)

ABBREVIATIONS

3-MP: 3-mercaptopyruvate

γ-GCS: γ-glutamyl cysteine synthetase

ACACA: Acetyl-coenzyme A carboxylase

ADIPOQ: Adiponectin

AKT: Serine-threonine protein kinase

AOE: Antioxidant enzymes

ARE: Antioxidant response elements

ASC52telo: Immortalized human adipose-derived mesenchymal stem cells

ATP: Adenosine triphosphate

BAT: Brown adipose tissue

BAX: BCL2 associated X

BMI: Body mass index

CAT: Catalase

CAT: Cysteine aminotransferase

CBS: Cystathionine-β-Synthase

CDO: Cysteine dioxygenase

CEBPα: CCAAT/enhancer-binding protein alpha

C/EBPβ: CCAAT/enhancer-binding protein beta

C/EBPδ: CCAAT/enhancer-binding protein delta

CO: Carbon monoxide

CSAD: Cysteine sulfinic acid decarboxylase

CSE-KO: Cystathionine γ-lyase knockout

CTH/CSE: Cystathionine γ-lyase

DAO: D-amino acid oxidase

DHLA: Dihydrolipoic acid

DTT: Dithiothreitol

ETHE1: Sulfur dioxygenase

FABP4: Fatty acid-binding protein 4

FASN: Fatty acid synthase

FOXO3: Forkhead box O3

GC: Gas chromatography

GPx: Glutathione peroxidase

GS: Glutathione synthetase

GSH: Glutathione

GSSG: Glutathione disulfide

GSSH: Glutathione persulfide

GST: Glutathione-S-transferase

H_2S: Hydrogen Sulfide

hAMSC: Human adipose-derived mesenchymal stem cells

HbA1c: Glycated haemoglobin / haemoglobin A1c

HDL: High-density lipoprotein

HFD: High-fat diet

HOMA-IR: Homeostatic Model Assessment for Insulin Resistance

HPLC: High-pressure liquid chromatography

HS^-: Hydrosulfide anion

HTAU-DH: Hypotaurine dehydrogenase

IL-1: Interleukin-1

IL-6: Interleukin-6

IRS1: Insulin receptor substrate 1

ISE: Ion sulfide electrode

KD: Knock-down

KEAP1: Kelch-like ECH-associated protein 1

LC3: Microtubule Associated Protein 1 Light Chain 3 Alpha

LC-MS: Liquid chromatography-mass spectrometry

LDL: Low-density lipoprotein

LR: Lawesson's reagent

MBB: Monobromobimane

MMTS: S-methyl methanethiosulfonate

MPO: Myeloperoxidase

MPST: 3-mercapto-pyruvate sulfurtransferase

mRNA: messenger RNA

MSBT: Methylsulfonylbenzothiazole

MSCs: Mesenchymal stem cells

MTHFR: N5,N10-methylenetetrahydrofolate reductase

Na_2S: Sodium sulfide

NADH: Nicotinamide adenine dinucleotide

NADPH: Nicotinamide adenine dinucleotide phosphate

NaHS: Sodium hydrosulfide

NFκB: Nuclear factor kappa-light-chain-enhancer of activated B cells

NO: Nitric oxide

NRF2: Nuclear factor (erythroid-derived 2)-like 2

PLP: Pyridoxal-5'-phosphate

PPARγ: Peroxisome proliferator-activated receptor gamma

PPG: Propargylglycine

RNS: Reactive nitrogen species

ROS: Reactive oxygen species

S^0: Sulfur atom

S^{2-}: Sulfide anion

$S_2O_3^{2-}$: Thiosulfate

SAH: S-Adenosylhomocysteine

SAM: S-adenosylmethionine

SAT: Subcutaneous adipose tissue

SIRT1: Sirtuin 1

SIRT3: Sirtuin 3

SIRTs: Sirtuins

SLC2A4: Glucose transporter 4

SO_3^{2-}: Sulfite

SO_4^{2-}: Sulfate

SOD2: Superoxide dismutase 2

SQR: Sulfide quinone oxidoreductase

SREBP1: Sterol regulatory element-binding protein 1

SVF: Stromal vascular fraction

TNF-α: Tumor-necrosis factor-alpha

TP53: Tumor protein p53

TRX: Thioredoxin

TST: Thiosulfate sulfurtransferase

UCP1: Uncoupling protein 1

VAT: Visceral adipose tissue

WAT: White adipose tissue

WHO: World Health Organization

WT: Wild type

LIST OF FIGURES

TABLE OF CONTENTS

SUMMARY

Hydrogen sulfide (H_2S), regarded as the third gasotransmitter, plays diverse physiological and pathological roles in the body along with another two gasotransmitters, including nitric oxide (NO) and carbon monoxide (CO). Endogenous H_2S metabolisms (production and catabolism) take part in both normal physiology and in some human disorders. Manipulation of H_2S levels by inhibiting H_2S synthesis or administration of H_2S-releasing molecules revealed beneficial as well as harmful effects of H_2S. However, the impact of H_2S in the pathophysiology of obesity and its importance in the physiology of human adipose tissue has been scarcely investigated. Here we aimed to investigate circulating H_2S according to obesity, and the impact of H_2S on adipocyte and adipose tissue physiology.

Circulating serum sulfide concentrations were increased in subjects with morbid obesity in proportion to fat mass and inversely associated with circulating markers of heme degradation. In addition, serum sulfide concentration decreased in morbidly obese subjects with impaired compared to those with normal fasting glucose. Longitudinally, weight gain resulted in increased serum sulfide concentration, whereas weight loss had opposite effects. These data suggested the possible role of hydrogen sulfide in the physiology of human adipose tissue. To investigate the impact of H_2S on adipocyte physiology, experiments in mouse 3T3-L1 cell line, immortalized human adipose-derived mesenchymal stem cells (ASC52telo) and human preadipocytes were performed. In 3T3-L1 mouse cell line, GYY4137 slow-releasing H_2S improved adipocyte differentiation in inflammatory conditions, and H_2S proadipogenic effect depended on dose, donor and exposure time. In immortalized human adipose-derived mesenchymal stem cells (ASC52telo) permanent knockdown of cystathionine-β-Synthase (*CBS*), an important H_2S-synthesising gene in these cells, promoted a cellular senescence phenotype, characterized by increased cellular inflammation and oxidative stress, reduced cellular rejuvenation-related gene expression markers and especially increased adipogenic potential, which resulted in a non-physiological enhanced adipocyte differentiation with excessive lipid storage. Of note, in human

preadipocytes, adipocytes and adipose tissue, the relevance of H_2S biosynthesis in adipogenesis was confirmed, and a new mechanism of its action through the identification of persulfidated proteins involved in adipogenesis was suggested. To sum up, H_2S-synthesizing enzymes were recognized as important actors in the human adipose tissue physiology and systemic insulin sensitivity possibly, avoiding cellular senescence and inflammation, and in consequence preserving adipose tissue adipogenesis.

Altogether, this doctorate thesis provides sound and novel proofs addressing the role of H_2S in the pathophysiology of obesity and its importance in the physiology of human adipose tissue, including the discovery of increased circulating serum sulfide concentrations in subjects with morbid obesity in proportion to fat mass, and unravels the importance of H_2S-synthesizing enzymes and H_2S as a previously unrecognized targets in the modulation of human adipocyte physiology.

RESUM

El sulfur d'hidrogen (H_2S), considerat el tercer gasotransmissor, té diversos rols fisiològics i patològics en el cos juntament amb altres dos gasotransmissors, incloent l'òxid nítric (NO) i el monòxid de carboni (CO). Els metabolismes endògens H_2S (producció i catabolisme) participen tant en la fisiologia normal com en alguns trastorns humans. La manipulació dels nivells d'H_2S inhibint-ne la seva síntesi o degut a l'administració de molècules alliberadores d'H_2S s'han utilitzat per revelar efectes beneficiosos i nocius del H_2S. Tot i això, l'impacte de l'H_2S amb prou feines s'ha investigat en la fisiopatologia de l'obesitat i la seva importància en la fisiologia del teixit adipós humà. En aquesta tesi ens hem proposat investigar l'H_2S circulant en relació a l'obesitat, i l'impacte de l'H_2S en la fisiologia de l'adipòcit i el teixit adipós.

Les concentracions de sulfur sèric circulant van augmentar en subjectes amb obesitat mòrbida en proporció a la massa grassa i inversament associades a marcadors circulants de la degradació de productes hemo. A més, la concentració de sulfur sèric va disminuir en subjectes amb obesitat mòrbida i amb la glucosa en dejú alterada en comparació aquells amb un nivells normals. Longitudinalment, l'augment de pes va provocar una major concentració de sulfur sèric, mentre que la pèrdua de pes va tenir efectes oposats. Aquestes dades van suggerir el possible rol del sulfur d'hidrogen en la fisiologia del teixit adipós humà. Per tal d'investigar l'impacte de l'H_2S en la fisiologia dels adipòcits, es van realitzar experiments en la línia cel·lular murínica 3T3-L1, en cèl·lules mare mesenquimals inmortalitzades derivades del teixit adipós (ASC52telo) i en preadipòcits humans. En la línia cel·lular de ratolí 3T3-L1, el GYY4137 com a donador lent de H_2S va millorar la diferenciació adipòcitaria en condicions inflamatòries, i de fet l'efecte proadipogènic de l'H_2S depenia de la dosi, del donador i del temps d'exposició. En cèl·lules mare mesenquimals inmortalitzades derivades del teixit adipós (ASC52telo), el silenciament permanent de la cistationina-β-sintetasa (*CBS*), un gen important en implicat en la síntesi de H_2S en aquestes cèl·lules, promovia un fenotip de senescència cel·lular, caracteritzat per un augment en l'expressió gènica de marcadors de la inflamació cel·lular i l'estrès oxidatiu, una reducció de marcadors relacionats amb el rejoveniment cel·lular, i sobretot, un augment del potencial

adipogènic, que va donava lloc a un increment no fisiològic de la diferenciació i a un excés d'emmagatzematge de lípids. Es rellevant destacar que en preadipòcits, adipócits i en el teixit adipós es va confirmar la importància de la biosíntesi d'H_2S en l'adipogenesis, i es va suggerir un nou mecanisme de la seva acció mitjançant la identificació de proteïnes persulfidatades implicades en l'adipogènesi. En conclusió, els enzims encarregats de la síntesi de H_2S van ser reconeguts com a actors importants en la fisiologia del teixit adipós humà i la sensibilitat sistèmica a la insulina, possiblement evitant la senescència i la inflamació cel·lular i, en conseqüència, preservant l'adipogènesi del teixit adipós.

En conjunt, aquesta tesi doctoral proporciona proves sòlides i novedoses sobre el paper de l'H_2S en la fisiopatologia de l'obesitat i la seva importància en la fisiologia del teixit adipós humà, incloent el descobriment de concentracions incrementades de sulfurs sèrics circulants en subjectes amb obesitat mòrbida en proporció a la massa grassa, i revela la importància dels enzims que sintetitzen H_2S i l'H_2S com a dianes no reconegudes prèviament en la modulació de la fisiologia dels adipòcits humans.

RESUMEN

El sulfuro de hidrógeno (H_2S), considerado el tercer gasotransmissor, tiene varios roles fisiológicos y patológicos en el cuerpo junto con otros dos gasotransmissors, que incluyen el óxido nítrico (NO) y el monóxido de carbono (CO). Los metabolismos endógenos del H_2S (producción y catabolismo) participan tanto en la fisiología normal como en varios trastornos humanos. La manipulación de los niveles de H_2S por la inhibición de las enzimas implicadas en su síntesis o debido a la administración de moléculas liberadoras de H_2S se has utilizado para revelar los efectos beneficiosos y nocivos del H_2S. Aún así, el impacto del H_2S apenas se ha investigado en la fisiopatología de la obesidad y su importancia en la fisiología del tejido adiposo humano. En esta tesis nos hemos propuesto investigar el H_2S circulante en relación a la obesidad, y el impacto del H_2S en la fisiología del adipocito y el tejido adiposo.

Las concentraciones de sulfuro sérico circulante aumentaron en sujetos con obesidad mórbida en proporción a la masa grasa e inversamente asociadas a marcadores circulantes de la degradación de productos hemo. Además, la concentración de sulfuro sérico disminuyó en sujetos con obesidad mórbida y con la glucosa en ayunas alterada en comparación aquellos con niveles normales. Longitudinalmente, el aumento de peso provocó una mayor concentración de sulfuro sérico, mientras que la pérdida de peso tenia efectos opuestos. Estos datos sugirieron un posible rol del sulfuro de hidrógeno en la fisiología del tejido adiposo humano. Para poder investigar el impacto del H_2S en la fisiología de los adipocitos, se realizaron experimentos en la línea celular de ratón 3T3-L1, en células madre mesenquimales inmortalizadas derivades del tejido adiposo (ASC52telo) y en preadipocitos humanos. En la línea celular de ratón 3T3-L1, el GYY4137 como donador lento de H_2S mejoró la diferenciación adipocitaria en condiciones inflamatorias, y de hecho el efecto proadipogenico del H_2S dependía de la dosis, el donador y del tiempo de exposición. En células madre mesenquimales inmortalizadas derivadas de tejido adiposo (ASC52telo), el silenciamiento permanente de la cistationina-β-sintasa (*CBS*), un gen importante implicado en la síntesis de H_2S en dichas células , promovía un fenotipo de senescencia celular, caracterizado por el aumento en la expresión génica de marcadores de la inflamación celular y

estrés oxidativo, una reducción de marcadores relacionados con el rejuvenecimiento celular, y sobre todo, un aumento del potencial adipogénico, que daba lugar a un augmento no fisiológico de la diferenciación y un exceso en el almacenamiento de lípidos. Es relevante destacar que en preadipocitos, adipocitos y en el tejido adiposo humano se confirmó la importancia de la biosíntesis de H_2S en la adipogénesis, y se sugirió un nuevo mecanismo de su acción mediante la identificación de proteínas persulfidatadas implicadas en la adipogénesis. En conclusión, las enzimas encargadas de la síntesis de H_2S fueron reconocidas como actores importantes en la fisiología del tejido adiposo humano y la sensibilidad sistémica a la insulina, posiblemente evitando la senescencia y la inflamación celular y, en consecuencia, preservando la adipogénesis del tejido adiposo.

En conjunto, esta tesis doctoral proporciona pruebas sólidas y novedosas sobre el papel del H_2S en la fisiopatología de la obesidad y su importancia en la fisiología del tejido adiposo humano, incluyendo el descubrimiento de concentraciones incrementadas de sulfuros séricos circulantes en sujetos con obesidad mórbida en proporción a la masa grasa, y revela la importancia de las enzimas que sintetizan H_2S y el propio H_2S como dianas no reconocidas previamente implicadas en la modulación de la fisiología de los adipocitos humanos.

1. INTRODUCTION

1.1 OBESITY

1.1.1 Definition of Obesity

Obesity is characterized by the excessive accumulation and storage of fat in the body (regionally, globally or both) that may be harmful to health and is defined by a body mass index (BMI) of 30 kg/m^2 or greater. A BMI of 35 and higher is considered morbid obesity.

The epidemic of obesity presents a serious threat to human health around the world. The worldwide prevalence of obesity has increased dramatically over the past 30 years, fueled by economic growth, industrialization, mechanized transport, urbanization, an increasingly sedentary lifestyle, and a nutritional transition to processed foods and high calorie diets[1]. According to the World Health Organization (WHO) actually 30% of Americans and 10-20% of Europeans are obese, and estimates than more than 1.9 billion adults worldwide were overweight. Of these over 650 million were obese.

High body mass carries with it an increased risk of the development of a number of serious cardiovascular and metabolic diseases, such as type 2 diabetes, hypertension, dyslipidemia, stroke, osteoarthritis as well as several different forms of cancer[2].

The most accurate measures of body fat (the major component of body weight responsible for adverse outcomes) such as underwater weighing, dual-energy x-ray absorptiometry scanning, computed tomography, and magnetic resonance imaging are impractical for use in everyday clinical encounters. Estimates of body fat including body mass index (BMI, calculated by dividing the body weight in kilograms by height in meters squared, or kg/m^2) and waist circumference do have limitations compared to these imaging methods, but still provide relevant information and are easily implemented in a variety of practice settings[3].

1.2 ADIPOSE TISSUE

1.2.1 Adipose tissue

Adipose tissue is one of the most abundant in the human body, but for a long time, it has been given little importance and it was considered only as a passive energy storage site[4]. The worldwide epidemic of obesity and type 2 diabetes has greatly increased interest in the biology and physiology of adipose tissues. Actually, it is now known that apart from the energy reservoir function, adipose tissue functions as a thermal insulator, mechanical shock absorber, and more importantly as an endocrine organ[5]. Two types of adipose tissue coexist in humans, the white adipose tissue (WAT) and brown (BAT), each performing different functions.

White adipose tissue is one of the most abundant in mammals especially subcutaneous and visceral depots, where it performs numerous complex functions. The primary role of the WAT is to store large amounts of excess energy in the form of triglycerides for future use by other cells of the organism during periods of energy deprivation. That requires the process of lipogenesis as well as the uptake of triglycerides for accumulation fat, and the mobilization of this energy by the use of other cells in the body through the process of lipolysis. In addition, WAT has an endocrine function that contributes to the regulation and homeostasis of all the energy stored in the body by secreting different hormones, including peptides (adipokines), lipids (lipokines) and exosomal miRNAs derived from the adipose tissue[6]. The white adipocytes contain a single, large lipid droplet, leaving the nucleus and cytoplasm in the periphery of the cell[7].

Brown adipose tissue is specialized to generate heat by dissipating chemical energy as a defense against cold and obesity. The total mass of BAT in adults is small, that's why it was initially believed to be of relevance only in human newborns and infants. However, research during recent years provided unequivocal evidence of active BAT in human adults[8]. The distribution of BAT in adults varied widely and was categorized by six anatomically distinct depots: cervical, supraclavicular, axillary, paraspinal, mediastinal, and abdominal, being the supraclavicular region the depot with the highest proportion of total body BAT volume[9]. Thermogenesis in the BAT is mediated through a brown fat-specific mitochondrial protein, uncoupling protein 1 (UCP1),

which plays an important role in the control of energy homeostasis[10]. It's important to mention that humans possess at least two types of thermogenic adipocytes, the classical brown adipocytes present in BAT depots and beige or brite adipocytes, known to differentiate from a sub-population of progenitors resident in WAT, induced by cold exposure or β-adrenergic stimulation among other factors, with specific gene expression pattern distinct from either white or brown fat[11].

1.2.2 Adipogenesis and obesity

Obesity is characterized by adipose tissue expansion due to two main processes, the increase in the number of cells by adipocyte differentiation (hyperplasia) and by the increase of adipocyte size (hypertrophy)[12]. Hypertrophy to some extent is characteristic of individuals with obesity-associated metabolic disturbances, including insulin resistance and dyslipidemia, and increased risk of type 2 diabetes and non-alcoholic fatty liver disease[13–15]. In contrast, hyperplasia is strongly correlated with healthy obesity, being required to achieve morbidly obesity[16]. The number of adipocytes present in a tissue is determined mostly by the process of adipocyte differentiation, therefore understanding the origin and development of adipocytes and adipose tissue is key to generate treatments for obesity[17]. Prolonged periods of weight gain in adults usually involves an increase in the number of adipocytes and adipocyte size[18]. New adipocytes are constantly generated from a pre-existing population of undifferentiated progenitor cells or through the dedifferentiation of adipocytes to preadipocytes, which again differentiate into adipocytes[19]. Therefore in both cases, the generation of new adipocytes plays a key role in obesity.

A reduced ability of adipose tissue to expand when challenged with excess nutrients due to decreased adipogenic potential can lead to insulin resistance[20,21], since this leads to adipocyte hypertrophy, which is associated with increased inflammation, oxidative stress, systemic insulin resistance, reduced mitochondrial function, membrane modifications, DNA damage and cell death [21–24]. This hypertrophy leads to a higher release of adipokines as proinflammatory cytokines such as interleukin-1 (IL-1), interleukin-6 (IL-6) and tumor-necrosis factor-alpha (TNF-α), resulting in low-grade chronic inflammation, which begins in adipose tissue and eventually reaches the circulation and other organs[25,26]. One of the first consequences of inflammation is

insulin resistance, since TNF-α prevents the phosphorylation of insulin receptors, interfering in their cascade action and preventing their functioning[27]. Another cause of inflammation is oxidative stress, which can be triggered by adipocytes. Oxidative stress plays an important role in the pathogenesis of insulin resistance by disrupting the release of adipokines by adipose tissue such as TNF-α and IL-6, which can trigger inflammation. The high senescent cell burden in hypertrophic obesity may be more a cause of the development of fat cell hypertrophy, rather than being secondary to obesity itself[28]. Reduced adipogenesis as a consequence of increased senescent cell burden is also associated with increased ectopic lipid accumulation in other tissues, such as liver and muscle[28,29], which in turn is associated with the development of insulin resistance.

1.3 THE ADIPOCYTE AND EXPERIMENTAL *IN VITRO* MODELS

1.3.1 Adipocyte

Over the last several years, the increasing prevalence of obesity has favored an intense study of adipose tissue biology and the precise mechanisms involved in adipocyte differentiation and adipogenesis. Adipose tissue contains adipocytes in addition to a wide population of cells, such as macrophages, fibroblasts, pericytes, blood cells, endothelial cells, smooth muscle cells, mesenchymal stem cells (MSCs), and adipose precursor cells[30]. All of these cells are located in the stromal vascular fraction (SVF), and the cell composition and phenotype of the SVF are usually different depending on the location of the adipose tissue depot and the adiposity[31].

Adipocyte commitment and differentiation are complex processes, which can be investigated thanks to the development of diverse *in vitro* cell models and molecular biology techniques that allow for a better understanding of adipogenesis and adipocyte dysfunction associated with obesity[30]. *In vitro* models have been invaluable in determining the mechanisms involved in adipocyte proliferation, differentiation, adipokine secretion and gene/protein expression[32].

Essentially all work on adipogenesis has used either predetermined clonal cell lines or primary cultures of adipose tissue-derived stromal-vascular precursor cells, which have been effectively

cultured from several species including humans[33–35]. Explant culture, known as *ex vivo* adipose tissue explants, derived from primary tissues contain cells at different stages of development and can not be as scientifically controlled as preadipose cell lines, but they probably reflect more accurately the normal condition *in vivo*[36]. In addition, primary cells can be isolated from various species and from different fat depots, as well as from animals of different physiological states and ages, allowing comparisons between cells of different origins.

1.3.2 Adipocyte differentiation

Adipogenesis refers to the process where adipocyte progenitors are differentiated into mature adipocytes. Adipogenesis can be briefly divided into two phases: determination and terminal differentiation[37]. During the determination phase, mesenchymal stem cells are committed to the adipose lineage and become preadipocytes in response to appropriate adipogenic stimulation[38]. Terminal differentiation, on the other hand, describes the process by which preadipocytes acquire the characteristics of the mature adipocytes[37]. MSCs are known to contribute to tissue repair and are capable of differentiating into different lineages such as osteoblasts (bone), adipocytes (fat), chondrocytes (cartilage), or myotubes (muscle)[39] (**Figure 1**).

A commonly employed cellular model to study adipogenesis is 3T3-L1 cell line, which has already been committed to the adipocyte lineage. The cellular and molecular changes that occur during adipogenesis from studies using 3T3-L1 cells, then the knowledge is on the regulation of the terminal differentiation process[37]. However, little is known about the regulation of determination of adipogenesis, particularly *in vivo*. Thus, to study the role of hydrogen sulfide during determination and terminal steps of adipogenesis, both human adipose-derived mesenchymal stem cells (hAMSC) and 3T3-L1 adipocyte cell lines are used in this thesis.

3T3-L1 preadipocytes have to withdraw from the cell cycle before adipose conversion. Upon reaching confluence, proliferative preadipocytes become growth-arrested by contact inhibition[40]. After growth arrest at confluence, those preadipocytes re-enter the cell cycle and must receive an appropriate combination of mitogenic and adipogenic signals to undergo terminal adipocyte

differentiation. During this step, cells undergo at least one round of DNA replication and cell doubling. Re-entry into the cell cycle of growth-arrested preadipocytes is known as the clonal expansion phase[41]. However, primary preadipocytes derived from human adipose tissue do not require cell division to enter the differentiation process[42]. The whole process of differentiation is accompanied by specific sequential changes in the expression of different genes, which vary depending on the cell line and the experimental treatments.

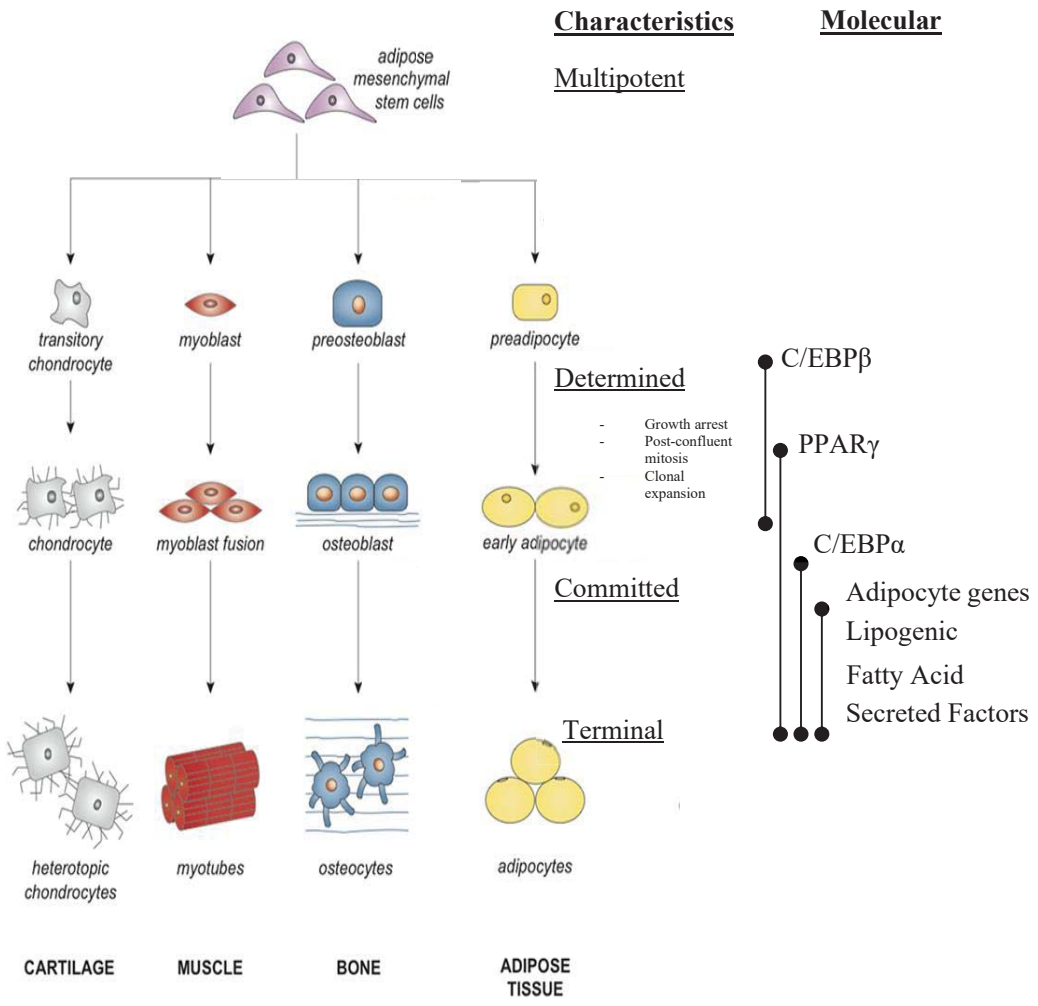

Figure 1. Schematic overview of signaling molecules and transcription factors involved in the regulation of differentiation of adipose-derived mesenchymal stem cells (MSCs**)** into adipocytes, and their potential lineages. *Figure taken and adapted from Bateman M.E. (2017)* [38].

A rapid and transient increase in transcription and expression of CCAAT / enhancer-binding protein beta (*C/EBP*β) and delta (*C/EBP*δ) is observed in preadipocytes differentiation, accelerating the induction of two transcription factors in this first phase of growth arrest, the peroxisome proliferator-activated receptor gamma (PPARγ) and CCAAT / enhancer-binding protein alpha (CEBPα) playing a key role in activating the set of genes involved in adipogenesis (including genes involved in lipogenesis, lipolysis, and formation of lipid vacuole)[43,44]. The expression of another transcription factor called sterol regulatory element-binding protein 1 (SREBP1) is also overexpressed in the early stages of adipogenesis, which stimulates PPARγ activation[45]. During the late stages of adipogenesis, the expression of genes associated with lipogenesis, such as glucose transporter 4 (SLC2A4)[46], acetyl-coenzyme A carboxylase (ACACA)[47] and fatty acid synthase (FASN)[48] are overexpressed, through SREBP1 regulation. The process of differentiation of preadipocytes is also accompanied by morphological changes, such as the formation and fusion of small lipid droplets, and the change of a fibroblastic shape to a rounded shape. The process of differentiation is explained above (**Figure 1**).

1.4 HYDROGEN SULFIDE (H_2S)

Gasotransmitters are small molecules of endogenous gas that has the noticeable ability to diffuse into cells to interact with their targets, inducing an array of intracellular signaling and pathophysiological responses[49,50]. Hydrogen sulfide is the most recent addition to the gasotransmitters family, the first two being nitric oxide (NO) and carbon monoxide (CO)[51].

Instead of binding to plasma membrane receptors, the high solubility of gasotransmitters in lipids facilitate them to penetrate cell membranes without requiring a specific transporter or receptor. Gasotransmitters are generated endogenously by specific enzymes and can generate various functions at physiologically relevant concentrations by targeting specific cellular and molecular targets[52]. A gaseous substance is not readily stored in vesicular structures and so must be resynthesized as needed. This implies that the biosynthetic enzymes must be subject to tightly

regulatory mechanisms[53]. Abnormal generation and metabolism of these gasotransmitters have been extensively demonstrated to affect diverse biological processes, such as vascular biology, immune functions, cellular survival, metabolism, longevity, development, and stress resistance[52].

Perhaps the most remarkably unique feature of gasotransmitters relates to the molecular mechanisms whereby they signal to their targets. Gasotransmitters chemically modify intracellular proteins, thus affecting cellular metabolism in a more immediate fashion than other signal transduction mechanisms[53].

H_2S has been traditionally considered only as a toxic agent for living organisms[54]. Nowadays, is considered as a gaseous mediator that plays important regulatory roles in innate immunity and inflammatory responses impacting the development of cardiovascular and metabolic diseases[55–59].

H_2S is an inorganic, colorless, flammable water-soluble gas with a characteristic odor of rotten eggs. In physiological solutions, approximately 20-30% of H_2S exist in a non-dissociated form and 70-80% spontaneously hydrolyses H_2S into hydrosulfide anion (HS^-), which is partially transformed into sulfide anion (S^{2-}) as demonstrated by the following reaction, $H_2S \leftrightarrow H^+ + HS^- \leftrightarrow 2H^+ + S^{2-}$, by Dombkowski and collaborators[60]. Apart from free or unbound sulfide (S^{2-}, HS^- or H_2S), H_2S pools exist in different biochemical forms in physiological, including, acid-labile sulfide (bound to the sulfur-iron clusters of proteins), and bound sulfane sulfur (bound to proteins)[61–63] (**Figure 2)**. Bound sulfane sulfur includes various compounds such as persulfides, polysulfides, thiosulfate, polythionates, thiosulfonates, bisorganylpolysulfanes or monoarylthiosulfonates, elemental sulfur, and many others. Total H_2S refers to all these forms together. The precise chemistry through which these different biological pools of H_2S interact to affect their pathophysiological functions is an area of active research. However, differences in bioavailability of these biochemical pools of sulfide remain largely unknown in part due to difficulties in measuring them[64]. HS^- is capable of conversion to S^{2-} (pKa_2 11.96) but only $2.8x10^{-3}$ % is present in this form at physiological pH values, the S^{2-} concentration in solution is therefore negligible[65,66]. In the alkaline mitochondrial matrix (pH 8.0), HS^- reaches 92%, while

the remaining 8% corresponds to H_2S. Contrarily, under the acidic conditions in lysosomes (pH 4.7), >99% of hydrogen sulfide is in its H_2S form and is slightly polar, allowing it to freely diffuse across and accumulate in an aqueous or hydrophobic environment such as biological membranes[67].

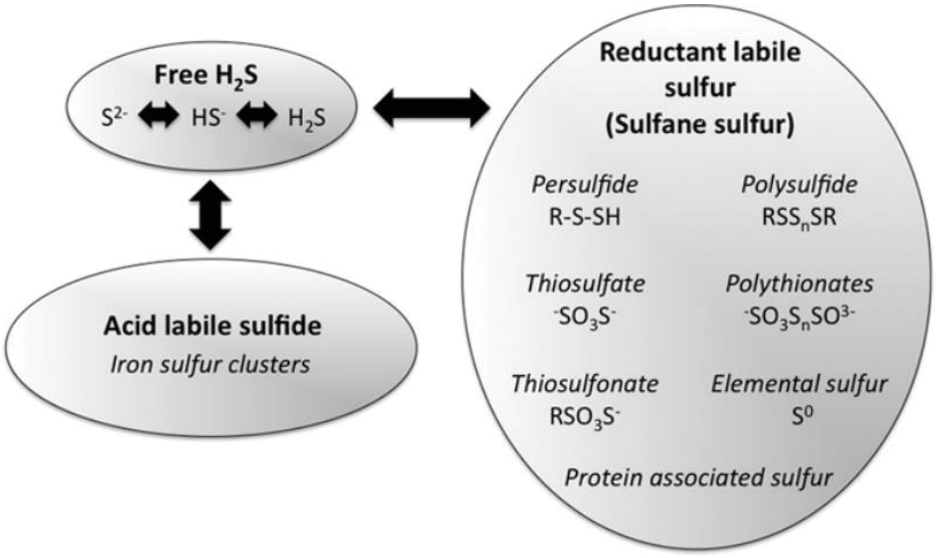

Figure 2. Different pools of H_2S and its biochemical forms. *Figure taken from Shen X. (2012)*[62].

1.5 BIOSYNTHESIS OF H_2S

Hydrogen sulfide biosynthesis has been identified in a variety of mammalian tissues via enzymatic and non-enzymatic pathways[68]. In enzymatic biosynthesis, the endogenous generation of H_2S from L-cysteine in the cytosol of cells is mainly mediated by two pyridoxal-5'-phosphate (PLP) dependent enzymes known as cystathionine β-synthase (CBS)[69] and cystathionine γ-lyase (CTH or CSE)[70]. H_2S is also produced by L-cysteine aminotransferase (CAT) and 3-mercapto-pyruvate sulfurtransferase (MPST) in the cytosol and mitochondria[71]. The expression of these enzymes is tissue-specific, in some tissues, CBS, CTH and MPST are all need for the generation of H_2S, whereas in others one enzyme serves. A small portion of endogenous H_2S is derived *via* non-enzymatic reduction sulfur species present in certain metabolites[68].

1.5.1 Enzymatic synthesis of H_2S

1.5.1.1 Generation of H_2S from the transsulfuration pathway

The transsulfuration pathway plays a central role in sulfur metabolism and redox regulation in cells. The pathway leads to the generation of several sulfur metabolites, which include L-cysteine, glutathione (GSH), taurine and the gaseous signalling molecule hydrogen sulfide[72]. In mammals, the pathway involves the transfer of sulfur from homocysteine to cysteine via cystathionine and is the only route for the biosynthesis of cysteine. Homocysteine, which is derived from dietary methionine, is converted to cystathionine by cystathionine β-synthase (CBS), which is acted on by cystathionine γ-lyase (CTH) to generate L-cysteine[72] (**Figure 3**).

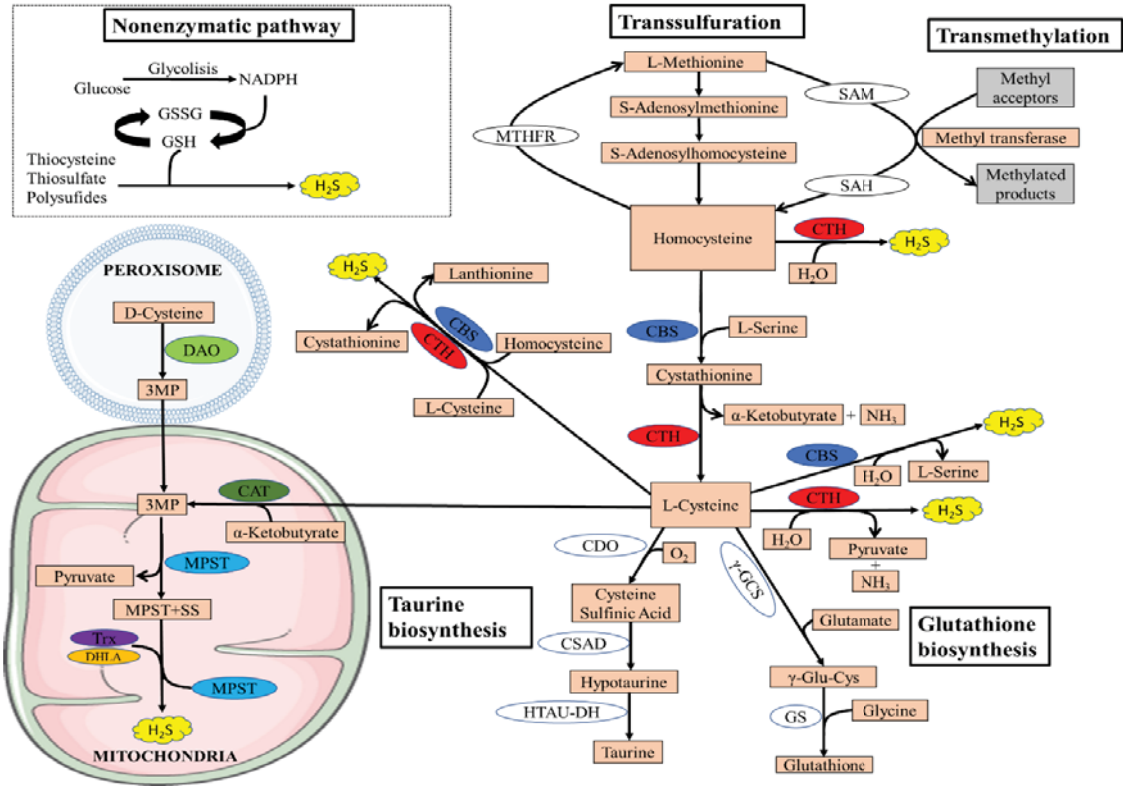

Figure 3. Overview of the transsulfuration pathway. There are four enzymatic pathways for the biosynthesis of H_2S, including CBS, CSE, MPST coupled with CAT, and MPST coupled with DAO. Non-enzymatic H_2S generation occurs in the presence of reducing equivalents such as NADPH and NADH, reactive sulfur species in persulfides, thiosulfate, and polysulfides that are reduced into H_2S and other metabolites. The transsulfuration pathway intersects with the transmethylation pathway at homocysteine. Methionine is an indispensable amino acid and is transmethylated intracellularly via *S*-adenosylmethionine (SAM), an important methyl donor for most biological methylation reactions, to S-Adenosylhomocysteine (SAH) produced in this process and then is hydrolyzed to homocysteine. Homocysteine can be remethylated back to regenerate methionine by N5,N10-methylenetetrahydrofolate reductase (MTHFR). The cysteine generated by the pathway can be conducted into GSH synthesis by the action of the enzymes, γ-glutamyl cysteine synthetase (γ-GCS) and glutathione synthetase (GS) or converted to other sulfur-containing molecules such as taurine. Taurine is generated by the action of three enzymes, CDO, cysteine sulfinic acid decarboxylase (CSAD) and hypotaurine dehydrogenase (HTAU-DH).

In addition to its essential role in protein synthesis, cysteine is also a component of the major antioxidant GSH and a potent antioxidant itself [73]. Disruption of cysteine and GSH metabolism has been frequently linked to aberrant redox homeostasis and neurodegeneration[73,74]. Both CTH and CBS play important roles in the regulation of redox balance. It has been reported that approximately 50% of the cysteine generated by the transsulfuration pathway is utilized for GSH biosynthesis in hepatic cells[75,76]. Cysteine is also the precursor of the gaseous signalling molecule hydrogen sulfide and other sulfur metabolites[77,78]. Besides GSH and H_2S, cysteine is converted to the sulfur-containing molecule taurine by the action of the enzyme cysteine dioxygenase (CDO) to form cysteinesulfinic acid, which can then be decarboxylated to hypotaurine by cysteinesulfinic acid decarboxylase, and the hypotaurine generated, oxidized to taurine[79]. Since CDO acts directly on cysteine, it can modulate H_2S production by influencing substrate availability. Mice lacking CDO have elevated cysteine and H_2S production capacity[80,81]. Taurine plays a role in osmoregulation, immunomodulation, neuromodulation, Ca^{2+} homeostasis, ocular function and possesses antioxidant and anti-inflammatory effects[82]. Transsulfuration pathway is intimately linked to the transmethylation pathway via homocysteine, which can be remethylated to generate methionine or be irreversibly converted to cysteine (**Figure 3**). This doctoral thesis will focus on the regulation of the transsulfuration pathway pertaining to cysteine and H_2S metabolism and its role during normal and pathological conditions in adipose tissue.

1.5.1.2 Other enzymatic pathways of H_2S generation: CAT/MPST

Recently, an alternative enzymatic pathway to the transsulfuration pathway has been identified for the enzymatic generation of H_2S within mitochondria, as the 3-mercaptopyruvate pathway. The pathway requires two enzymes, 3-mercaptopyruvate sulfurtransferase and the PLP-dependent enzyme cysteine aminotransferase (CAT). 3-mercaptopyruvate (3MP) is produced by CAT from L-cysteine and α-ketoglutarate[71]. Thereafter, MPST transfers a sulfur atom from 3MP onto itself, which leads to the formation of persulfide, MPST-SS. H_2S and MPST are then released from the persulfide of MPST-SS in the presence of reductants such as thioredoxin (TRX) and dihydrolipoic acid (DHLA)[83]. Recently, another source of 3MP was found in mammals by Shibuya *et al*., D-

cysteine[84]. Specifically, D-cysteine is transformed into 3MP by peroxisome located d-amino acid oxidase (DAO). Metabolite exchanges between peroxisome and mitochondria can import 3MP into mitochondria where it is further catalyzed into H_2S by MPST. Because of the exclusive location of DAO in the brain and kidney, this H_2S-generating pathway is currently believed to uniquely exist in the two organs[68].

1.5.2 Non-enzymatic synthesis of H_2S

There have been several non-enzymatic H_2S productions reported, suspected to represent a small proportion of generated endogenous H_2S. It is postulated that coordinated activities of PLP and iron (Fe^{3+}) catalyzed the generation of H_2S using cysteine as substrate, in a non-enzymatic manner in specific circumstances. Regulation of H_2S production via this pathway may contribute to the pathophysiology of conditions with iron dysregulation such as hemolysis, iron overload, and hemorrhagic disorders[85].

H_2S can also be generated from sulfane sulfur via non-enzymatical reduction, in the presence of an endogenous reductant, such as nicotinamide adenine dinucleotide phosphate (NADPH) and nicotinamide adenine dinucleotide (NADH), which are supplied by oxidation of glucose *via* glycolysis or from phosphogluconate *via* NADPH oxidase[86]. In the presence of such reductants, reactive sulfur species in persulfides, thiosulfate, and polysulfides can be reduced into H_2S and other metabolites[87]. Essentially, all the components of this non-enzymatic route are available in mammals including reducible sulfur, suggesting the necessity of this pathway in mammalian systems. In accordance with this, hyperglycemia is demonstrated to promote H_2S generation by enhancing this pathway[88].

1.6 CATABOLISM OF H_2S

The roles of H_2S consumption enzymes via catabolic effects on either H_2S directly or on the amino-acid cysteine, may not appear obvious at first sight, but their potential influence on H_2S tissue levels can't be forgotten[80]. Even with their recognised association with H_2S detoxification, only now are we beginning to see how these enzymes influence physiological levels of this gas. H_2S is removed quickly from the cellular environment via two main catabolic pathways, described below: i) H_2S oxidation, which takes place mainly in mitochondria, initially to thiosulfate, followed by its conversion to sulfite and sulfate; and ii) scavenged by hemoglobin to form sulfhemoglobin, as well as other metalloproteins.

1.6.1 Mitochondrial oxidation

Mitochondria is known to be the main site where the oxidation and removal of H_2S takes place. In the body, the process of H_2S oxidation and detoxification occurs predominantly in the liver and colon, and subsequently products are excreted in the urine[89]. Interestingly, Norris et al. also reported that liver might have an important role in the regulation of H_2S levels in the circulation, as a consequence of its location and an enhanced capacity to clearance blood H_2S through H_2S oxidation[90].

The very sequence of reactions and acceptors in the mitochondrial H_2S oxidation pathway is uncertain, leading to contradictory depictions of sulfide oxidation. It is generally accepted that the first step of sulfide breakdown is catalyzed by the action of membrane-associated sulfide quinone oxidoreductase (SQR). This flavoprotein transfers electrons from H_2S to coenzyme Q in the mitochondrial electron transfer chain, thus making H_2S the first inorganic substrate that is able to sustain mitochondrial respiration, indicating that H_2S oxidation and elimination can promote adenosine triphosphate (ATP) synthesis[91]. Concomitantly, SQR transfers the H_2S sulfur atom (S^0) to an acceptor, the physiological persulfide acceptor is postulated to be reduced glutathione (GSH) resulting in the formation of glutathione persulfide (GSSH). Persulfide groups are further oxidised to sulfite (SO_3^{2-}) by sulfur dioxygenase (ETHE1) present in the mitochondrial matrix[92,93].

Sulfite is then directly oxidised to sulfate (SO_4^{2-}) by sulfite oxidase or thiosulfate ($S_2O_3^{2-}$) by rhodanese and excreted in the urine[93]. Then major oxidation products of H_2S are thiosulfate ($S_2O_3^{2-}$) and sulfate (SO_4^{2-}) whose ratio and production rate vary in a tissue-specific manner[94] (**Figure 4 A)**.

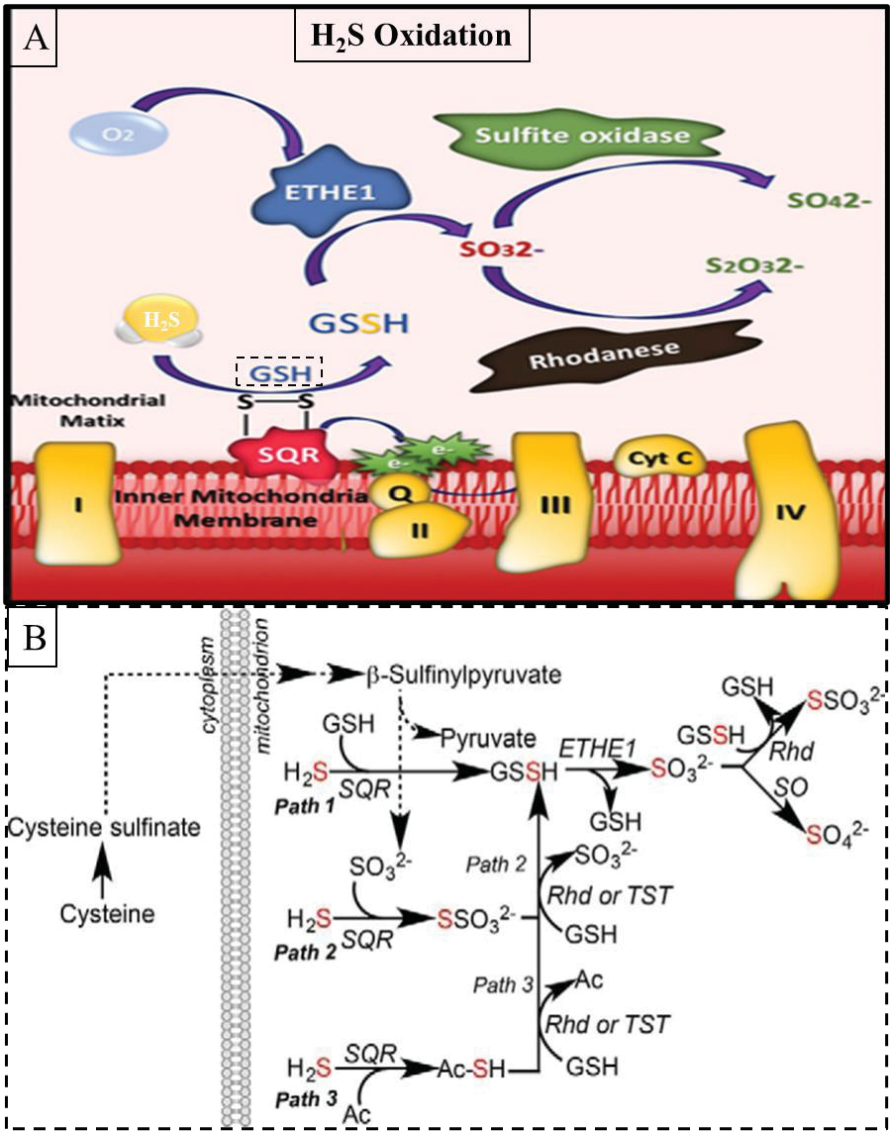

Figure 4. Oxidation of H_2S. A) First step of sulfide oxidation is catalyzed by the action of membrane-associated sulfide quinone oxidoreductase (SQR), which transfers the H_2S sulfur atom to GSH as an acceptor, to form GSSH. GSSH is further oxidised to sulfite (SO_3^{2-}) by sulfur dioxygenase (ETHE1). Sulfite is then directly oxidised to sulfate (SO_4^{2}) by sulfite oxidase (SO) or thiosulfate ($S_2O_3^{2-}$) by rhodanese (TST). **B)** Alternative sulfide oxidation pathways, with an unknown acceptor or sulfite as acceptors coupled to SQR. In the sulfite pathway, sulfite is originated via cysteine catabolic pathway in which cysteine sulfinate in the cytoplasm is converted to β-sulfinylpyruvate in the mitochondria. *Figure taken and adapted from Murphy B. (2019)*[298] *and Libiad M. (2014)*[91].

Instead of reduced glutathione as persulfide acceptor, it is also suggested to be sulfite or an unknown acceptor[92,95]. Thus case, persulfide groups are indirectly transferred to GSH to yield GSSH, the only known substrate for ETHE1. The proposed reaction assumes that sulfite is the acceptor, possibly derived via the cysteine catabolic pathway in which cysteine sulfinic acid formed in the cytoplasm is converted to β-sulfinylpyruvate in the mitochondrion. Then originated sulfite or unknown acceptor is oxidized to thiosulfate or oxidized acceptor respectively, which in turn persulfidate GSH thanks to the action of thiosulfate sulfurtransferase (TST) to form GSSH and sulfite or acceptor again[91] (**Figure 4 B)**.

1.6.2 Scavenging

Besides being metabolized through the mitochondrial sulfide-oxidizing pathway, H_2S can be oxidized by several metalloproteins such as globins, heme-based sensors of diatomic gaseous molecules (such as O_2, NO, CO), cytochrome c oxidase, catalase and peroxidases (lactoperoxidase, myeloperoxidase and thyroid peroxidase), as reported by several groups[96–100].

1.7 METABOLISM AND H_2S

H_2S has been shown to regulate a myriad of cellular processes with multiple physiological consequences. As such, dysfunctional tissue H_2S metabolism is increasingly implicated in different pathologies, from cardiovascular and neurodegenerative diseases to cancer[67]. However, the impact of H_2S has been scarcely investigated in the pathophysiology of obesity and its importance in the physiology of human adipose tissue. Understanding the precise mechanisms that control H_2S homeostasis and their dysregulation during obesity and its role in adipose tissue a major research focus. Despite decades of molecular and cellular studies on the enzymatic systems involved in H_2S synthesis and breakdown, it appears at times that this field of biology is still in its infancy, with new targets of H_2S and related species being consistently identified and new mechanistic details being unrevealed.

1.7.1 H_2S and obesity

There is emerging evidence supporting the importance of H_2S in the pathophysiology of obesity and type 2 diabetes[101]. Exogenous H_2S administration led to increased insulin sensitivity and improved glucose tolerance after a high-fat diet-fed in mice in parallel to weight gain[102,103]. Supplementation with H_2S donors or increasing endogenous H_2S biosynthesis was sufficient to stimulate fat mass accumulation in mice and fruit flies, whereas depletion of endogenous H_2S biosynthesis prevented HFD-induced fat mass[103,104].

In humans, the role of circulating H_2S has been scarcely investigated. Plasma H_2S levels were found to be significantly decreased in non-obese individuals with type-2 diabetes and in overweight participants with altered glucose tolerance[101,105]. To the best of our knowledge, circulating H_2S levels in morbidly obese subjects have not been yet investigated.

1.7.2 The role of H_2S in adipose tissue

Feng et al.[106], first identified the endogenous CTH and CBS gene expression pathway in adipose tissue, and suggested CTH as the primary pathway of H_2S generation in adipose tissue[106]. The same year, Fang et al. first demonstrated that CTH protein expression and endogenous H_2S production in rat perivascular adipose tissue were detectable and that the endogenous H_2S generated was predominantly CTH-catalysed[107]. Following studies confirmed that CBS, CTH and MPST genes were expressed in adipose tissue depots[108,109], and suggested that H_2S affects diverse metabolisms that take place in the adipose tissue, such as lipid, glucose, and mitochondrial metabolism. H_2S is also involved in the regulation of inflammatory and oxidative stress associated response in adipose tissue, through adipokine and antioxidant control[110]. *In vitro* 3T3-L1 mouse cell line model, point to a possible role of H_2S in adipocyte differentiation through the modulation of PPARγ activity[103,104,111]. The overexpression of the H_2S generation enzyme CTH and the administration of the H_2S donor sodium hydrosulfide (NaHS) to 3T3-L1 cells in an environment of high glucose restored adiponectin secretion and decreased the secretion of proinflammatory cytokines[112]. However, the impact of H_2S on human adipocytes and adipose tissue has not been investigated, while its possible role in adipogenesis is not yet completely understood.

1.8 PHYSIOLOGICAL PROPERTIES OF H_2S

The effects of H_2S are well documented to be biphasic, mainly due to the wide range of H_2S concentrations used. At low concentrations, H_2S was demonstrated to be cytoprotective via acting as an antioxidant and anti-inflammatory agent, whereas at high concentrations H_2S becomes an oxidant and a pro-inflammatory agent.

1.8.1 Redox role of H_2S

Oxidative stress involves molecular or cellular damage, resulting from deficiency of antioxidants and/or antioxidant enzyme systems, and disrupting the cellular reduction-oxidation balance[113,114]. The human body is equipped with a variety of antioxidants that serve to counterbalance the effect of oxidants, being H_2S one of the most important. In fact, H_2S protects cells in various diseases by acting as an antioxidant that reduces excessive amounts of reactive oxygen species (ROS) and reactive nitrogen species (RNS)[115]. ROS are highly reactive molecules and can damage cell structures such as carbohydrates, nucleic acids, lipids, and proteins and alter their functions[116].

Several studies have highlighted the role of H_2S in cellular redox homeostasis, which can be summarized in two main mechanisms: i) modulating levels and activity of classic cellular antioxidants, such as glutathione (GSH) and thioredoxin (TRX), ii) and increasing the activity or expression of the transcription nuclear factor (erythroid-derived 2)-like 2 (NRF2) and the histone deacetylase protein family of sirtuins (SIRTs), which in turn increase the expression of antioxidant enzymes (AOE).

As mentioned before, one such way H_2S may exert its antioxidant effects is through modulating the expression and activity of classic antioxidants, like GSH and TRX. GSH is a tripeptide made of cysteine, glycine and glutamate, existing often as a reduced form, and it is synthesized from cysteine. GSH reduces disulfide bonds formed within cytoplasmic proteins to cysteines by serving as an electron donor. In the process, GSH is converted to its oxidized form, glutathione disulfide (GSSG)[117]. GSH is synthesized by the consecutive catalysis of two enzymes, γ-glutamyl cysteine synthetase (γ-GCS) and glutathione synthetase (GS)[117,118]. H_2S administration has been shown to

enhance γ-GCS activity, without changing its expression[119]. H_2S administration is also associated with augmented levels of GSH in the mitochondria. As cytoplasmic GSH is transported into mitochondria, because mitochondria cannot synthesize GSH, the enhanced mitochondrial GSH concentration following H_2S administration is suggested to depend on the increased cytoplasmic GSH levels and enhanced transport into the mitochondria[119] (**Figure 5**).

As mentioned above, the NRF2 transcription nuclear factor mediates the expression of antioxidant enzymes. Under normal physiologic conditions, this transcription factor is confined to the cytoplasm by binding to Kelch-like ECH-associated protein 1 (KEAP1) dimer forming an inactive complex. Whenever a change in redox status occurs by increased cellular ROS levels, KEAP1 dimer changes conformation due to the breaking of disulfide bonds between cysteine residues, and releases NRF2, which translocates to the nucleus and induces the transcription of AOE genes to attain redox homeostasis[120]. Various studies have shown that persulfidation of KEAP1 at the cysteine-151 residue, leading to NRF2 dissociation, increased nuclear translocation and expression of antioxidant genes through binding to antioxidant response elements (ARE) promoters sites[121]. In addition, H_2S can S-sulfhydrate KEAP1 at the cysteine-226 and cysteine-613 residues, leading to Keap1 inactivation, NRF2 release and promotion of NRF2-dependent gene expression[122].

The sirtuins are a family of highly conserved NAD+-dependent deacetylases that mediate a variety of cellular functions and are regulated in response to a wide range of stimuli, including nutritional and metabolic changes, inflammatory signals and oxidative stress. The idea that sirtuins are involved in redox signaling comes from their strong connections to several of the molecules of the antioxidant response element, which mediates signaling events involved in transcriptional regulation of gene expression in cells exposed to oxidative stress[123]. Disruption of redox cellular homeostasis affects SIRTs at different levels, including inducing or repressing their expression, and leading to post-translational modifications such as cysteine oxidation and nitrosylation, which can lead to loss of their function[124].

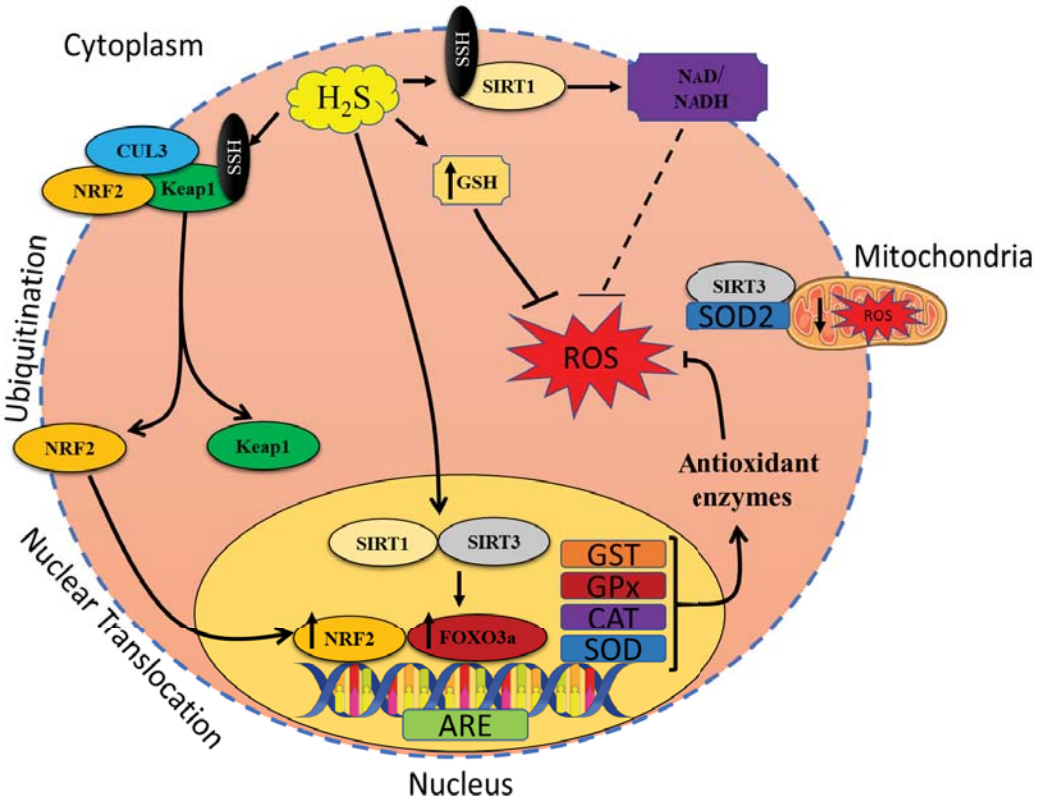

Figure 5. Overview of oxidative stress regulation and antioxidant effect of H_2S. When H_2S levels are increased, Kelch-like ECH-associated protein 1 (KEAP1) is persulfidated, which brings a conformational change of the protein and NRF2 release from KEAP1, allowing the translocation of NRF2 to the nucleus, where it binds to the promoter containing antioxidant response element (ARE) sequences and increased transcription of antioxidant genes such as catalase (CAT), superoxide dismutase (SOD), glutathione-S-transferase (GST) and glutathione peroxidase (GPx). H_2S can also induce GSH synthesis, which blocks ROS production. During oxidative stress, H_2S induces SIRT1 through persulfidation, to regulate the levels of nicotinamide adenine dinucleotide and nicotinamide adenine dinucleotide phosphate NAD/NADH to prevent ROS generation. SIRT1 and SIRT3 induced the expression of transcription factor FOXO3, which regulate the transcription of antioxidant enzymes. In the mitochondria, H_2S can induce SOD2 through SIRT3 to regulate oxidative stress.

Two sirtuins that are known to be central to the control oxidative stress processes are mammalian sirtuin 1 (SIRT1) and sirtuin 3 (SIRT3), which are localized to the nucleus and mitochondria, respectively. Studies suggest that SIRT1 is sensitive to intracellular redox radicals and maybe a key regulator of cell survival in response to oxidative stress[125]. During oxidative stress, H_2S induces *SIRT1* through persulfidation to regulate the levels of NAD/NADH to prevent ROS generation. In addition, H_2S has been shown to induce the expression of activator protein-1, which promotes the expression of SIRT3[126]. Then SIRT3 induces the expression of transcription factor forkhead box O3 (FOXO3) and consequent ROS production, promoting the activator protein-1.

Additionally, H_2S can induce superoxide dismutase 2 (SOD2) through SIRT3 in mitochondria and regulate oxidative stress[126] (**Figure 5**).

1.8.2 Role of H_2S in inflammation

Inflammation is an adaptive response to injury, but uncontrolled inflammation can lead to tissue damage and disease. H_2S has recently gained significant attention as an inflammation biological mediator. Antiinflammatory effect of H_2S has been reported in acute lung injury[127,128], and in kidney injury caused by urinary-derived sepsis[129]. *In vitro* studies confirmed this antiinflammatory role[130] through the modulation of nuclear factor kappa-light-chain-enhancer of activated B cells (NFκB) activity[56]. Antiinflammatory effect of H_2S is supported by the fact that H_2S deficiency contributes to the switch of adipose tissue macrophages anti-inflammatory M2 phenotype to proinflammatory M1 phenotype associated with obesity[131]. However, other studies reported that H_2S has a proinflammatory effect in the liver and aggravated LPS-induced liver damage [132–135].

1.9 H_2S SIGNALLING

Hydrogen sulfide plays important regulatory roles in innate immunity and inflammatory responses impacting on the development of cardiovascular and metabolic diseases[55–59], through different molecular mechanisms, including scavenging of reactive oxygen species[136] and a new revealed mechanism known as persulfidation[137].

1.9.1 Protein persulfidation

Persulfidation is a post-translational modification in which thiol groups (R–SH) from reactive cysteine residues are converted into perthiols (R–SSH). Persulfidation is known to modulate the structure and biological activity of target proteins, preventing irreversible cysteine overoxidation, and in consequence, preserving protein function[137–139]. Persulfidation usually increases the

reactivity of target proteins, modulating their biological activities, whereas other post-translational modifications, such as S-nitrosylation often decrease protein activity[140].

1.10 WORKING WITH H_2S

1.10.1 Hydrogen sulfide donors

Compounds that degrade in response to a specific trigger to release H_2S, termed H_2S donors, include a wide variety of functional groups and delivery systems, some of which mimic the tightly controlled endogenous production in response to specific, biologically relevant conditions[137]. Today, a lot of H_2S donors are available and have been developed.

The most common class of H_2S donors employed in biological studies are the sulfide salts, sodium hydrosulfide (NaHS) and sodium sulfide (Na_2S). These salts release H_2S almost instantly on contacting water. Although, the sulfide salts have the advantage of boosting H_2S concentration rapidly, this rapid and spontaneous release of H_2S may become toxic if not controlled. Additionally, due to the very high volatility of H_2S, the concentration of the solution may decrease rapidly, resulting in a non-physiological role of hydrogen sulfide[141].

Synthetic donors that provide tunable H_2S release rates via structural modification with discrete byproducts allow for a more in-depth analysis of the physiological roles of H_2S and, optimistically, clinically relevant H_2S-releasing prodrugs. GYY4137 is a synthetic water-soluble derivative of Lawesson's reagent (LR), which also releases H_2S via hydrolysis[142]. GYY4137 is generally regarded as a slow-releasing H_2S donor, because GYY4137 released H_2S with a peaking time of 10 min versus 10 seconds for NaHS in phosphate buffer[142]. The GYY4137 has proven to be a useful tool, particularly in investigating the importance of H_2S release rate on physiological outcomes[137].

1.10.2 Methods to detect hydrogen sulfide

Due to the widespread interest in its biological functions, detection methods for sulfide have evolved from simple colorimetric assays to the more recently used techniques, including high-pressure liquid chromatography (HPLC) and gas chromatography (GC)[61,143,144], monobromobimane (MBB)[145–148], methylene blue method[149,150], fluorescence probes[151], and electrochemical sensors (ion-sensitive electrodes and polarographic H_2S sensors)[152,153].

The best method for H_2S measurement has caused considerable controversy. H_2S exists in various chemical forms: free (hydro- sulphide anion, HS), acid-labile (bound to the sulfur-iron clusters of proteins), bound sulfane sulfur (bound to proteins, i.e. poly- sulfides, persulfides, etc.). Total H_2S refers to all these forms together. Certainly, each technique has its advantages and limitations. An ideal method for the detection should be able to distinguish between free and bound labile sulfides.

Total H_2S levels can be measured with different methods, as mentioned, among which the most commonly used is the monobromobimane method with spectrophotometric detection, recently fluorescent probes gained attention. Chromatography based methods, which have been used to measure both plasma and tissue H_2S sensitivity, however, do not have the capability of real-time measuring in biological samples and require hypoxic or anoxic conditions[144,145,154]. In a typical MBB assay, H_2S reacts with two molecules of monobromobimane to form the fluorescent sulfide-dibimane, followed by HPLC assay with fluorescence detection. This method requires relatively expensive equipment, and its time-consuming process results in unknown reactions in blood samples, thus interfering in the detection of sulfide and making real-time measurements of H_2S impossible[145–148].

The methylene-blue method is one of the most commonly used spectrometric methods for measuring plasma H_2S, which involves the reaction of H_2S with N,N-dimethyl-p-phenylenediamine sulfate to produce the light-absorbing methylene blue. However, this method allows quantifying free H_2S, although, due to acidic sample pre-treatment, acid-labile sulfide can be also freed to some extent, thus possibly and unpredictably decreasing overall accuracy[155].

Some other spectroscopic methods offer high sensitivity and selectivity for H_2S. For example, it is noteworthy that the most recently developed sulfide-sensitive fluorescent probes enable H_2S measurement in cell and blood samples at low concentrations[147,151,156]. Compared with traditional methods, the detection of reactive sulfur species via fluorescence can lower the external influence on the endogenous species distribution, can reduce the time of sample preparation, and can achieve real-time detection[151].

Electrochemical sensors have several advantages including high sensitivity, high selectivity, low detection limit, fast response time, repeatability[157]. However, electrochemical sensors have several limitations that make them a pointless method to measure reliable free sulfide due to their high sensitivity to temperature, light, interference from other gases or the use of strong alkaline antioxidant buffers, resulting in sulfide release from other biological sources such as cysteine or small molecular weight thiols[155,158]. Ion-sensitive electrodes (ISEs) and amperometric (polarographic) H_2S sensors are two well-known devices that have been applied to detect H_2S concentration in biological samples.

Sulfide-specific ion-selective electrodes (ISEs), utilizing a micro-electrode that measure the ion S^{2-} directly have also been used on biological samples, but results provided by this method may be inaccurate, and/or difficult to interpret. Formation of S^{2-} requires mixing the sample with a strong alkaline solution (pH>11), generally referred to as the “antioxidant buffer,” to drive the equilibrium between H_2S, HS^-, and S^{2-} to favor S^{2-}. These alkaline conditions appear to promote hydroxyl replacement of cysteine sulfur from the bound sulfane sulfur and acid-labile sulfur thereby producing erroneously high sulfide concentrations that continue to increase with time[155,158].

The polarographic electrode directly measures the concentration of dissolved H_2S gas in real-time[158]. Because this method only measures H_2S gas, total sulfide must be calculated from concomitant pH measurements. Polarographic electrodes also consume sulfide, albeit slowly. However, this can become problematic when measurements are made in a small volume in which there is an increased probability of lowering the total sulfide concentration, or in unstirred

conditions in which electrode consumption can reduce sulfide concentration in the immediate area surrounding the tip of the electrode. Amperometric electrodes are generally pressure and temperature-sensitive and prone to drift, necessitating frequent calibration[155].

1.10.3 Methods to detect protein persulfidation

Having a selective method for persulfide detection is of most importance in order to fully understand the physiological and pathophysiological role of H_2S. Several methods have been proposed for the detection of protein persulfidation, all of which are detailed below.

1.10.3.1 Modified Biotin-Switch Method

This method was a modification of the method originally used for the detection of protein S-nitrosation in proteins, known as the biotin switch assay[159]. Protein persulfides were postulated to remain unreacted after the blocking of thiols with S-methyl methanethiosulfonate (MMTS)[53]. Hence after the excess MMTS is removed, the free persulfides can be labeled with the use of biotin-HPDP, as shown in **Figure 6**.

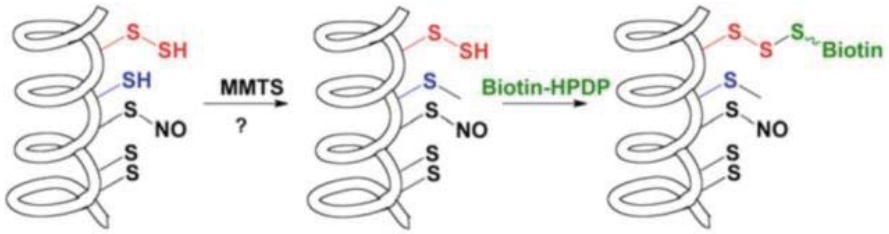

Figure 6. Diagram of modified Biotin Switch Assay. This method is a modification of Jaffrey et al. "Biotin Switch" method. First, free -SH groups are blocked with S-methyl methanethiosulfonate (MMTS), without affecting protein persulfides. Then, persulfides are labeled with biotin-HPDP. *Figure taken and adapted from Kouroussis E. (2019)*[160].

1.10.3.2 Cy5-Maleimide Labelling

Cy5-labeled maleimide was used as a thiol-blocking reagent, to block both the persulfides and free thiol of tested protein sample. The product of Cy5-maleimide and persulfide is actually a disulfide that can be cleaved by dithiothreitol (DTT). The samples were then treated with DTT and the decrease of in-gel fluorescent signal was monitored as a readout for the persulfide levels (**Figure 7**).

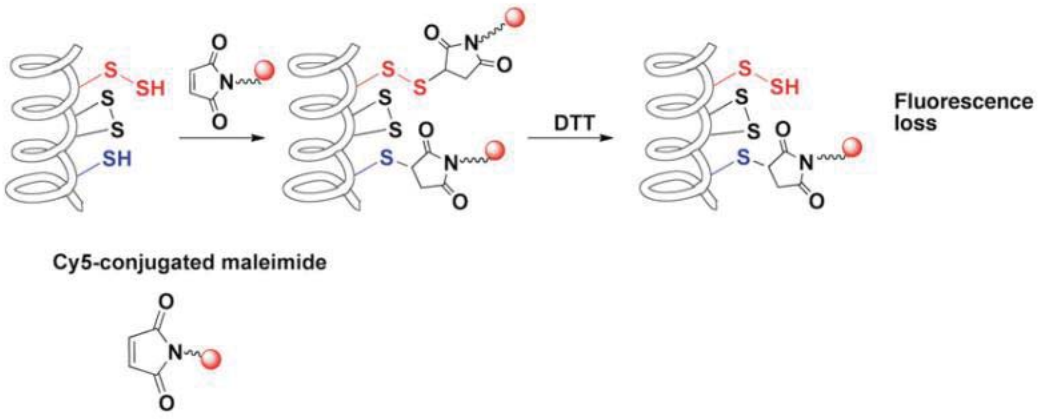

Figure 7. Diagram of Cy5-conjugated maleimide method. Cyanine5 maleimide is a mono-reactive dye which selectively couples with thiol groups (persulfidated proteins and free thiols) to give labeled conjugates. DTT, then cleaves the bound between Cy5-conjugated maleimide with protein persulfides, resulting in a decrease of fluorescence signal, proportional to sample persulfides. *Figure taken and adapted from Kouroussis E. (2019)*[160].

1.10.3.3 Tag-Switch Method

Using the first described method, the modified biotin switch assay, a large number of persulfidated proteins were identified in animal and plant systems[53,161]. Nevertheless, the specificity of the blocking reagent S-methyl-methanothiosulfonate (MMTS) has been questioned by several authors. Thus, a new approach to detect persulfidated proteins was recently described, the tag-switch method[162]. This method employs methylsulfonylbenzothiazole (MSBT) to block both thiols and persulfide groups in the first step; then, the disulfide bonds in persulfide adducts possess enhanced reactivity to nucleophilic attack by the cyanoacetate-based reagent derivates (such as CN-biotin, CN-BOT or CN-Cy3), while thiol adducts are thioethers that do not react with nucleophiles (**Figure 8)**. To identify and quantify presulfidated proteins, persulfidated proteins

tagged with cyanoacetate-biotin are purified with streptavidin-beads and analyzed by liquid chromatography-mass spectrometry (LC-MS).

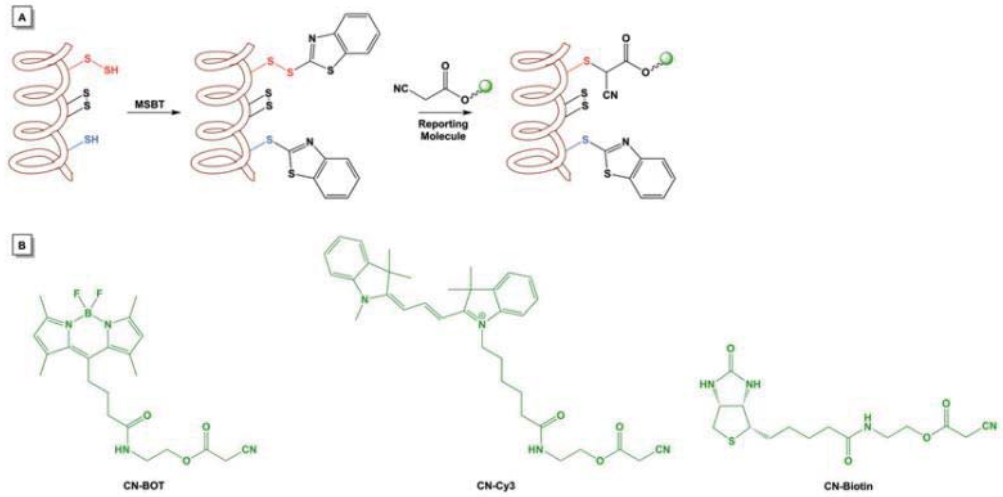

Figure 8. Diagram of the tag-switch method. This method employs methylsulfonylbenzothiazole (MSBT) to block both thiols and persulfide groups in the first step. Then, the disulfide bonds in persulfide adducts possess enhanced reactivity to nucleophilic attack by the reporting molecule (such as cyanoacetate-based reagent CN-biotin, Cy3-dye (CN-Cy3) and CN-BOT) while thiol adducts do not react with the reporting molecule.

Despite all this knowledge, many things about the regulatory mechanisms of H_2S on physiological roles in human adipose tissue have not been investigated. We here report the first observations, to our knowledge, linking H_2S to the physiology of human adipose tissue.

2. HYPOTHESIS

This thesis examines H_2S in obesity and its possible role in adipose tissue physiology.

Taking into account the H_2S physiological properties and previous studies in mice[102,103] and humans without morbidly obesity[101], we hypothesize that hydrogen sulfide is altered in obesity, and impacts on adipogenesis and human adipose tissue physiology modulating inflammation and insulin action.

3. OBJECTIVES

To test this hypothesis, we aimed:

1. To evaluate circulating H_2S in humans according to obesity.

2. To evaluate the role of H_2S on 3T3-L1 adipocyte differentiation and inflammation.

3. To evaluate the importance of CBS in ASC52telo cells.

4. To evaluate the role of H_2S-synthesizing enzymes and H_2S in human preadipocytes, adipocytes and in adipose tissue physiology according to insulin sensitivity.

5. To determine the protein persulfidation profile associated with adipogenesis in preadipocytes and human differentiated adipocytes.

4. MANUSCRIPTS

MANUSCRIPT 1

Ferran Comas, Jèssica Latorre, Francisco Ortega, María Arnoriaga Rodríguez, Aina Lluch, Mònica Sabater, Ferran Rius, Xavier Ribas, Miquel Costas, Wifredo Ricart, Albert Lecube, José Manuel Fernández-Real, José María Moreno-Navarrete. **Morbidly obese subjects show increased serum hydrogen sulfide in proportion to fat mass.** *Int J Obes (London).* 2020 Oct; doi: 10.1038/s41366-020-00696-z.

Impact factor (2019): 4.419 (Q1, Nutrition & Dietetics)

International Journal of Obesity
https://doi.org/10.1038/s41366-020-00696-z

ARTICLE

Clinical research

Morbidly obese subjects show increased serum sulfide in proportion to fat mass

Ferran Comas[1] · Jèssica Latorre[1] · Francisco Ortega[1] · María Arnoriaga Rodríguez[1] · Aina Lluch[1] · Mònica Sabater[1] · Ferran Rius[2] · Xavier Ribas[3] · Miquel Costas[3] · Wifredo Ricart[1,4] · Albert Lecube[2] · José Manuel Fernández-Real[1,4] · José María Moreno-Navarrete[1,4]

Received: 23 April 2020 / Revised: 8 September 2020 / Accepted: 26 September 2020

Abstract

Background and objectives The importance of hydrogen sulfide is increasingly recognized in the pathophysiology of obesity and type 2 diabetes in animal models. Very few studies have evaluated circulating sulfides in humans, with discrepant results. Here, we aimed to investigate serum sulfide levels according to obesity.

Subjects and methods Serum sulfide levels were analyzed, using a selective fluorescent probe, in two independent cohorts [cross-sectionally in discovery ($n = 139$) and validation ($n = 71$) cohorts, and longitudinally in 82 participants from discovery cohort]. In the validation cohort, blood gene expression of enzymes contributing to H_2S generation and consumption were also measured.

Results In the discovery cohort, serum sulfide concentration was significantly increased in subjects with morbid obesity at baseline and follow-up, and positively correlated with BMI and fat mass, but negatively with total cholesterol, haemoglobin, serum ferritin, iron and bilirubin after adjusting by age, gender and fat mass. Fat mass ($\beta = 0.51$, $t = 3.67$, $p < 0.0001$) contributed independently to age-, gender-, insulin sensitivity- and BMI-adjusted serum sulfide concentration variance. Importantly, receiver operating characteristic analysis demonstrated the relevance of fat mass predicting serum sulfide levels, which was replicated in the validation cohort. In addition, serum sulfide concentration was decreased in morbidly obese subjects with impaired compared to those with normal fasting glucose. Longitudinally, weight gain resulted in increased serum sulfide concentration, whereas weight loss had opposite effects, being the percent change in serum sulfide positively correlated with the percent change in BMI and waist circumference, but negatively with bilirubin. Whole blood *CBS, CTH, MPST, SQOR, TST* and *MPO* gene expression was not associated to obesity or serum sulfide concentration.

Conclusions Altogether these data indicated that serum sulfide concentrations were increased in subjects with morbid obesity in proportion to fat mass and inversely associated with circulating markers of haem degradation.

Introduction

Hydrogen sulfide has emerged as an important factor in diverse physiological and pathophysiological processes, such as neurodegeneration, regulation of inflammation and blood pressure and metabolism [1]. A variety of diseases, such as cancer, diabetes and metabolic disorders, are associated with altered endogenous levels of H_2S [2]. H_2S is endogenously generated from cysteine by pyridoxal-5′-phosphate-dependent enzymes, cystathionine β-synthase

✉ José Manuel Fernández-Real
jmfreal@idibgi.org

✉ José María Moreno-Navarrete
jmoreno@idibgi.org

[1] Department of Diabetes, Endocrinology and Nutrition, Institut d'Investigació Biomèdica de Girona (IdIBGi), CIBEROBN (CB06/03/010) and Instituto de Salud Carlos III (ISCIII), Girona, Spain

[2] Endocrinology and Nutrition Department, University Hospital Arnau de Vilanova, Obesity, Diabetes and Metabolism (ODIM) research group, IRBLleida, University of Lleida, Lleida, Spain

[3] Grup de Química Bioinspirada, Supramolecular i Catàlisi (QBIS-CAT), Institut de Química Computacional i Catàlisi (IQCC), Departament de Química, Universitat de Girona, C/M. Aurèlia Capmany 69, 17003 Girona, Spain

[4] Department of Medicine, Universitat de Girona, Girona, Spain

Published online: 10 October 2020

(CBS) and cystathionine γ-lyase (CTH or CSE), through the transsulfuration pathway [3], but also 3-mercaptopyruvate sulfurtransferase (MPST) activity has been described as a source of H_2S [4]. In addition, the major H_2S-metabolizing enzyme sulfide quinone oxidoreductase (SQOR) [5], and other enzymes such as thiosulfate sulfurtransferase (TST) and myeloperoxidase (MPO) also modulate H_2S levels by increasing H_2S consumption and oxidation [6, 7].

There is emerging evidence supporting the importance of H_2S in the pathophysiology of obesity and type 2 diabetes [8]. Exogenous H_2S administration led to increased insulin sensitivity and improved glucose tolerance after a high-fat diet-fed in mice in parallel to weight gain [9, 10]. Supplementation with H_2S donors or increasing endogenous H_2S biosynthesis was sufficient to stimulate fat mass accumulation in mice and fruit flies, whereas depletion of endogenous H_2S biosynthesis prevented HFD-induced increase in fat mass [9, 11].

In humans, the role of circulating sulfide has been scarcely investigated. Plasma sulfide levels were found to be significantly decreased in non-obese individuals with type 2 diabetes and in overweight participants with altered glucose tolerance [8, 12]. However, to the best of our knowledge, serum sulfide levels have not been previously investigated in subjects with obesity. Here, we aimed to investigate (cross-sectionally and longitudinally) serum sulfide in morbidly obese subjects in two independent cohorts. In addition, expression of H_2S-synthesising (CTH, CBS and MPST) and H_2S-removing (SQOR, TST and MPO) enzymes in whole blood according to obesity status was also analyzed.

Materials/Subjects and methods

Participants recruitment

Discovery cohort

From January 2016 to October 2017, a cross-sectional case-control study was undertaken in the Endocrinology Department of Josep Trueta University Hospital. We included 139 consecutive subjects, 85 obese (BMI ≥ 30 kg/m^2) participants and 54 non-obese (BMI < 30 kg/m^2) similar in age (age range of 28–66 years) and sex distribution. Furthermore, 16 morbidly obese participants were recruited at Arnau de Vilanova University Hospital. Normal fasting glucose (NFG) was defined according to ADA recommendations [13], with fasting glucose < 100 mg/dl), and impaired fasting glucose (IFG), with fasting glucose between 100 and 126 mg/dl).

Longitudinal changes in discovery cohort

To evaluate longitudinally the relationship between serum sulfide and metabolic parameters, 82 participants (29 non-obese and 53 obese) were followed during 1 year. After the initial assessment, obese patients were instructed to reduce their daily caloric intake between 500 and 800 kcal. A hypocaloric diet containing 20–25 kcal/kg and composed by 30% fat (10% saturated fat), 15% protein, 20–25 g dietary fibre and 55% carbohydrates was recommended. The subjects were followed every 4 months to monitor dietary compliance. In addition, 22 of 53 obese participants underwent bariatric surgery via Roux-en-Y gastric bypass. Exclusion criteria were: type 2 diabetes mellitus, chronic inflammatory systemic diseases, acute or chronic infections in the previous month, severe disorders of eating behaviour or major psychiatric antecedents; neurological diseases, history of trauma or injured brain, language disorders and excessive alcohol intake (≥40 g OH/day in women or 80 g OH/day in men).

The institutional review board—Ethics Committee for Clinical Research (CEIC) of Dr. Josep Trueta University Hospital (Girona, Spain) and Arnau de Vilanova University Hospital (Lleida, Spain)—approved the study protocol and informed written consent was obtained from all participants.

Validation cohort

This cohort includes 71 (18 non-obese and 53 obese) non-diabetic participants of Caucasian origin recruited at the Endocrinology Service of the Hospital Universitari Dr. Josep Trueta (Girona, Spain). Exclusion criteria were type 2 diabetes, clinically significant hepatic, neurological or other major systemic disease, including malignancy, infection in the previous month, an elevated serum creatinine concentration, acute major cardiovascular event in the previous 6 months, acute illnesses and current evidence of high grade chronic inflammatory or infective diseases, serious chronic illness, >20 g ethanol intake/day or use of medications that might interfere with insulin action. Liver and thyroid dysfunction were specifically excluded by biochemical work-up. Samples and data from patients included in this study were provided by the FATBANK platform promoted by the CIBEROBN and coordinated by the IDIBGI Biobank (Biobanc IDIBGI, B.0000872), integrated in the Spanish National Biobanks' Network and they were processed following standard operating procedures with the appropriate approval of the Ethics, External Scientific and FATBANK Internal Scientific Committees. To ensure blinding in outcome analyses, all samples were codified.

Anthropometric measurements and analytical methods

BMI was calculated as the weight in kilograms divided by height in metres squared. The waists of participants were measured with a soft tape midway between the lowest rib

and the iliac crest, and hip circumference was measured at the widest part of the gluteal region. Body composition was assessed using a dual energy x-ray absorptiometry (GE lunar, Madison, Wisconsin). Serum glucose concentrations were measured in duplicate by the glucose oxidase method using a Beckman glucose analyzer II (Beckman Instruments, Brea, California). Glycated haemoglobin (HbA1c) was measured by the high-performance liquid chromatography method (Bio-Rad, Muenchen, Germany, and autoanalyser Jokoh HS-10, respectively). Serum insulin was measured by Human Insulin ELISA kit (RIS006R, Biovendor—Laboratorni medicina, a.s., Brno, Czech Republic) with intra- and inter-assay coefficient of variation < 7% and <10%, respectively. Insulin resistance was estimated by using the formula of the homoeostatic model assessment of insulin resistance (HOMA-IR) as: (Fasting glucose (mg/dl) × fasting insulin (μIU/ml))/405) [14]. HDL cholesterol was quantified following precipitation with polyethylene glycol at room temperature. The Friedewald formula was used to calculate the concentration of LDL cholesterol. Total serum triglycerides were measured through the reaction of glycerol-phosphate-oxidase and peroxidase on a Hitachi 917 instrument (Roche, Mannheim, Germany). C-reactive protein (ultrasensitive assay; 110 Beckman, Fullerton, CA), total bilirubin, haemoglobin, ferritin and iron were determined by a routine laboratory test.

Hyperinsulinemic-euglycemic venous clamp

Insulin action was determined by hyperinsulinemic-euglycemic clamp. After an overnight fast, two catheters were inserted into an antecubital vein, one for each arm, used to administer constant infusions of glucose and insulin and to obtain arterialized venous blood samples. A 2-h hyperinsulinemic-euglycemic clamp was initiated by a two-step primed infusion of insulin (80 mU/m^2/min for 5 min, 60 mU/m^2/min for 5 min) immediately followed by a continuous infusion of insulin at a rate of 40 mU/m^2/min (regular insulin [Actrapid; Novo Nordisk, Plainsboro, NJ]). Glucose infusion began at minute 4 at an initial perfusion rate of 2 mg/kg/min being then adjusted to maintain plasma glucose concentration at 88.3–99.1 mg/dl. Blood samples were collected every 5 min for determination of plasma glucose and insulin. Insulin sensitivity was assessed as the mean glucose infusion rate during the last 40 min. In the stationary equilibrium, the amount of glucose administered (M) equals the glucose taken by the body tissues and is a measure of overall insulin sensitivity.

Fluorescence probe sulfide quantification

To measure blood sulfide levels, avoiding the possible interference of some anticoagulants such as EDTA, required to obtain plasma samples, we only used serum samples. Blood samples were collected and transferred in a BD Vacutainer tube with clot activator and separating gel (Ref: 366468, BD, Plymouth, UK), and centrifuged at 1600 × g during 15 min at 4 °C to obtain serum, which was stored at −80 °C in 0.5 ml aliquots of sterile air tight vials (Ref: 72.694.005 Sarstedt Inc Nümbrecht, Germany) to avoid repeated freeze/thawing cycles, and thawed only once before sulfide measurement. The stability of sulfide in serum samples was previously reported [15]. This study demonstrated that one freeze/thawing cycle had no significant effect on measured sulfide levels in comparison with freshly withdrawn serum samples [15]. Both baseline and follow-up samples were analyzed at the same time. Importantly, eight samples were reanalyzed 8 months later, and no significant differences in serum sulfide levels were found (9.63 ± 6.6 vs 11.11 ± 7.5, $p = 0.7$), indicating that storage of samples for long of a period did not impact on serum sulfide levels.

Sulfide concentration in serum was assessed using a naphthalimide-based fluorescent sensor 6-Azido-2-(2-(2-(2-hydroxyethoxy) ethoxy)ethyl)-1H-benzo[de]isoquinoline-1,3 (2H)-dione [L1 probe azido group (R-N3)], which was chemically synthesized in Institute of Computational Chemistry and Catalysis (Chemistry Department, University of Girona) as described previously [16]. To measure sulfide levels, serum and standard curve were incubated 70 min at 37 °C in the dark with 5 μmol/l of L1 probe. Standard curve was generated from a 10 mM stock solution of sodium sulfide (Na_2S) in phosphate buffered saline containing 5 μmol/l of L1 at various concentrations (0, 3.8, 7.8, 15.6, 31.25, 62.5, 125 and 250 μmol/l Na_2S). After incubation, fluorescence was read in a BioTek Cytation 5 reader at λ ex = 435 ± 20 and λ em = 550 ± 20 nm. Blank control of serum samples was performed in the same incubation conditions without L1 probe. Intra- and inter-assay coefficients of variation for these determinations were <9.7% and <10.5%, respectively. Serum sulfide levels are mentioned as L1-sulfide levels to specify the method used.

RNA expression

To preserve RNA, whole blood collected in PAXgene Blood RNA tubes (Qiagen, Hilden, Germany). Gene expression was assessed by real-time PCR using a LightCycler® 480 Real-Time PCR System (Roche Diagnostics SL, Barcelona, Spain), using TaqMan® technology suitable for relative genetic expression quantification. The commercially available and pre-validated TaqMan® primer/probe sets used were as follows: peptidylprolyl isomerase A (cyclophilin A) (4333763, PPIA as endogenous control), cystathionine γ-lyase (CTH, Hs00542284_m1),

Table 1 Serum L1-sulfide and anthropometric and clinical parameters according to obesity in cohort 1 at baseline, and bivariate correlations between serum L1-sulfide and these parameters.

	Non-obese	Obese	p^1	r	p^2
N	54	85			
Sex (men/women)	20/34	26/59			
Age (years)	47.8 ± 10.4	46.2 ± 10.1	0.4	−0.06	0.4
BMI (kg/m^2)	24.9 ± 2.8	43.9 ± 6.9	**<0.0001**	0.40	**<0.0001**
Waist circumference (cm)	90.2 ± 10.2	127.7 ± 15.9	**<0.0001**	0.37	**<0.0001**
Fat mass (%)	31.9 ± 8.1	49.9 ± 5.3	**<0.0001**	0.54	**<0.0001**
Fasting glucose (mg/dl)	94.3 ± 12.5	95.6 ± 10.9	0.5	0.01	0.9
Fasting insulin (µIU/ml)	9.6 ± 5.5	26.7 ± 11.1	**<0.0001**	0.36	**<0.0001**
HOMA-IR	2.29 ± 1.4	6.28 ± 2.7	**<0.0001**	0.37	**<0.0001**
HbA1c (%)	5.4 ± 0.2	5.6 ± 0.3	**0.009**	0.16	0.05
M (mg/(kg × min))	10.4 ± 3.4	4.3 ± 2.6	**<0.0001**	−0.34	**<0.0001**
Total cholesterol (mg/dl)	200.3 ± 41.1	187.4 ± 37.1	0.06	−0.20	**0.02**
HDL cholesterol (mg/dl)	65.5 ± 18.2	50.3 ± 11.8	**<0.0001**	−0.21	**0.02**
LDL cholesterol (mg/dl)	121.4 ± 33.6	116.6 ± 38.7	0.5	−0.17	0.05
Triglycerides (mg/dl)[a]	75.5 (57.7–97)	111 (78.5–139.5)	**<0.0001**	0.11	0.2
hsCRP (mg/dl)[a]	0.65 (0.39–1.71)	5.41 (2.97–9.22)	**<0.0001**	0.45	**<0.0001**
Haemoglobin (g/dl)	13.8 ± 1.2	13.9 ± 1.5	0.7	−0.26	**0.002**
Serum iron (µg/dl)	92.9 ± 32.8	75.8 ± 25.4	**0.001**	−0.37	**<0.0001**
Serum ferritin (ng/ml)[a]	91.5 (38.2–198.1)	91.2 (40.5–190.5)	0.8	−0.29	**<0.0001**
Total bilirubin (mg/dl)	0.54 ± 0.25	0.43 ± 0.21	**0.01**	−0.37	**<0.0001**
Serum L1-sulfide (µmol/l)	5.67 ± 3.3	10.08 ± 4.5	**<0.0001**	–	–

p^1: p value from unpaired t-test, p^2: p value from Spearman's correlation and r was the coefficient of correlation. Bold values mean that p value reached statistical significance.

[a]Median and interquartile range.

CBS (Hs00163925_m1) and MPST (Hs05579360_s1), SQOR (SQOR or SQRDL, Hs01126963_m1), TST (Hs00361812_m1) and MPO (Hs00165162_m1).

Statistical analyses

Statistical analyses were performed using SPSS 12.0 software. Unless otherwise stated, descriptive results of continuous variables are expressed as mean and SD for Gaussian variables or median and interquartile range. Unpaired t-test was used to compare circulating sulfide concentration according to obesity. Student's paired two-sample t test was used to compare anthropometric parameters and serum sulfide concentrations in longitudinal study. The correlation between variables was analyzed by simple correlation (Spearman's test) and multivariate regression analysis. Receiver operating characteristic (ROC) analysis was conducted to determine the ability of fat mass to discriminate between patients with increased and decreased serum sulfide levels. Area under the curve and 95% confidence interval were determined. Levels of statistical significance were set at $p < 0.05$.

Results

Serum L1-sulfide levels were associated to obesity and fat mass

Discovery cohort

Serum L1-sulfide concentration was significantly increased in morbid obesity (Table 1, Fig. 1a), and positively correlated with BMI, waist circumference, fat mass (Fig. 1b), fasting insulin, HOMA-IR and hsCRP, but negatively with insulin sensitivity, total and HDL cholesterol, haemoglobin, serum ferritin, iron and total bilirubin (Table 1). Multivariate regression analysis revealed that fat mass ($\beta = 0.51$, $t = 3.67$, $p < 0.0001$) contributed independently to age-, gender-, insulin sensitivity- and BMI-adjusted serum L1-sulfide concentration variance. Of note, additional analysis revealed that circulating iron-related parameters [iron ($\beta = -0.23$, $t = -2.84$, $p = 0.005$), haemoglobin ($\beta = -0.22$, $t = -2.35$, $p = 0.02$), ferritin ($\beta = -0.21$, $t = -2.28$, $p = 0.02$)], total bilirubin ($\beta = -0.31$, $t = -4.01$, $p < 0.0001$) and total cholesterol ($\beta = -0.18$, $t = -2.26$, $p = 0.02$), but not fasting insulin

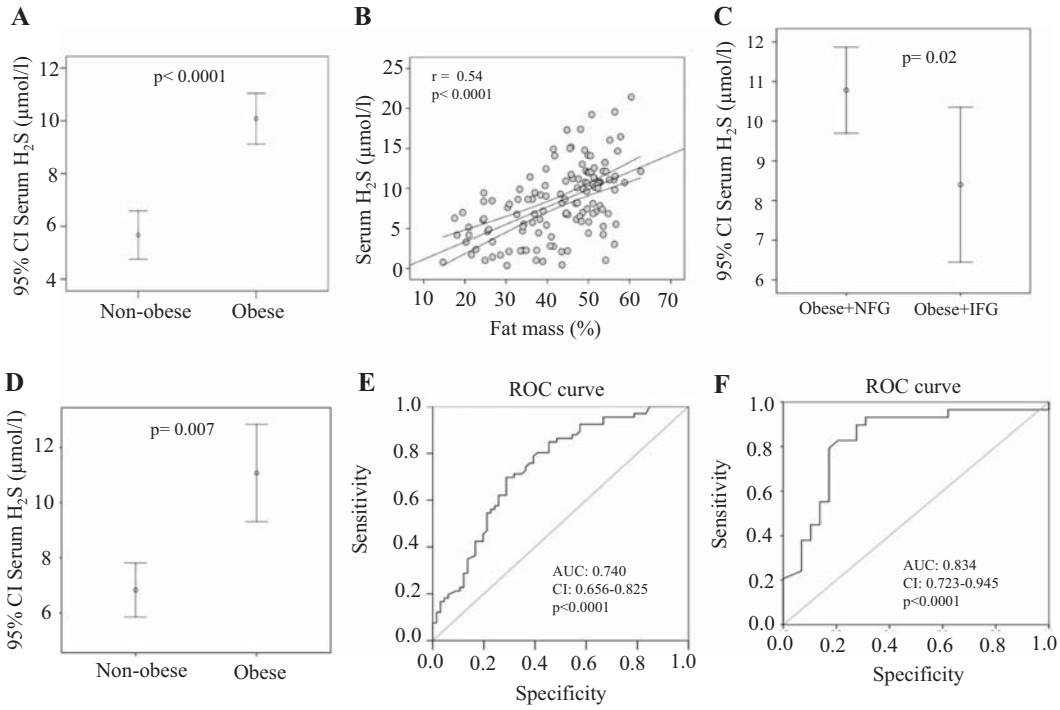

Fig. 1 Serum sulfide in association with obesity, fat mass and fasting glucose in cohort 1. a Serum sulfide concentration according to obesity at baseline. **b** Bivariate correlation between serum sulfide concentration and fat mass at baseline. **c** Serum sulfide concentration in obese participants according to fasting glucose at baseline. **d** Serum sulfide concentration according to obesity at follow-up. Receiver operating characteristic (ROC) curve for fat mass in the prediction of sulfide levels at baseline (**e**) and at follow-up (**f**).

($\beta = 0.09$, $t = 0.86$, $p = 0.4$), HOMA-IR ($\beta = 0.07$, $t = 0.66$, $p = 0.5$), insulin sensitivity ($\beta = -0.13$, $t = -1.18$, $p = 0.2$), hsCRP ($\beta = 0.08$, $t = 0.87$, $p = 0.4$) and HDL cholesterol ($\beta = -0.09$, $t = -1.06$, $p = 0.3$), contributed to age-, gender- and fat mass-adjusted serum L1-sulfide concentration variance.

Interestingly, serum L1-sulfide concentration was decreased in morbidly obese subjects with impaired (IFG) compared to those with normal (NFG) fasting glucose (Fig. 1c) similar to insulin sensitivity (3.44 ± 2.1 vs 4.73 ± 2.7, $p = 0.04$), and contrary to HOMA-IR (7.31 ± 3.4 vs 5.92 ± 2.3, $p = 0.06$).

At follow-up, serum L1-sulfide levels were still increased in participants with morbid obesity (Fig. 1d), and positively correlated with BMI, waist circumference, fat mass (Table 2), strengthening the association between serum L1-sulfide levels and obesity. In addition, the correlations between serum L1-sulfide and hsCRP, fasting insulin, insulin sensitivity, total cholesterol, haemoglobin, serum ferritin, iron and total bilirubin were replicated at follow-up (Table 2). In multivariate regression analysis, fat mass ($\beta = 0.49$, $t = 2.90$, $p = 0.005$) contributed independently to age-, gender-, insulin sensitivity- and BMI-adjusted serum L1-sulfide concentration variance. Circulating iron-related parameters [iron ($\beta = -0.28$, $t = -2.48$, $p = 0.01$), haemoglobin ($\beta = -0.32$, $t = -2.51$, $p = 0.01$), ferritin ($\beta = -0.26$, $t = -2.05$, $p = 0.04$)], total bilirubin ($\beta = -0.45$, $t = -4.72$, $p < 0.0001$), hsCRP ($\beta = 0.35$, $t = 3.03$, $p = 0.003$), total cholesterol ($\beta = -0.32$, $t = -2.82$, $p = 0.006$) and LDL cholesterol ($\beta = -0.29$, $t = -2.72$, $p = 0.008$), but not fasting insulin ($\beta = 0.05$, $t = 0.37$, $p = 0.7$) or insulin sensitivity ($\beta = -0.11$, $t = -0.77$, $p = 0.4$), contributed to age-, gender- and fat mass-adjusted serum L1-sulfide concentration variance.

Importantly, the area under the curve for fat mass to predict L1-sulfide levels was 0.740 (0.656–0.825) at baseline and 0.834 (0.723–0.0.945) at follow-up (both with $p < 0.0001$) (Fig. 1e, f).

Next, longitudinal changes in anthropometric, clinical parameters and serum L1-sulfide concentration were analyzed comparing baseline and follow-up data. In non-obese participants, no significant changes in obesity measures, metabolic parameters (except for fasting triglycerides, fasting insulin and HOMA-IR) and serum L1-sulfide concentration were observed (Table 3). In obese participants, we found that weight gain resulted in increased serum L1-sulfide concentration, whereas weight loss had opposite effects (Table 3). In fact, the percent change in L1-sulfide was positively correlated with the percent change in BMI ($r = 0.33$, $p = 0.003$), waist circumference ($r = 0.42$,

Table 2 Serum L1-sulfide and anthropometric and clinical parameters according to obesity in cohort 1 at follow-up, and bivariate correlations between serum L1-sulfide and these parameters.

	Non-obese	Obese	p^1	r	p^2
N	42	40			
Sex (men/women)	17/25	14/26			
Age (years)	48.1 ± 10.4	46.3 ± 10.6	0.4	−0.04	0.7
BMI (kg/m^2)	25.5 ± 2.7	39.7 ± 8.1	**<0.0001**	0.35	**0.001**
Waist circumference (cm)	89.3 ± 9.6	117.7 ± 17.5	**<0.0001**	0.42	**<0.0001**
Fat mass (%)	31.5 ± 7.7	46.6 ± 7.3	**<0.0001**	0.59	**<0.0001**
Fasting glucose (mg/dl)	92.9 ± 20.4	101.1 ± 7.8	**0.04**	0.06	0.6
Fasting insulin (μIU/ml)	11.8 ± 5.1	20.9 ± 9.9	**<0.0001**	0.24	**0.03**
HOMA-IR	2.71 ± 1.3	5.24 ± 2.7	**<0.0001**	0.19	0.07
HbA1c (%)	5.5 ± 0.7	5.6 ± 0.4	0.8	0.01	0.9
M (mg/(kg × min))	9.46 ± 2.7	4.07 ± 2.4	**<0.0001**	−0.42	**<0.0001**
Total cholesterol (mg/dl)	193.4 ± 35.7	178.4 ± 39.7	0.08	−0.32	**0.005**
HDL cholesterol (mg/dl)	59.1 ± 12.5	53.6 ± 12.7	0.06	−0.10	0.4
LDL cholesterol (mg/dl)	116.8 ± 28.5	104.6 ± 34.3	0.09	−0.34	**0.002**
Triglycerides (mg/dl)[a]	74 (64–98.2)	97.5 (70.5–132)	0.07	−0.04	0.7
hsCRP (mg/dl)[a]	1.16 (0.37–2.76)	2.97 (1.91–6.16)	**0.006**	0.37	**0.001**
Haemoglobin (g/dl)	13.81 ± 1.2	13.86 ± 1.3	0.9	−0.36	**0.001**
Serum iron (μg/dl)	87.2 ± 25.1	77.9 ± 31.2	0.1	−0.35	**0.001**
Serum ferritin (ng/ml)[a]	90 (33–170)	61 (22.7–139)	0.1	−0.37	**<0.0001**
Total bilirubin (mg/dl)	0.51 ± 0.18	0.44 ± 0.22	0.1	−0.55	**<0.0001**
Serum L1-sulfide (μmol/l)	7.35 ± 3.3	10.31 ± 5.3	**0.007**	–	–

p^1: p value from unpaired t-test, p^2: p value from Spearman's correlation and r was the coefficient of correlation. Bold values mean that p value reached statistical significance.

[a]Median and interquartile range.

$p < 0.0001$), but negatively correlated with total bilirubin ($r = -0.28$, $p = 0.01$).

Validation cohort

To reinforce the relationship between serum L1-sulfide and obesity, a second independent cohort was examined. Data from this independent cohort confirmed the association between serum L1-sulfide and obesity, being significantly increased in obese subjects (Fig. 2a), positively correlated with BMI and fat mass and negatively correlated with serum iron and total bilirubin (Table 4). In this cohort, the area under the curve for fat mass to predict L1-sulfide levels was 0.706 (0.588–0.825) (Fig. 2b).

Expression of putative enzymes in whole blood that might modulate circulating L1-sulfide levels was not associated to obesity

Taking advantage of whole blood RNA samples availability in validation cohort, expression of putative enzymes in whole blood that might modulate circulating sulfide levels, including H_2S-synthesising (CTH, CBS and MPST) and H_2S-removing (SQOR, TST and MPO) gene expression, was analysed (Fig. 2c). Expression of these genes was not associated to obesity (BMI or fat mass) or serum L1-sulfide concentration (Tables 4 and 5). Expression of most of these enzymes was positively correlated among themselves (Table 5). *CBS* mRNA levels were positively correlated with *SQOR* and *TST*; *MPST* with *SQOR*, *TST* and *MPO*; *SQOR* with *TST* and *MPO*; and *TST* with *MPO* mRNA levels (Table 5). *CTH* mRNA levels were negatively correlated with haemoglobin, serum ferritin and iron, and *MPO* mRNA levels were positively correlated with fasting glucose, haemoglobin and serum ferritin (Table 5).

Discussion

The novel results of this study show increased serum L1-sulfide levels in subjects with morbid obesity in parallel to fat mass accumulation. Cross-sectionally in both discovery (at baseline and follow-up) and validation cohort, multivariate regression and ROC analysis demonstrated the relevance of fat mass predicting serum sulfide levels. Longitudinally, changes in BMI and waist circumference were correlated to changes in serum sulfide, resulting weight gain in increased and weight loss in reduced serum sulfide levels. Searching the possible source of serum sulfide, key enzymes in H_2S biosynthesis were investigated in

Table 3 Longitudinal changes in anthropometric, clinical parameters and serum L1-sulfide concentrations in cohort 1.

	Non-obese		Obese with weight gain		Obese with weight loss	
	Baseline	Follow-up	Baseline	Follow-up	Baseline	Follow-up
N	29		24		29	
Age (years)	50.0 ± 8.9	51.1 ± 8.9[c]	46.1 ± 10.1	47.3 ± 9.9[c]	41.5 ± 10.8	42.6 ± 10.8[c]
BMI (kg/m^2)	25.3 ± 2.5	25.5 ± 2.7	43.1 ± 6.8	44.7 ± 8.1[a]	43.9 ± 7.1	30.5 ± 6.1[c]
Waist circumference (cm)	90.1 ± 9.3	89.8 ± 9.2	125.3 ± 12.2	128.1 ± 14.4	127.3 ± 17.1	98.6 ± 15.8[c]
Fasting glucose (mg/dl)	97.1 ± 15.1	94.1 ± 21.4	96.2 ± 10.4	103.7 ± 7.1[b]	88.8 ± 10.1	91.1 ± 9.1
Fasting insulin (μIU/ml)	9.5 ± 5.4	11.5 ± 4.7[a]	23.7 ± 11.5	20.8 ± 9.3	25.9 ± 12.8	16.4 ± 10.6[c]
HOMA-IR	2.33 ± 1.6	2.86 ± 1.5[a]	6.35 ± 3.3	5.59 ± 2.5	6.31 ± 2.9	4.62 ± 3.1[a]
HbA1c (%)	5.46 ± 0.25	5.50 ± 0.26	5.62 ± 0.32	5.59 ± 0.28	5.63 ± 0.62	5.29 ± 0.34[a]
M (mg/(kg × min))	10.45 ± 2.4	9.53 ± 2.6	4.42 ± 2.2	3.68 ± 2.1	3.87 ± 1.5	6.14 ± 3.4[a]
Total cholesterol (mg/dl)	199.4 ± 39.3	206.4 ± 31.2	184.7 ± 46.5	181.4 ± 41.5	184.8 ± 30.2	166.7 ± 30.4[b]
HDL cholesterol (mg/dl)	62.9 ± 17.6	60.1 ± 14.1	53.2 ± 13.5	51.9 ± 12.6	46.8 ± 9.7	54.1 ± 9.5[b]
LDL cholesterol (mg/dl)	125.9 ± 28.1	126.9 ± 25.1	111.1 ± 38.1	107 ± 32.7	113.7 ± 28.8	95.6 ± 29.2[b]
Triglycerides (mg/dl)*	77.5 (59.5–92.2)	81 (73–108.5)[a]	95.5 (57.5–146.5)	104.5 (71.7–148.2)	107 (78–151)	73 (62.5–95.5)[b]
hsCRP (mg/dl)*	0.79 (0.45–1.76)	1.46 (0.58–2.76)	4.21 (2.43–7.40)	3.76 (2.42–10.19)	3.12 (2.17–15.85)	1.91 (0.48–3.09)[a]
Haemoglobin (g/dl)	13.83 ± 1.1	13.92 ± 1.1	13.93 ± 1.1	14.07 ± 1.4	13.81 ± 1.5	13.87 ± 1.3
Serum iron (μg/dl)	80.55 ± 21.3	92.14 ± 26.6	79.33 ± 23.1	80.67 ± 28.8	79.45 ± 31.4	77.58 ± 33.9
Serum ferritin (ng/ml)*	81.5 (37.7–179.5)	113 (33–178.5)	89 (38–159)	85 (38–166)	84 (30–204)	45 (17–138)[b]
Total bilirubin (mg/dl)	0.49 ± 0.21	0.52 ± 0.16	0.39 ± 0.14	0.37 ± 0.13	0.42 ± 0.14	0.48 ± 0.19
Serum L1-sulfide (μmol/l)	5.95 ± 3.5	6.47 ± 3.01	9.48 ± 4.2	11.95 ± 5.1[a]	10.15 ± 3.9	7.61 ± 4.3[b]

p value was obtained from paired *t*-test.

[a]$p < 0.05$, [b]$p < 0.01$ and [c]$p < 0.001$ compared to baseline parameters. *Median and interquartile range.

whole blood, being *MPST* gene the most expressed. Supporting this finding, a previous study proposed that blood H_2S levels were produced via MPST in red blood cells [17]. However, in the current study, no significant associations between expression of *MPST* (and the other enzymes, *CTH* or *CBS*) and obesity (BMI or fat mass) or serum sulfide levels were found, indicating that additional endogenous H_2S sources might contribute to serum sulfide levels. Otherwise, H_2S-metabolizing enzymes (*SQOR, TST* and *MPO*) mRNA levels were also not associated with obesity or correlated with serum L1-sulfide levels. Since mRNA is not always in proportion to protein levels, an important limitation of current study was the absence of protein data. Additional studies are required to investigate blood *CTH*, *CBS*, *MPST*, *SQOR*, *TST* and *MPO* protein amount and enzymatic activity according to obesity status.

Another consistent finding of current study was the negative association between L1-sulfide levels and circulating products of haem degradation, such as iron and bilirubin, suggesting a possible inhibitory activity of serum sulfide on haem degradation. Supporting this suggestion, Saravanan et al. reported that administration of S-allylcysteine, a sulfur containing amino acid, resulted in decreased iron, ferritin, bilirubin and haem oxygenase (a key enzyme in haem degradation) activity in diabetic rats [18]. Otherwise and also in line with current findings, increased haem oxygenase activity and carbon monoxide (CO, the third product of haem degradation) levels were associated with decreased H_2S levels [19]. Of note, this and other studies demonstrated that exogenous CO administration or increased endogenous CO levels reduced enzymatic H_2S production [19–21]. Current findings and these latter studies [18–21] suggest a bidirectional modulation between enzymatic H_2S production and haem degradation. The importance of haem biosynthesis on adipogenesis, adipocyte physiology [22, 23] and fat mass accretion [24] has been well substantiated. Together with current findings, it could be proposed that increased fat mass accretion and haem biosynthesis result in decreased circulating iron, bilirubin and CO levels. The consequence would be raised enzymatic H_2S biosynthesis and serum L1-sulfide levels. Strengthening this hypothesis, we found that total bilirubin and serum iron were decreased in obese participants. In line with these findings, other studies have reported a negative association between bilirubin and obesity status. In fact, increased bilirubin production attenuated fat mass accretion, weight

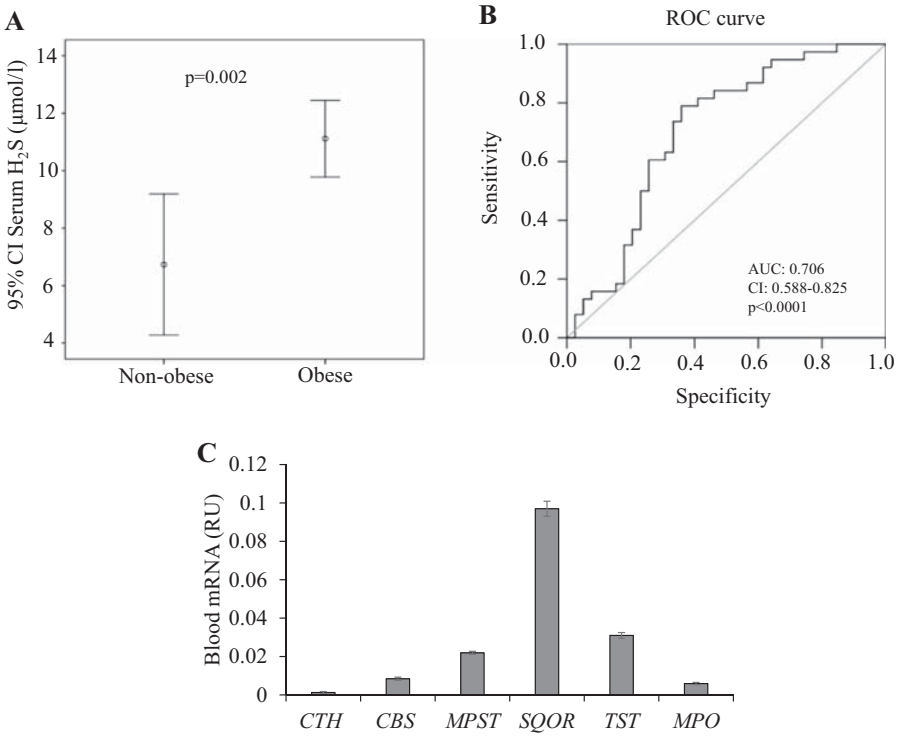

Fig. 2 Serum sulfide in association with obesity and fat mass in cohort 2. a Serum sulfide concentration according to obesity. **b** ROC curve for fat mass in the prediction of sulfide levels. **c** Blood *CTH*, *CBS*, *MPST*, *SQOR*, *TST* and *MPO* mRNA levels in participants from cohort 2.

gain and liver fat accumulation [25–29]. Decreased serum iron levels in obesity have also been reported [30].

Current data also indicated a negative association between serum L1-sulfide levels and total and LDL cholesterol. In line with these associations, Mani et al. reported that plasma total cholesterol and LDL cholesterol levels were significantly increased in CSE-KO compared to WT HFD-fed mice [31]. Interestingly, CSE-KO displayed decreased H_2S liver production, suggesting that H_2S was involved in liver cholesterol metabolism.

H_2S biosynthesis has been identified in a variety of mammalian tissues via enzymatic and non-enzymatic pathways, all contributing to the total amount of circulating H_2S [32, 33]. Previous studies demonstrated that CBS and CTH enzymes are secreted into the bloodstream by the liver and vascular endothelial cells, circulating as components of the plasma proteome and producing H_2S in human blood [34]. Supporting liver H_2S biosynthesis in obesity, mice fed with high-fat diet for 5 weeks displayed increased expression of *CBS* and *CTH* genes and H_2S production in the liver [35]. Against this argument, other studies demonstrated that liver H_2S production was attenuated in high-fat diet-induced obesity, but increased in conditions of dietary restriction [36, 37]. In addition, Norris et al. reported that liver might have an important role in the regulation of H_2S levels in the circulation, as a consequence of its location and enhanced capacity to clearance blood H_2S through H_2S oxidation [38]. Current data suggested that liver capacity to disposal of blood H_2S might be attenuated in obesity. However, further studies are required to examine in depth this suggestion.

Otherwise, adipose tissue, which is proportional to fat mass, also might be considered an additional H_2S source in obese subjects [11]. Yang et al. demonstrated that high-fat diet-induced fat mass accretion was associated with increased adipose tissue H_2S biosynthesis in mice and fruit flies [11]. However, the relative contribution of adipose tissue to serum sulfide levels has not been previously investigated and needs to be confirmed in further studies.

In contrast to enzymatic synthesis pathways, endogenous production of H_2S through non-enzymatic processes in mammalian tissues is not well understood or characterized. Yang et al. reported that apart from the liver and kidney, where the production of H_2S was mainly through the CTH enzyme, H_2S was non-enzymatically produced by iron and vitamin B6, and using cysteine as a substrate in other organs and at circulatory level [39]. However, taking into account the negative correlation between L1-sulfide and circulating iron-related parameters, this mechanism might be discarded.

It is important to note that increased levels of plasma cysteine predispose to obesity and its associated metabolic disturbances [40, 41]. Even though L1 probe azido group (R-N3) has been shown to be around 20–50 times more selective to H_2S, when compared to other thiols such as cysteine and glutathione [12], the higher amount of these interfering thiols in serum [42] might increase L1

Table 4 Anthropometric and clinical parameters, serum L1-sulfide and whole blood *CTH, CBS, MPST, SQOR, TST* and *MPO* mRNA levels according to obesity and bivariate correlations between serum L1-sulfide and anthropometric and clinical characteristics and mRNA levels in cohort 2.

	Non-obese	Obese	p^1	r	p^2
N	18	53			
Sex (men/women)	7/11	13/40			
Age (years)	49.4 ± 12.4	46.4 ± 9.5	0.3	0.05	0.7
BMI (kg/m^2)	23.8 ± 2.9	44.5 ± 7.6	**<0.0001**	0.24	**0.02**
Waist circumference (cm)	80.8 ± 12.4	122.8 ± 21.8	**<0.0001**	0.17	0.2
Fat mass (%)	27.1 ± 12.1	48.4 ± 5.1	**<0.0001**	0.38	**0.001**
Total cholesterol (mg/dl)	217.2 ± 38.7	203.7 ± 32.6	0.1	−0.07	0.6
LDL cholesterol (mg/dl)	137.2 ± 38.8	132.2 ± 30.2	0.6	−0.10	0.4
HDL cholesterol (mg/dl)	63.6 ± 16.1	47.1 ± 9.5	**<0.0001**	−0.02	0.8
Triglycerides (mg/dl)[a]	63 (46.7–102.7)	112 (86.5–159.5)	**0.001**	0.05	0.7
Fasting insulin (μIU/ml)[a]	4.8 (2.1–7.2)	12.4 (8.5–18.8)	**0.005**	0.08	0.5
HOMA-IR	0.94 (0.44–1.66)	2.75 (1.73–4.43)	**0.001**	0.06	0.6
Fasting glucose (mg/dl)	90.7 ± 9.1	91.8 ± 9.4	0.6	0.04	0.7
HbA1c (%)	5.4 ± 0.2	5.6 ± 0.3	0.06	0.13	0.3
hsCRP (mg/dl)[a]	0.11 (0.04–0.29)	0.55 (0.31–1.07)	**0.002**	0.14	0.3
Haemoglobin (g/dl)	14.15 ± 1.4	13.90 ± 1.5	0.5	−0.20	0.07
Serum iron (μg/dl)	92.85 ± 26.2	72.31 ± 26.8	**0.003**	−0.27	**0.01**
Serum ferritin (ng/ml)[a]	45 (36–142)	54 (22–174)	0.3	−0.07	0.5
Total bilirubin (mg/dl)	0.61 ± 0.31	0.44 ± 0.17	**0.02**	−0.34	**0.002**
Serum L1-sulfide (μmol/l)	6.73 ± 4.7	11.15 ± 5.3	**0.002**	–	
CTH (RU)	0.0013 ± 0.0005	0.0012 ± 0.0003	0.5	0.06	0.6
CBS (RU)	0.0058 ± 0.004	0.0081 ± 0.005	0.09	0.02	0.8
MPST (RU)	0.021 ± 0.005	0.022 ± 0.007	0.6	−0.09	0.4
SQOR (RU)	0.095 ± 0.027	0.105 ± 0.051	0.4	0.03	0.7
TST (RU)	0.031 ± 0.013	0.029 ± 0.013	0.6	−0.04	0.7
MPO (RU)	0.0059 ± 0.004	0.0061 ± 0.004	0.9	−0.05	0.7

p^1: p value from unpaired t-test, p^2: p value from Spearman's correlation and r was the coefficient of correlation. Bold values mean that p value reached statistical significance.

[a]Median and interquartile range.

fluorescence by non-specific reactions with cysteine-thiols. However, the following points indicated that current measurements could discriminate from cysteine-thiols: (i) Bariatric surgery-induced weight loss did not change total cysteine levels [43], whereas a longitudinal reduction of serum L1-sulfide in association with fat mass and weight loss was observed in the current study. (ii) Pre-treatment with reducing agent was not required in L1 measurements. Thus, it is less likely to pick up sulfur from disulfide bonded cysteine.

Another source of non-enzymatic H_2S is produced by the microbiota residing in the gastrointestinal tract belonging to the sulfate-reducing bacteria, such as *Desulfovibrio, Desulfomicrobium, Desulfobulbus, Desulfobacter, Desulfomonas* and *Desulfotomaculum* genera [44]. Germ-free mice, which were resistant to high-fat diet-induced obesity [45], were shown to have 50–80% less H_2S in their circulation and tissues [46], indicating that sulfate-reducing bacteria could be a significant contributor to H_2S concentration in obesity. Of note, metagenomic studies pointed to increased sulfate-reducing bacteria in obesogenic conditions [47, 48]. Expansion of Desulfovibrio in detriment to Clostridia reduction enhanced lipid absorption and adiposity, and was associated to obesity in mice and humans with metabolic syndrome [48].

Another important finding from current study was that morbidly obese participants with impaired fasting glucose displayed decreased serum L1-sulfide levels similar to decreased insulin sensitivity or increased insulin resistance (HOMA-IR), suggesting that endogenous H_2S biosynthesis might contribute to maintain NFG levels. Supporting this idea, exogenous H_2S administration led to improved glucose tolerance in high-fat diet-fed mice [9, 11] and decreased circulating sulfide levels were previously reported in men with poor glycemic control and type 2 diabetes [8, 12]. Otherwise, other studies reported opposite effects in relation to glucose metabolism [49, 50], showing that H_2S decreased hepatocyte glucose uptake and increased hepatic gluconeogenesis [50], and inhibited insulin release from β-cells [49]. In fact these findings go in the opposite

Table 5 Bivariate correlations among *CBS, CTH, MPST, SQOR, TST* and *MPO* mRNA levels and anthropometric and clinical characteristics in cohort 2.

	CTH r	*CBS* r	*MPST* r	*SQOR* r	*TST* r	*MPO* r
Age (years)	−0.08	0.05	0.10	0.04	0.08	0.22
BMI (kg/m^2)	−0.05	0.19	−0.06	0.01	0.01	−0.02
Waist circumference (cm)	−0.16	0.20	−0.04	0.04	0.08	0.11
Fat mass (%)	0.01	0.22	−0.12	0.09	0.09	−0.17
Total cholesterol (mg/dl)	0.03	−0.01	0.19	0.17	0.14	0.16
LDL cholesterol (mg/dl)	0.01	−0.03	0.13	0.12	0.11	0.18
HDL cholesterol (mg/dl)	0.01	−0.01	0.13	−0.05	−0.06	−0.12
Triglycerides (mg/dl)	−0.08	0.16	−0.07	0.06	0.07	0.01
Fasting insulin (μIU/ml)	−0.06	0.14	−0.06	−0.03	0.10	0.11
HOMA-IR	−0.07	0.15	−0.07	−0.04	0.09	0.11
Fasting glucose (mg/dl)	−0.05	−0.03	0.04	0.06	0.11	**0.24**[a]
HbA1c (%)	−0.10	−0.05	0.08	−0.15	−0.09	−0.05
hsCRP (mg/dl)	−0.11	0.17	−0.06	0.012	0.01	0.09
Haemoglobin (g/dl)	**−0.41**[c]	0.03	0.01	−0.02	0.17	**0.29**[a]
Serum iron (μg/dl)	**−0.23**[a]	−0.03	0.16	0.09	0.18	0.16
Serum ferritin (ng/ml)	**−0.39**[b]	−0.01	0.01	−0.05	0.12	**0.48**[c]
Total bilirubin (mg/dl)	−0.16	−0.13	0.09	0.01	0.16	0.06
CTH (RU)	–	−0.02	0.09	0.17	0.1	−0.09
CBS (RU)	−0.02	–	0.08	**0.31**[b]	**0.33**[b]	0.22
MPST (RU)	0.09	0.08	–	**0.43**[c]	**0.74**[c]	**0.39**[c]
SQOR (RU)	0.17	**0.31**[b]	**0.43**[c]	–	**0.71**[c]	**0.31**[b]
TST (RU)	0.11	**0.33**[b]	**0.74**[c]	**0.71**[c]	–	**0.53**[c]
MPO (RU)	−0.09	0.22	**0.39**[c]	**0.31**[b]	**0.53**[c]	–

Bold values mean that *p* value (obtained from Spearman's correlation) reached statistical significance, and *r* was the coefficient of correlation.

[a] $p < 0.05$.

[b] $p < 0.01$.

[c] $p < 0.001$.

direction from the correlations of serum sulfide with insulin sensitivity or insulin resistance observed in all participants, which were not maintained after adjusting by age, gender and fat mass.

A possible limitation of current study was that it was designed to investigate changes in serum sulfide levels according to obesity status in non-diabetic participants, so the impact of H_2S on obesity-associated metainflammation disorders, such as type 2 diabetes and cardiovascular diseases cannot be examined in depth. However, these issues were previously investigated in humans [8, 12, 51, 52] and rats [53, 54]. Other study limitations were that distinct biological pools for H_2S, such as free gaseous, sulfane sulfur bound and acid-labile [55], were not analysed, and that only-one method was used to measure serum sulfide levels. To gain insight in to the differences between serum L1-sulfide levels between lean and obese patients, the analysis of these three biological pools of serum H_2S and the validation of sulfide measurements using common alternative methods (such Monobromobimane derivatization/HPLC-based method and assays to measure H_2S production) should be considered in future studies.

In conclusion, altogether these data demonstrated a potential link between serum sulfide concentration and obesity, being circulating sulfide increased in proportion to fat mass accumulation, and suggesting haem degradation as a negative regulator, and adipose tissue, plasma cysteine and gut microbiota as putative additional sources of serum sulfide levels.

Acknowledgements This work was partially supported by research grants PI15/01934, PI16/01173 and PI19/01712 from the Instituto de Salud Carlos III from Spain and VII Spanish Diabetes Association grants to Basic Diabetes Research Projects led by young researchers, CIBEROBN Fisiopatología de la Obesidad y Nutrición is an initiative from the Instituto de Salud Carlos III and Fondo Europeo de Desarrollo Regional (FEDER) from Spain. Project ThinkGut (EFA345/19) 65% co-financed by the European Regional Development Fund (ERDF) through the Interreg V-A Spain-France-Andorra programme (POCTEFA 2014-2020). We acknowledge the technical assistance of Oscar Rovira (IdIBGi). We want to particularly acknowledge the patients, the FATBANK platform promoted by the CIBEROBN and

the IDIBGI Biobank (Biobanc IDIBGI, B.0000872), integrated in the Spanish National Biobanks' Network, for their collaboration and coordination.

Compliance with ethical standards

Conflict of interest The authors declare that they have no conflict of interest.

Publisher's note Springer Nature remains neutral with regard to jurisdictional claims in published maps and institutional affiliations.

References

1. Whiteman M, Le Trionnaire SL, Chopra M, Fox B, Whatmore J. Emerging role of hydrogen sulfide in health and disease: critical appraisal of biomarkers and pharmacological tools. Clin. Sci. 2011;121:459–88.
2. Yang CT, Chen L, Xu S, Day JJ, Li X, Xian M. Recent development of hydrogen sulfide releasing/stimulating reagents and their potential applications in cancer and glycometabolic disorders. Front. Pharmacol. 2017;8:664.
3. Kamoun P. Endogenous production of hydrogen sulfide in mammals. Amino Acids. 2004;26:243–54.
4. Kuo MM, Kim DH, Jandu S, Bergman Y, Tan S, Wang H, et al. MPST but not CSE is the primary regulator of hydrogen sulfide production and function in the coronary artery. Am J Physiol. 2016;310:H71–9.
5. Landry AP, Ballou DP, Banerjee R. Modulation of catalytic promiscuity during hydrogen sulfide oxidation. ACS Chem Biol. 2018;13:1651–8.
6. Pálinkás Z, Furtmüller PG, Nagy A, Jakopitsch C, Pirker KF, Magierowski M, et al. Interactions of hydrogen sulfide with myeloperoxidase. Br. J. Pharmacol. 2015;172:1516–32.
7. Morton NM, Beltram J, Carter RN, Michailidou Z, Gorjanc G, McFadden C, et al. Genetic identification of thiosulfate sulfurtransferase as an adipocyte-expressed antidiabetic target in mice selected for leanness. Nat Med. 2016;22:771–9.
8. Whiteman M, Gooding KM, Whatmore JL, Ball CI, Mawson D, Skinner K, et al. Adiposity is a major determinant of plasma levels of the novel vasodilator hydrogen sulphide. Diabetologia. 2010;53:1722–6.
9. Cai J, Shi X, Wang H, Fan J, Feng Y, Lin X, et al. Cystathionine γ lyase–hydrogen sulfide increases peroxisome proliferator-activated receptor γ activity by sulfhydration at C139 site thereby promoting glucose uptake and lipid storage in adipocytes. Biochim Biophys Acta. 2016;1861:419–29.
10. Geng B, Cai B, Liao F, Zheng Y, Zeng Q, Fan X. et al. Increase or decrease hydrogen sulfide exert opposite lipolysis, but reduce global insulin resistance in high fatty diet induced obese mice. PLoS ONE. 2013;8:e73892.
11. Yang G, Ju Y, Fu M, Zhang Y, Pei Y, Racine M, et al. Cystathionine gamma-lyase/hydrogen sulfide system is essential for adipogenesis and fat mass accumulation in mice. Biochim Biophys Acta. 2018;1863:165–76.
12. Suzuki K, Sagara M, Aoki C, Tanaka S, Aso Y. Clinical implication of plasma hydrogen sulfide levels in Japanese patients with type 2 diabetes. Intern Med. 2017;56:17–21.
13. Association AD. 2. Classification and diagnosis of diabetes: Standards of medical care in diabetes—2019. Diabetes Care. 2019;42:S13–28.
14. Matthews DR, Hosker JP, Rudenski AS, Naylor BA, Treacher DF, Turner RC. Homeostasis model assessment: insulin resistance and β-cell function from fasting plasma glucose and insulin concentrations in man. Diabetologia. 1985;28:412–9.
15. Ditrói T, Nagy A, Martinelli D, Rosta A, Kožich V, Nagy P. Comprehensive analysis of how experimental parameters affect H2S measurements by the monobromobimane method. Free Radic Biol Med. 2019;136:146–58.
16. Choi SA, Park CS, Kwon OS, Giong HK, Lee JS, Ha TH. et al. Structural effects of naphthalimide-based fluorescent sensor for hydrogen sulfide and imaging in live zebrafish. Sci Rep. 2016;6:26203
17. Vitvitsky V, Yadav PK, Kurthen A, Banerjee R. Sulfide oxidation by a noncanonical pathway in red blood cells generates thiosulfate and polysulfides. J Biol Chem. 2015;290:8310–20.
18. Saravanan G, Ponmurugan P, Begum MS. Effect of S-allylcysteine, a sulphur containing amino acid on iron metabolism in streptozotocin induced diabetic rats. J Trace Elem Med Biol. 2013;27:143–7.
19. Yu S, Yan Z, Che N, Zhang X, Ge R. Impact of carbon monoxide/heme oxygenase on hydrogen sulfide/cystathionine-γ-lyase pathway in the pathogenesis of allergic rhinitis in guinea pigs. Otolaryngol Neck Surg. 2015;152:470–6.
20. Hishiki T, Yamamoto T, Morikawa T, Kubo A, Kajimura M, Suematsu M. Carbon monoxide: impact on remethylation/transsulfuration metabolism and its pathophysiologic implications. J Mol Med. 2012;90:245–54.
21. Bin GuoS, Duan ZJ, Wang QM, Zhou Q, Li Q, Sun XY. Endogenous carbon monoxide downregulates hepatic cystathionine-γ-lyase in rats with liver cirrhosis. Exp Ther Med. 2015;10:2039–46.
22. Galmozzi A, Kok BP, Kim AS, Montenegro-Burke JR, Lee JY, Spreafico R, et al. PGRMC2 is an intracellular haem chaperone critical for adipocyte function. Nature. 2019;576:138–42.
23. Moreno-Navarrete JM, Rodríguez A, Ortega F, Becerril S, Girones J, Sabater-Masdeu M, et al. Heme biosynthetic pathway is functionally linked to adipogenesis via mitochondrial respiratory activity. Obesity. 2017;25:1723–33.
24. Nunes-Souza N, Dias-Júnior NM, Eleutério-Silva MA, Ferreira-Neves VP, Moura FA, Alenina N, et al. 3-Amino-1,2,4-triazole induces quick and strong fat loss in mice with high fat-induced metabolic syndrome. Oxid Med Cell Longev. 2020;2020. https://doi.org/10.1155/2020/3025361.
25. Takei R, Inoue T, Sonoda N, Kohjima M, Okamoto M, Sakamoto R, et al. Bilirubin reduces visceral obesity and insulin resistance by suppression of inflammatory cytokines. PLoS ONE. 2019;14. https://doi.org/10.1371/journal.pone.0223302.
26. Stec DE, John K, Trabbic CJ, Luniwal A, Hankins MW, Baum J, et al. Bilirubin binding to PPARα inhibits lipid accumulation. PLoS ONE. 2016;11. https://doi.org/10.1371/journal.pone.0153427.
27. Gordon DM, Neifer KL, Hamoud A-RA, Hawk CF, Nestor-Kalinoski AL, Miruzzi SA, et al. Bilirubin remodels murine white adipose tissue by reshaping mitochondrial activity and the coregulator profile of peroxisome proliferator-activated receptor α. J Biol Chem. 2020;295. https://doi.org/10.1074/jbc.RA120.013700.
28. Cimini FA, Arena A, Barchetta I, Tramutola A, Ceccarelli V, Lanzillotta C, et al. Reduced biliverdin reductase-A levels are associated with early alterations of insulin signaling in obesity. Biochim Biophys Acta. 2019;1865:1490–501.
29. Gordon DM, Adeosun SO, Ngwudike SI, Anderson CD, Hall JE, Hinds TD, et al. CRISPR Cas9-mediated deletion of biliverdin reductase A (BVRA) in mouse liver cells induces oxidative stress and lipid accumulation. Arch Biochem Biophys. 2019;672. https://doi.org/10.1016/j.abb.2019.108072.
30. Zhao L, Zhang X, Shen Y, Fang X, Wang Y, Wang F. Obesity and iron deficiency: a quantitative meta-analysis. Obes. Rev. 2015;16:1081–93.
31. Mani S, Li H, Untereiner A, Wu L, Yang G, Austin RC, et al. Decreased endogenous production of hydrogen sulfide accelerates atherosclerosis. Circulation. 2013;127:2523–34.

32. Rose P, Moore PK, Zhu YZ. H_2S biosynthesis and catabolism: new insights from molecular studies. Cell Mol Life Sci. 2017;74:1391–412.
33. Szijártó IA, Markó L, Filipovic MR, Miljkovic JL, Tabeling C, Tsvetkov D, et al. Cystathionine γ-lyase-produced hydrogen sulfide controls endothelial no bioavailability and blood pressure. Hypertension. 2018;71:1210–7.
34. Bearden SE, Beard RS, Pfau JC. Extracellular transsulfuration generates hydrogen sulfide from homocysteine and protects endothelium from redox stress. Am J Physiol. 2010;299: H1568–76.
35. Hwang SY, Sarna LK, Siow YL, Karmin O. High-fat diet stimulates hepatic cystathionine β-synthase and cystathionine γ-lyase expression. Can J Physiol Pharmacol. 2013;91:913–9.
36. Yang Y, Wang Y, Sun J, Zhang J, Guo H, Shi Y, et al. Dietary methionine restriction reduces hepatic steatosis and oxidative stress in high-fat-fed mice by promoting H2S production. Food Funct. 2019;10:61–77.
37. Hine C, Harputlugil E, Zhang Y, Ruckenstuhl C, Lee BC, Brace L, et al. Endogenous hydrogen sulfide production is essential for dietary restriction benefits. Cell. 2015;160:132–44.
38. Norris EJ, Culberson CR, Narasimhan S, Clemens MG. The liver as a central regulator of hydrogen sulfide. Shock. 2011;36:242–50.
39. Yang J, Minkler P, Grove D, Wang R, Willard B, Dweik R, et al. Non-enzymatic hydrogen sulfide production from cysteine in blood is catalyzed by iron and vitamin B6. Commun Biol. 2019;2:1–14.
40. Carter RN, Morton NM. Cysteine and hydrogen sulphide in the regulation of metabolism: Insights from genetics and pharmacology. J Pathol. 2016;238:321–32.
41. Elshorbagy AK, KoziC HV, David Smith A, Refsum H. Cysteine and obesity: consistency of the evidence across epidemiologic, animal and cellular studies. Curr Opin Clin Nutr Metab Care. 2012;15:49–57.
42. Giustarini D, Dalle-Donne I, Lorenzini S, Milzani A, Rossi R. Age-related influence on thiol, disulfide, and protein-mixed disulfide levels in human plasma. J Gerontol A Biol Sci Med Sci. 2006;61:1030–8.
43. Aasheim ET, Elshorbagy AK, My Diep L, Søvik TT, Mala T, Valdivia-Garcia M, et al. Effect of bariatric surgery on sulphur amino acids and glutamate. Br J Nutr. 2011;106:432–40.
44. Rey FE, Gonzalez MD, Cheng J, Wu M, Ahern PP, Gordon JI. Metabolic niche of a prominent sulfate-reducing human gut bacterium. Proc Natl Acad Sci USA. 2013;110:13582–7.
45. Bäckhed F, Manchester JK, Semenkovich CF, Gordon JI. Mechanisms underlying the resistance to diet-induced obesity in germ-free mice. Proc Natl Acad Sci USA. 2007;104:979–84.
46. Shen X, Carlström M, Borniquel S, Jädert C, Kevil CG, Lundberg JO. Microbial regulation of host hydrogen sulfide bioavailability and metabolism. Free Radic Biol Med. 2013;60:195–200.
47. Hildebrandt MA, Hoffmann C, Sherrill-Mix SA, Keilbaugh SA, Hamady M, Chen YY, et al. High-fat diet determines the composition of the murine gut microbiome independently of obesity. Gastroenterology. 2009;137:1716.
48. Petersen C, Bell R, Klag KA, Lee S-H, Soto R, Ghazaryan A, et al. T cell-mediated regulation of the microbiota protects against obesity. Science. 2019;80-:365:eaat9351.
49. Kaneko Y, Kimura Y, Kimura H, Niki I. L-cysteine inhibits insulin release from the pancreatic β-cell: Possible involvement of metabolic production of hydrogen sulfide, a novel gasotransmitter. Diabetes. 2006;55:1391–7.
50. Zhang L, Yang G, Untereiner A, Ju Y, Wu L, Wang R. Hydrogen sulfide impairs glucose utilization and increases gluconeogenesis in hepatocytes. Endocrinology. 2013;154:114–26.
51. Rajpal S, Katikaneni P, Deshotels M, Pardue S, Glawe J, Shen X, et al. Total sulfane sulfur bioavailability reflects ethnic and gender disparities in cardiovascular disease. Redox Biol. 2018;15:480–9.
52. Guo R, Wu Z, Jiang J, Liu C, Wu B, Li X, et al. New mechanism of lipotoxicity in diabetic cardiomyopathy: deficiency of Endogenous H2S Production and ER stress. Mech Ageing Dev. 2017;162:46–52.
53. Jeddi S, Gheibi S, Kashfi K, Carlström M, Ghasemi A. Protective effect of intermediate doses of hydrogen sulfide against myocardial ischemia-reperfusion injury in obese type 2 diabetic rats. Life Sci. 2020;256. https://doi.org/10.1016/j.lfs.2020.117855.
54. Gomez CB, de la Cruz SH, Medina-Terol GJ, Beltran-Ornelas JH, Sánchez-López A, Silva-Velasco DL, et al. Chronic administration of NaHS and L-Cysteine restores cardiovascular changes induced by high-fat diet in rats. Eur J Pharmacol. 2019;863. https://doi.org/10.1016/j.ejphar.2019.172707.
55. Shen X, Peter EA, Bir S, Wang R, Kevil CG. Analytical measurement of discrete hydrogen sulfide pools in biological specimens. Free Radic Biol Med. 2012;52:2276–83.

MANUSCRIPT 2

Ferran Comas, Jèssica Latorre, Olaf Cussó, Francisco Ortega, Aina Lluch, Mònica Sabater, Anna Castells-Nobau, Wifredo Ricart, Xavier Ribas, Miquel Costas, José Manuel Fernández-Real, José María Moreno-Navarrete. **Hydrogen sulfide impacts on inflammation-induced adipocyte dysfunction.** *Food Chem Toxicol*. 2019 Sep; doi:10.1016/j.fct.2019.05.051.

Impact factor (2019): 4.679 (D1, Food Science & Technology)

Food and Chemical Toxicology 131 (2019) 110543

Contents lists available at ScienceDirect

Food and Chemical Toxicology

journal homepage: www.elsevier.com/locate/foodchemtox

Hydrogen sulfide impacts on inflammation-induced adipocyte dysfunction

Ferran Comas[a], Jèssica Latorre[a], Olaf Cussó[b], Francisco Ortega[a], Aina Lluch[a], Mònica Sabater[a], Anna Castells-Nobau[a], Wifredo Ricart[a,c], Xavier Ribas[b], Miquel Costas[b], José Manuel Fernández-Real[a,c,**], José María Moreno-Navarrete[a,c,*]

[a] Department of Diabetes, Endocrinology and Nutrition, Hospital of Girona 'Dr Josep Trueta'Institut d'Investigació Biomèdica de Girona (IdIBGi), CIBEROBN (CB06/03/010) and Instituto de Salud Carlos III (ISCIII), Girona, Spain
[b] Grup de Química Bioinspirada, Supramolecular i Catàlisi (QBIS-CAT), Institut de Química Computacional i Catàlisi (IQCC), Departament de Química, Universitat de Girona, C/M. Aurèlia Capmany 69, 17003, Girona, Catalonia, Spain
[c] Department of Medicine, Universitat de Girona, Girona, Spain

ARTICLE INFO

Keywords:
Hydrogen sulfide
3T3-L1
Adipocyte
Inflammation
GYY4137
Na_2S*Keywords:*
Hydrogen sulfide
3T3-L1 cell differentiation
Inflammation
GYY4137
Na_2S

ABSTRACT

A dual role of hydrogen sulfide (H_2S) in inflammation is well-reported and recent studies demonstrated adipogenic effects of H_2S in 3T3-L1 cells. Here, we aimed to investigate the effects of H_2S on adipocyte differentiation and inflammation. H_2S concentration in 3T3-L1 culture media was increased during adipocyte differentiation in parallel to adipogenic and *Cth* gene expression, and its inhibition using DL-Propargyl Glycine (PPG) impaired 3T3-L1 differentiation. GYY4137 and Na_2S administration only in the first or in the last stage of adipocyte differentiation resulted in a significant increased expression of adipogenic genes. However, when GYY4137 or Na_2S were administrated during all process no significant effects on adipogenic gene expression were found, suggesting that excessive H_2S administration might exert negative effects on adipogenesis. In fact, continuous addition of Na_2S, which resulted in Na_2S excess, inhibited adipogenesis, whereas time-expired Na_2S had no effect. In inflammatory conditions, GYY4137, but not Na_2S, administration attenuated the negative effects of inflammation on adipogenesis and insulin signaling-related gene expression during adipocyte differentiation. In inflamed adipocytes, Na_2S administration enhanced the negative effects of inflammatory process. Altogether these data showed that slow-releasing H_2S improved adipocyte differentiation in inflammatory conditions, and that H_2S proadipogenic effects depend on dose, donor and exposure time.

1. Introduction

Hydrogen sulfide (H_2S) biosynthesis has been identified in a variety of mammalian tissues, notably in the brain, heart, and the gastrointestinal tract, (Stipanuk, 2004; Yang et al., 2008), with a number of possible physiologic and pathophysiologic roles and a range of potential therapeutic uses (Li et al., 2009; Szabó, 2007; Whiteman and Moore, 2009). There is emerging evidence supporting the importance of H_2S in adipocytes, offering new insight into their role in the pathogenesis of obesity. Recent studies showed a possible role of H_2S in adipogenesis, enhancing PPARγ activity and stability and increasing glucose uptake and lipid storage (Cai et al., 2016). In fact, the CSE/H_2S system has been demonstrated to promote adipogenesis and fat mass accumulation in mice (Yang et al., 2018). However, opposite findings have been reported in other in vitro studies (Kim et al., 2012; Lii et al., 2012).

H_2S has recently gained significant attention as inflammation biological mediator. Antiinflammatory effect of H_2S has been reported in acute lung injury (Tokuda et al., 2012; Ang et al., 2011; Chen et al., 2009), and in kidney injury caused by urinary-derived sepsis (Chen et al., 2014). In vitro studies confirmed this antiinflammatory role (Yang et al., 2011) through the modulation of NFκB activity (Du et al., 2014). Antiinflammatory effect of H_2S is supported by the fact that H_2S deficiency contributes to switch of adipose tissue macrophages antiinflammatory M2 phenotype to proinflammatory M1 phenotype associated with obesity (Velmurugan et al., 2015). However, other studies reported that H_2S has proinflammatory effect in liver and aggravated LPS-induced liver damage (Yan et al., 2013; Zhang et al., 2007; Collin et al., 2005; Badiei et al., 2016).

Taking together these results it is evident that H_2S is implicated in the regulation of adipocyte differentiation and inflammation. Here, we hypothesize that a possible role of H_2S in the modulation of adipocyte inflammation might underlie its adipogenic effects. To test this

* Corresponding author. Department of Medicine, Universitat de Girona, Institut d'Investigació Biomèdica de Girona (IdIBGi), Girona, Spain.
** Corresponding author. Section of Diabetes, Endocrinology and Nutrition Hospital of Girona "Dr Josep Trueta" Carretera de França s/n, 17007, Girona, Spain.
E-mail addresses: jmfreal@idibgi.org (J.M. Fernández-Real), jmoreno@idibgi.org (J.M. Moreno-Navarrete).

https://doi.org/10.1016/j.fct.2019.05.051
Received 16 January 2019; Received in revised form 9 May 2019; Accepted 29 May 2019
Available online 30 May 2019

hypothesis, we aimed to investigate the possible role of GYY4137, a long-acting H_2S releasing donor, and sodium sulfide (Na_2S), a fast-releasing H_2S donor on adipocyte differentiation and inflammation.

2. Materials and methods

2.1. 3T3-L1 cell culture and differentiation

The embryonic fibroblast mouse cell line 3T3-L1 (American Type Culture Collection) was cultured in DMEM containing 4.5 g/L glucose, 10% FBS, 100 U/ml penicillin, and 100 μg/ml streptomycin. At 2 days after confluence, insulin (5 μg/ml), dexamethasone (0.25μM), and isobutylmethylxanthine (0.25 mM) mixture was added for 2 days, followed by 5 days with insulin (5 μg/ml) alone. DL-Propargyl Glycine (PPG, 0.25 and 1 mM) and H_2S donors [Na_2S (50 μM), GYY4137 (50 μM)] and time-expired Na_2S (50 μM) were directly added into the differentiation or adipocyte maintenance media. For hydrogen sulfide excess experiments, Na_2S and time-expired Na_2S were added every 12 h in first two days of adipocyte differentiation process and then every 24 h from day 2–7. Time-expired Na_2S, which was administrated to control the effects of sodium and oxidized sulfur species accumulation in the medium, was obtained as previously described by Tsai et al. (2015). Briefly, time-expired Na_2S was prepared in Dulbecco's phosphate buffered saline (pH = 7.4) (D-PBS, Sigma Chemical) at room temperature, and was obtained leaving Na_2S (50 μM) solution in an opened falcon 50 mL centrifuge tube in aseptic conditions during ~30 h.

Cells were then considered mature adipocytes, harvested, and stored at −80 °C for RNA extraction to study adipogenic and H_2S biosynthesis-related gene expression levels during 3T3-L1 differentiation.

Inflammatory conditions during 3T3-L1 differentiation and in mature adipocytes were induced by macrophage-conditioned media (MCM, 2%) and lipopolysaccharide (1 μg/ml) administration. During 3T3-L1 differentiation, MCM (2%) and LPS (1 μg/ml) was added in two steps of the differentiation process. To obtain inflamed adipocytes, MCM (2%) and LPS (1 μg/ml) administration during 24 h on fully 3T3-L1 differentiated adipocytes was performed.

Macrophage-conditioned medium was obtained as previously described (Moreno-Navarrete et al., 2009). Briefly, the human monocyte cell line THP-1 (American Type Culture Collection, Barcelona, Spain) was cultured in Rosswell Park Memmorial Institute (RPMI media 1640; Cat. No. 21870–076) 1640 medium containing 10% fetal bovine serum, 5 mM glucose, 2 mM L-glutamine, 50 μg/ml gentamicine and 20 mM 4-(2-hydroxyethyl)-1-piperazineethanesulfonic acid (HEPES) at 37 °C in a humidified 5%CO_2 per 95 °C air atmosphere. The mature macrophage-like state was induced by treating THP-1 cells ($1{,}2 \times 10^6$ cells) with 0.162 μM phorbol 12-myristate 13-acetate (PMA) (Sigma Chemical, Madrid, Spain) in 6-well culture dishes for 24 h. Differentiated, plastic-adherent cells were washed with cold Dulbecco's phosphate buffered saline (D-PBS, Sigma Chemical) and then incubated with fresh medium without phorbol 12-myristate 13-acetate during additional 24 h. The supernatants (macrophage-conditioned media (MCM)) were collected, centrifuged at 900 *g* for 5 min, aliquoted and stored at −80 °C until testing.

All in vitro experiments were performed in four independent replicates.

2.2. Quantification of H_2S media concentration

H_2S concentration in cultured media was assessed using a naphthalimide-based fluorescent sensor 6-Azido-2-(2-(2-(2-hydroxyethoxy) ethoxy)ethyl)-1H-benzo[de]isoquinoline-1,3 (2H)-dione(L1), as described previously (Choi et al., 2016). To measure H_2S production, 3T3-L1 cells were incubated 24 h in DMEM media containing 10% (vol/vol) FBS and 5 μM of L1 probe, during different days of differentiation (0, 2 and 7). After incubation, media were transferred to new eppendorf tubes to be homogenized. To measure H_2S levels, a standard curve was generated from a 10 mM stock solution of sodium sulfide (Na_2S) in DMEM containing 10% (vol/vol) and 5 μM of L1 at various concentrations (0, 7.8, 15.6, 31.25, 62.5, 125, 250 and 500 μM Na_2S). Before reading standard curve was incubated during 90 min at 37 °C. After incubation, fluorescence was read in a BiotekCytation 5 reader at λ ex = 435 ± 10 nm and λ em = 550 ± 10 nm in duplicate.

2.3. RNA expression

RNA purification and gene expression procedures and analyses were performed as previously described (Moreno-Navarrete et al., 2014). Briefly, RNA purification was performed using an RNeasy Lipid Tissue Mini kit (QIAgen, Izasa S.A., Barcelona, Spain), and the integrity was checked by Agilent Bioanalyzer (Agilent Technologies, Palo Alto, CA). Gene expression was assessed by real time PCR using a LightCycler 480 Real-Time PCR System (Roche Diagnostics, Barcelona, Spain), using TaqMan technology suitable for relative genetic expression quantification. The RT-PCR reaction was performed in a final volume of 12 μl. The cycle program consisted of an initial denaturing of 10 min at 95 °C then 40 cycles of 15 s denaturizing phase at 95 °C and 1 min annealing and extension phase at 60 °C. A threshold cycle (Ct value) was obtained for each amplification curve and then a ΔΔCt value was calculated as follows: (Ct, target gene - Ct, endogenous control) treatment - (Ct, target gene - Ct, endogenous control) control or vehicle. Eukaryotic 18S rRNA was used as endogenous control. Fold changes compared with the endogenous control were then determined by calculating $2^{-\Delta\Delta Ct}$, so that gene expression results are expressed as expression ratio relative to *18S* gene expression according to the manufacturer's guidelines. The following primer/probe sets were used: Adiponectin (Adipoq, Mm00456425_m1), peroxisome proliferator-activated receptor gamma (Pparg, Mm0000440940_m1), glucose transporter type 4 (Slc2a4, Mm00436615_m1), perlipin 1 (Plin1, Mm00558672_m1), CCAAT/enhancer-binding protein alpha (Cebpa, Mm00514283_s1), fatty acid synthase (Fasn, Mm00662319_m1), interleukin 6 (Il6, Mm00446190_m1), fatty acid binding protein 4 (Fabp4, Mm00445880_m1), tumor necrosis factor alpha (Tnf, Mm99999068_m1), diacylglycerol O-acyltransferase 1 (Dgat1, Mm00515643_m1), patatin Like Phospholipase Domain Containing 2 (Pnpla2, Mm00503040_m1), lipase E (Lipe, Mm00495359_m1), cystathionine gamma-lyase (Cth, Mm00461247) and cystathionine beta-synthase (Cbs, Mm00460654_m1).

2.4. Oil Red O staining

Intracellular lipid accumulation was assessed by Oil Red O staining. Cells were washed twice with PBS, fixed in 4% formaldehyde for 1 h, and stained for 30 min with 0.2% Oil Red O solution in 60% isopropanol. Cells were then washed several times with water, and excess water was evaporated by placing the stained cultures at 32 °C. Oil-red staining was quantified, as previously described (Lee et al., 2018) with Fiji software (Schindelin et al., 2012). The area occupied by lipid droplets stained by Oil Red O was selected and quantified using color threshold plugin (*Hue*: exclusion criteria 41–211) to identify red color regions. Then, Oil Red O staining was represented as % of selected stained area in comparison with image total area.

2.5. Statistical analysis

Statistical analyses were performed using SPSS statistical software (SPSS v21.0; IBM, Chicago, IL, USA). The non-parametric Mann–Whitney test was used. Levels of statistical significance were set at $p < 0.05$.

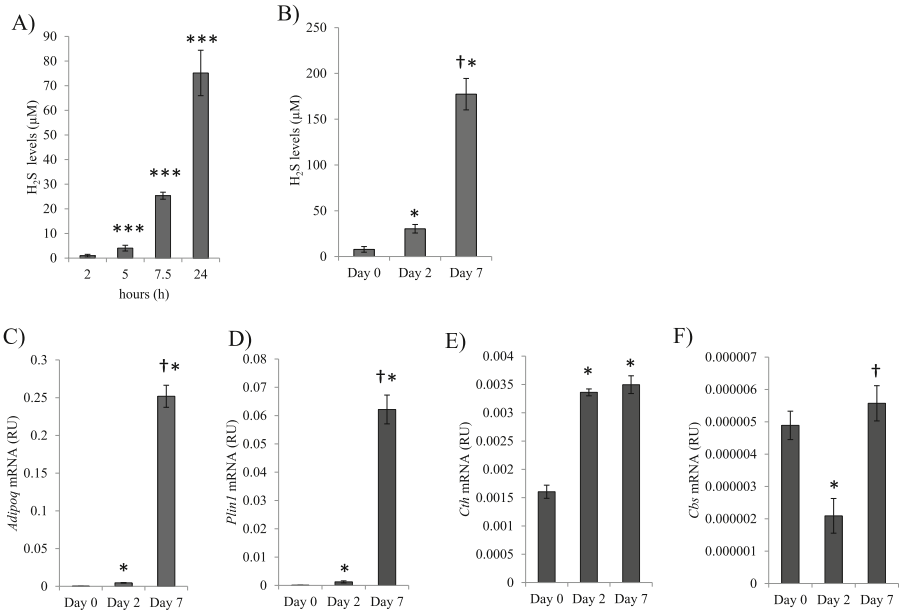

Fig. 1. A) Effects of L1 incubation (for 2, 5, 7.5 and 24 h) in 3T3-L1 cells (day 3 of adipocyte differentiation) on 3T3-L1-conditioned media H_2S concentration measurement. ***p < 0.001 compared to 2 h. **B–F)** H_2S levels **(B)**, *Adipoq* **(C)**, *Plin1* **(D)**, *Cth* **(E)** and *Cbs* **(F)** gene expression at days 0, 2 and 7 during adipocyte differentiation. *p < 0.05 compared with day 0 and †p < 0.05 compared with day 2.

3. Results

3.1. H_2S production during adipogenesis

Given the marked effects of hydrogen sulfide on adipocytes differentiation, we decided to explore H_2S synthesis in 3T3-L1 during adipogenesis. First, cell culture media from day 0, 2 or 7 plus L1 probe (5 μM) were incubated for 1 h, but H_2S levels was undetectable at any day. Then, to increase the performance and taking advantage of solubility and non-toxicity of L1 probe, 3T3-L1 cells were incubated with L1 probe (5 μM) for 2, 5, 7.5 and 24 h. A significant and cumulative increase in H_2S concentration was found, achieving the maximum levels at 24 h (Fig. 1A). Interestingly, 24 h H_2S (μM) accumulation in media increased significantly from day 0 to day 2 and from day 2 to day 7, confirming that H_2S is generated during adipogenesis (Fig. 1B). The maximum levels of H_2S accumulation in the media were associated with the higher adipogenic gene expression (Fig. 1C and D). Then, expression of H_2S-generating genes Cth (also named CSE) and Cbs were analysed. *Cth* was highly expressed compared to *Cbs* gene [0.0034962 ± 0.0001561 (Ct value 25.49 ± 0.21) *vs* 0.0000055 ± 0.0000005 (Ct value 34.81 ± 0.36) RU, p < 0.0001], supporting Cth as the main source of adipogenesis-associated H_2S biosynthesis (Yang et al., 2018). In fact, *Cth* gene expression was increased in the first stage of adipocyte differentiation process (from day 0–2), and then these levels were maintained until the end of the process (day 7) (Fig. 1E), whereas *Cbs* mRNA decreased at day 2, and recovered at day 7 (Fig. 1F).

3.2. Effects of PPG in 3T3-L1 during adipogenesis

We decided to study the effect of CTH inhibitor (PPG, 0.25 and 1 mM) on adipogenic related gene expression, as a way to identify the effect of decreased H_2S synthesis during adipogenesis. During adipogenesis, 0.25 and 1 mM PPG administration during adipogenesis led to decreased adipogenic (*Pparg, Adipoq, Glut4, Plin1* and *Cebpa*), lipogenic (*Fasn* and *Dgat1*) and lipolytic (*Pnpla2* and *Lipe*) gene expression at dose dependent-manner, and increased expression of inflammatory related gene *Il6* (Fig. 2A). As shown by Red Oil O staining, PPG (1 mM) treatment significantly decreased adipogenesis and adipocytes lipid accumulation in concordance with gene expression results (Fig. 2B). Even though, no significant effects of PPG on hydrogen sulfide synthesis related genes (*Cth* and *Cbs*) were observed (Fig. 1B), PPG administration led to decreased H_2S accumulation at day 7 (Fig. 2C).

These findings reveal that certain levels of hydrogen sulfide are necessary for adipocyte differentiation.

3.3. Effects of Na_2S and GYY4137 in 3T3-L1 during adipogenesis

Treatment with GYY4137 and Na_2S during all the differentiation process of 3T3-L1 (Day 0–7) had no significant effects (Fig. 3A). At day 7, increased H_2S accumulation in Na_2S, but not GYY4137, was observed (Fig. 3B). Interestingly, administration of GYY4137 and Na_2S in the first stage (Day 0–2) and late stage (Day 2–7) of adipocyte differentiation resulted in a significant increase of adipogenic (*Adipoq, Pparg, Glut4* and *Fabp4*) and lipogenic (*Fasn*) genes (Fig. 3C and D).

3.4. Effects of Na_2S excess and time-expired Na_2S in 3T3-L1 during adipogenesis

First, to evaluate the stability and the effects of one single dose of Na_2S (50 μM) on H_2S levels, the loss of H_2S concentration in phosphate-buffered saline (PBS) was measured in cell culture conditions (without cells) during 4 days at several points (0, 24, 48, 72 and 96 h, Fig. 4A). This experiment showed a 60% reduction of H_2S levels at 24 h. This information led to estimate excess H_2S levels in daily Na_2S administration experiment, suggesting the following concentrations: ~35 μM at 12 h, ~59.6 μM at 24 h, ~76.6 μM at 36 h, ~88.6 μM at 48 h, ~55.4 μM at 72 h, ~42.2 μM at 96 h, ~36.9 μM at 120 h, ~34.7 μM at 144 h and ~33.9 μM at 168 h.

Next, the effect of H_2S excess on adipogenesis was assessed. Continuous addition of Na_2S (50 μM) or time-expired Na_2S administration during adipocyte differentiation process were performed as detailed in methods. Time-expired Na_2S had undetectable H_2S levels. Na_2S excess led to decreased adipogenic (*Pparg, Adipoq, Glut4* and *Fapb4*), lipogenic (*Fasn*) and lipolytic (*Pnpla2* and *Lipe*) gene expression, and tend to increase expression of *Il6* (Fig. 4B). Red Oil O staining confirmed that Na_2S daily administration inhibited adipogenesis (Fig. 4C). In contrast, time-expired Na_2S had no significant effects in the expression of adipogenic and lipogenic genes, whilst significant decreased lipolytic (*Pnpla2*) and inflammatory (*Il6*) gene expression was reported (Fig. 4B).

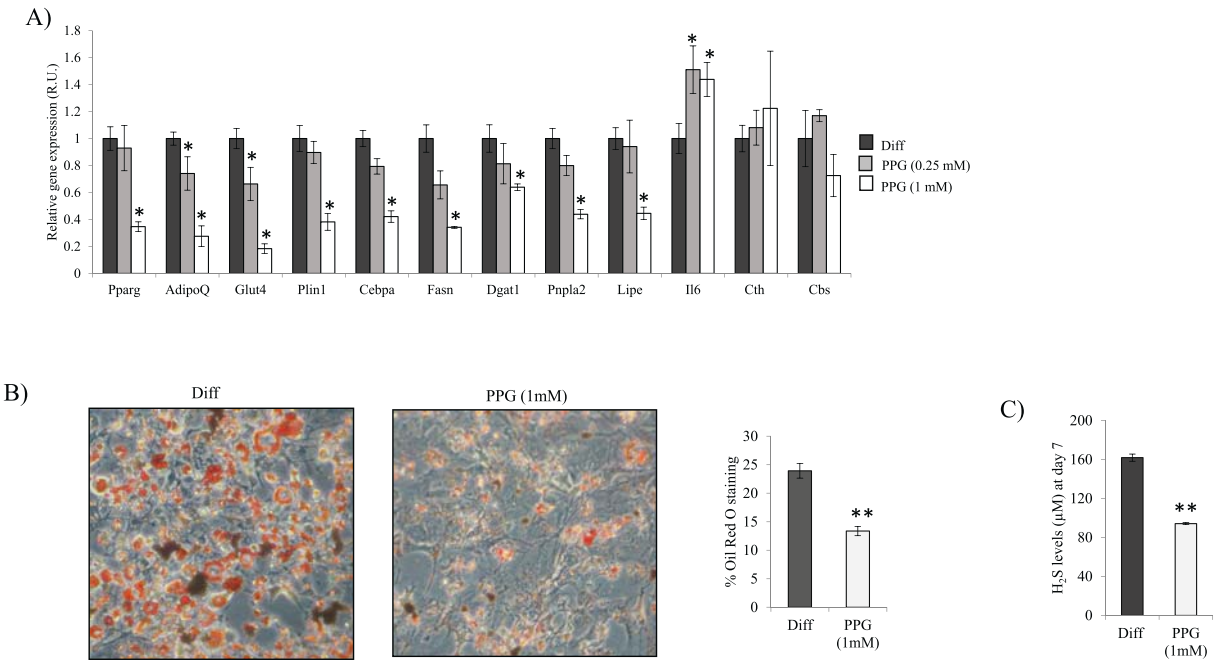

Fig. 2. A-C) Effects of PPG (0,25 and 1 mM) administration during 3T3-L1 differentiation on adipogenic, lipogenic, lipolytic, inflammatory and hydrogen sulfide synthesis gene expression (**A**), intracellular lipid accumulation using Red Oil staining (**B**) and H_2S levels at day 7 **(C)**. Control differentiated (black bars), 0.25 mM PPG (grey bars) and 1 mM PPG (white bars). *p < 0.05 and **p < 0.01 compared with control differentiated. These data are expressed as mean ± SEM. (For interpretation of the references to color in this figure legend, the reader is referred to the Web version of this article.)

3.5. Effects of Na_2S and GYY4137 in 3T3-L1 during adipocyte differentiation in inflammatory conditions

Inflammatory conditions (Diff + MCM) resulted in decreased adipogenesis (*Adipoq* and *Fasn*) and insulin action (*Glut4*)-related gene expression and increased expression of *Il6* gene (Fig. 5A). GYY4137, but not Na_2S, administration attenuated the negative effects of inflammation on *Adipoq*, *Fasn* and *Glut4* gene expression, but not *Il6*, during adipocyte differentiation (Fig. 5A).

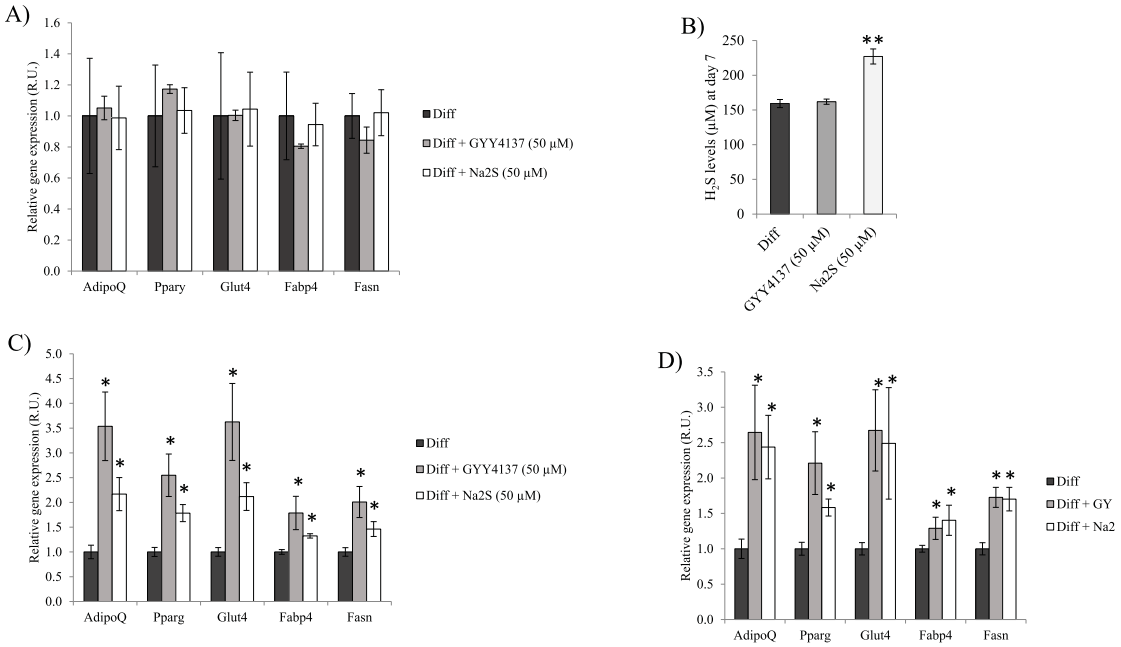

Fig. 3. A-B) Effects of GYY4137 (50 µM) and Na_2S (50 µM) treatments on expression of adipogenic and lipogenic related genes **(A)** and H_2S levels **(B)** at day 7, administrating hydrogen sulfide donors from day 0–7 during 3T3-L1 adipogenesis. **C-D)** Effects of GYY4137 (50 µM) and Na_2S (50 µM) treatments on expression of adipogenic and lipogenic related genes at day 7, administrating hydrogen sulfide donors only from day 0–2 **(C)** or from day 2–7 **(D)**. Control differentiated (black bars), GYY4137 (grey bars) and Na_2S (white bars). *p < 0.05 and **p < 0.01 compared with control differentiated. These data are expressed as mean ± SEM.

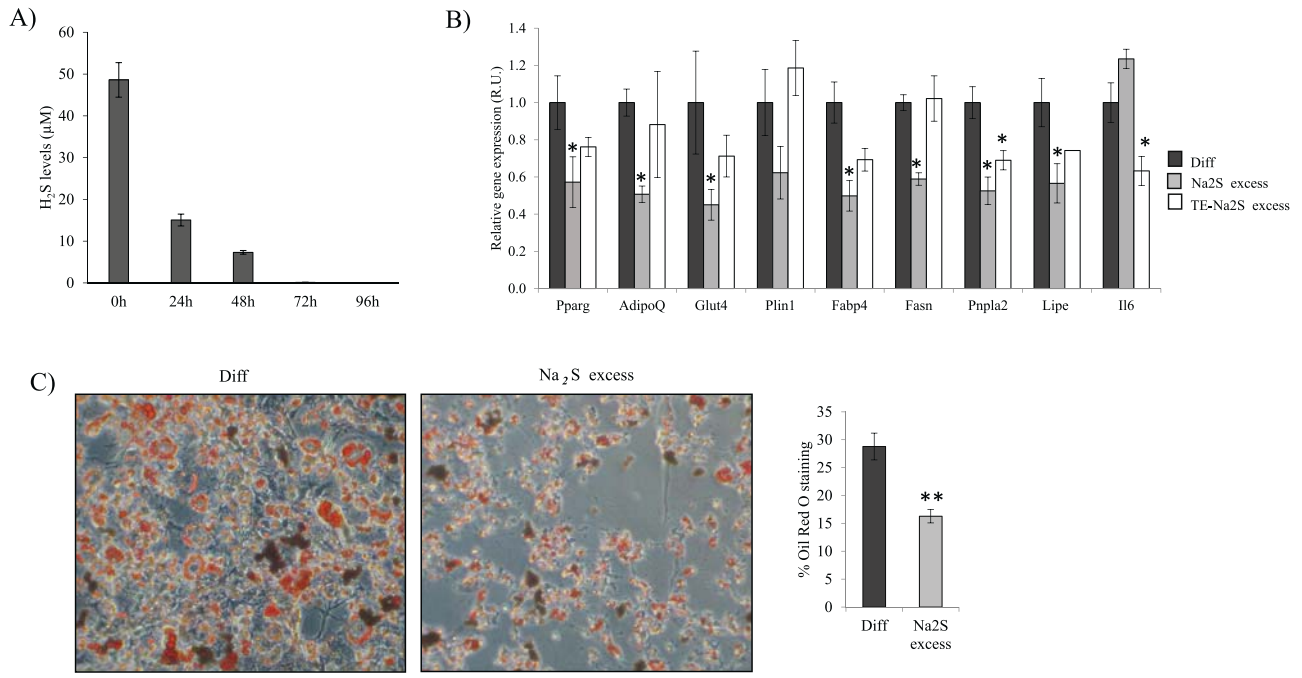

Fig. 4. A) Effects of one single dose of Na_2S (50 µM diluted in PBS) on H_2S levels in cell culture conditions (without cells) at several points (0, 24, 48, 72 and 96 h). **B–C)** Effects of Na_2S and time-expired Na_2S excess administration on expression of adipogenic, lipogenic and lipolytic related genes during 3T3-L1 adipogenesis (**B**), and intracellular lipid accumulation using Oil red staining (**C**). Control differentiated (black bars), Na_2S excess (grey bars) and time-expired Na_2S excess (white bars). *$p < 0.05$ compared with control differentiated. These data are expressed as mean ± SEM. (For interpretation of the references to color in this figure legend, the reader is referred to the Web version of this article.)

3.6. Effects of Na_2S and GYY4137 in fully differentiated 3T3-L1 adipocytes in inflammatory conditions

Treatment of inflamed adipocytes with Na_2S led to decreased adipogenic gene expression (*Adipoq, Pparg* and *Fabp4*) and insulin action (*Glut4*) related gene expression and increases inflammatory gene expression (*Il6*), whereas GYY4137 treatment only increases significantly *Pparg*, tend to decrease the expression of *Il6*, and had no significant effect in the expression of the other adipogenic-related genes studied (Fig. 5B).

4. Discussion

To best of our knowledge this is the first study exploring the role of H_2S in 3T3-L1 preadipocytes during differentiation and in mature adipocytes in inflammatory conditions using different H_2S donors. Specifically, H_2S biosynthesis was increased during adipocyte differentiation, and H_2S donor (GYY4137 and Na_2S) administration at different stages of adipocyte differentiation process resulted in enhanced adipogenesis, whereas treatments with a specific inhibitor of endogenous H_2S biosynthesis (PPG) impaired adipogenesis and increased inflammation. Even though, several studies reported H_2S concentration in human serum in a range of 10–200 µM (Karunya et al., 2019; Chen et al., 2005; Li et al., 2005; Peng et al., 2011) or higher (Hamidi Shishavan et al., 2017), other studies (Whitfield et al., 2008; Furne et al., 2008; Olson, 2009; Shen et al., 2012) argue reduced H_2S levels in serum using sound arguments. In current study, to evaluate H_2S biosynthesis at different stage of adipocyte differentiation (day 0, 2 and 7), the 24 h cumulative H_2S concentration were measured, indicating cell capacity for H_2S production, but not its physiological levels. In line with these studies (Whitfield et al., 2008; Furne et al., 2008; Olson, 2009; Shen et al., 2012), when adipocyte conditioned medium with L1 probe was incubated for 1 h, H_2S concentration (physiological levels) were undetectable.

In addition, GYY4137 administration attenuated the negative effects of inflammation during adipogenesis (Constant et al., 2008; Yarmo et al., 2010), whereas Na_2S aggravates the negative effects of inflammation on mature inflamed adipocytes.

These adipogenic and antiinflammatory activities of GYY4137 might be explained through the sulfhydration of PPARγ and NFκB cysteine residues (Cai et al., 2016; Du et al., 2014). Sulfhydrated PPARγ increased its nuclear accumulation, DNA binding activity and adipogenesis gene expression, thereby increasing glucose uptake and lipid storage (Cai et al., 2016), whereas sulfhydrated p65 subunit of NF-κB at cysteine-38 inhibited macrophage inflammation by suppressing NFκB pathway activation (Du et al., 2014). Supporting current data, Na_2S and GYY4137 administration was found to be associated positively with adipogenic and lipogenic gene expression in 3T3-L1 cells, whereas ZYJ1122 (a structural analogue of GYY4137 lacking sulfur) had not any effects in these gene expression (Tsai et al., 2015). Furthermore, Lee and colleagues demonstrated that hydrogen sulfide donor, diallyl disulfide, promotes adipogenesis in 3T3-L1 cells (Lee et al., 2007). On the other hand, other studies reported antiadipogenic effect of hydrogen sulfide donors derived from garlic (Kim et al., 2012; Lii et al., 2012). Of note, daily administration of Na_2S during 3T3-L1 differentiation inhibited adipogenesis, suggesting that H_2S excess suppressed adipogenic differentiation. No significant effects of time-expired Na_2S on adipogenic markers were found, indicating that H_2S from donors was the responsible of adipogenic effect. Donors used in current study released H_2S at different rates, Na_2S is a fast-releasing H_2S donor and GYY4137 is a slow-releasing H_2S donor, producing in consequence different concentrations of the H_2S at several times (Whiteman et al., 2010). These differences in H_2S availability and concentration could explain why GYY4137 was more effective than Na_2S in promoting adipocyte differentiation and attenuating the negative effects of inflammation on adipogenesis.

Inflammation in adipocytes is known to decrease adipogenesis in parallel to increased insulin resistance (Gustafson and Smith, 2006), so

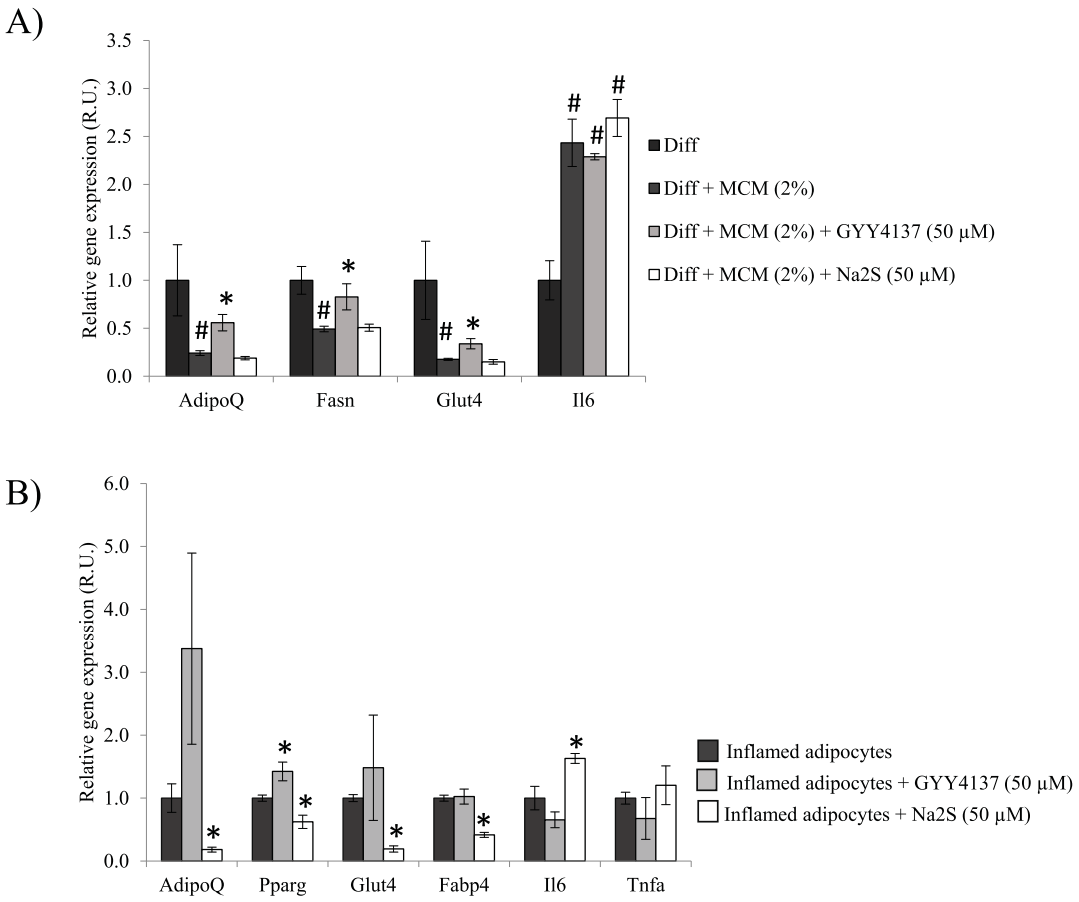

Fig. 5. A) Effects of GYY4137 (50 µM) and Na_2S (50 µM) administration on adipogenic and inflammatory gene expression during 3T3-L1 differentiation in inflammatory conditions at day 7. **B)** Effects of GYY4137 (50 µM) and Na_2S (50 µM) administration during 48 h on adipogenic and inflammatory gene expression in inflamed fully differentiated 3T3-L1 adipocytes. Control differentiated (black bars), inflamed control (dark grey bars), GYY4137 (grey bars) and Na_2S (white bars). #p < 0.05 compared with control differentiated and *p < 0.05 compared with inflamed control. These data are expressed as mean ± SEM.

novel therapeutic strategies targeting adipose tissue to mitigate inflammation are emerging (Kusminski et al., 2016). Current findings reveal that GYY4137 may represent an innovative therapeutic tool against obesity-related adipose tissue inflammation.

It is well known that GYY4137 release is slower than Na_2S (Powell et al., 2018; Rose et al., 2015). A previous study demonstrated that the rate of H_2S release from GYY4137 (1 mM, pH 7.4, 37 °C) was 4.17 ± 0.5 nmol/25 min (Li et al., 2008). In agreement with these studies, GYY4137 (50 µM) administration did not result in a significant increase in H_2S levels in adipocyte conditioned media.

In conclusion, altogether these data demonstrated that H_2S in adipocytes plays a pivotal role regulating adipogenesis under normal and pro-inflammatory conditions. Interactions between adipocytes and H_2S may represent a novel target for restoring adipocytes physiologic function.

Funding

This work was partially supported by research grants PI15/01934 and PI16/01173 from the Instituto de Salud Carlos III from Spain and VII Spanish Diabetes Association grants to Basic Diabetes Research Projects led by young researchers. CIBEROBN Fisiopatología de la Obesidad y Nutrición is an initiative from the Instituto de Salud Carlos III and Fondo Europeo de Desarrollo Regional (FEDER) from Spain.

Declarations of interest

None.

Conflicts of interest

The authors declare no conflict of interest.

Authors' contributions.

FC, JMF-R and JMM-N participated in conception and design of the study, acquisition of data and analysis and interpretation of data, and drafted the article. JL, OC, FO, AL, MS, AC-N, WR, XR, MC participated in acquisition and analysis of data, and read the article critically for important intellectual content. All authors read and approved the final manuscript, and agreed to be accountable for all aspects of the work.

Acknowledgements

This work was partially supported by research grants PI15/01934 and PI16/01173 from the Instituto de Salud Carlos III from Spain and VII Spanish Diabetes Association grants to Basic Diabetes Research Projects led by young researchers. CIBEROBN Fisiopatología de la Obesidad y Nutrición is an initiative from the Instituto de Salud Carlos III and Fondo Europeo de Desarrollo Regional (FEDER) from Spain.

References

Ang, S.-F., Sio, S.W.S., Moochhala, S.M., MacAry, P.A., Bhatia, M., 2011. Hydrogen sulfide upregulates cyclooxygenase-2 and prostaglandin E metabolite in sepsis-evoked acute lung injury via transient receptor potential vanilloid type 1 channel activation. J. Immunol. 187 (9), 4778–4787. https://doi.org/10.4049/jimmunol.1101559.

Badiei, A., Chambers, S.T., Gaddam, R.R., Bhatia, M., 2016. Cystathionine-γ-lyase gene silencing with siRNA in monocytes/macrophages attenuates inflammation in cecal ligation and puncture-induced sepsis in the mouse. J. Bio Sci. 41 (1), 87–95. http://www.ncbi.nlm.nih.gov/pubmed/26949091, Accessed date: 4 December 2018.

Cai, J., Shi, X., Wang, H., et al., 2016. Cystathionine γ lyase–hydrogen sulfide increases peroxisome proliferator-activated receptor γ activity by sulfhydration at C139 site thereby promoting glucose uptake and lipid storage in adipocytes. Biochim. Biophys. Acta Mol. Cell Biol. Lipids 1861 (5), 419–429. https://doi.org/10.1016/j.bbalip.2016.03.001.

Chen, Y.H., Yao, W.Z., Geng, B., Ding, Y.L., Lu, M., Zhao, M.W., Tang, C.S., 2005. Endogenous hydrogen sulfide in patients with COPD. Chest 128 (5), 3205–3211. https://doi.org/10.1378/chest.128.5.3205.

Chen, Y.-H., Wu, R., Geng, B., et al., 2009. Endogenous hydrogen sulfide reduces airway inflammation and remodeling in a rat model of asthma. Cytokine 45 (2), 117–123. https://doi.org/10.1016/j.cyto.2008.11.009.

Chen, X., Xu, W., Wang, Y., et al., 2014. Hydrogen sulfide reduces kidney injury due to urinary-derived sepsis by inhibiting NF-κB expression, decreasing TNF-α levels and increasing IL-10 levels. Exp. Ther. Med. 8 (2), 464–470. https://doi.org/10.3892/etm.2014.1781.

Choi, S.-A., Park, C.S., Kwon, O.S., et al., 2016. Structural effects of naphthalimide-based fluorescent sensor for hydrogen sulfide and imaging in live zebrafish. Sci. Rep. 6 (1), 26203. https://doi.org/10.1038/srep26203.

Collin, M., Anuar, F.B.M., Murch, O., Bhatia, M., Moore, P.K., Thiemermann, C., 2005. Inhibition of endogenous hydrogen sulfide formation reduces the organ injury caused by endotoxemia. Br. J. Pharmacol. 146 (4), 498–505. https://doi.org/10.1038/sj.bjp.0706367.

Constant, V.A., Gagnon, A., Yarmo, M., Sorisky, A., 2008. The antiadipogenic effect of macrophage-conditioned medium depends on ERK1/2 activation. Metabolism 57 (4), 465–472. https://doi.org/10.1016/j.metabol.2007.11.005.

Du, J., Huang, Y., Yan, H., Zhang, Q., Zhao, M., Zhu, M., Liu, J., Chen, S.X., Bu, D., Tang, C., Jin, H., 2014. Hydrogen sulfide suppresses oxidized low-density lipoprotein (ox-LDL)-stimulated monocyte chemoattractant protein 1 generation from macrophages via the nuclear factor κB (NF-κB) pathway. J. Biol. Chem. 289 (14), 9741–9753. https://doi.org/10.1074/jbc.M113.517995.

Furne, J., Saeed, A., Levitt, M.D., 2008. Whole tissue hydrogen sulfide concentrations are orders of magnitude lower than presently accepted values. Am. J. Physiol. Regul. Integr. Comp. Physiol. 295 (5), R1479–R1485. https://doi.org/10.1152/ajpregu.90566.2008.

Gustafson, B., Smith, U., 2006. Cytokines promote wnt signaling and inflammation and impair the normal differentiation and lipid accumulation in 3t3-L1 preadipocytes. J. Biol. Chem. 281 (14), 9507–9516. https://doi.org/10.1074/jbc.M512077200.

Hamidi Shishavan, M., Henning, R.H., van Buiten, A., Goris, M., Deelman, L.E., Buikema, H., 2017. Metformin improves endothelial function and reduces blood pressure in diabetic spontaneously hypertensive rats independent from glycemia control: comparison to vildagliptin. Sci. Rep. 7 (1), 10975. https://doi.org/10.1038/s41598-017-11430-7.

Karunya, R., Jayaprakash, K.S., Gaikwad, R., Sajeesh, P., Ramshad, K., Muraleedharan, K.M., Dixit, M., Thangaraj, P.R., Sen, A.K., 2019. Rapid measurement of hydrogen sulphide in human blood plasma using a microfluidic method. Sci. Rep. 9 (1), 3258. https://doi.org/10.1038/s41598-019-39389-7.

Kim, E.J., Lee, D.H., Kim, H.J., et al., 2012. Thiacremonone, a sulfur compound isolated from garlic, attenuates lipid accumulation partially mediated via AMPK activation in 3T3-L1 adipocytes. J. Nutr. Biochem. 23 (12), 1552–1558. https://doi.org/10.1016/j.jnutbio.2011.10.008.

Kusminski, C.M., Bickel, P.E., Scherer, P.E., 2016. Targeting adipose tissue in the treatment of obesity-associated diabetes. Nat. Rev. Drug Discov. 15 (9), 639–660. https://doi.org/10.1038/nrd.2016.75.

Lee, J.-H., Kim, K.-A., Kwon, K.-B., et al., 2007. Diallyl disulfide accelerates adipogenesis in 3T3-L1 cells. Int. J. Mol. Med. 20 (1), 59–64. http://www.ncbi.nlm.nih.gov/pubmed/17549389, Accessed date: 4 December 2018.

Lee, M., Katerelos, M., Gleich, K., Galic, S., Kemp, B.E., Mount, P.F., Power, D.A., 2018. Phosphorylation of acetyl-CoA carboxylase by AMPK reduces renal fibrosis and is essential for the anti-fibrotic effect of metformin. J. Am. Soc. Nephrol. 29 (9), 2326–2336. https://doi.org/10.1681/ASN.2018010050.

Li, L., Bhatia, M., Zhu, Y.Z., Zhu, Y.C., Ramnath, R.D., Wang, Z.J., Anuar, F.B., Whiteman, M., Salto-Tellez, M., Moore, P.K., 2005. Hydrogen sulfide is a novel mediator of lipopolysaccharide-induced inflammation in the mouse. FASEB J. 19 (9), 1196–1198. https://doi.org/10.1096/fj.04-3583fje.

Li, L., Whiteman, M., Guan, Y.Y., Neo, K.L., Cheng, Y., Lee, S.W., Zhao, Y., Baskar, R., Tan, C.H., Moore, P.K., 2008. Characterization of a novel, water-soluble hydrogen sulfide-releasing molecule (GYY4137): new insights into the biology of hydrogen sulfide. Circulation 117 (18), 2351–2360. https://doi.org/10.1161/CIRCULATIONAHA.107.753467.

Li, L., Hsu, A., Moore, P.K., 2009. Actions and interactions of nitric oxide, carbon monoxide and hydrogen sulphide in the cardiovascular system and in inflammation — a tale of three gases!. Pharmacol. Ther. 123 (3), 386–400. https://doi.org/10.1016/j.pharmthera.2009.05.005.

Lii, C.-K., Huang, C.-Y., Chen, H.-W., et al., 2012. Diallyl trisulfide suppresses the adipogenesis of 3T3-L1 preadipocytes through ERK activation. Food Chem. Toxicol. 50 (3–4), 478–484. https://doi.org/10.1016/j.fct.2011.11.020.

Moreno-Navarrete, J.M., Ortega, F.J., Ricart, W., Fernandez-Real, J.M., 2009. Lactoferrin increases (172Thr)AMPK phosphorylation and insulin-induced (p473Ser)AKT while impairing adipocyte differentiation. Int. J. Obes. 33 (9), 991–1000. https://doi.org/10.1038/ijo.2009.143.

Moreno-Navarrete, J.M., Ortega, F., Moreno, M., Serrano, M., Ricart, W., Fernández-Real, J.M., 2014. Lactoferrin gene knockdown leads to similar effects to iron chelation in human adipocytes. J. Cell Mol. Med. 18 (3), 391–395. https://doi.org/10.1111/jcmm.12234.

Olson, K.R., 2009. Is hydrogen sulfide a circulating "gasotransmitter" in vertebrate blood? Biochim. Biophys. Acta 1787 (7), 856–863. https://doi.org/10.1016/j.bbabio.2009.03.019.

Peng, H., Cheng, Y., Dai, C., King, A.L., Predmore, B.L., Lefer, D.J., Wang, B., 2011 Oct 4. A fluorescent probe for fast and quantitative detection of hydrogen sulfide in blood. Angew Chem. Int. Ed. Engl. 50 (41), 9672–9675. https://doi.org/10.1002/anie.201104236.

Powell, C.R., Dillon, K.M., Matson, J.B., 2018. A review of hydrogen sulfide (H2S) donors: chemistry and potential therapeutic applications. Biochem. Pharmacol. 149, 110–123. https://doi.org/10.1016/j.bcp.2017.11.014.

Rose, P., Dymock, B.W., Moore, P.K., 2015. GYY4137, a novel water-soluble, H2S-releasing molecule. Methods Enzymol. 554, 143–167. https://doi.org/10.1016/bs.mie.2014.11.014.

Schindelin, J., Arganda-Carreras, I., Frise, E., Kaynig, V., Longair, M., Pietzsch, T., Preibisch, S., Rueden, C., Saalfeld, S., Schmid, B., Tinevez, J.Y., White, D.J., Hartenstein, V., Eliceiri, K., Tomancak, P., Cardona, A., 2012. Fiji: an open-source platform for biological-image analysis. Nat. Methods 9 (7), 676–682. https://doi.org/10.1038/nmeth.2019.

Shen, X., Peter, E.A., Bir, S., Wang, R., Kevil, C.G., 2012. Analytical measurement of discrete hydrogen sulfide pools in biological specimens. Free Radic. Biol. Med. 52 (11–12), 2276–2283. https://doi.org/10.1016/j.freeradbiomed.2012.04.007.

Stipanuk, M.H., 2004. SULFUR AMINO ACID METABOLISM: pathways for production and removal of homocysteine and cysteine. Annu. Rev. Nutr. 24 (1), 539–577. https://doi.org/10.1146/annurev.nutr.24.012003.132418.

Szabó, C., 2007. Hydrogen sulphide and its therapeutic potential. Nat. Rev. Drug Discov. 6 (11), 917–935. https://doi.org/10.1038/nrd2425.

Tokuda, K., Kida, K., Marutani, E., et al., 2012. Inhaled hydrogen sulfide prevents endotoxin-induced systemic inflammation and improves survival by altering sulfide metabolism in mice. Antioxidants Redox Signal. 17 (1), 11–21. https://doi.org/10.1089/ars.2011.4363.

Tsai, C.-Y., Peh, M.T., Feng, W., Dymock, B.W., Moore, P.K., 2015. Hydrogen sulfide promotes adipogenesis in 3T3L1 cells. PLoS One 10 (3). https://doi.org/10.1371/journal.pone.0119511. e0119511.

Velmurugan, G.V., Huang, H., Sun, H., et al., 2015. Depletion of H_2S during obesity enhances store-operated Ca2+ entry in adipose tissue macrophages to increase cytokine production. Sci. Signal. 8 (407), ra128. https://doi.org/10.1126/scisignal.aac7135.

Whiteman, M., Moore, P.K., 2009. Hydrogen sulfide and the vasculature: a novel vasculoprotective entity and regulator of nitric oxide bioavailability? J. Cell Mol. Med. 13 (3), 488–507. https://doi.org/10.1111/j.1582-4934.2009.00645.x.

Whiteman, M., Li, L., Rose, P., Tan, C.-H., Parkinson, D.B., Moore, P.K., 2010. The effect of hydrogen sulfide donors on lipopolysaccharide-induced formation of inflammatory mediators in macrophages. Antioxidants Redox Signal. 12 (10), 1147–1154. https://doi.org/10.1089/ars.2009.2899.

Whitfield, N.L., Kreimier, E.L., Verdial, F.C., Skovgaard, N., Olson, K.R., 2008. Reappraisal of H2S/sulfide concentration in vertebrate blood and its potential significance in ischemic preconditioning and vascular signaling. Am. J. Physiol. Regul. Integr. Comp. Physiol. 294 (6), R1930–R1937. https://doi.org/10.1152/ajpregu.00025.2008.

Yan, Y., Chen, C., Zhou, H., et al., 2013. Endogenous hydrogen sulfide formation mediates the liver damage in endotoxemic rats. Res. Vet. Sci. 94 (3), 590–595. https://doi.org/10.1016/j.rvsc.2012.10.009.

Yang, G., Wu, L., Jiang, B., et al., 2008 Oct 24. H2S as a physiologic vasorelaxant: hypertension in mice with deletion of cystathionine gamma-lyase. Science 322 (5901), 587–590. https://doi.org/10.1126/science.1162667.

Yang, C., Yang, Z., Zhang, M., et al., 2011. Hydrogen sulfide protects against chemical hypoxia-induced cytotoxicity and inflammation in HaCaT cells through inhibition of ROS/NF-κB/COX-2 pathway. Agarwal, S. (Ed.), PLoS One 6 (7), e21971. https://doi.org/10.1371/journal.pone.0021971.

Yang, G., Ju, Y., Fu, M., et al., 2018. Cystathionine gamma-lyase/hydrogen sulfide system is essential for adipogenesis and fat mass accumulation in mice. Biochim. Biophys. Acta Mol. Cell Biol. Lipids 1863 (2), 165–176. https://doi.org/10.1016/j.bbalip.2017.11.008.

Yarmo, M.N., Gagnon, A., Sorisky, A., 2010. The anti-adipogenic effect of macrophage-conditioned medium requires the IKKβ/NF-κB pathway. Horm. Metab. Res. 42 (12), 831–836. https://doi.org/10.1055/s-0030-1263124.

Zhang, H., Zhi, L., Moochhala, S., Moore, P.K., Bhatia, M., 2007. Hydrogen sulfide acts as an inflammatory mediator in cecal ligation and puncture-induced sepsis in mice by upregulating the production of cytokines and chemokines via NF-κB. Am. J. Physiol. Lung Cell Mol. Physiol 292 (4), L960–L971. https://doi.org/10.1152/ajplung.00388.2006.

MANUSCRIPT 3

Ferran Comas, Jèssica Latorre, Francisco Ortega, Núria Oliveras, Aina Lluch, Wifredo Ricart, José Manuel Fernandez-Real, José Maria Moreno-Navarrete. **Permanent cystathionine-β-Synthase gene knockdown promotes inflammation and oxidative stress in immortalized human adipose-derived mesenchymal stem cells, enhancing their adipogenic capacity.** *Redox Biol.* 2020 Aug; doi: 10.1016/j.redox.2020.101668.

Impact factor (2019): 9.986 (D1, Biochemistry & Molecular biology)

Graphical abstract

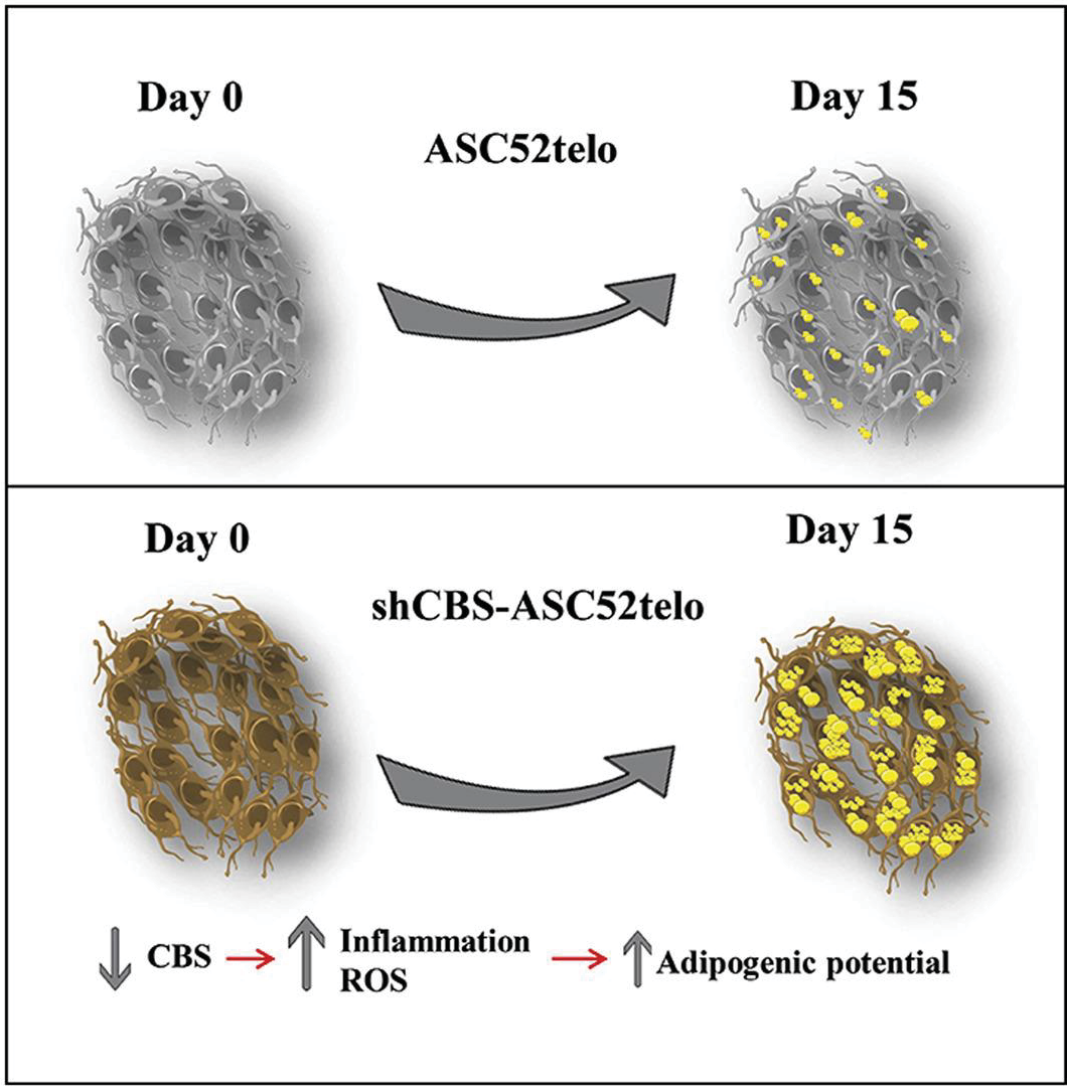

ARTICLE IN PRESS

Redox Biology xxx (xxxx) xxx

Contents lists available at ScienceDirect

Redox Biology

journal homepage: www.elsevier.com/locate/redox

Research Paper

Permanent cystathionine-β-Synthase gene knockdown promotes inflammation and oxidative stress in immortalized human adipose-derived mesenchymal stem cells, enhancing their adipogenic capacity

Ferran Comas [a], Jèssica Latorre [a], Francisco Ortega [a], Núria Oliveras-Cañellas [a], Aina Lluch [a], Wifredo Ricart [a], José Manuel Fernández-Real [a,b,**], José María Moreno-Navarrete [a,b,*]

[a] Department of Diabetes, Endocrinology and Nutrition, Institut d'Investigació Biomèdica de Girona (IdIBGi), CIBEROBN (CB06/03/010) and Instituto de Salud Carlos III (ISCIII), Girona, Spain
[b] Department of Medicine, Universitat de Girona, Girona, Spain

ARTICLE INFO

Keywords:
Human adipose-derived mesenchymal stem cells
Cystathionine β-synthase
Cellular senescence
Inflammation
Oxidative stress and adipogenesis

ABSTRACT

In the present study, we aimed to investigate the impact of permanent cystathionine-β-Synthase (CBS) gene knockdown in human telomerase reverse transcriptase (hTERT) immortalized human adipose-derived mesenchymal stem cells (ASC52telo) and in their capacity to differentiate into adipocytes. *CBS* gene KD in ASC52telo cells led to increased cellular inflammation (*IL6, CXCL8, TNF*) and oxidative stress markers (increased intracellular reactive oxygen species and decreased reduced glutathione levels) in parallel to decreased H_2S production and rejuvenation (*LC3* and *SIRT1*)-related gene expression. In addition, *CBS* gene KD in ASC52telo cells resulted in altered mitochondrial respiratory function, characterised by decreased basal respiration (specifically proton leak) and spare respiratory capacity, without significant effects on cell viability and proliferation. In this context, shCBS-ASC52telo cells displayed enhanced adipogenic (*FABP4, ADIPOQ, SLC2A4, CEBPA, PPARG*)-, lipogenic (*FASN, DGAT1*)- and adipocyte (*LEP, LBP*)-related gene expression markers, decreased expression of proinflammatory cytokines, and increased intracellular lipid accumulation during adipocyte differentiation compared to control ASC52telo cells. Otherwise, the increased adipogenic potential of shCBS-ASC52telo cells was detrimental to the ability to differentiate into osteogenic linage. In conclusion, this study demonstrated that permanent *CBS* gene KD in ASC52telo cells promotes a cellular senescence phenotype with a very increased adipogenic potential, promoting a non-physiological enhanced adipocyte differentiation with excessive lipid storage.

1. Introduction

Recent studies in 3T3-L1 cells pointed to a relevant role of transulfuration pathway in adipogenesis [1–4]. Even though Tsai et al. reported that both transulfuration pathway enzymes [cystathionine β-synthase (CBS) and cystathionine γ-lyase (CTH or CSE)] were important in adipocyte differentiation [1], the latter studies demonstrated that only CTH exerted a relevant role in adipogenesis increasing PPARγ activity during adipocyte differentiation [2,3]. In fact, in a previous study, in which *Cth* and *Cbs* gene expression in 3T3-L1 cells was analysed and compared, we found that *Cth* was highly expressed in preadipocytes and increased during adipocyte differentiation, whereas expression of *Cbs* gene was almost undetectable in preadipocytes and did not change during adipocyte differentiation, even tending to decrease in the first two days of the process [4].

Human adipose-derived mesenchymal stem cells (hAMSC), the adipocyte precursor cells located in adipose tissue stromal vascular fraction, are required for adipose tissue hyperplasia and functionality [5,6]. A previous study reported a useful human telomerase reverse transcriptase (hTERT) immortalized hAMSC (ASC52telo) cell model to study

* Corresponding author. Department of Diabetes, Endocrinology and Nutrition, Institut d'Investigació Biomèdica de Girona (IdIBGi), Parc Hospitalari Martí i Julià - Edifici M2, C/ Dr. Castany s/n, 17190, Salt, Spain.
** Corresponding author. Section of Diabetes, Endocrinology and Nutrition, Institut d'Investigació Biomèdica de Girona (IdIBGi), Hospital of Girona "Dr Josep Trueta", Carretera de França s/n, 17007, Girona, Spain.
E-mail addresses: jmfreal@idibgi.org (J.M. Fernández-Real), jmoreno@idibgi.org (J.M. Moreno-Navarrete).

https://doi.org/10.1016/j.redox.2020.101668
Received 23 June 2020; Accepted 29 July 2020
Available online 2 August 2020

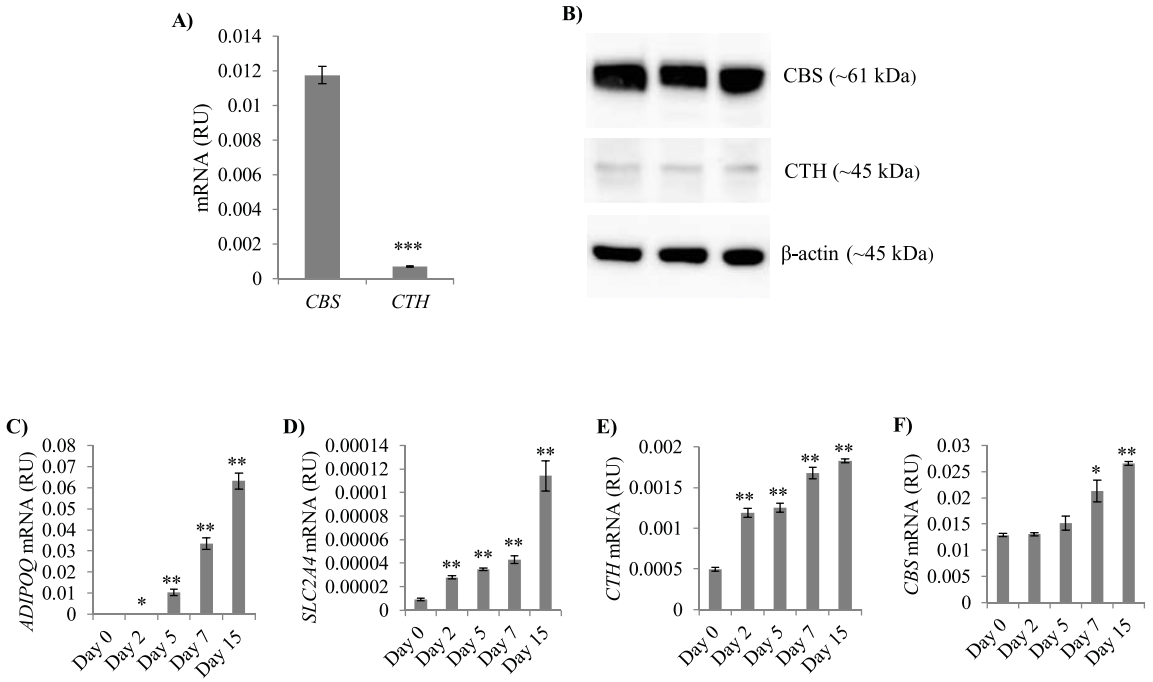

Fig. 1. A) *CBS* and *CTH* mRNA levels in ASC52telo cells,***p < 0.001. **B)** Representative Western blot of CBS and CTH protein in ASC52telo cell lysates. **C–F)** *ADIPOQ, SLC2A4, CTH* and *CBS* mRNA levels during adipocyte differentiation of ASC52telo cells. *p < 0.05 and **p < 0.01 *vs* day 0.

adipocyte differentiation [7].

To the best of our knowledge, the importance of transulfuration pathway in hAMSC adipogenesis has not been yet examined. Taking advantage of ASC52telo cells, in the present study, we aimed to investigate the possible role of CBS enzyme in hAMSC during adipocyte differentiation.

2. Material and methods

2.1. Differentiation of human immortalized adipose-derived mesenchymal stem cells

Human telomerase reverse transcriptase immortalized adipose-derived MSC (ASC52telo, SCRC-4000, ATCC, LGC Standards SLU, Barcelona, Spain) cells were cultured in Mesenchymal Stem Cell Basal Medium (ATCC PCS-500-030) plus FBS (2%), rhFGF basic (5 ng/ml), rhFGF acidic (5 ng/ml), rhEGF (5 ng/ml), L-Alanyl-L-Glutamine (2.4 mM) and G418 (0.2 mg/ml) at 37 °C in a 5% CO2 in air atmosphere.

Adipogenic differentiation. ASC52telo cells were cultured in three repetitive cycles of 72 h in adipogenic differentiation medium composed of DMEM/Nutrient Mix F-12 medium, FBS (10%), penicillin, streptomycin, human insulin (10 μg/mL), DXM (1 μmol/L), isobutylmethylxanthine (0.5 mmol/L), and PPARγ agonists (rosiglitazone, 1 μmol/L), followed by 72 h in adipogenic maintenance medium composed of DMEM/Nutrient Mix F-12 medium, FBS (10%), penicillin, streptomycin, and human insulin (10 μg/mL).

Osteogenic differentiation. ASC52telo cells were cultured with osteogenic differentiation medium composed of DMEM/Nutrient Mix F-12 medium, FBS (10%), 50 μg/ml ascorbic 2-phosphate, 10 nM dexamethasone and 10 mM β-glycerophosphate. Osteogenic medium was refreshed every 3 days. After 9 days, the cells were harvested.

2.2. Short hairpin (sh) RNA-mediated knockdown of CBS gene

Permanent silencing was performed using *CBS*-targeted and control (scrambled) shRNA lentiviral particles (sc-60335-V and sc-108080, Santa Cruz Biotechnology, CA, USA) and following the manufacturer instructions. Positive hAMSC harboring shRNA cassette for *CBS* were selected by puromycin (3 μg/mL) selection 60 h after infection.

2.3. In vitro measurements

Intracellular reactive oxygen species were measured using Fluorometric Intracellular ROS Kit (Cat. nº MAK142, Sigma, Madrid, Spain), reduced and total glutathione was measured using Glutathione Colorimetric Assay Kit (Cat. nº K261-100, Biovision, CA, USA). LDH activity and 3-(4,5-dimethyl-2-yl)-2,5-diphenyltetrazolium bromide (MTT) assay were performed with specific commercial kits, Cytotoxicity Detection Kit (LDH) (Cat. nº 11644793001, Roche Diagnostics SL, Barcelona, Spain) and Cell Proliferation Kit (MTT) (Cat. nº 11465007001, Roche Diagnostics SL, Barcelona, Spain). H_2S concentration in cultured medium was assessed as detailed elsewhere [4], using a naphthalimide-based fluorescent sensor 6-Azido-2-[2-[2-(2-hydroxyethoxy)ethoxy]ethyl]benzo[de]isoquinoline-1,3-dione (L1), which was chemically synthesised in Institute of Computational Chemistry and Catalysis (Chemistry Department, University of Girona) as described previously [8]. Intracellular lipid accumulation was assessed by Oil Red O staining as detailed elsewhere [4].

2.4. Mitochondrial respiratory function

Mitochondrial respiratory function was assessed using Seahorse XFp Extracellular Flux Analyzer (Seahorse Bioscience, Agilent Technologies) using Seahorse XFp Cell Mito Stress Test Kit as detailed elsewhere [9].

2.5. RNA expression

Briefly, RNA purification was performed using RNeasy Lipid Tissue Mini Kit (QIAgen, Izasa SA, Barcelona, Spain) and the integrity was checked by Agilent Bioanalyzer (Agilent Technologies, Palo Alto, CA). Gene expression was assessed by real time PCR using an LightCycler® 480 Real-Time PCR System (Roche Diagnostics SL, Barcelona, Spain),

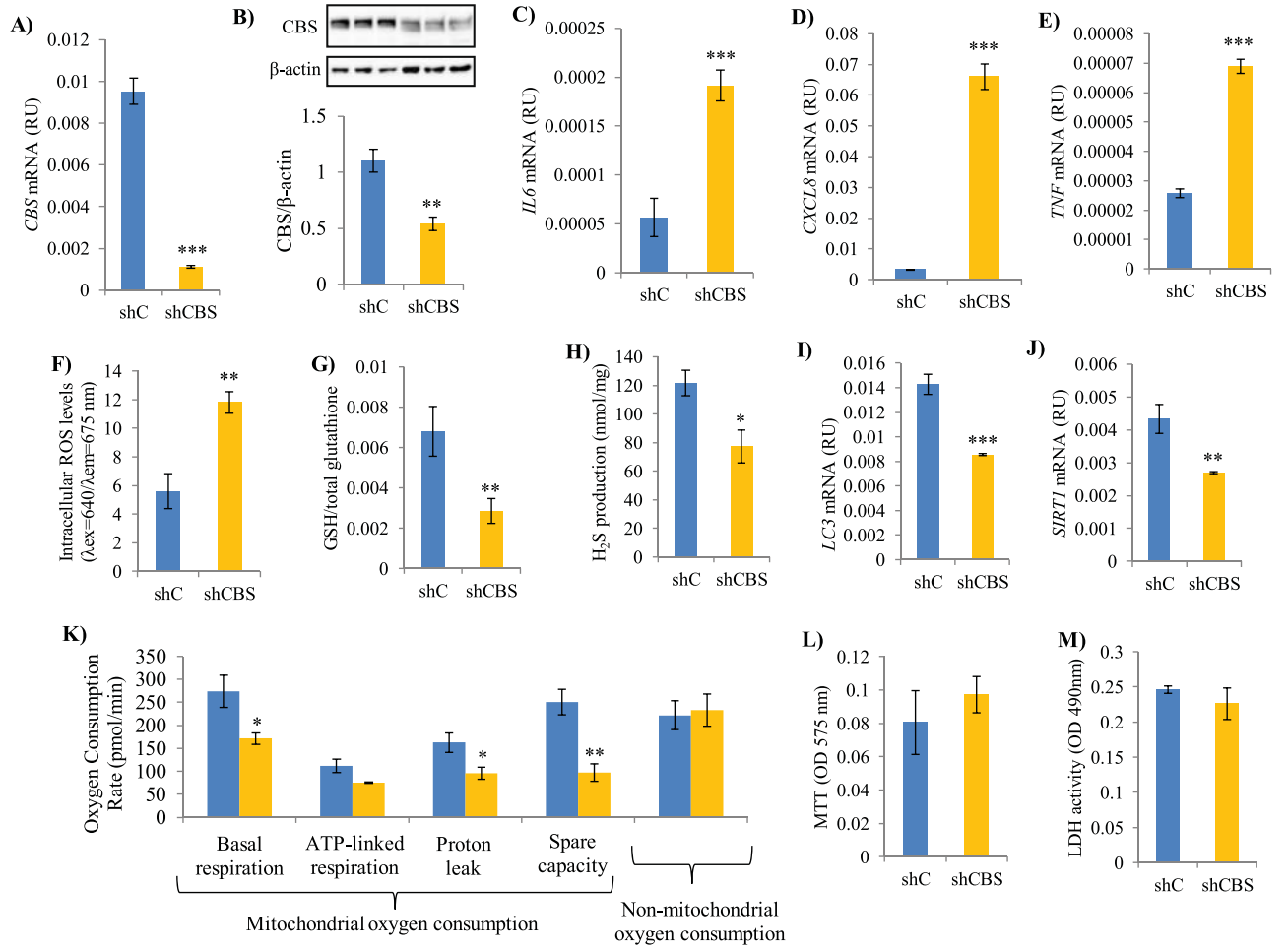

Fig. 2. A-M) Effect of permanent *CBS* gene knockdown (shCBS) on *CBS* mRNA **(A)** and CBS protein **(B)** levels, *IL6* **(C)**, *CXCL8* **(D)** and *TNF* **(E)** mRNA levels, intracellular ROS levels **(F)**, GSH/total glutathione **(G)**, H_2S production **(H)**, *LC3* **(I)** and *SIRT1* **(J)** mRNA levels, mitochondrial respiration **(K)**, MTT assay **(L)** and LDH activity **(M)** in ASC52telo cells. *p < 0.05, **p < 0.01 and ***p < 0.001 *vs* shC-ASC52telo cells.

using TaqMan® and SYBRgreen technology suitable for relative genetic expression quantification. The commercially available and pre-validated TaqMan® primer/probe sets used were as follows: Peptidylprolyl isomerase A (cyclophilin A) (4333763, PPIA as endogenous control), cystathionine γ-lyase (CTH, Hs00542284_m1), cystathionine β-synthase (CBS, Hs00163925_m1), adiponectin (ADIPOQ, Hs00605917_m1), peroxisome proliferator-activated receptor gamma (PPARG, Hs00234592_m1), fatty acid synthase (FASN, Hs00188012_m1), diacylglycerol O-acyltransferase 1 (DGAT1, Hs01020362_g1), CCAAT/enhancer binding protein alpha (CEBPA, Hs00269972_s1), solute carrier family 2 member 4 (SLC2A4 or GLUT4, Hs00168966_m1), insulin receptor substrate 1 (IRS1, Hs00178563_m1), Leptin (LEP, Hs00174877_m1), lipopolysaccharide binding protein (LBP, Hs01084621_m1), interleukin 6 (interferon, beta 2) (IL6, Hs00985639_m1), tumor necrosis factor (TNF, Hs00174128_m1), C-X-C motif chemokine ligand 8 (CXCL8 or IL8, Hs00174103_m1), C–C motif chemokine ligand 2 (CCL2 or MCP1, Hs00234140_m1), microtubule associated protein 1 light chain 3 alpha (MAP1LC3A or LC3, Hs00738808_m1), sirtuin 1 (SIRT1, Hs01009005_m1) and fatty acid binding protein 4, adipocyte (FABP4, Hs01086177_m1).

2.6. Protein preparation and Western blot analysis

Cellular protein were extracted directly in radioimmnuno precipitation assay (RIPA) buffer (0.1% SDS, 0.5% sodium deoxycholate, 1% Nonidet P-40, 150 mM NaCl, and 50 mM Tris-HCl, pH 8.0), supplemented with protease inhibitors (1 mM phenylmethylsulfonyl fluoride). Cellular debris and lipids were eliminated by centrifugation of the solubilized samples at 13000 rpm for 10 min at 4 °C, recovering the soluble fraction. Protein concentration was determined using the RC/DC Protein Assay (Bio-Rad Laboratories, Hercules, CA). RIPA protein extracts (25 μg) were separated by SDS-PPGE and transferred to nitrocellulose membranes by conventional procedures. Membranes were immunoblotted with anti-CTH, CBS and β-actin (sc-365382, sc-133154, sc-47778, Santa Cruz Biotechnology, CA, USA). Anti-mouse IgG coupled to horseradish peroxidase was used as a secondary antibody. Horseradish peroxidase activity was detected by chemiluminescence, and quantification of protein expression was performed using scion image software.

2.7. Statistical analyses

Statistical analyses were performed using SPSS 12.0 software. Unpaired *t*-test and nonparametric test (Mann Whitney test) was used to analyse *in vitro* experimental data. Levels of statistical significance were set at $p < 0.05$.

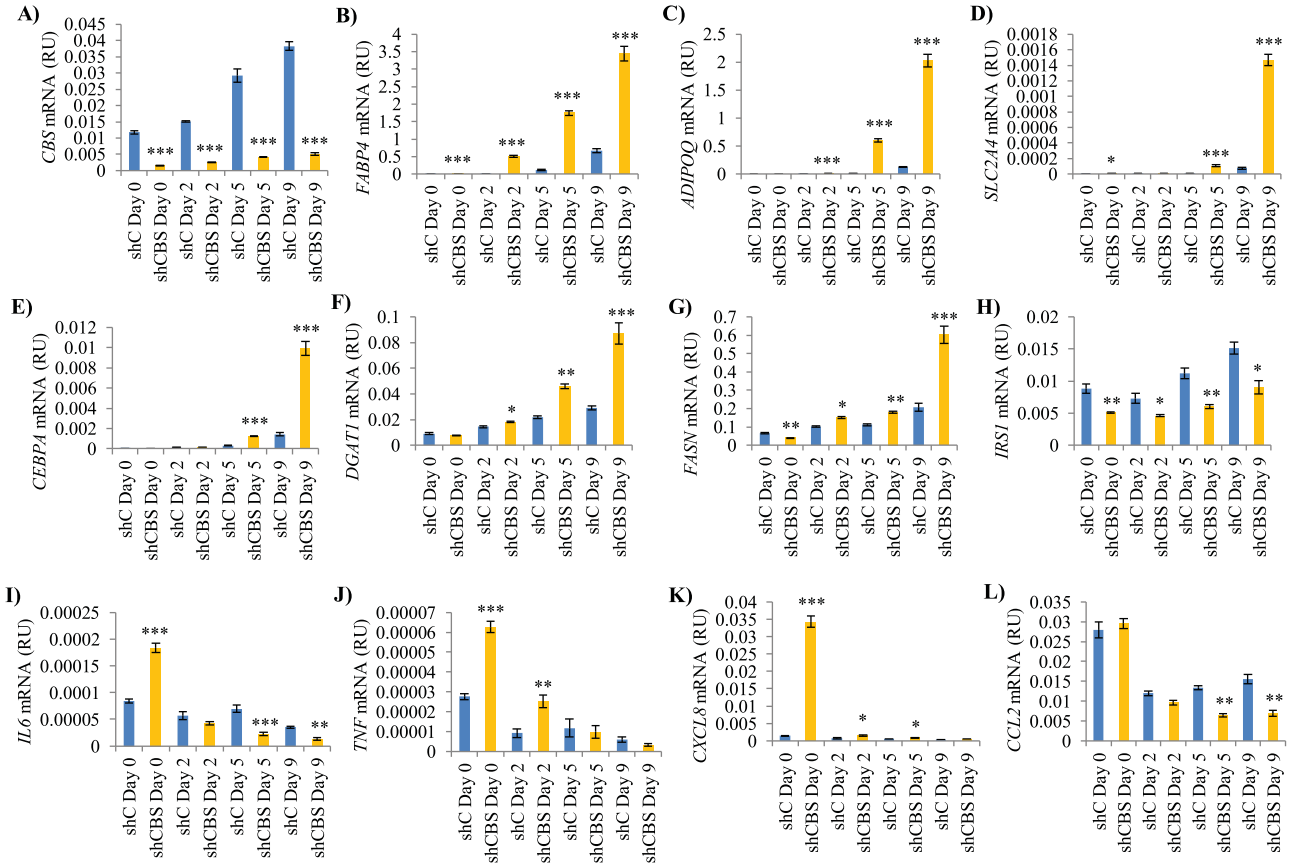

Fig. 3. A-L) Effect of permanent *CBS* gene knockdown (shCBS) on *CBS, FABP4, ADIPOQ, SLC2A4, CEBPA, DGAT1, FASN, IRS1, IL6, TNF, CXCL8* and *CCL2* mRNA levels in a time course experiment during ASC52telo cell adipocyte differentiation. *p < 0.05, **p < 0.01 and ***p < 0.001 *vs* shC-ASC52telo cells.

3. Results

3.1. CBS is much more abundant than CTH in ASC52telo cells

In ASC52telo cells, and contrary to 3T3-L1 cells [4], *Cbs* gene expression and CBS protein levels were significantly increased compared to CTH (Fig. 1A and B).

When adipocyte differentiation was examined in ASC52telo cells, we found a significant increased of adipogenic (*ADIPOQ* and *SLC2A4*) gene expression (Fig. 1C and D) in a time course experiment, confirming that adipogenesis has been appropriately induced in these cells. Similar to the observations in 3T3-L1 cells [4], *CTH* gene expression increased during hAMSC adipocyte differentiation in parallel to adipogenic genes (Fig. 1C–E), whereas *CBS* gene expression also increased but only in the last days of adipocyte differentiation process (Fig. 1F).

3.2. CBS gene KD in ASC52telo cells promotes inflammation and oxidative stress

Considering the higher CBS compared CTH protein levels, the effect of permanent *CBS* gene knockdown (KD) on ASC52telo cells was tested. *CBS* gene KD in these cells (Fig. 2A and B) led to a significant increase in cellular inflammation (*IL6, CXCL8, TNF*) and oxidative stress markers, including increased intracellular reactive oxygen species and decreased intracellular reduced glutathione levels, in parallel to decreased H_2S production (Fig. 2C–H). In addition, *SIRT1* and *LC3* mRNA were also decreased (Fig. 2I and J). Importantly, when mitochondrial respiration was evaluated, we found that *CBS* gene KD in ASC52telo cells resulted in decreased basal respiration (specifically proton leak) and spare respiratory capacity (Fig. 2K). Otherwise, no significant effects *CBS* gene knockdown on cell proliferation (MTT assay, Fig. 2L) or necrosis (LDH activity, Fig. 2M) were found.

3.3. CBS gene KD in ASC52telo cells enhances differentiation into adipocytes

In this context, *CBS* gene KD during ASC52telo adipocyte differentiation (Fig. 3A) led to enhanced adipocyte differentiation, with increased expression of adipogenic genes (*FABP4*, *ADIPOQ, SLC2A4*, *CEBPA, DGAT1, FASN*), but decreased *IRS1*, in a time course experiment (Fig. 3B–H; Suppl Figure 1). Consistent with previous findings (Fig. 2C–E), proinflammatory cytokines (*IL6, TNF* and *CXCL8*), but not the chemokine *CCL2*, were significantly increased at day 0 (Fig. 3I-L). Of interest, *IL6, TNF, CXCL8* and *CCL2* mRNA were strongly reduced during adipocyte differentiation, being significantly decreased *IL6* and *CCL2* at day 5 and 9 in shCBS-ASC52telo cells compared to shC-ASC52telo (control) cells (Fig. 3I-L).

To confirm these enhanced adipogenic capacity of shCBS-ASC52telo, in an independent experiment, we evaluated these cells in adipogenic conditions at day 15 (Fig. 4A). Reinforcing previous observations, shCBS-ASC52telo cells displayed enhanced adipogenic (*FABP4, ADIPOQ, SLC2A4, CEBPA, PPARG*)-, lipogenic (*FASN, DGAT1*)- and adipocyte (*LEP, LBP*)-related gene expression markers (Fig. 4B–J), decreased expression of proinflammatory cytokines (*IL6* and *TNF*) (Fig. 4K-L), and increased intracellular lipid accumulation (Fig. 4M–N) at day 15.

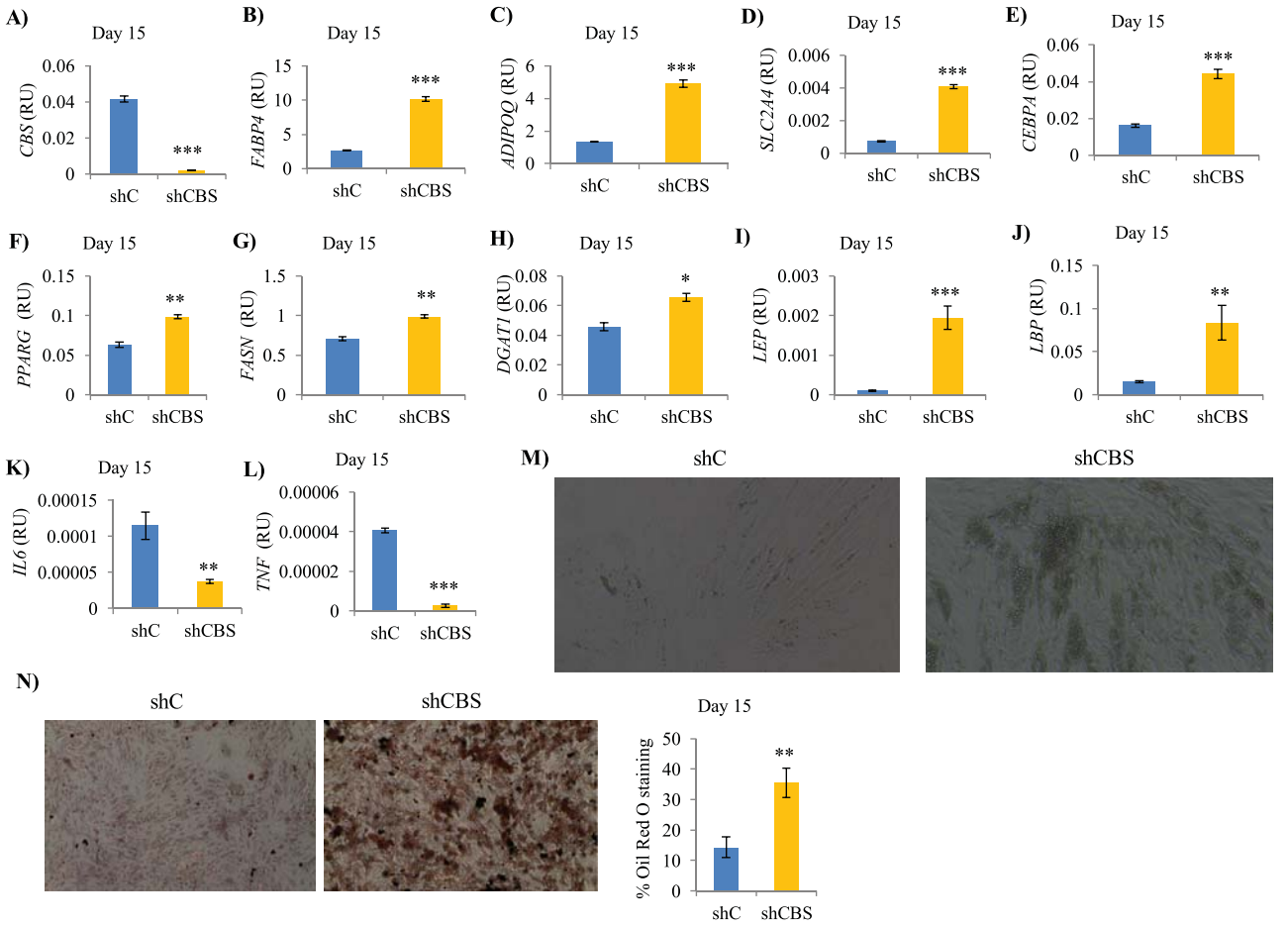

Fig. 4. A-L) Effect of permanent *CBS* gene knockdown (shCBS) on *CBS, FABP4, ADIPOQ, SLC2A4, CEBPA, PPARG, FASN, DGAT1, LEP, LBP, IL6* and *TNF* mRNA levels. **M-N)** Effect of permanent *CBS* gene knockdown (shCBS) on intracellular lipid accumulation, visually assessed at 10x magnifications **(M)** and measured by Oil Red O staining **(N)** at day15 of ASC52telo cell adipocyte differentiation. *p < 0.05, **p < 0.01 and ***p < 0.001 *vs* shC-ASC52telo cells. (For interpretation of the references to colour in this figure legend, the reader is referred to the Web version of this article.)

3.4. CBS gene KD in ASC52telo cells decreased osteogenic markers

Next, to evaluate the capacity of shCBS-ASC52telo cells to differenciate into another cell type, these cells were cultured in osteogenic conditions during 9 days. shCBS-ASC52telo cells (Fig. 5A) displayed reduced osteogenic markers (such as *RUNX2, BGLAP* and *TFGB1*) (Fig. 5B–D) in parallel to decreased rejuvenation (*LC3* and *SIRT1*)-related genes (Fig. 5E and F), but increased *FABP4* (Fig. 5G) and proinflammatory cytokines (*IL6, TNF* and *IL8)* (Fig. 5H–J).

4. Discussion

The current study demonstrated that, contrary to 3T3-L1 cells in which CTH levels were significantly increased but CBS was almost undetectable [4], ASC52telo cells showed an increased CBS/CTH ratio, characterized by increased CBS but very low levels of CTH mRNA and protein. In line with these findings, previous studies also demonstrated increased CBS *vs* CTH mRNA and protein levels in human mesenchymal stem cells [10,11].

These data indicate a major role of CBS in intracellular H_2S biosynthesis compared to CTH in ASC52telo cells. In fact, *CBS* gene KD in ASC52telo cells resulted in a significant increased in cellular inflammation and oxidative stress in parallel to decreased capacity to produce endogenous H_2S. A large number of studies demonstrated anti-inflammatory and anti-oxidant effects of H_2S in mesenchymal stem cells [10,12] and other cells [13–15]. However, the pro-oxidant and pro-inflammatory effects of CBS depletion might be also explained by other causes, including:

i) Altered mitochondrial respiratory function, characterized by decreased proton leak and spare respiratory capacity, two functional measures of mitochondrial function [16,17]. Supporting these findings, a recent study demonstrated the importance of CBS on mitochondrial function in endothelial cells [18]. It is important to note that proton leak (uncoupled respiration), which was significantly decreased in CBS KD ASC52telo (shCBS-ASC52telo) cells (Fig. 2K), is key mitochondrial process in the prevention of oxidative stress [19,20].
ii) Decreased expression of rejuvenation (*LC3* and *SIRT1*)-related genes. The protective effects of increased *SIRT1* [21–27] and *LC3* [28–31] mRNA levels in the prevention of cellular inflammation, oxidative stress and mitochondrial function are widely reported.
iii) Increased homocysteine/cysthationine ratio. CBS enzyme inhibition results in increased homocysteine in detrimental of cysthationine levels [32,33]. The pro-oxidant and pro-inflammatory effects of excess homocysteine have been demonstrated in *in vitro* and *in vivo* experiments [33–38]. Otherwise, similar to ASC52telo cells, breast tumor tissue displayed increased CBS, but very low CTH mRNA levels, resulting in increased intracellular levels of cysthationine, and in consequence preserving mitochondrial

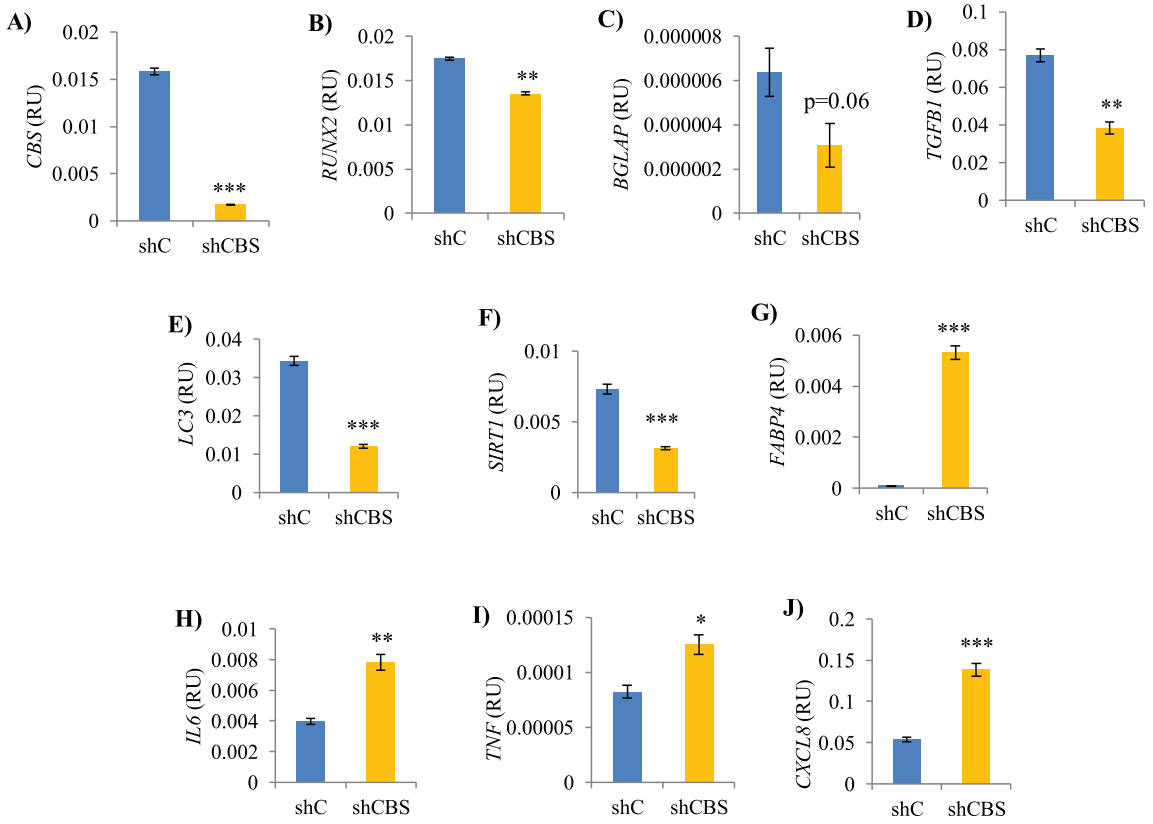

Fig. 5. A-J) Effect of permanent CBS gene knockdown (shCBS) on *CBS* mRNA levels **(A)**, expression of osteogenic-related genes (*RUNX2, BGLAP, TGFB1*) **(B–D)**, rejuvenation-related genes (*LC3, SIRT1*) **(E–F)**, *FABP4* **(G)** and proinflammatory cytokines (*IL6, TNF, CXCL8*) **(H–J)** during ASC52telo cell osteocyte differentiation (at day 9). *p < 0.05, **p < 0.01 and ***p < 0.001 *vs* shC-ASC52telo cells.

function and preventing oxidative and endoplasmic reticulum stress [39].

Another important finding of current study was that *CBS* gene knockdown in ASC52telo cells greatly enhanced their capacity to differentiate into adipocytes in detrimental to the ability to differentiate into osteogenic linage. It is well-stablished that increased oxidative stress (ROS levels) in adipose-derived mesenchymal stem cells promotes a cellular senescence and inflammation phenotype characterised by increased capacity for differenciate into adipocyte at the expense of decreased stemness capacity [40–42]. In fact, antioxidant treatment in mesenchymal stem cells prevented adipocyte differentiation [42]. In agreement with current data, the administration of diallyl disulfide, a slow H_2S donor [43], restored hAMSC stemness via inhibition of intracellular ROS levels [44]. The relevance of CBS on osteogenesis has been previously reported [45–47]. Interestingly, one of these studies demonstrated that exogenous homocysteine administration increased intracellular homocysteine levels, and resulted in increased ROS, altered mitochondrial function, reduced expression of *CBS* gene and intracellular H_2S level, and in consequence, inhibiting its capacity to differentiate into osteogenic linage [47]. Otherwise, to the best of our knowledge, the impact of CBS depletion enhancing hAMSC adipogenesis has not been previously shown. These findings could seem controversial with one previous study in 3T3-L1 cells, in which CBS gene knockdown decreased adipogenesis [1], whereas other studies demonstrated that CTH was the only enzyme of transulfuration pathway with adipogenic properties [2–4]. In line with these studies, increased CTH/CBS ratio was associated to increased adipogenic potential in ASC52telo cells, which was characterised with very high expression of adipogenic genes (such as FABP4 and SLC2A4), even before adding the adipogenic media (at day 0). Moreover, supporting the cellular inflammation-associated adipogenic potential observed in shCBS-ASC52telo cells, two recent studies demonstrated that cellular inflammation promoted the generation of new adipocytes and adipose tissue expansion [48,49]. Otherwise, *IRS1* gene expression was significantly decreased in shCBS-ASC52telo cells at day 0 and during adipocyte differentiation. In line with this, even though IRS-1 is important for lipid storage in adipose tissue [50], a recent study reported that IRS-1 knockdown in bone marrow mesenchymal stem cells increased their capacity to differentiate into adipocytes [51]. Current findings and these studies [45,46,48] suggest that cellular senescence and inflammation might promote a non-physiological increased adipocyte differentiation.

5. Conclusions

Altogether these findings demonstrated that permanent *CBS* gene KD in ASC52telo cells promotes a cellular senescence phenotype, characterized by increased cellular inflammation and oxidative stress, reduced cellular rejuvenation-related gene expression markers and a very increased adipogenic potential, which resulted in a non-physiological enhanced adipocyte differentiation with excessive lipid storage.

Author contributions

FC, JL, FO, NO-C and AL researched data; WR and JMF-R contributed to the discussion and reviewed the manuscript; JMMN researched data and wrote the manuscript.

Declaration of competing interest

The authors have nothing to disclose.

Acknowledgements

This work was partially supported by research grants PI15/01934, PI16/01173 and PI19/01712 from the Instituto de Salud Carlos III from Spain and VII Spanish Diabetes Association grants to Basic Diabetes Research Projects led by young researchers, CIBEROBN Fisiopatología de la Obesidad y Nutrición is an initiative from the Instituto de Salud Carlos III and Fondo Europeo de Desarrollo Regional (FEDER) from Spain. We acknowledge the technical support in L1 synthesis of Xavier Ribas (UdG) and Miquel Costas (UdG).

Appendix A. Supplementary data

Supplementary data to this article can be found online at https://doi.org/10.1016/j.redox.2020.101668.

References

[1] C.Y. Tsai, M.T. Peh, W. Feng, B.W. Dymock, P.K. Moore, Hydrogen sulfide promotes adipogenesis in 3T3L1 cells, PLoS One 10 (2015) e0119511–e0119511.
[2] G. Yang, Y. Ju, M. Fu, Y. Zhang, Y. Pei, M. Racine, S. Baath, T.J.S. Merritt, R. Wang, L. Wu, Cystathionine gamma-lyase/hydrogen sulfide system is essential for adipogenesis and fat mass accumulation in mice, Biochim. Biophys. Acta Mol. Cell Biol. Lipids 1863 (2018) 165–176.
[3] J. Cai, X. Shi, H. Wang, J. Fan, Y. Feng, X. Lin, J. Yang, Q. Cui, C. Tang, G. Xu, B. Geng, Cystathionine γ lyase-hydrogen sulfide increases peroxisome proliferator-activated receptor γ activity by sulfhydration at C139 site thereby promoting glucose uptake and lipid storage in adipocytes, Biochim. Biophys. Acta Mol. Cell Biol. Lipids 1861 (2016) 419–429.
[4] F. Comas, J. Latorre, O. Cussó, F. Ortega, A. Lluch, M. Sabater, A. Castells-Nobau, W. Ricart, X. Ribas, M. Costas, J.M. Fernández-Real, J.M. Moreno-Navarrete, Hydrogen sulfide impacts on inflammation-induced adipocyte dysfunction, Food Chem. Toxicol. 131 (2019) 110543.
[5] Z. Pan, Z. Zhou, H. Zhang, H. Zhao, P. Song, D. Wang, J. Yin, W. Zhao, Z. Xie, F. Wang, Y. Li, C. Guo, F. Zhu, L. Zhang, Q. Wang, CD90 serves as differential modulator of subcutaneous and visceral adipose-derived stem cells by regulating AKT activation that influences adipose tissue and metabolic homeostasis, Stem Cell Res. Ther. 10 (2019).
[6] B. Gustafson, A. Nerstedt, U. Smith, Reduced subcutaneous adipogenesis in human hypertrophic obesity is linked to senescent precursor cells, Nat. Commun. 10 (2019).
[7] S. Wolbank, G. Stadler, A. Peterbauer, A. Gillich, M. Karbiener, B. Streubel, M. Wieser, H. Katinger, M. Van Griensven, H. Redl, C. Gabriel, J. Grillari, R. Grillari-Voglauer, Telomerase immortalized human amnion- and adipose-derived mesenchymal stem cells: maintenance of differentiation and immunomodulatory characteristics, Tissue Eng. A 15 (2009) 1843–1854.
[8] S.A. Choi, C.S. Park, O.S. Kwon, H.K. Giong, J.S. Lee, T.H. Ha, C.S. Lee, Structural effects of naphthalimide-based fluorescent sensor for hydrogen sulfide and imaging in live zebrafish, Sci. Rep. 6 (2016), 26203–26203.
[9] J.M. Moreno-Navarrete, M. Jové, T. Padró, J. Boada, F. Ortega, W. Ricart, R. Pamplona, L. Badimón, M. Portero-Otín, J.M. Fernández-Real, Adipocyte lipopolysaccharide binding protein (LBP) is linked to a specific lipidomic signature, Obesity 25 (2017) 391–400.
[10] B. Fox, J.T. Schantz, R. Haigh, M.E. Wood, P.K. Moore, N. Viner, J.P.E. Spencer, P. G. Winyard, M. Whiteman, Inducible hydrogen sulfide synthesis in chondrocytes and mesenchymal progenitor cells: is H2S a novel cytoprotective mediator in the inflamed joint? J. Cell Mol. Med. 16 (2012) 896–910.
[11] T.A. Markel, N.A. Drucker, A.R. Jensen, K.R. Olson, Human mesenchymal stem cell hydrogen sulfide production critically impacts the release of other paracrine mediators after injury, J. Surg. Res. 254 (2020) 75–82.
[12] I. Cacciotti, M. Ciocci, E. Di Giovanni, F. Nanni, S. Melino, Hydrogen sulfide-releasing fibrous membranes: potential patches for stimulating human stem cells proliferation and viability under oxidative stress, Int. J. Mol. Sci. 19 (2018).
[13] J. Li, X. Teng, S. Jin, J. Dong, Q. Guo, D. Tian, Y. Wu, Hydrogen sulfide improves endothelial dysfunction by inhibiting the vicious cycle of NLRP3 inflammasome and oxidative stress in spontaneously hypertensive rats, J. Hypertens. 37 (2019) 1633–1643.
[14] Z. Lin, N. Altaf, C. Li, M. Chen, L. Pan, D. Wang, L. Xie, Y. Zheng, H. Fu, Y. Han, Y. Ji, Hydrogen sulfide attenuates oxidative stress-induced NLRP3 inflammasome activation via S-sulfhydrating c-Jun at Cys269 in macrophages, Biochim. Biophys. Acta (BBA) - Mol. Basis Dis. 1864 (2018) 2890–2900.
[15] W. P, C. F, W. W, Z. XD, Hydrogen sulfide attenuates high glucose-induced human retinal pigment epithelial cell inflammation by inhibiting ROS formation and NLRP3 inflammasome activation, Mediat. Inflamm. 2019 (2019).
[16] Y.X. Xiao, I.R. Lanza, J.M. Swain, M.G. Sarr, K.S. Nair, M.D. Jensen, Adipocyte mitochondrial function is reduced in human obesity independent of fat cell size, J. Clin. Endocrinol. Metab. 99 (2014).
[17] J.M. Moreno-Navarrete, F. Ortega, A. Rodríguez, J. Latorre, S. Becerril, M. Sabater-Masdeu, W. Ricart, G. Frühbeck, J.M. Fernández-Real, HMOX1 as a marker of iron excess-induced adipose tissue dysfunction, affecting glucose uptake and respiratory capacity in human adipocytes, Diabetologia 60 (2017) 915–926.
[18] G. Rao, B. Murphy, A. Dey, S.K.D. Dwivedi, Y. Zhang, R.V. Roy, P. Chakraborty, R. Bhattacharya, P. Mukherjee, Cystathionine beta synthase regulates mitochondrial dynamics and function in endothelial cells, Faseb. J. (2020), https://doi.org/10.1096/fj.202000173R.
[19] S. Cadenas, Mitochondrial uncoupling, ROS generation and cardioprotection, Biochim. Biophys. Acta Bioenerg. 1859 (2018) 940–950.
[20] P.S. Brookes, Mitochondrial H + leak and ROS generation: an odd couple, Free Radic. Biol. Med. 38 (2005) 12–23.
[21] G.-Z. Zhang, Y.-J. Deng, Q.-Q. Xie, E.-H. Ren, Z.-J. Ma, X.-G. He, Y.-C. Gao, X.-W. Kang, Sirtuins and intervertebral disc degeneration: roles in inflammation, oxidative stress, and mitochondrial function, Clin. Chim. Acta 508 (2020) 33–42.
[22] L. S, B. SH, K. YJ, P. JH, D.L. B, J. WB, J. S, L. NK, D. L, K. DY, K. S, S. HJ, Y. J, L. DH, M. HR, C. HY, K. SM, MHY2233 attenuates replicative cellular senescence in human endothelial progenitor cells via SIRT1 signaling, Oxid. Med. Cell. Longev. 2019 (2019), 6492029–6492029.
[23] J.R. Baker, C. Vuppusetty, T. Colley, S. Hassibi, P.S. Fenwick, L.E. Donnelly, K. Ito, P.J. Barnes, MicroRNA-570 is a novel regulator of cellular senescence and inflammaging, Faseb. J. 33 (2019) 1605–1616.
[24] P. Wang, C. Lv, T. Zhang, J. Liu, J. Yang, F. Guan, T. Hong, FOXQ1 regulates senescence-associated inflammation via activation of SIRT1 expression, Cell Death Dis. 8 (2017), e2946.
[25] Y. Guo, P. Li, L. Gao, J. Zhang, Z. Yang, G. Bledsoe, E. Chang, L. Chao, J. Chao, Kallistatin reduces vascular senescence and aging by regulating microRNA-34a-SIRT1 pathway, Aging Cell 16 (2017) 837–846.
[26] Y. Yuan, V.F. Cruzat, P. Newsholme, J. Cheng, Y. Chen, Y. Lu, Regulation of SIRT1 in aging: roles in mitochondrial function and biogenesis, Mech. Ageing Dev. 155 (2016) 10–21.
[27] J.W. Hwang, H. Yao, S. Caito, I.K. Sundar, I. Rahman, Redox regulation of SIRT1 in inflammation and cellular senescence, Free Radic. Biol. Med. 61 (2013) 95–110.
[28] S. D'Adamo, S. Cetrullo, S. Guidotti, Y. Silvestri, M. Minguzzi, S. Santi, L. Cattini, G. Filardo, F. Flamigni, R.M. Borzì, Spermidine rescues the deregulated autophagic response to oxidative stress of osteoarthritic chondrocytes, Free Radic. Biol. Med. 153 (2020) 159–172.
[29] J. W, Z. P, Z. X, Apelin promotes ECM synthesis by enhancing autophagy Flux via TFEB in human degenerative NP cells under oxidative stress, BioMed Res. Int. 2020 (2020), 4897170–4897170.
[30] S. Bhansali, A. Bhansali, P. Dutta, R. Walia, V. Dhawan, Metformin upregulates mitophagy in patients with T2DM: a randomized placebo-controlled study, J. Cell Mol. Med. 24 (2020) 2832–2846.
[31] R. Li, J. Shang, W. Zhou, L. Jiang, D. Xie, G. Tu, Overexpression of HIPK2 attenuates spinal cord injury in rats by modulating apoptosis, oxidative stress, and inflammation, Biomed. Pharmacother. 103 (2018) 127–134.
[32] K. Zuhra, F. Augsburger, T. Majtan, C. Szabo, Cystathionine-β-synthase: molecular regulation and pharmacological inhibition, Biomolecules 10 (2020).
[33] K. Robert, J. Nehmé, E. Bourdon, G. Pivert, B. Friguet, C. Delcayre, J. Delabar, N. Janel, Cystathionine β synthase deficiency promotes oxidative stress, fibrosis, and steatosis in mice liver, Gastroenterology 128 (2005) 1405–1415.
[34] K. AnandBabu, P. Sen, N. Angayarkanni, Oxidized LDL, homocysteine, homocysteine thiolactone and advanced glycation end products act as pro-oxidant metabolites inducing cytokine release, macrophage infiltration and pro-angiogenic effect in ARPE-19 cells, PLoS One 14 (2019) e0216899–e0216899.
[35] X. Wu, L. Zhang, Y. Miao, J. Yang, X. Wang, C. chen Wang, J. Feng, L. Wang, Homocysteine causes vascular endothelial dysfunction by disrupting endoplasmic reticulum redox homeostasis, Redox Biol. 20 (2019) 46–59.
[36] A. Longoni, B. Bellaver, L.D. Bobermin, C.L. Santos, Y. Nonose, J. Kolling, T.M. dos Santos, A.M. de Assis, A. Quincozes-Santos, A.T.S. Wyse, Homocysteine induces glial reactivity in adult rat astrocyte cultures, Mol. Neurobiol. 55 (2018) 1966–1976.
[37] D. Zhang, P. Fang, X. Jiang, J. Nelson, J.K. Moore, W.D. Kruger, R.M. Berretta, S. R. Houser, X. Yang, H. Wang, Severe hyperhomocysteinemia promotes bone marrow-derived and resident inflammatory monocyte differentiation and atherosclerosis in LDLr/CBS-deficient mice, Circ. Res. 111 (2012) 37–49.
[38] L. Papatheodorou, N. Weiss, Vascular oxidant stress and inflammation in hyperhomocysteinemia, Antioxidants Redox Signal. 9 (2007) 1941–1958.
[39] S. Sen, B. Kawahara, S.K. Mahata, R. Tsai, A. Yoon, L. Hwang, K. Hu-Moore, C. Villanueva, A. Vajihuddin, P. Parameshwar, M. You, D.L. Bhaskar, O. Gomez, K. F. Faull, R. Farias-Eisner, G. Chaudhuri, Cystathionine: a novel oncometabolite in human breast cancer, Arch. Biochem. Biophys. 604 (2016) 95–102.
[40] C.H. Lin, N.T. Li, H.S. Cheng, M.L. Yen, Oxidative stress induces imbalance of adipogenic/osteoblastic lineage commitment in mesenchymal stem cells through decreasing SIRT1 functions, J. Cell Mol. Med. 22 (2018) 786–796.
[41] K. Marycz, K.A. Tomaszewski, K. Kornicka, B.M. Henry, S. Wroński, J. Tarasiuk, M. Maredziak, Metformin decreases reactive oxygen species, enhances osteogenic properties of adipose-derived multipotent mesenchymal stem cells in vitro, and increases bone density in vivo, Oxid. Med. Cell. Longev. 2016 (2016) 9785890.
[42] D. de Villiers, M. Potgieter, M.A. Ambele, L. Adam, C. Durandt, M.S. Pepper, The role of reactive oxygen species in adipogenic differentiation, in: Adv. Exp. Med. Biol, Springer New York LLC, 2018, pp. 125–144.

[43] D. Liang, H. Wu, M.W. Wong, D. Huang, Diallyl trisulfide is a fast H_2S donor, but diallyl disulfide is a slow one: the reaction pathways and intermediates of glutathione with polysulfides, Org. Lett. 17 (2015) 4196–4199.
[44] K. Bahrampour Juybari, T. Kamarul, M. Najafi, D. Jafari, A.M. Sharifi, Restoring the IL-1β/NF-κB-induced impaired chondrogenesis by diallyl disulfide in human adipose-derived mesenchymal stem cells via attenuation of reactive oxygen species and elevation of antioxidant enzymes, Cell Tissue Res. 373 (2018) 407–419.
[45] Y. Liu, R. Yang, X. Liu, Y. Zhou, C. Qu, T. Kikuiri, S. Wang, E. Zandi, J. Du, I. S. Ambudkar, S. Shi, Hydrogen sulfide maintains mesenchymal stem cell function and bone homeostasis via regulation of Ca2+ channel sulfhydration, Cell Stem Cell 15 (2014) 66–78.
[46] L. Gambari, G. Lisignoli, E. Gabusi, C. Manferdini, F. Paolella, A. Piacentini, F. Grassi, Distinctive expression pattern of cystathionine-β-synthase and cystathionine-γ-lyase identifies mesenchymal stromal cells transition to mineralizing osteoblasts, J. Cell. Physiol. 232 (2017) 3574–3585.
[47] Y. Zhai, J. Behera, S.C. Tyagi, N. Tyagi, Hydrogen sulfide attenuates homocysteine-induced osteoblast dysfunction by inhibiting mitochondrial toxicity, J. Cell. Physiol. 234 (2019) 18602–18614.
[48] Q. Zhu, Y.A. An, M. Kim, Z. Zhang, S. Zhao, Y. Zhu, I.W. Asterholm, C. M. Kusminski, P.E. Scherer, Suppressing adipocyte inflammation promotes insulin resistance in mice, Mol. Metab. 39 (2020) 101010.
[49] I. Wernstedt Asterholm, C. Tao, T.S. Morley, Q.A. Wang, F. Delgado-Lopez, Z. V. Wang, P.E. Scherer, Adipocyte inflammation is essential for healthy adipose tissue expansion and remodeling, Cell Metabol. 20 (2014) 103–118.
[50] Y.H. Tseng, A.J. Butte, E. Kokkotou, V.K. Yechoor, C.M. Taniguchi, K. M. Kriauciunas, A.M. Cypess, M. Niinobe, K. Yoshikawa, M.E. Patti, C.R. Kahn, Prediction of preadipocyte differentiation by gene expression reveals role of insulin receptor substrates and necdin, Nat. Cell Biol. 7 (2005) 601–611.
[51] N. Wang, Y. Li, Z. Li, J. Ma, X. Wu, R. Pan, Y. Wang, L. Gao, X. Bao, P. Xue, IRS-1 targets TAZ to inhibit adipogenesis of rat bone marrow mesenchymal stem cells through PI3K-Akt and MEK-ERK pathways, Eur. J. Pharmacol. 849 (2019) 11–21.

Supplementary Figure 1. A-D) Effect of permanent *CBS* gene knockdown (shCBS) on *FABP4*, *ADIPOQ*, *SLC2A4* and *CEBPA* mRNA levels during ASC52telo cell adipocyte differentiation at day 0, 2 and 5. *p<0.05 and ***p<0.001 *vs* shC-ASC52telo cells.

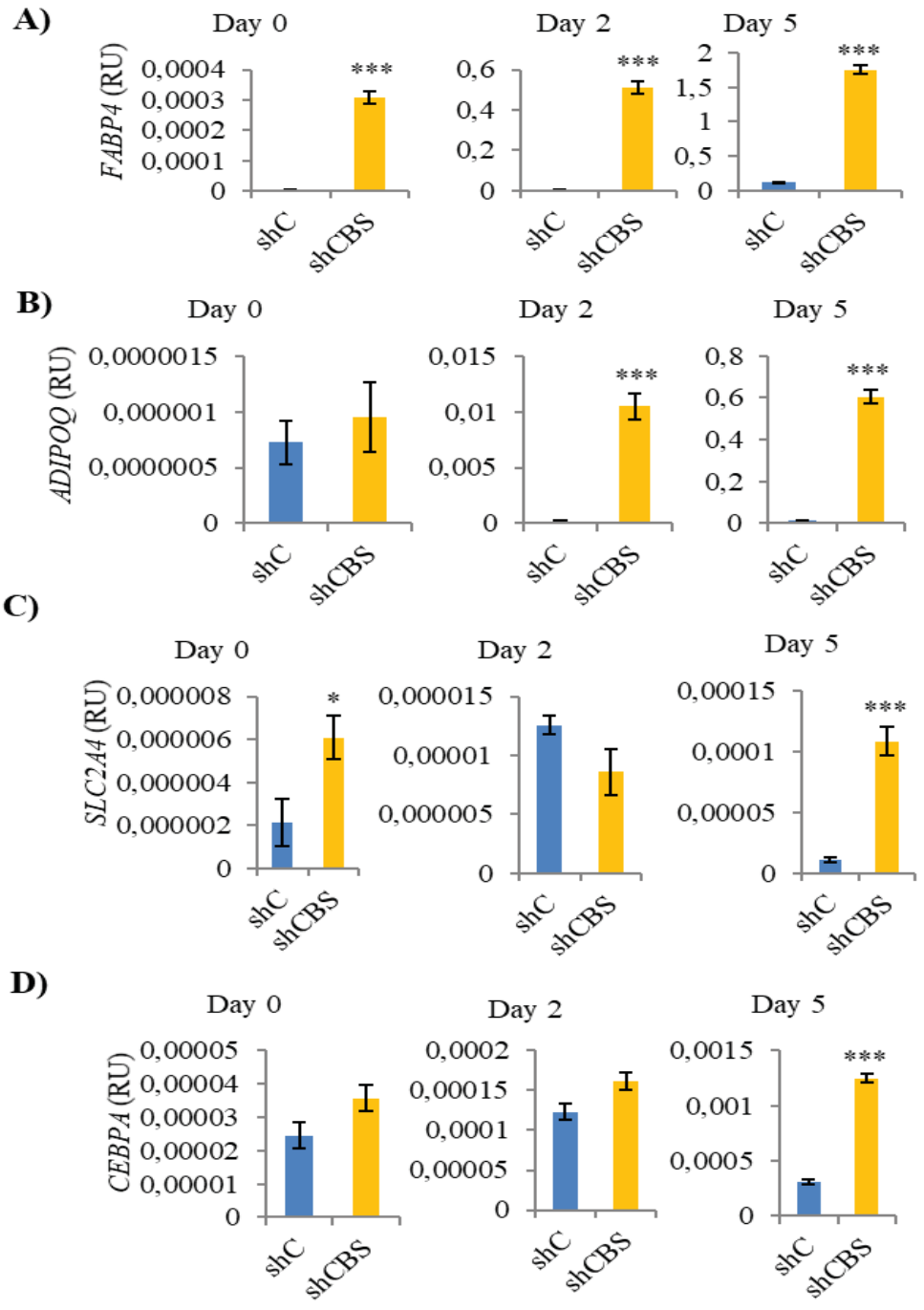

MANUSCRIPT 4

Ferran Comas, Jèssica Latorre, Francisco Ortega, María Arnoriaga Rodríguez, Matthias Kern, Aina Lluch, Wifredo Ricart, Matthias Blüher, Cecilia Gotor, Luis C. Romero, José Manuel Fernández-Real, José María Moreno-Navarrete. **Activation of endogenous H_2S biosynthesis or supplementation with exogenous H_2S enhances adipose tissue adipogenesis and preserves adipocyte physiology in humans.** Antioxid Redox Signal. 2021 Feb; doi:10.1089/ars.2020.8206

Impact factor (2019): 7.040 (D1, Endocrinology)

Activation of endogenous H_2S biosynthesis or supplementation with exogenous H_2S enhances adipose tissue adipogenesis and preserves adipocyte physiology in humans

Ferran Comas[1], Jèssica Latorre[1], Francisco Ortega[1], María Arnoriaga Rodríguez[1], Matthias Kern[2], Aina Lluch[1], Wifredo Ricart[1], Matthias Blüher[2], Cecilia Gotor[3], Luis C. Romero[3], José Manuel Fernández-Real[1,4*], José María Moreno-Navarrete[1,4*]

[1]Department of Diabetes, Endocrinology and Nutrition, Institut d'Investigació Biomèdica de Girona (IdIBGi), CIBEROBN (CB06/03/010) and Instituto de Salud Carlos III (ISCIII), Girona, Spain.

[2]Department of Medicine, University of Leipzig, Leipzig, Germany.

[3]Instituto de Bioquímica Vegetal y Fotosíntesis, Consejo Superior de Investigaciones Científicas and Universidad de Sevilla, Seville, Spain.

[4]Department of Medical Sciences, Universitat de Girona, Girona, Spain.

Abbreviated Title: H_2S in human adipose tissue adipogenesis

*Corresponding author and person to whom reprint requests should be addressed**:**
J.M. Moreno-Navarrete, Ph.D. e-mail: jmoreno@idibgi.org
J.M. Fernández-Real, M.D. Ph.D. e-mail: jmfreal@idibgi.org
Section of Diabetes, Endocrinology and Nutrition
Hospital of Girona "Dr Josep Trueta"
Carretera de França s/n, 17007, Girona, SPAIN.
Phone: 34-972-94 02 00
Fax: 34-972-94 02 70

Keywords: adipogenesis, adipose tissue, hydrogen sulfide, obesity, protein persulfidation.

Abstract

Aims: To investigate the impact of exogenous hydrogen sulfide (H_2S) and its endogenous biosynthesis on human adipocytes and adipose tissue in the context of obesity and insulin resistance.

Results: Experiments in human adipose tissue explants and in isolated preadipocytes demonstrated that exogenous H_2S or the activation of endogenous H_2S biosynthesis resulted in increased adipogenesis, insulin action, sirtuin deacetylase and PPARγ transcriptional activity, whereas chemical inhibition and gene knockdown of each enzyme generating H_2S (*CTH*, *CBS*, *MPST*) led to altered adipocyte differentiation, cellular senescence and increased inflammation. In agreement with these experimental data, visceral and subcutaneous adipose tissue expression of H_2S-synthesising enzymes was significantly reduced in morbidly obese subjects in association with attenuated adipogenesis and increased markers of adipose tissue inflammation and senescence. Interestingly, weight loss interventions (including bariatric surgery or diet/exercise) improved expression of H_2S biosynthesis-related genes. In human preadipocytes, expression of *CTH*, *CBS* and *MPST* genes and hydrogen sulfide production were dramatically increased during adipocyte differentiation. More importantly, the adipocyte proteome exhibiting persulfidation was characterized, disclosing that different proteins involved in fatty acid and lipid metabolism, the citrate cycle, insulin signalling, several adipokines and PPAR experienced the most dramatic persulfidation (85-98%).

Innovation: No previous studies investigated the impact of H_2S on human adipose tissue. This study suggests that the potentiation of adipose tissue H_2S biosynthesis is a possible therapeutic approach to improve adipose tissue dysfunction in patients with obesity and insulin resistance.

Conclusion: Altogether these data supported the relevance of H_2S biosynthesis in the modulation of human adipocyte physiology.

Abbreviations

AT, adipose tissue; DDA; data-dependent acquisition; DIA, data-independent acquisition; FDR, False Discovery Rate; HOMA-IR, Homeostasis Model Assessment – Insulin Resistance Index; KD, gene knockdown; LDH, Lactate Dehydrogenase; PLP, pyridoxal 5'-phosphate; PPG, DL-propargylglycine; SAT, subcutaneous adipose tissue; sc, subcutaneous; shRNA, short hairpin RNA; SVF, stromal vascular cells; VAT, visceral adipose tissue.

Introduction

Adipose tissue dysfunction, characterised by increased inflammation and cellular senescence and reduced adipogenesis, is an important contributor to obesity-associated metabolic disturbances, including insulin resistance (10, 33, 44). Increased oxidative stress and reactive oxygen species (ROS) levels in adipose tissue have been extensively demonstrated in obesity in association to insulin resistance and adipocyte dysfunction (1, 2, 13, 24, 62). The attenuation of adipose tissue oxidative stress might be an important therapeutic approach to prevent adipose tissue dysfunction and improve obesity-associated metabolic disturbances (50).

Hydrogen sulfide (H_2S) is a gaseous mediator that plays important regulatory roles in innate immunity and inflammatory responses impacting on the development of cardiovascular and metabolic diseases (8, 23, 32, 70, 81). In mammalian systems, H_2S is endogenously generated from cysteine by pyridoxal-5'-phosphate (PLP)-dependent enzymes, cystathionine β-synthase (CBS) and cystathionine γ-lyase (CTH or CSE), through the transsulfuration pathway (34). In the absence of PLP, 3-mercaptopyruvate sulfurtransferase (MPST) converts 3-mercaptopyruvate into H_2S (39, 68).

H_2S exerts its biological actions attenuating oxidative stress through different molecular mechanisms, including scavenging of ROS (69) and protein persulfidation (63). Protein persulfidation is a post-translational modification in which thiol groups (R–SH) from reactive cysteine residues are converted into perthiols (R–SSH). Persulfidation is known to modulate the structure and biological activity of target proteins, preventing irreversible cysteine overoxidation, and in consequence, preserving protein function (22, 56, 63, 84).

A recent study reported increased serum sulfide levels in subjects with morbid obesity in positive correlation with fat mass (17), but negatively associated with hyperglycemia (17, 77), showing decreased serum sulfide levels in obese subjects with altered glucose tolerance. In line with this study, previous studies also demonstrated decreased plasma sulfide levels in association to type 2 diabetes (77) or decreased adipose tissue H_2S production capacity in mice models of obesity and diabetes (high fat diet and db/db) (35).

In fact, there is emerging evidence in the 3T3-L1 mouse cell line pointing to a possible role of H_2S in adipocyte differentiation through the modulation of PPARγ activity (9, 73, 80). The overexpression of the H_2S generation enzyme CTH and the administration of the H_2S donor NaHS to 3T3-L1 cells in an environment of high glucose restored adiponectin secretion and decreased the secretion of proinflammatory cytokines (59). However, the impact of H_2S on human adipocytes has not been investigated, while its possible role in human adipose tissue physiology and adipogenesis is not yet completely understood.

We here aimed to investigate the possible role of H_2S on human adipogenesis and adipose tissue in the context of obesity and insulin resistance, reporting the first observations, to our knowledge, linking H_2S to the physiology of human adipose tissue.

Results

To examine the impact of H_2S on adipose tissue, *ex vivo* experiments were performed in adipose tissue explants from cohort 1, in which paired SAT and VAT were obtained from 20 morbidly obese participants with different degrees of systemic insulin sensitivity. Anthropometric and clinical parameters are shown in Suppl Table 1. As detailed in methods, the effects of GYY4137 in 5 consecutive participants and induction of endogenous H_2S biosynthesis in all participants (n=20) were tested, with sulfide levels being analyzed in 8 consecutive participants.

Exogenous H_2S administration increased adipogenesis, sirtuin and PPARγ activity in human adipose tissue explants

The most common class of H_2S donors are the sulfide salts [such as sodium hydrosulfide (NaSH) and sodium sulfide (Na_2S)] and GYY4137. Sulfide salts produced a fast release of H_2S triggering acute supraphysiological effects, and then H_2S levels drop rapidly. In contrast, GYY4137 induces a slower but more prolonged H_2S release, with increased peaking time (10 min vs 10 s for NaSH), but decreased peaking concentration (400-fold lower than for NaSH) (63). In human adipose tissue *ex vivo*, GYY4137 (5 μM, 16h at 37ºC) administration increased *ADIPOQ, FASN, SLC2A4* and *SIRT1* mRNAs in parallel to sulfide levels in tissue culture media (Figure 2A). GYY4137 (200 μM, 1h at 37ºC) also increased sirtuin deacetylase (Figure 2B) and PPARγ transcriptional (Figure 2C) activities in adipose tissue lysates.

Ex vivo stimulation of H_2S biosynthesis enhances the expression of adipogenic genes and *SIRT1* in association with insulin sensitivity

Then, H_2S biosynthesis was examined in human adipose tissue explants (Suppl Table 1), after adding L-cysteine and pyridoxal 5'-phosphate (PLP), known to induce H_2S biosynthesis through CBS and CTH. We observed increased endogenous H_2S

biosynthesis (Figure 2D) in parallel to raised *CTH* and *CBS* mRNAs levels (Table 1, Figure 2E-F), pointing that *CTH* and *CBS* gene expression is associated to H_2S biosynthesis. The induction of endogenous H_2S biosynthesis resulted in increased sulfide levels in tissue culture media and enhanced expression of adipogenic (*ADIPOQ, PPARG, SLC2A4, CIDEA* and *FASN*) and *SIRT1* genes in both subcutaneous (SAT) and visceral (VAT) adipose tissue (Table 1, Figure 2D). Sulfide concentration in the media positively correlated with *ADIPOQ*, *PPARG, SLC2A4* and *SIRT1* gene expression in both SAT and VAT (Figure 2E-F). The increase in SAT, but not VAT, *ADIPOQ, SLC2A4, FASN* and *SIRT1* gene expression after endogenous H_2S biosynthesis induction in AT explants was higher in those morbidly obese participants with decreased Hb1Ac (Figure 3A-D), but increased insulin sensitivity (Figure 3E-H).

Supporting these experimental data, VAT and SAT H_2S-synthesising enzymes (*CTH*, *CBS*, *MPST*) gene expression, which is ~~i~~n association to H_2S biosynthesis, were associated to systemic insulin sensitivity and adipose tissue adipogenesis in two cross-sectional (cohort 2 and 3) and three longitudinal (cohort 4, 5, 6) cohorts, in which bariatric surgery or diet/exercise interventions were performed.

Insulin sensitivity is associated to *CTH* expression in human adipose tissue

In cohort 2, VAT and SAT *CTH*, *CBS* and SAT *MPST* gene expression were significantly decreased in obese subjects (Suppl Table 2, Figure 4A-C) in association with homeostasis model assessment – insulin resistance index (HOMA-IR) and fasting triglycerides (Table 2). HOMA-IR was the main factor contributing to decreased SAT *CTH* (β= -0.29, p=0.04) and SAT *CBS* (β= -0.42, p=0.02) after adjusting for sex, age and body mass index (BMI). In a subgroup of 12 participants, in which CTH protein levels were analysed, a positive correlation between CTH protein and mRNA levels in both SAT and VAT were found (Figure 4D).

In an independent cohort of morbidly obese participants (cohort 3, Suppl Table 3), insulin sensitivity (euglycemic clamp) was positively correlated with SAT *CTH* (r=0.55, p=0.02, Figure 4E) and *CBS* (r=0.45, p=0.06, Figure 4F), but not *SAT MPST* (r=0.34, p=0.1) after excluding participants with type 2 diabetes. VAT *CTH* gene expression was also negatively correlated with HOMA-IR (Table 3).

Association of *CTH, CBS* and *MPST* with markers of adipose tissue functionality and the effects of weight loss

In cohort 2, in both VAT and SAT, *CTH*, *CBS* and *MPST* gene expression was positively correlated with adipogenic (*FASN, ACACA, PPARG*), insulin signaling pathway-related (*IRS1, SLC2A4*), *SIRT1* and *PPARGC1A* gene expression and negatively associated with expression of *LEP*, *LBP* and *TNF* (only *MPST*) genes (Table 2). In cohort 3, concordant associations were found for *CTH* and *MPST*, but not for *CBS* gene expression (Table 3). *CTH* gene expression correlated with expression of adipogenic (*ADIPOQ, PPARG*), mitochondrial biogenesis (*PPARGC1A*), and insulin signaling pathway-related (*IRS1*) genes, and markers of cellular senescence (positively with *SIRT1* and negatively with *BAX, TP53* and *TNF* gene expression (Table 3). *MPST* mRNA also positively correlated with *PPARG, ADIPOQ* and *SLC2A4* genes (Table 3).

In cohort 4, bariatric surgery-induced weight loss resulted in increased *CTH* (29.7%, p=0.0005), *CBS* (9.6%, p=0.05) and *MPST* (15.2%, p=0.01) mRNAs in parallel to improved insulin sensitivity and systemic inflammation (53, 57). Interestingly, the increase in *CTH* mRNA was positively correlated with the increase in *ADIPOQ* (r= 0.71, p= 0.002), *SIRT1* (r= 0.53, p= 0.03) and *PPARGC1A* (r= 0.56, p= 0.02) mRNAs. Similar findings were observed in an independent cohort after bariatric surgery-induced weight loss (cohort 6) and also after diet or exercise-induced weight loss (cohort 5), with increased SAT *CTH* mRNA levels (55% and 29%, respectively, both p<0.01).

In adipose tissue cell fractions, *CTH* and *MPST* gene expression significantly increased in human adipocytes in comparison with stromal vascular cells (SVF) (Figure 4G-H), whereas no significant differences in *CBS* gene expression between these 2 cell types were detected (Figure 4I).

Expression of H_2S-synthesising enzymes increases with adipocyte differentiation

Next, H_2S biosynthesis was investigated at cellular level, in human preadipocytes and adipocytes. We found that an adipocyte endogenous source of H_2S is prominent in human adipocytes. Sulfide levels were detectable and quantified in the culture media of human adipocytes and consistently increased by a ~30% with adipocyte differentiation (Figure 5A-B). *CTH* and *MPST* gene expression increased progressively during human adipocyte differentiation (Figure 5C-D) in close parallelism with adipogenic genes (*ADIPOQ,* Figure 5E). *CBS* increased slightly only in the last days of differentiation (day 12 and day 14, Figure 5F). These findings were confirmed at the protein level, observing high levels of sulfide-producer enzyme accumulation after differentiation (Figure 5G).

Exogenous H_2S potentiates insulin action and adipogenesis in human adipocytes

GYY4137 had no apparent effects on PPARγ transcriptional activity in preadipocytes (Figure 6A) (72 h) but led to a significantly increased sirtuin deacetylase activity (Figure 6B). In contrast, GYY4137 increased PPARγ transcriptional activity in adipocytes (Figure 6C), without significantly affecting sirtuin deacetylase activity (Figure 6D). GYY4137 treatment resulted in a 3-fold increase ($p<0.001$) in ^{pSer473}Akt/Akt ratio in response to insulin (Figure 6E).

GYY4137 dose-dependently increased the expression of adipogenic genes (*ADIPOQ, FABP4* and *CEBPA*) and *SLC2A4* in the last days of adipocyte differentiation and this effect was reverted by the CTH inhibitor propargylglycine (PPG) (Figure 6F-I).

Chemical inhibition of H_2S-synthesising enzymes attenuates adipogenesis and impacts inflammation in human adipocytes

Propargylglycine (PPG) is a known specific chemical inhibitor of the CTH enzyme, which led to a significant reduction of intracellular lipid accumulation (Figure 7A), fatty acid synthase protein levels (Figure 7B) and adipogenic gene expression (*ADIPOQ, FABP4, PPARG, FASN, PLIN1*) (Figure 7C-G) during adipogenesis. PPG led to raised markers of cellular senescence (*BAX, TP53*), proinflammatory cytokines (*IL6, TNF*) and ^{pSer536}NFκB (p65)/NFκB (p65) ratio, without changing LDH activity (a direct measure of cellular damage and necrosis) ((Figure 7H-M).

In fully differentiated adipocytes, PPG also attenuated insulin-induced ^{Ser473}Akt phosphorylation (Figure 7N), reduced *ADIPOQ, FASN, DGAT1*, *PPARG*, *IRS1*, *PPARGC1A* and *SIRT1* (Suppl Figure 1A-G), but did not affect inflammatory or cellular senescence-related gene expression or LDH activity (Suppl Figure 1H-L).

Gene knockdown (KD) of *CTH, CBS* and *MPST* in human preadipocytes impairs adipocyte differentiation

The effects of chemical compounds such as GYY4137 or PPG up- or downregulating H_2S production could be due to off-target mechanisms acting at multiple levels. For this reason, we studied how *CTH, CBS* and *MPST* gene KD affect adipogenesis during human adipocyte differentiation. The silencing of all these genes resulted in significantly decreased expression of adipogenic, lipogenic and insulin pathway-related genes while increasing inflammatory gene expression (Figure 8A-C). *CTH* gene KD resulted in a significantly decreased expression in adipogenic (*ADIPOQ, FABP4, FASN, PPARG, CEBPA*) and insulin pathway (*SLC2A4, IRS1*)-related genes while increasing inflammatory mRNAs (*IL6, TNF*) (Figure 8A).

CBS gene KD also resulted in decreased *ADIPOQ, FABP4, FASN, CEBPA, SLC2A4* and *IRS1*, and increased *IL6* mRNA levels (Figure 8B). *MPST* gene KD led to decreased *ADIPOQ, FABP4, FASN, PPARG, CEBPA* and *SLC2A4*, and increased *IL6* and *TNF* mRNA levels (Figure 8C). Of note, the most antiadipogenic effect was observed in CTH gene KD, since expression of all adipogenic and insulin pathway-related genes was reduced between 45-55% ($p<0.005$).

Persulfidation affects proteins involved in adipogenesis

Between 10 -30% of the cellular proteome is susceptible to being modified by persulfidation as it has been reported in mammals and plants, being this a highly prevalent protein post-translational modification (6, 60). For this reason, to gain insight into the mechanism underlying the adipogenic effects of H_2S, whole proteome persulfidation in preadipocytes and adipocytes was analysed and compared. To assess that, a sequential window acquisition of all theoretical spectra-mass spectrometry (SWATH-MS) quantitative approach with the tag-switch method (83) was combined for identification of protein persulfidation in preadipocyte and differentiated human cell cultures. Protein samples from four biological replicates extracted from preadipocyte and differentiated adipocyte cell cultures were isolated and subjected to the chemoselective tag-switch method to label persulfidated proteins. The enriched samples in persulfidated proteins obtained were digested, and the peptide solutions analyzed in two sequential steps: a shotgun data-dependent acquisition (DDA) approach to generate the spectral library, and SWATH acquisition by a data-independent acquisition (DIA) method. In the first step, after integrating the eight datasets, a total of 19,053 peptides [1% false discovery rate (FDR) and 92.8 % confidence] and 2,016 unique proteins (1% FDR) were identified and used as spectral library (Suppl dataset 1, available in PRIDE with identifier PXD018720). In the second step, to quantify protein levels using SWATH acquisition, the same eight

biological samples were analyzed twice each (technical replicas) by a DIA method. For quantitation, the fragment spectra were obtained for the sixteen runs and 1,590 proteins were quantified (Suppl dataset 2, available in PRIDE with identifier PXD018720), of which 954 were differentially more or less abundant in each culture with a fold change of ± 1.5 and p value < 0.05 (Suppl dataset 3, available in PRIDE with identifier PXD018720). From these proteins, 332 proteins were more persulfidated in differentiated adipocytes and in addition, we detected in the spectral library generated by the DDA approach 496 proteins that were only identified in the adipocyte samples and were under the detection limit in preadipocyte cultures (Suppl Table 4). Therefore, a total of 828 proteins were only persulfidated or were more persulfidated in differentiated adipocyte cultures.

In differentiated human adipocytes, persulfidation was significantly increased in proteins involved in fatty acid and lipid metabolism, the citrate cycle, adipokine, PPAR and insulin signalling (Figure 9A-B), Among them, we identified PLIN1, previously described as susceptible of persulfidation (21), which validated the proteomic approach used, and other important proteins and enzymes in adipocyte physiology, such as FASN, SCD, ACACA, THRSP, PLIN4, LIPE, ACSL1, SLC2A4 (GLUT4) and FABP4 (all with $p<0.0000001$), but not non-adipogenic control proteins, such as ACTB, ENO1 and PARK7 (61) that showed similar level of persulfidation in both cell cultures (Figure 9C). Considering that persulfidation preserved protein integrity and function in conditions of oxidative stress where cysteine residues may be partially oxidized (22, 63, 84), current data suggested that persulfidation in adipocytes might have a crucial role preserving those proteins involved in adipogenesis and adipocyte physiology. These proteins mainly included enzymes, lipid droplet-associated proteins, membrane transporters and receptors that modulate lipogenesis, lipolysis, mitochondrial function and insulin action (Suppl

dataset 2 and Figure 9A-B). On the other hand, in preadipocytes the proteins that were persulfidated belonged to pathways involved in immune response, cell migration, glycosaminoglycan degradation, complement and coagulation cascades and bacterial invasion of epithelial cells (Suppl Figure 2A-B).

Discussion

The current study provides sound and novel evidences supporting the importance of H_2S biosynthesis in the physiology of human adipose tissue. Altogether current findings pointed to a crucial role of H_2S and H_2S-synthetizing enzymes in human adipose tissue physiology at different cellular levels. Even though, the specific molecular mechanism to explain the possible effects of H_2S on human adipogenesis has not been fully resolved in this study, some mechanisms might be inferred from current findings. These putative mechanisms were as follows:

i) Preserving adipogenic-related proteins through protein persulfidation. Persulfidation often increases the reactivity of target proteins, modulating their biological activities, whereas other post-translational modifications, such as S-nitrosylation often decreases protein activity (25). In fact, a recent study showed experimentally, for the first time, a higher chemical reactivity in proteins with persulfidated cysteines compared to proteins with cysteines with sulfur in the thiol state (26). Even though, the most reported impact of persulfidation is to activate protein function, some studies demonstrated inhibitory effects in some important proteins (26).

Taking into account that we found increased persulfidation in FASN, SCD, ACACA, THRSP, PLIN4, LIPE, ACSL1, GLUT4 and FABP4, and that an appropriate functionality of these proteins is required for adipogenesis and adipocyte physiology (3, 14, 19, 31, 42, 46, 66, 82), the current results suggest that endogenous H_2S biosynthesis might preserve the function of those proteins involved in adipogenesis. However, further experiments are required to confirm this suggestion.

Supporting the importance of H_2S in the physiology of adipose cells, *CTH*, *CBS* and *MPST* mRNA levels were detected at substantial levels in adipocytes, increasing during human adipocyte differentiation in parallel to *ADIPOQ*. The knockdown of *CTH*, *CBS*

and *MPST* promoted the development of dysfunctional adipocytes during adipocyte differentiation, decreasing markers of adipogenesis and increasing the expression of proinflammatory cytokines in parallel to decreased H_2S biosynthesis. Of note, the most anti-adipogenic effect was observed in *CTH* gene KD. The chemical inhibition of CTH activity resulted in decreased adipogenesis during human adipocyte differentiation and in fully differentiated adipocytes. In fact, anti-adipogenic and inflammatory effects of high PPG dose (250 μM) during human adipocyte differentiation were comparable with the effects of *CTH* gene KD. In contrast, no significant effects of low PPG dose (25 μM) were found. This discrepancy could be explained by the previously reported low potency, low selectivity and the limited cell-membrane permeability of PPG (7). However, considering that inhibiting CBS, CTH and MPST may have effects independent of H_2S, such as perturbations in homocysteine metabolism, the results of PPG or gene knockdown experiments should be interpreted with caution. In addition, it should be considered that knockdown of one of these enzymes might be compensated by H_2S production by the remaining ones. Otherwise, the administration of GYY4137 in the last stage of the process resulted in a dose-dependent increased expression of adipogenic genes. Interestingly, when endogenous H_2S production was inhibited with PPG (250 μM), GYY4137 sustained adipogenic gene expression (Figure 6), preventing the reduction observed in Figure 7. Previous studies demonstrated that adipogenic (73) and anti-cancer (41) effects of GYY4137 were not observed when cells were treated with ZYJ1122, its structural analogue lacking sulfur, indicating that GYY4137 effects were dependent of H_2S moiety. *Ex vivo* experiments also demonstrated that the activation of H_2S-producing enzymes in adipose tissue increased expression of adipogenic genes in correlation to H_2S biosynthesis. Consistent with the suggested impact of H_2S on protein persulfidation in adipose cells (current study), a recent study demonstrated that persulfidation depends on

intracellular H_2S levels, observing in those situations of decreased H_2S biosynthesis, such as aging, a significant decline in protein persulfidation, whereas conditions of enhanced H_2S production (such as dietary restriction) were associated with increased protein persulfidation (84).

ii) *Preventing inflammatory processes in human preadipocytes through the induction of sirtuin deacetylase activity*. Specifically, in human preadipocytes, exogenous H_2S (GYY4137) treatment enhanced sirtuin activity, whereas when endogenous H_2S biosynthesis was inhibited (using PPG or in *CTH, CBS* and *MPST* KD) markers of cellular senescence (*TP53*), apoptosis (*BAX*) and inflammation (*TNF, IL6*) increased. These findings suggest that the previously reported anti-senescence effects of H_2S (20, 51, 65) might contribute to improve the adipogenic function of preadipocytes, and preserve adipose tissue functionality (4). In addition, increased *SIRT1* mRNA levels and sirtuin activity after transsulfuration pathway activation or GYY4137 administration in *ex vivo* experiment (adipose tissue explants) or the consistent association between H_2S-producing enzymes and *SIRT1* gene expression in human adipose tissue reinforced this idea. Furthermore, both SAT and VAT *CTH* gene expression negatively correlated with markers of cellular senescence (*TP53*), inflammation (*TNF*) and apoptosis (*BAX*) in obese subjects, which were all associated to adipose tissue dysfunction and insulin resistance (36, 37, 52, 71). Even though, TP53, inflammatory cytokines (IL6 and TNF) or apoptosis markers has all been previously used to characterize senescence-associated adipose tissue dysfunction (36, 37, 52, 71), a more accurate measurement of cellular senescence (such as β-galactosidase activity) should be considered to confirm current associations in further studies.

Strengthening current findings, increased SIRT1 activity led to enhanced adipose tissue rejuvenation (characterized by increased cellular stemness) and decreased inflammation

(12, 29, 43, 64, 78) and H_2S administration resulted in enhanced Sirt1 expression and activity (20, 51, 65), preventing vascular aging (20) and cellular senescence in human fibroblasts (65). In line with these findings, in immortalized human adipose-derived mesenchymal stem cells, which unlike human preadipocytes and adipocytes (current study) displayed a much higher expression of CBS than CTH gene (18), *CBS* gene knockdown promotes a cellular senescence phenotype characterized by increased inflammation and oxidative stress, and decreased H_2S production (18). Of note, this cellular senescence phenotype resulted in adipocyte hypertrophy, when these cells differentiated into adipocytes, and attenuated their ability to differentiate into osteogenic linage (18).

iii) *Increasing insulin action through the activation of PPARγ transcriptional activity in differentiated adipocytes.* GYY4137 administration resulted in a significant increase~~d~~ of insulin-induced Akt phosphorylation at serine 473, whereas PPG administration had opposite effects. A fine regulation of insulin action is associated to adipogenesis and adipose tissue physiology (55, 67). *Ex vivo* experiments indicated that the adipogenic effect resulting from transsulfuration pathway activation was increased in association with insulin sensitivity, and negatively correlated with HbA1c levels, supporting the relationship between H_2S and adipose tissue insulin action. In addition, AT *CTH* gene expression was positively correlated to systemic insulin sensitivity in both cross-sectional studies (cohort 1 and cohort 2) and increased after bariatric surgery-induced weight los similar to insulin sensitivity. H_2S improved insulin action in mice (28, 48, 49, 79). GYY4137 administration improved high fat diet-induced insulin resistance through the activation of PPARγ in adipose tissue, whereas PPG exerted opposite effects (9). Mechanistically, H_2S-induced PPARγ transactivation is mediated by enhanced PPARγ persulfidation in cysteine residues from DNA binding domain (9, 80). Since PPG

administration also increased ^{pSer536}NFκB (p65)/NFκB ratio and proinflammatory cytokines (*IL6* and *TNF*), another potential mechanism to explain H_2S effects on insulin action was the inhibition of NFκB-induced inflammation (23).

In support of current findings, CBS deficiency is known to be associated with decreased fat mass in both mice and humans (30, 38). CTH is involved in adipogenesis in phylogenetically distant species from drosophila to mice (9, 73, 80) with *cth* knockout mice developing decreased fat mass under cysteine-limited diets (47).

Decreased levels of H_2S-synthetizing enzymes in morbidly obese subjects seems in contradiction with the relevance of these enzymes in adipogenesis and fat mass accretion. However, in conditions of obesity and insulin resistance, adipogenesis is attenuated (40, 54, 74), and size enlargement of pre-existing adipocytes acquires more relevance in fat mass sustaining (45). The findings in human adipose tissue are in agreement with decreased adipose tissue H_2S production reported in db/db and high-fat diet-fed mice (35). Even though, adipose tissue as a possible source of increased serum sulfide levels, recently described in morbidly obese subjects (17), cannot be discarded. Alternative hypothesis should be investigated: i) Expression of H_2S-synthesizing enzymes could be higher in early phases of obesity but decrease in more advanced disease as a consequence of adipose tissue inflammation and insulin resistance. ii) In addition, H_2S production depends not only by the expression/activity of synthesizing enzymes but also on its oxidation. Decreased oxidation may be the result of environmental hypoxia as that present in adipose tissue from subjects with obesity (72). In this context, decreased oxidation could result in persistently higher serum sulfide levels.

Current data might anticipate clinical applications and also suggest that the modulation of adipose tissue H_2S biosynthesis may play a role in glucose metabolism. Dietary raw garlic homogenate (a complex mixture containing several H_2S precursors) administration

restored plasma H_2S levels in diabetic rats and led to increased insulin sensitivity (58). Therapeutically, the potentiation of adipose tissue H_2S-synthetizing enzymes to improve adipose tissue physiology in patients with type 2 diabetes should be investigated in depth in further studies.

Conclusions

This study sustains adipose tissue H_2S-synthetizing enzymes as important actors in human adipose tissue physiology and systemic insulin sensitivity, possibly avoiding cellular senescence and inflammation, and in consequence preserving adipose tissue adipogenesis.

Innovation

Even though the role of H_2S on adipogenesis has been previously studied in mice, no previous studies investigated the impact of H_2S on human adipose tissue. The current study demonstrates the relevance of H_2S biosynthesis in human adipogenesis and adipose tissue physiology. This study also shows the first whole proteome persulfidation analysis in human adipocytes, suggesting that persulfidation might preserve the function of those proteins involved in adipogenesis. Altogether these data point to the potentiation of adipose tissue H_2S biosynthesis as a possible therapeutic approach to improve adipose tissue dysfunction in patients with obesity and insulin resistance (Figure 1).

Material and Methods

Subjects' recruitment for adipose tissue samples

Ex vivo experiments in adipose tissue explants

Cohort 1. Paired SAT and VAT were obtained from 20 obese participants undergoing open abdominal surgery (gastrointestinal bypass) under general anesthesia after an overnight fast. Anthropometric and clinical parameters were detailed in Suppl Table 1. The study had the approval of the ethical committee, and all patients gave informed written consent.

These experiments were performed as previously described (53). In brief, samples of adipose tissue were immediately transported to the laboratory (5–10 min). The handling of tissue was carried out under strictly aseptic conditions. The tissue was cut with scissors into small pieces (5–10 mg) and incubated in buffer plus albumin (3 ml/g of tissue) for 30 min. After incubation, the tissue explants were centrifuged for 30 s at 400*g*. Then ∼100 mg of minced tissue was placed into 1 ml M199 (Life Technologies, Invitrogen) containing 10% fetal bovine serum (Hyclone, Thermo Fisher Scientific), 100 unit/ml penicillin (Life Technologies, Invitrogen), and 100 μg/ml streptomycin (Life Technologies, Invitrogen) and incubated for 16 h in suspension culture under aseptic conditions. The following treatments were performed: i) Vehicle or GYY4137 (5 μM) administration during 16 h at 37ºC to evaluate the effects of exogenous H_2S administration (N=5); and ii) Vehicle or L-cysteine (10 mM) and pyridoxal 5'-phosphate (2 mM), as an inductor of the transsulfuration pathway (H_2S-synthesising enzymes), during 16 h at 37ºC to evaluate the effects of endogenous H_2S biosynthesis (N=20). In addition, the effect of GYY4137 (200 μM, 1 h at 37ºC) in adipose tissue lysates were also tested.

Cross-sectional studies

In cohort 2, a group of 241 [122 visceral (VAT) and 119 subcutaneous (SAT) adipose tissues] from participants with normal body weight and different degrees of obesity, with body mass index (BMI) within 20 and 68 kg/m^2, were analyzed. In a third cohort of morbidly obese (BMI > 35 kg/m^2) subjects with different degrees of insulin action (measured using hyperinsulinemic-euglycemic clamp), 35 paired SAT and VAT samples (Cohort 3) were studied. Altogether these subjects were recruited at the Endocrinology Service of the Hospital of Girona "Dr Josep Trueta". All subjects were of Caucasian origin and reported that their body weight had been stable for at least three months before the study. Subjects were studied in the post-absorptive state. BMI was calculated as weight (in kg) divided by height (in m) squared. They had no systemic disease other than obesity or type 2 diabetes, and all were free of any infections in the previous month before the study. Type 2 diabetes was diagnosed following the criteria of the Expert Committee on the Diagnosis and Classification of Diabetes (85). The characteristics of patients with type 2 diabetes are described in Suppl Table 2 and Suppl Table 3. Liver diseases (specifically tumoral disease and HCV infection) and thyroid dysfunction were specifically excluded by biochemical work-up. All subjects gave written informed consent, validated and approved by the ethical committee of the Hospital of Girona "Dr Josep Trueta", after the purpose of the study was explained to them. Samples and data from patients included in this study were provided by the FATBANK platform promoted by the CIBEROBN and coordinated by the IDIBGI Biobank (Biobanc IDIBGI, B.0000872), integrated in the Spanish National Biobanks Network and they were processed following standard operating procedures with the appropriate approval of the Ethics, External Scientific and FATBANK Internal Scientific Committees.

Interventional studies

In cohort 4, twenty-five Caucasian obese (BMI= 43.7 ± 4.6 kg/m^2, age=47 ± 9 years [mean ±SD]) subjects, who underwent bariatric surgery thought Roux-en-Y gastric bypass in Hospital of Girona "Dr Josep Trueta" were part of an ongoing study (57). Inclusion criteria were age between 30 and 60 years, BMI $\geq$ 35 kg/m^2 and ability to understand the study protocol. Exclusion criteria were use of medications able to interfere with insulin action and history of a chronic systemic disease. Adipose tissue samples from the SAT depot were obtained during bariatric surgery. Postoperative samples of SAT were obtained by subcutaneous biopsy at the mesogastric level after 2 years from surgery. Fasting blood samples were obtained at the same day of the biopsy. All subjects gave written informed consent, validated and approved by the ethical committee of the Hospital of Girona "Dr Josep Trueta", after the purpose of the study was explained to them.

In cohorts 5 and 6, SAT gene expression was analyzed before and 6 months after a multimodal weight reduction program consisting of a -800kcal calorie restricted diet combined with a structured (twice a week for 60min) exercise program (cohort 5, n=15; mean age: 46.2±2.5years, mean BMI: 34.5±1.8kg/m², no type 2 diabetes, no concomitant medication) and before and 12 months after bariatric surgery (cohort 6, n=32), as previously described (11). All study protocols have been approved by the ethics committee of the University of Leipzig. All participants gave written informed consent before taking part in the study.

Adipose tissue samples were obtained from SAT and VAT depots during elective surgical procedures (cholecystectomy, surgery of abdominal hernia and gastric by-pass surgery). Both SAT and VAT samples were collected from the abdomen, following standard procedures. Samples of adipose tissue were immediately transported to the laboratory (5-10 min). The handling of tissue was carried out under strictly aseptic conditions. Adipose

tissue samples were washed in PBS, cut off with forceps and scalpel into small pieces (100 mg), and immediately flash-frozen in liquid nitrogen before stored at -80ºC. The isolation of adipocyte and stromal vascular fraction cells (SVF) was performed from 8 SAT and 8 VAT non-frozen adipose tissue samples. These samples were washed three to four times with phosphate-buffered saline (PBS) and suspended in an equal volume of PBS supplemented with 1% penicillin-streptomycin and 0.1% collagenase type I prewarmed to 37°C. The tissue was placed in a shaking water bath at 37°C with continuous agitation for 60 minutes and centrifuged for 5 minutes at 300 to 500g at room temperature. The supernatant, containing mature adipocytes, was recollected. The pellet was identified as the SVF. Isolated mature adipocytes and SVF stored at -80ºC for gene expression analysis.

Hyperinsulinemic-euglycemic clamp

Insulin action was determined by hyperinsulinemic-euglycemic clamp. After an overnight fast, two catheters were inserted into an antecubital vein, one for each arm, used to administer constant infusions of glucose and insulin and to obtain arterialized venous blood samples. A 2-h hyperinsulinemic-euglycemic clamp was initiated by a two-step primed infusion of insulin (80 mU/m^2/min for 5 min, 60 mU/m^2/min for 5 min) immediately followed by a continuous infusion of insulin at a rate of 40 mU/m^2/min (regular insulin [Actrapid; Novo Nordisk, Plainsboro, NJ]). Glucose infusion began at minute 4 at an initial perfusion rate of 2 mg/kg/min being then adjusted to maintain plasma glucose concentration at 88.3–99.1 mg/dL. Blood samples were collected every 5 min for determination of plasma glucose and insulin. Insulin sensitivity was assessed as the mean glucose infusion rate during the last 40 min. In the stationary equilibrium, the amount of glucose administered (*M*) equals the glucose taken by the body tissues and is a measure of overall insulin sensitivity.

Analytical methods

Serum glucose concentrations were measured in duplicate by the glucose oxidase method using a Beckman glucose analyser II (Beckman Instruments, Brea, California). Glycosylated haemoglobin (HbA1c) was measured by the high-performance liquid chromatography method (Bio-Rad, Muenchen, Germany, and autoanalyser Jokoh HS-10, respectively). Intra- and inter-assay coefficients of variation were less than 4% for all these tests. Serum insulin was measured in duplicate by RIA (Medgenix Diagnostics, Fleunes, Belgium). The intra-assay coefficient of variation was 5.2% at a concentration of 10 mU/l and 3.4% at 130 mU/l. The interassay coefficients of variation were 6.9 and 4.5% at 14 and 89 mU/l, respectively. HOMA-IR was calculated using the following formula: [Insulin (mU/l) x Glucose mmol/l]/22.5. Roche Hitachi Cobas c711 instrument (Roche, Barcelona, Spain) was used to do HDL cholesterol and total serum triglycerides determinations. HDL cholesterol was quantified by a homogeneous enzymatic colorimetric assay through the cholesterol esterase / cholesterol oxidase / peroxidase reaction (Cobas HDLC3). Serum fasting triglycerides were measured by an enzymatic, colorimetric method with glycerol phosphate oxidase and peroxidase (Cobas TRIGL). LDL cholesterol was calculated using the Friedewald formula.

Differentiation of human pre-adipocytes

Isolated human subcutaneous preadipocytes (Zen-Bio Inc., Research Triangle Park, NC) were plated on T-75 cell culture flasks and cultured at 37 C and 5% CO2 in DMEM/nutrient mix F-12 medium (1:1, vol/vol) supplemented with 10 U/ml penicillin/streptomycin, 10% fetal bovine serum (FBS), 1% HEPES, and 1% glutamine (all from GIBCO, Invitrogen S.A, Barcelona, Spain). One week later, the isolated and expanded human sc preadipocytes were cultured (~40,000 cells/cm2) in 12-well plates with preadipocytes medium (Zen-Bio) composed of DMEM/nutrient mix F-12 medium

(1:1, vol/vol), HEPES, FBS, penicillin, and streptomycin in a humidified 37 C incubator with 5% CO2. Twenty-four hours after plating, cells were checked for complete confluence (d 0), and differentiation was induced using differentiation medium (Zen-Bio) composed of preadipocytes medium, human insulin, dexamethasone, isobutylmethylxanthine, and PPARγ agonists (rosiglitazone). After 7 day (d7), differentiation medium was replaced with fresh adipocyte medium (Zen-Bio) composed of DMEM/nutrient mix F-12 medium (1:1, vol/vol), HEPES, FBS, biotin, pantothenate, human insulin, dexamethasone, penicillin, streptomycin, and amphotericin. Negative control (nondifferentiated cell) was performed with preadipocyte medium during all differentiation process. Fourteen days after the initiation of differentiation, cells appeared rounded with large lipid droplets apparent in the cytoplasm. Cells were then considered mature adipocytes, harvested, and stored at -80ºC for RNA/protein purification. For time course experiment, Cells were harvested and stored at -80ºC for RNA/protein purification at day 0, 2, 5, 7, 9, 12 and 14. To evaluate cell integrity, lactate dehydrogenase (LDH) activity was analyzed by Cytotoxicity Detection Kit (LDH) (Cat. nº 11644793001, Roche Diagnostics SL, Barcelona, Spain) according to the manufacturer's instructions.

Treatments CTH inhibitor DL-propargylglycine (PPG, 25 and 250 μM) administration was performed during sc adipocyte differentiation. Otherwise, after adipocyte differentiation (at d 14), sc fully differentiated adipocytes were incubated with fresh medium (control) and fresh medium containing PPG (25 and 250 μM) for 48h. GYY4137 (0.1, 1 and 5 μM, a slow H_2S donor) was administrated during the last stage (from day 7 to 14) of sc adipocyte differentiation process. At the end of each experiment, cells were harvested, and pellets and supernatants were stored at -80 ºC. All *in vitro* experiments were performed in three or four independent replicates.

Short hairpin (sh) RNA-mediated knockdown of CTH, CBS and MPST gene

Gene knockdown was performed using *CTH, CBS* and *MPST*-targeted and control (scrambled) shRNA lentiviral particles (sc-78973-V, sc-60335-V, sc-75821-V and sc-108080, Santa Cruz Biotechnology, CA, USA) following the manufacturer instructions in human subcutaneous preadipocytes at 80% of cell confluence. Adipocyte differentiation started 24 h after lentiviral transfection and no antibiotic selection was performed.

Media sulfide quantification

Sulfide concentration in cultured medium was assessed as previously described (16), using a naphthalimide-based fluorescent sensor 6-Azido-2-[2-[2-(2-hydroxyethoxy)ethoxy]ethyl]benzo[de]isoquinoline-1,3-dione (L1). This probe was chemically synthesised in Institute of Computational Chemistry and Catalysis (Chemistry Department, University of Girona) as described previously (15). L1 probe (5 μM) was included and incubated in adipose tissue (16h) or adipocyte (24h) maintenance media. In each experiment, a negative control that consisted in the incubation of cell culture media plus L1 probe (5 μM) without adipose tissue explants or adipocytes was also performed. This negative control was used to subtract spontaneous H_2S production. After incubation, media were transferred to new eppendorf tubes to be homogenized, and were kept at –80ºC in the dark, until the read. Fluorescence was read in a Biotek Cytation 5 reader at λ ex = 435 nm and λ em = 550nm in duplicate and quantified with a Na_2S standard curve (0, 7.8, 15.6, 31.25, 62.5, 125, 250 and 500 μM). Media sulfide levels were normalized by total protein amount in cell lysates in *in vitro* experiments or by total adipose tissue amount in *ex vivo* experiments.

Oil red O staining

Intracellular lipid accumulation was measured by oil red O staining. For oil red O staining, cells were washed twice with PBS, fixed in 4% formaldehyde for 1 h, and stained for 30 min with 0.2% oil red O solution in 60% isopropanol. Cells were then washed several times with water, and excess water was evaporated by placing the stained cultures at ~32°C. To determine the extent of adipose conversion, 0.2 ml of isopropanol was added to the stained culture dish. The extracted dye was immediately removed by gentle pipetting and its optical density was monitored spectrophotometrically at 500 nm using a multiwell plate reader (Model Anthos Labtec 2010 1.7 reader).

Insulin action, sirtuin and PPARγ activities

To study insulin signaling, basal- and insulin-induced Akt phosphorylation at Ser473 normalized by total Akt protein levels (^{pSer473}Akt/Akt ratio) were measured after adipocyte differentiation (at d 14). Insulin stimulus was performed with insulin (100 nM) administration during 10 min. Sirtuin deacetylase and PPARγ transcriptional activities were measured using Sirtuin Activity Assay Kit (Fluorometric) (K324-100, BioVision, CA, USA) and PPAR gamma Transcription Factor Assay Kit (ab133101, Abcam, UK), respectively, strictly following the manufacturer's instructions.

RNA expression

RNA purification, gene expression procedures and analyses were performed, as previously described (53, 57). Briefly, RNA purification was performed using RNeasy Lipid Tissue Mini Kit (QIAgen, Izasa SA, Barcelona, Spain) and the integrity was checked by Agilent Bioanalyzer (Agilent Technologies, Palo Alto, CA). Gene expression was assessed by real time PCR using a LightCycler® 480 Real-Time PCR System (Roche Diagnostics SL, Barcelona, Spain), using TaqMan® technology suitable for relative genetic expression quantification. The RT-PCR reaction was performed in a final volume

of 12 µl. The cycle program consisted of an initial denaturing of 10 min at 95 °C then 40 cycles of 15 s denaturizing phase at 95 °C and 1 min annealing and extension phase at 60 °C. A threshold cycle (Ct value) was obtained for each amplification curve and then a ΔCt was first calculated by subtracting the Ct value for human cyclophilin A (*PPIA*) RNA from the Ct value for each sample. Fold changes compared with the endogenous control were then determined by calculating $2^{-\Delta Ct}$, so that gene expression results are expressed as expression ratio relative to *PPIA* gene expression according to the manufacturer's guidelines. TaqMan® primer/probe sets (Thermo Fisher Scientific, Waltham, MA, USA) used were as follows: Peptidylprolyl isomerase A (cyclophilin A) (4333763, PPIA as endogenous control), cystathionine γ-lyase (CTH, Hs00542284_m1), cystathionine β-synthase (CBS, Hs00163925_m1), mercaptopyruvate sulfurtransferase (MPST, Hs00560401_m1), adiponectin (ADIPOQ, Hs00605917_m1), peroxisome proliferator-activated receptor gamma (PPARG, Hs00234592_m1), fatty acid synthase (FASN, Hs00188012_m1), acetyl-CoA carboxylase alpha (ACACA, Hs00167385_m1), CCAAT/enhancer binding protein alpha (CEBPA, Hs00269972_s1), solute carrier family 2 member 4 (SLC2A4, Hs00168966_m1), insulin receptor substrate 1 (IRS1, Hs00178563_m1), Leptin (LEP, Hs00174877_m1), lipopolysaccharide binding protein (LBP, Hs01084621_m1), interleukin 6 (interferon, beta 2) (IL6, Hs00985639_m1), tumor necrosis factor (TNF, Hs00174128_m1), CD68 molecule (CD68, Hs00154355_m1), BCL2-associated X protein (BAX, Hs00180269_m1), tumor protein p53 (TP53, Hs01034249_m1) and fatty acid binding protein 4, adipocyte (FABP4, Hs01086177_m1).

Protein analysis

Protein were extracted directly in radioimmnuno precipitation assay (RIPA) buffer (0.1% SDS, 0.5% sodium deoxycholate, 1% Nonidet P-40, 150mM NaCl, and 50mM Tris-HCl,

pH 8.0), supplemented with protease inhibitors (1 mM phenylmethylsulfonyl fluoride). Cellular debris and lipids were eliminated by centrifugation of the solubilized samples at 13000 rpm for 10 min at 4ºC, recovering the soluble fraction. Protein concentration was determined using the RC/DC Protein Assay (Bio-Rad Laboratories, Hercules, CA). RIPA protein extracts (25 μg) were separated by SDS-PPGE and transferred to nitrocellulose membranes by conventional procedures. Membranes were immunoblotted with anti-CTH, CBS, MPST, FASN, β-actin (sc-365382**,** sc-133154, sc-376168, sc-20140, sc-47778, Santa Cruz Biotechnology, CA, USA), ^{pSer536}NFκB (p65), NFκB (p65), ^{pSer473}Akt and Akt (Cell Signaling Technology, Inc, MA, USA). Anti-rabbit IgG and anti-mouse IgG coupled to horseradish peroxidase was used as a secondary antibody. Horseradish peroxidase activity was detected by chemiluminescence, and quantification of protein expression was performed using Scion image software.

Label-free protein quantitation by SWATH-MS acquisition and analysis

Protein samples from human preadipocyte cell cultures and differentially mature adipocytes were isolated from three biological samples. Culture medium was removed by aspiration and washed once with PBS solutions. Culture cells were incubated with a trypsin solution at 37 ºc for 5 min and collected by centrifugation at 2000 rpm for 5 min. The supernatant was collected by aspiration and cell pellet freezed to -80 ºC until used. Samples were prepared by resuspension in 1 x Cell Lysis Buffer containing 20 mM Tris-HCl (pH 7.5),150 mM NaCl, 1 mM Na_2EDTA, 1 mM EGTA, 1% Triton, 2.5 mM sodium pyrophosphate, 1 mM **ß**-glycerophosphate, 1 mM Na_3VO_4, 1 μg/ml leupeptin, 0.5 mM PMSF, 1x protease inhibitor cocktail (Roche), at a ratio of 1 ml of buffer per 100 mg of tissue. Cells were vortexed and incubated 25 min at 4 ºC (on ice) and sonicated 4 times in a sonicator bath for 10 s. The extract was centrifugated at 14000 g at 4ºC for 15 min and supernatant used as protein source. 1 mg of protein per sample were TCA/acetone

precipitated, resuspended in 50 mM TRIS-HCl, pH 8.0 containing 2.5% SDS, 1x protease inhibitor (Roche) and submitted to the tag-switch labelling for persulfidation protein enrichment as described (5). After elution from the streptavidin-beads proteins were precipitated by TCA/acetone procedure. Precipitated samples were resupended in 50 mM ammonium bicarbonate with 0.2 % Rapigest (Waters) for protein determination. 50 µg of protein were alkylated and trypsin-digested as previously described (27, 76), and the SWATH-MS analyses were performed at the Proteomic Facility of the Institute of Plant Biochemistry and Photosynthesis, Seville, Spain. A data-dependent acquisition (DDA) approach using nano-LC-MS/MS was first performed to generate the SWATH-MS spectral library as described by García *et al.* (27).

The peptide and protein identifications were performed using Protein Pilot software (version 5.0.1, Sciex) with the Paragon algorithm. The search was conducted against a Uniprot proteome database ID: UP000005640 (March 2019), specifying iodoacetamide with other possible Cys modifications. The false discovery rate (FDR) was set to 0.01 for both peptides and proteins. The MS/MS spectra of the identified peptides were then used to generate the spectral library for SWATH peak extraction using the add-in for PeakView Software (version 2.1, Sciex) MS/MSALL with SWATH Acquisition MicroApp (version 2.0, Sciex). Peptides with a confidence score above 99 % (as obtained from the Protein Pilot database search) were included in the spectral library.

For relative quantitation using SWATH analysis, the same samples used to generate the spectral library were analyzed using a data-independent acquisition (DIA) method. Each sample (2 µL) was analyzed using the LC-MS equipment and LC gradient described above to build the spectral library but instead used the SWATH-MS acquisition method. The method consisted of repeating an acquisition cycle of TOF MS/MS scans (230 to 1500 m/z, 60 ms acquisition time) of 60 overlapping sequential precursor isolation

windows of variable width (1 m/z overlap) covering the 400 to 1250 m/z mass range with a previous TOF MS scan (400 to 1250 m/z, 50 ms acquisition time) for each cycle. The total cycle time was 3.7 s.

The targeted data extraction of the fragment ion chromatogram traces from the SWATH runs was performed by PeakView (version 2.1) with the MS/MSALL with SWATH Acquisition MicroApp (version 2.0). This application processed the data using the spectral library created from the shotgun data. Up to 10 peptides per protein and 7 fragments per peptide were selected, based on signal intensity. Any shared and modified peptides were excluded from the processing. Windows of 12 min and 20 ppm width were used to extract the ion chromatograms. SWATH quantitation was attempted for all proteins in the ion library that were identified by Protein Pilot with an FDR below 1 %. The extracted ion chromatograms were then generated for each selected fragment ion. The peak areas for the peptides were obtained by summing the peak areas from the corresponding fragment ions. PeakView computed an FDR and a score for each assigned peptide according to the chromatographic and spectra components. Only peptides with an FDR below 5% were used for protein quantitation. Protein quantitation was calculated by adding the peak areas of the corresponding peptides. To test for differential protein abundance between the two groups, MarkerView (version 1.2.1, Sciex) was used for signal normalization.

The mass spectrometry proteomics data have been deposited in the ProteomeXchange Consortium via the PRIDE (75) partner repository with identifier PXD018720.

Statistical analyses

Statistical analyses were performed using SPSS 12.0 software. The relation between variables was analyzed by simple correlation (Pearson's test and Spearman's test) and multiple regression analyses in a stepwise manner. One factor ANOVA with post-hoc

Bonferroni test, paired t-test and unpaired t-test were used to compare *CTH, CBS* and *MPST* gene expression in human cohorts and *ex vivo* experiment. Nonparametric test (Mann Whitney test) was used to analyse *in vitro* experiments. Levels of statistical significance were set at $p<0.05$.

Electronic laboratory notebook was not used.

ACKNOWLEDGEMENTS

We acknowledge the technical support in L1 synthesis of Xavier Ribas (UdG) and Miquel Costas (UdG). We want to particularly acknowledge the patients, the FATBANK platform promoted by the CIBEROBN and the IDIBGI Biobank (Biobanc IDIBGI, B.0000872), integrated in the Spanish National Biobanks Network, for their collaboration and coordination.

Author contributions: FC participated in this study conducting experiments, acquiring and analyzing data; JL, FO, MAR, MK, AL, CG and LCR participated in this study acquiring and analyzing data; WR, MB and LCR contributed to the discussion and reviewed the manuscript; JMFR and JMMN contributed to research study design, conducting experiments, analyzing and writing the manuscript.

Author Disclosure: The authors have nothing to disclose.

Funding statements: This work was partially supported by research grants PI15/01934, PI16/01173 and PI19/01712 from the Instituto de Salud Carlos III from Spain and VII Spanish Diabetes Association grants to Basic Diabetes Research Projects led by young researchers, CIBEROBN Fisiopatología de la Obesidad y Nutrición is an initiative from the Instituto de Salud Carlos III and Fondo Europeo de Desarrollo Regional (FEDER) from Spain. This work was also supported in part by FEDER through the Agencia Estatal de Investigación grant BIO2016-76633-P.

Data availability: All data generated or analyzed during this study are included in the published article (and its online supplementary files). The datasets generated during and/or analyzed during the current study are available in the ProteomeXchange Consortium via the PRIDE with identifier PXD018720.

Supplementary files: 3 Suppl tables and 8 Suppl figures.

References

1. Acín-Pérez R, Iborra S, Martí-Mateos Y, Cook ECL, Conde-Garrosa R, Petcherski A, Muñoz M [a]M, Martínez de Mena R, Krishnan KC, Jiménez C, Bolaños JP, Laakso M, Lusis AJ, Shirihai OS, Sancho D, and Enríquez JA. Fgr kinase is required for proinflammatory macrophage activation during diet-induced obesity. *Nat Metab* 2: 974–988, 2020.

2. Akl MG, Fawzy E, Deif M, Farouk A, and Elshorbagy AK. Perturbed adipose tissue hydrogen peroxide metabolism in centrally obese men: Association with insulin resistance. *PLoS One* 12, 2017.

3. Albert JS, Yerges-Armstrong LM, Horenstein RB, Pollin TI, Sreenivasan UT, Chai S, Blaner WS, Snitker S, O'Connell JR, Gong D-W, Breyer RJ, Ryan AS, McLenithan JC, Shuldiner AR, Sztalryd C, and Damcott CM. Null Mutation in Hormone-Sensitive Lipase Gene and Risk of Type 2 Diabetes. *N Engl J Med* 370: 2307–2315, 2014.

4. Arner E, Westermark PO, Spalding KL, Britton T, Rydén M, Frisén J, Bernard S, and Arner P. Adipocyte turnover: Relevance to human adipose tissue morphology. *Diabetes* 59: 105–109, 2010.

5. Aroca A, Benito JM, Gotor C, and Romero LC. Persulfidation proteome reveals the regulation of protein function by hydrogen sulfide in diverse biological processes in Arabidopsis. *J Exp Bot* 68: 4915–4927, 2017.

6. Aroca A, Gotor C, and Romero LC. Hydrogen sulfide signaling in plants: emerging roles of protein persulfidation. *Front Plant Sci* 9, 2018.

7. Asimakopoulou A, Panopoulos P, Chasapis CT, Coletta C, Zhou Z, Cirino G, Giannis A, Szabo C, Spyroulias GA, and Papapetropoulos A. Selectivity of commonly used pharmacological inhibitors for cystathionine β synthase (CBS) and cystathionine γ lyase (CSE). *Br J Pharmacol* 169: 922–932, 2013.

8. Benavides GA, Squadrito GL, Mills RW, Patel HD, Isbell TS, Patel RP, Darley-Usmar VM, Doeller JE, and Kraus DW. Hydrogen sulfide mediates the vasoactivity of garlic. *Proc Natl Acad Sci U S A* 104: 17977–17982, 2007.

9. Cai J, Shi X, Wang H, Fan J, Feng Y, Lin X, Yang J, Cui Q, Tang C, Xu G, and Geng B. Cystathionine γ lyase–hydrogen sulfide increases peroxisome proliferator-activated receptor γ activity by sulfhydration at C139 site thereby promoting glucose uptake and lipid storage in adipocytes. *Biochim Biophys Acta - Mol Cell Biol Lipids* 1861: 419–429, 2016.

10. Carobbio S, Pellegrinelli V, and Vidal-Puig A. Adipose tissue function and expandability as determinants of lipotoxicity and the metabolic syndrome. *Adv Exp Med Biol.* 960: 161–196, 2017.

11. Chakaroun R, Raschpichler M, Klöting N, Oberbach A, Flehmig G, Kern M, Schön MR, Shang E, Lohmann T, Dreßler M, Fasshauer M, Stumvoll M, and Blüher M. Effects of weight loss and exercise on chemerin serum concentrations and adipose tissue expression in human obesity. *Metabolism* 61: 706–714, 2012.

12. Chalkiadaki A and Guarente L. High-fat diet triggers inflammation-induced cleavage of SIRT1 in adipose tissue to promote metabolic dysfunction. *Cell Metab* 16: 180–188, 2012.

13. Chattopadhyay M, Khemka VK, Chatterjee G, Ganguly A, Mukhopadhyay S, and Chakrabarti S. Enhanced ROS production and oxidative damage in subcutaneous white

adipose tissue mitochondria in obese and type 2 diabetes subjects. *Mol Cell Biochem* 399: 95–103, 2015.

14. Cheng X, Xi QY, Wei S, Wu D, Ye RS, Chen T, Qi QE, Jiang QY, Wang SB, Wang LN, Zhu XT, and Zhang YL. Critical role of miR-125b in lipogenesis by targeting stearoyl-CoA desaturase-1 (SCD-1). *J Anim Sci* 94: 65–76, 2016.

15. Choi SA, Park CS, Kwon OS, Giong HK, Lee JS, Ha TH, and Lee CS. Structural effects of naphthalimide-based fluorescent sensor for hydrogen sulfide and imaging in live zebrafish. *Sci Rep* 6: 26203–26203, 2016.

16. Comas F, Latorre J, Cussó O, Ortega F, Lluch A, Sabater M, Castells-Nobau A, Ricart W, Ribas X, Costas M, Fernández-Real JM, and Moreno-Navarrete JM. Hydrogen sulfide impacts on inflammation-induced adipocyte dysfunction. *Food Chem Toxicol* 131: 110543, 2019.

17. Comas F, Latorre J, Ortega F, Arnoriaga Rodríguez M, Lluch A, Sabater M, Rius F, Ribas X, Costas M, Ricart W, Lecube A, Fernández-Real JM, and Moreno-Navarrete JM. Morbidly obese subjects show increased serum sulfide in proportion to fat mass. *Int J Obes*, 2020.

18. Comas F, Latorre J, Ortega F, Oliveres N, Lluch A, Ricart W, Fernández-Real JM, and Moreno-Navarrete JM. Permanent cystathionine-β-Synthase gene knockdown promotes inflammation and oxidative stress in immortalized human adipose-derived mesenchymal stem cells, enhancing their adipogenic capacity. *Redox Biol*: 101668, 2020.

19. Cui Y, Liu Z, Sun X, Hou X, Qu B, Zhao F, Gao X, Sun Z, and Li Q. Thyroid hormone responsive protein spot 14 enhances lipogenesis in bovine mammary epithelial cells. *Vitr Cell Dev Biol - Anim* 51: 586–594, 2015.

20. Das A, Huang GX, Bonkowski MS, Longchamp A, Li C, Schultz MB, Kim LJ, Osborne B, Joshi S, Lu Y, Treviño-Villarreal JH, Kang MJ, Hung T tyng, Lee B, Williams EO, Igarashi M, Mitchell JR, Wu LE, Turner N, Arany Z, Guarente L, and Sinclair DA. Impairment of an Endothelial NAD+-H2S Signaling Network Is a Reversible Cause of Vascular Aging. *Cell* 173: 74–89.e20, 2018.

21. Ding Y, Wang H, Geng B, and Xu G. Sulfhydration of perilipin 1 is involved in the inhibitory effects of cystathionine gamma lyase/hydrogen sulfide on adipocyte lipolysis. *Biochem Biophys Res Commun* 521: 786–790, 2020.

22. Dóka, Ida T, Dagnell M, Abiko Y, Luong NC, Balog N, Takata T, Espinosa B, Nishimura A, Cheng Q, Funato Y, Miki H, Fukuto JM, Prigge JR, Schmidt EE, Arnér ESJ, Kumagai Y, Akaike T, and Nagy P. Control of protein function through oxidation and reduction of persulfidated states. *Sci Adv* 6: eaax8358, 2020.

23. Du J, Huang Y, Yan H, Zhang Q, Zhao M, Zhu M, Liu J, Chen SX, Bu D, Tang C, and Jin H. Hydrogen sulfide suppresses oxidized low-density lipoprotein (Ox-LDL)-stimulated monocyte chemoattractant protein 1 generation from macrophages via the nuclear factor κb (NF-κB) pathway. *J Biol Chem* 289: 9741–9753, 2014.

24. Elrayess MA, Almuraikhy S, Kafienah W, Al-Menhali A, Al-Khelaifi F, Bashah M, Zarkovic K, Zarkovic N, Waeg G, Alsayrafi M, and Jaganjac M. 4-hydroxynonenal causes impairment of human subcutaneous adipogenesis and induction of adipocyte insulin resistance. *Free Radic Biol Med* 104: 129–137, 2017.

25. Filipovic MR. Persulfidation (S-sulfhydration) and H2S. *Handb Exp Pharmacol* 230: 29–59, 2015.

26. Fu L, Liu K, He J, Tian C, Yu X, and Yang J. Direct Proteomic Mapping of Cysteine Persulfidation. *Antioxidants Redox Signal* 33: 1061–1076, 2020.

27. García I, Arenas-Alfonseca L, Moreno I, Gotor C, and Romero LC. HCN regulates cellular processes through posttranslational modification of proteins by s-cyanylation. *Plant Physiol* 179: 107–123, 2019.

28. Geng B, Cai B, Liao F, Zheng Y, Zeng Q, Fan X, Gong Y, Yang J, Cui Q hua, Tang C, and Xu G heng. Increase or Decrease Hydrogen Sulfide Exert Opposite Lipolysis, but Reduce Global Insulin Resistance in High Fatty Diet Induced Obese Mice. *PLoS One* 8: e73892–e73892, 2013.

29. Gillum MP, Kotas ME, Erion DM, Kursawe R, Chatterjee P, Nead KT, Muise ES, Hsiao JJ, Frederick DW, Yonemitsu S, Banks AS, Qiang L, Bhanot S, Olefsky JM, Sears DD, Caprio S, and Shulman GI. SirT1 regulates adipose tissue inflammation. *Diabetes* 60: 3235–3245, 2011.

30. Gupta S and Kruger WD. Cystathionine beta-synthase deficiency causes fat loss in mice. *PLoS One* 6: e27598–e27598, 2011.

31. Gustafson B, Hedjazifar S, Gogg S, Hammarstedt A, and Smith U. Insulin resistance and impaired adipogenesis. *Trends Endocrinol Metab* 26: 193–200, 2015.

32. Hine C, Harputlugil E, Zhang Y, Ruckenstuhl C, Lee BC, Brace L, Longchamp A, Treviño-Villarreal JH, Mejia P, Ozaki CK, Wang R, Gladyshev VN, Madeo F, Mair WB, and Mitchell JR. Endogenous hydrogen sulfide production is essential for dietary restriction benefits. *Cell* 160: 132–144, 2015.

33. Kahn CR, Wang G, and Lee KY. Altered adipose tissue and adipocyte function in the pathogenesis of metabolic syndrome. *J Clin Invest* 129: 3990–4000, 2019.

34. Kamoun P. Endogenous production of hydrogen sulfide in mammals. *Amino Acids* 26: 243–254, 2004.

35. Katsouda A, Szabo C, and Papapetropoulos A. Reduced adipose tissue H2S in obesity. *Pharmacol Res* 128: 190–199, 2018.

36. Khanahmadi M, Manafi B, Tayebinia H, Karimi J, and Khodadadi I. Downregulation of sirt1 is correlated to upregulation of p53 and increased apoptosis in epicardial adipose tissue of patients with coronary artery disease. *EXCLI J* 19: 1387–1398, 2020.

37. Krstic J, Reinisch I, Schupp M, Schulz TJ, and Prokesch A. P53 functions in adipose tissue metabolism and homeostasis. *Int J Mol Sci* 19, 2018.

38. Kruger WD. Cystathionine β-synthase deficiency: Of mice and men. *Mol Genet Metab* 121: 199–205, 2017.

39. Kuo MM, Kim DH, Jandu S, Bergman Y, Tan S, Wang H, Pandey DR, Abraham TP, Shoukas AA, Berkowitz DE, and Santhanam L. MPST but not CSE is the primary regulator of hydrogen sulfide production and function in the coronary artery. *Am J Physiol - Hear Circ Physiol* 310: H71–H79, 2016.

40. Kursawe R, Narayan D, Cali AMG, Shaw M, Pierpont B, Shulman GI, and Caprio S. Downregulation of ADIPOQ and PPARγ2 gene expression in subcutaneous adipose tissue of obese adolescents with hepatic steatosis. *Obesity* 18: 1911–1917, 2010.

41. Lee ZW, Zhou J, Chen CS, Zhao Y, Tan CH, Li L, Moore PK, and Deng LW. The slow-releasing Hydrogen Sulfide donor, GYY4137, exhibits novel anti-cancer effects in vitro and in vivo. *PLoS One* 6, 2011.

42. Levert KL, Waldrop GL, and Stephens JM. A biotin analog inhibits acetyl-CoA carboxylase activity and adipogenesis. *J Biol Chem* 277: 16347–16350, 2002.

43. Liu T, Ma X, Ouyang T, Chen H, Lin J, Liu J, Xiao Y, Yu J, and Huang Y. SIRT1 reverses senescence via enhancing autophagy and attenuates oxidative stress-induced apoptosis through promoting p53 degradation. *Int J Biol Macromol* 117: 225–234, 2018.

44. Liu Z, Wu KKL, Jiang X, Xu A, and Cheng KKY. The role of adipose tissue senescence in obesityand ageing-related metabolic disorders. *Clin Sci* 134: 315–330, 2020.

45. Longo M, Zatterale F, Naderi J, Parrillo L, Formisano P, Raciti GA, Beguinot F, and Miele C. Adipose tissue dysfunction as determinant of obesity-associated metabolic complications. *Int J Mol Sci* 20, 2019.

46. Lyu Y, Su X, Deng J, Liu S, Zou L, Zhao X, Wei S, Geng B, and Xu G. Defective differentiation of adipose precursor cells from lipodystrophic mice lacking perilipin 1. *PLoS One* 10, 2015.

47. Mani S, Yang G, and Wang R. A critical life-supporting role for cystathionine γ-lyase in the absence of dietary cysteine supply. *Free Radic Biol Med* 50: 1280–1287, 2011.

48. Manna P and Jain SK. Hydrogen sulfide and L-cysteine increase phosphatidylinositol 3,4,5-trisphosphate (PIP3) and glucose utilization by inhibiting phosphatase and tensin homolog (PTEN) protein and activating phosphoinositide 3-kinase (PI3K)/serine/threonine protein kinase (A. *J Biol Chem* 286: 39848–39859, 2011.

49. Manna P and Jain SK. Vitamin D up-regulates glucose transporter 4 (GLUT4) translocation and glucose utilization mediated by cystathionine-γ-lyase (CSE) activation and H2S formation in 3T3L1 adipocytes. *J Biol Chem* 287: 42324–32, 2012.

50. Masschelin PM, Cox AR, Chernis N, and Hartig SM. The Impact of Oxidative Stress on Adipose Tissue Energy Balance. *Front Physiol* 10, 2020.

51. Miller DL and Roth MB. Hydrogen sulfide increases thermotolerance and lifespan in Caenorhabditis elegans. *Proc Natl Acad Sci U S A* 104: 20618–20622, 2007.

52. Minamino T, Orimo M, Shimizu I, Kunieda T, Yokoyama M, Ito T, Nojima A, Nabetani A, Oike Y, Matsubara H, Ishikawa F, and Komuro I. A crucial role for adipose tissue p53 in the regulation of insulin resistance. *Nat Med* 15: 1082–1087, 2009.

53. Moreno-Navarrete JM, Escoté X, Ortega F, Serino M, Campbell M, Michalski M-C, Laville M, Xifra G, Luche E, Domingo P, Sabater M, Pardo G, Waget A, Salvador J, Giralt M, Rodriguez-Hermosa JI, Camps M, Kolditz CI, Viguerie N, Galitzky J, Decaunes P, Ricart W, Frühbeck G, Villarroya F, Mingrone G, Langin D, Zorzano A, Vidal H, Vendrell J, Burcelin R, Vidal-Puig A, and Fernández-Real JM. A role for adipocyte-derived lipopolysaccharide-binding protein in inflammation- and obesity-associated adipose tissue dysfunction. *Diabetologia* 56: 2524–2537, 2013.

54. Moreno-Navarrete JM, Ortega F, Serrano M, Rodriguez-Hermosa JI, Ricart W, Mingrone G, and Fernández-Real JM. CIDEC/FSP27 and PLIN1 gene expression run in parallel to mitochondrial genes in human adipose tissue, both increasing after weight loss. *Int J Obes* 38: 865–872, 2014.

55. Morley TS, Xia JY, and Scherer PE. Selective enhancement of insulin sensitivity in the mature adipocyte is sufficient for systemic metabolic improvements. *Nat Commun* 6: 7906, 2015.

56. Nagahara N, Nirasawa T, Yoshii T, and Niimura Y. Is novel signal transducer sulfur oxide involved in the redox cycle of persulfide at the catalytic site cysteine in a stable reaction intermediate of mercaptopyruvate sulfurtransferase? *Antioxidants Redox Signal* 16: 747–753, 2012.

57. Ortega FJ, Mercader JM, Moreno-Navarrete JM, Nonell L, Puigdecanet E, Rodriquez-Hermosa JI, Rovira O, Xifra G, Guerra E, Moreno M, Mayas D, Moreno-Castellanos N, Fernández-Formoso JA, Ricart W, Tinahones FJ, Torrents D, Malagón MM, and Fernández-Real JM. Surgery-induced weight loss is associated with the downregulation of genes targeted by MicroRNAs in adipose tissue. *J Clin Endocrinol Metab* 100: E1467–E1476, 2015.

58. Padiya R, Khatua TN, Bagul PK, Kuncha M, and Banerjee SK. Garlic improves insulin sensitivity and associated metabolic syndromes in fructose fed rats. *Nutr Metab* 8: 53, 2011.

59. Pan Z, Wang H, Liu Y, Yu C, Zhang Y, Chen J, Wang X, and Guan Q. Involvement of CSE/ H2S in high glucose induced aberrant secretion of adipokines in 3T3-L1 adipocytes. *Lipids Health Dis* 13: 155, 2014.

60. Paul BD and Snyder SH. H 2S signalling through protein sulfhydration and beyond. *Nat Rev Mol Cell Biol* 13: 499–507, 2012.

61. Pérez-Pérez R, López JA, García-Santos E, Camafeita E, Gómez-Serrano M, Ortega-Delgado FJ, Ricart W, Fernández-Real JM, and Peral B. Uncovering suitable reference proteins for expression studies in human adipose tissue with relevance to obesity. *PLoS One* 7: e30326, 2012.

62. Politis-Barber V, Brunetta HS, Paglialunga S, Petrick HL, and Holloway GP. Long-term, high-fat feeding exacerbates short-term increases in adipose mitochondrial reactive oxygen species, without impairing mitochondrial respiration. *Am J Physiol - Endocrinol Metab* 319: E373–E387, 2020.

63. Powell CR, Dillon KM, and Matson JB. A review of hydrogen sulfide (H2S) donors: Chemistry and potential therapeutic applications. *Biochem Pharmacol* 149: 110–123, 2018.

64. Rappou E, Jukarainen S, Rinnankoski-Tuikka R, Kaye S, Heinonen S, Hakkarainen A, Lundbom J, Lundbom N, Saunavaara V, Rissanen A, Virtanen KA, Pirinen E, and Pietiläinen KH. Weight Loss Is Associated With Increased NAD^+/SIRT1 Expression But Reduced PARP Activity in White Adipose Tissue. *J Clin Endocrinol {&} Metab* 101: 1263–1273, 2016.

65. Sanokawa-Akakura R, Akakura S, and Tabibzadeh S. Replicative senescence in human fibroblasts is delayed by hydrogen sulfide in a NAMPT/SIRT1 dependent manner. *PLoS One* 11: e0164710–e0164710, 2016.

66. Schmid B, Rippmann JF, Tadayyon M, and Hamilton BS. Inhibition of fatty acid synthase prevents preadipocyte differentiation. *Biochem Biophys Res Commun* 328: 1073–1082, 2005.

67. Shearin AL, Monks BR, Seale P, and Birnbaum MJ. Lack of AKT in adipocytes causes severe lipodystrophy. *Mol Metab* 5: 472–479, 2016.

68. Shibuya N, Tanaka M, Yoshida M, Ogasawara Y, Togawa T, Ishii K, and Kimura H. 3-Mercaptopyruvate sulfurtransferase produces hydrogen sulfide and bound sulfane sulfur in the brain. *Antioxidants Redox Signal* 11: 703–714, 2009.

69. Spassov SG, Donus R, Ihle PM, Engelstaedter H, Hoetzel A, and Faller S. Hydrogen Sulfide Prevents Formation of Reactive Oxygen Species through PI3K/Akt Signaling and Limits Ventilator-Induced Lung Injury. *Oxid Med Cell Longev* 2017: 3715037, 2017.

70. Szabó C. Hydrogen sulphide and its therapeutic potential. *Nat Rev Drug Discov* 6: 917–935, 2007.

71. Tinahones FJ, Araguez LCI, Murri M, Olivera WO, Torres MDM, Barbarroja N, Huelgas RG, Malagón MM, and Bekay R El. Caspase induction and BCL2 inhibition in human adipose tissue. *Diabetes Care* 36: 513–521, 2013.

72. Trayhurn P. Hypoxia and adipose tissue function and dysfunction in obesity. *Physiol Rev* 93: 1–21, 2013.

73. Tsai CY, Peh MT, Feng W, Dymock BW, and Moore PK. Hydrogen sulfide promotes adipogenesis in 3T3L1 cells. *PLoS One* 10: e0119511–e0119511, 2015.

74. Veilleux A, Blouin K, Rhéaume C, Daris M, Marette A, and Tchernof A. Glucose transporter 4 and insulin receptor substrate-1 messenger RNA expression in omental and subcutaneous adipose tissue in women. *Metabolism* 58: 624–631, 2009.

75. Vizcaíno JA, Csordas A, del-Toro N, Dianes JA, Griss J, Lavidas I, Mayer G, Perez-Riverol Y, Reisinger F, Ternent T, Xu Q-W, Wang R, and Hermjakob H. 2016 update of the PRIDE database and its related tools. *Nucleic Acids Res* 44: D447-56, 2016.

76. Vowinckel J, Capuano F, Campbell K, Deery MJ, Lilley KS, and Ralser M. The beauty of being (label)-free: Sample preparation methods for SWATH-MS and next-generation targeted proteomics. *F1000Research* 2: 272, 2014.

77. Whiteman M, Gooding KM, Whatmore JL, Ball CI, Mawson D, Skinner K, Tooke JE, and Shore AC. Adiposity is a major determinant of plasma levels of the novel vasodilator hydrogen sulphide. *Diabetologia* 53: 1722–1726, 2010.

78. Xu C, Cai Y, Fan P, Bai B, Chen J, Deng HB, Che CM, Xu A, Vanhoutte PM, and Wang Y. Calorie restriction prevents metabolic aging caused by abnormal sirt1 function in adipose tissues. *Diabetes* 64: 1576–1590, 2015.

79. Xue R, Hao DD, Sun JP, Li WW, Zhao MM, Li XH, Chen Y, Zhu JH, Ding YJ, Liu J, and Zhu YC. Hydrogen sulfide treatment promotes glucose uptake by increasing insulin receptor sensitivity and ameliorates kidney lesions in type 2 diabetes. *Antioxidants Redox Signal* 19: 5–23, 2013.

80. Yang G, Ju Y, Fu M, Zhang Y, Pei Y, Racine M, Baath S, Merritt TJS, Wang R, and Wu L. Cystathionine gamma-lyase/hydrogen sulfide system is essential for adipogenesis and fat mass accumulation in mice. *Biochim Biophys Acta - Mol Cell Biol Lipids* 1863: 165–176, 2018.

81. Yang G, Wu L, Jiang B, Yang W, Qi J, Cao K, Meng Q, Mustafa AK, Mu W, Zhang S, Snyder SH, and Wang R. H2S as a physiologic vasorelaxant: Hypertension in mice with deletion of cystathionine γ-lyase. *Science (80-)* 322: 587–590, 2008.

82. Zhan T, Poppelreuther M, Ehehalt R, and Füllekrug J. Overexpressed FATP1, ACSVL4/FATP4 and ACSL1 Increase the Cellular Fatty Acid Uptake of 3T3-L1 Adipocytes but Are Localized on Intracellular Membranes. *PLoS One 7: e45087, 2012.*

83. Zhang D, MacInkovic I, Devarie-Baez NO, Pan J, Park CM, Carroll KS, Filipovic MR, and Xian M. Detection of protein S-sulfhydration by a tag-switch technique. *Angew Chemie - Int Ed* 53: 575–581, 2014.

84. Zivanovic J, Kouroussis E, Kohl JB, Adhikari B, Bursac B, Schott-Roux S, Petrovic D, Miljkovic JL, Thomas-Lopez D, Jung Y, Miler M, Mitchell S, Milosevic V, Gomes JE, Benhar M, Gonzales-Zorn B, Ivanovic-Burmazovic I, Torregrossa R, Mitchell JR, Whiteman M, Schwarz G, Snyder SH, Paul BD, Carroll KS, and Filipovic MR. Selective Persulfide Detection Reveals Evolutionarily Conserved Antiaging Effects of S-Sulfhydration. *Cell Metab* 30: 1152–1170.e13, 2019.

85. 2. Classification and diagnosis of diabetes. *Diabetes Care* 38: S8–S16, 2015.

Table 1. Effects of transsulfuration pathway activation (PLP+CYS administration) on adipogenic, CTH and CBS gene expression and on H_2S production in cohort 1. These data were analysed using Paired T test. Bold values mean statistical significance ($p<0.05$).

	SAT (n=20)			VAT (n=20)		
	Control	**PLP+CYS**	**p**	**Control**	**PLP+CYS**	**P**
ADIPOQ (RU)	0.482±0.22	0.875±0.45	**<0.0001**	0.505±0.23	0.867±0.46	**<0.0001**
PPARG (RU)	0.022±0.009	0.035±0.015	**<0.0001**	0.025±0.013	0.040±0.017	**<0.0001**
SLC2A4 (RU)	0.0053±0.003	0.0085±0.004	**<0.0001**	0.0076±0.004	0.0119±0.007	**<0.0001**
FASN (RU)	0.167±0.08	0.232±0.13	**0.002**	0.203±0.08	0.274±0.16	**0.006**
LEP (RU)	0.125±0.06	0.209±0.12	**<0.0001**	0.075±0.07	0.142±0.13	**<0.0001**
IRS1 (RU)	0.0022±0.001	0.0022±0.001	0.9	0.0021±0.0008	0.0022±0.001	0.3
UCP3 (RU)	0.0003±0.0001	0.0003±0.0001	0.3	0.0005±0.0002	0.0004±0.0002	0.4
CIDEA (RU)	0.039±0.02	0.065±0.04	**0.001**	0.128±0.06	0.210±0.11	**<0.0001**
SIRT1 (RU)	0.017±0.005	0.026±0.008	**<0.0001**	0.025±0.009	0.035±0.013	**0.002**
CTH (RU)	0.0009±0.0003	0.0031±0.002	**<0.0001**	0.0031±0.001	0.0072±0.003	**0.001**
CBS (RU)	0.0024±0.001	0.0051±0.003	**<0.0001**	0.0048±0.002	0.0084±0.005	**0.001**
H_2S (nmol/mg AT)	0.57±0.4	2.05±1.1	**0.002**	0.48±0.3	2.11±1.5	**0.004**

Table 2. Correlation between *CTH, CBS* and *MPST* gene expression and anthropometric and clinical characteristics and selected gene expression in SAT (n=119) and VAT (n=122) from cohort 2. Bold values mean statistical significance (p<0.05).

	SAT *CTH*		**SAT *CBS***		**SAT *MPST***	
	r	**p**	**r**	**p**	**R**	**p**
Age (years)	0.05	0.6	0.01	0.9	-0.13	0.1
BMI (kg/m^2)	-0.52	**<0.0001**	-0.39	**<0.0001**	-0.32	**<0.0001**
Fasting glucose (mg/dl)	-0.09	0.3	-0.18	0.06	-0.22	**0.04**
HOMA-IR (n=34)	-0.61	**<0.0001**	-0.62	**<0.0001**	0.20	0.2
Total Cholesterol (mg/dl)	0.04	0.6	-0.05	0.6	-0.03	0.7
HDL Cholesterol (mg/dl)	0.18	0.06	-0.10	0.3	-0.02	0.8
LDL Cholesterol (mg/dl)	0.07	0.4	0.05	0.5	0.01	0.8
Fasting Triglycerides (mg/dl)	-0.22	**0.03**	-0.06	0.5	-0.21	**0.04**
FASN (R.U.)	0.50	**<0.0001**	0.45	**<0.0001**	0.46	**<0.0001**
ACACA (R.U.)	0.33	**0.001**	0.27	**0.006**	-0.02	0.8
PPARG (R.U.)	0.59	**<0.0001**	0.29	**0.01**	0.10	0.3
SLC2A4 (R.U.)	0.55	**<0.0001**	0.42	**<0.0001**	0.46	**<0.0001**
IRS1 (R.U.)	0.41	**<0.0001**	0.47	**<0.0001**	0.29	**0.004**
SIRT1 (R.U.)	0.52	**<0.0001**	0.36	**0.001**	-0.03	0.7
PPARGC1A (R.U.)	0.41	**<0.0001**	0.49	**<0.0001**	0.05	0.6
LEP (R.U.)	-0.37	**0.001**	-0.33	**0.008**	-0.22	**0.04**
LBP (R.U.)	-0.46	**<0.0001**	-0.26	**0.02**	-0.06	0.6
TNF (R.U.)	0.06	0.6	-0.03	0.7	-0.36	**<0.0001**
CD68 (R.U.)	0.05	0.6	0.03	0.7	-0.18	0.1
	VAT *CTH*		**VAT *CBS***		**VAT *MPST***	
	r	**p**	**r**	**p**	**r**	**p**
Age (years)	0.07	0.4	0.11	0.2	0.20	0.1
BMI (kg/m^2)	-0.46	**<0.0001**	-0.36	**<0.0001**	-0.26	**0.01**
Fasting glucose (mg/dl)	-0.17	0.08	-0.02	0.8	0.09	0.2
HOMA-IR (n=34)	-0.11	0.5	-0.08	0.6	-0.02	0.9
Total Cholesterol (mg/dl)	0.15	0.1	0.02	0.8	0.12	0.1
HDL Cholesterol (mg/dl)	-0.01	0.9	-0.09	0.4	-0.04	0.6
LDL Cholesterol (mg/dl)	0.20	0.05	0.02	0.8	0.17	0.1
Fasting Triglycerides (mg/dl)	0.02	0.8	0.11	0.2	-0.04	0.6
FASN (R.U.)	0.41	**<0.0001**	0.32	**0.001**	0.26	**0.01**
ACACA (R.U.)	0.35	**0.001**	0.37	**<0.0001**	-0.10	0.2
PPARG (R.U.)	0.44	**<0.0001**	0.39	**<0.0001**	0.12	0.3
SLC2A4 (R.U.)	0.48	**<0.0001**	0.39	**<0.0001**	0.41	**<0.0001**
IRS1 (R.U.)	0.44	**<0.0001**	0.39	**<0.0001**	0.30	**0.003**
SIRT1 (R.U.)	0.55	**<0.0001**	0.37	**<0.0001**	-0.08	0.5
PPARGC1A (R.U.)	0.25	**0.02**	0.12	0.3	-0.09	0.3
LEP (R.U.)	-0.39	**<0.0001**	-0.38	**<0.0001**	0.20	0.1
LBP (R.U.)	-0.25	**0.02**	-0.38	**<0.0001**	-0.02	0.9
TNF (R.U.)	-0.07	0.5	-0.02	0.8	-0.29	**0.005**
CD68 (R.U.)	0.05	0.5	0.19	0.1	-0.03	0.8

VAT, visceral adipose tissue; SAT, subcutaneous adipose tissue; HOMA-IR, Homeostasis Model Assessment – Insulin Resistance Index; R.U., relative gene expression units.

Table 3. Correlation between *CTH, CBS* and *MPST* gene expression and anthropometric and clinical characteristics and selected gene expression in SAT (n=35) and VAT (n=35) from cohort 3. Bold values mean statistical significance (p<0.05).

	SAT *CTH*		**SAT *CBS***		**SAT *MPST***	
	r	**p**	**r**	**p**	**r**	**p**
Age (years)	0.20	0.2	0.15	0.3	-0.16	0.4
BMI (kg/m^2)	0.05	0.7	-0.19	0.2	0.12	0.5
Waist circumference (cm)	-0.19	0.2	-0.23	0.2	-0.50	**0.002**
HOMA-IR	0.31	0.06	-0.29	0.08	-0.34	0.08
M (mg/kg·min)	0.24	0.2	0.40	**0.03**	0.35	0.07
Fasting Glucose (mg/dL)	-0.01	0.9	-0.13	0.4	-0.38	0.05
Total Cholesterol (mg/dl)	0.29	0.08	0.27	0.1	0.09	0.6
HDL Cholesterol (mg/dl)	0.32	0.05	0.06	0.7	-0.23	0.2
LDL Cholesterol (mg/dl)	0.21	0.2	0.28	0.1	0.07	0.7
Fasting triglycerides (mg/dl)	0.02	0.9	-0.05	0.7	0.16	0.4
PPARG (R.U.)	0.58	**<0.0001**	-0.33	0.05	0.23	0.2
ADIPOQ (R.U.)	0.56	**<0.0001**	0.17	0.3	0.38	0.05
SLC2A4 (R.U.)	0.13	0.4	0.53	**0.001**	0.44	**0.01**
IRS1 (R.U.)	0.41	**0.01**	0.23	0.2	0.32	0.1
SIRT1 (R.U.)	0.66	**<0.0001**	0.01	0.9	-0.11	0.6
PPARGC1A (R.U.)	0.85	**<0.0001**	0.04	0.8	0.15	0.4
TNF (R.U.)	-0.36	**0.04**	0.22	0.2	0.23	0.2
BAX (R.U.)	-0.66	**0.003**	0.24	0.2	0.05	0.8
TP53 (R.U.)	-0.65	**0.004**	0.28	0.1	-0.11	0.6
	VAT *CTH*		**VAT *CBS***		**VAT *MPST***	
	r	**p**	**r**	**p**	**r**	**p**
Age (years)	-0.16	0.3	0.07	0.7	0.13	0.4
BMI (kg/m^2)	-0.06	0.7	-0.08	0.6	-0.28	0.1
Waist circumference (cm)	-0.44	**0.008**	-0.08	0.6	-0.15	0.4
HOMA-IR	-0.37	**0.02**	0.08	0.6	-0.22	0.2
M (mg/kg·min)	0.21	0.2	0.16	0.4	0.33	0.08
Fasting Glucose (mg/dL)	-0.08	0.6	0.10	0.5	0.06	0.7
Total Cholesterol (mg/dl)	0.05	0.7	0.01	0.9	-0.10	0.5
HDL Cholesterol (mg/dl)	0.14	0.4	0.21	0.2	0.22	0.2
LDL Cholesterol (mg/dl)	0.05	0.7	-0.04	0.8	-0.18	0.3
Fasting triglycerides (mg/dl)	-0.22	0.1	-0.35	**0.04**	0.02	0.9
PPARG (R.U.)	0.28	0.1	-0.29	0.1	0.46	**0.005**
ADIPOQ (R.U.)	0.41	**0.01**	-0.15	0.3	0.42	**0.01**
SLC2A4 (R.U.)	0.19	0.2	0.18	0.3	0.61	**<0.0001**
IRS1 (R.U.)	0.46	**0.005**	0.27	0.1	0.14	0.4
SIRT1 (R.U.)	0.48	**0.005**	0.19	0.3	-0.30	0.1
PPARGC1A (R.U.)	0.43	**0.01**	0.16	0.3	-0.32	0.1
TNF (R.U.)	-0.31	0.06	0.18	0.3	-0.17	0.3
BAX (R.U.)	-0.44	**0.02**	0.23	0.2	0.29	0.1
TP53 (R.U.)	-0.42	**0.03**	0.27	0.1	0.09	0.6

VAT, visceral adipose tissue; SAT, subcutaneous adipose tissue; HOMA-IR, Homeostasis Model Assessment – Insulin Resistance Index; M, systemic insulin sensitivity measured by hyperinsulinemic-euglycemic clamp; R.U., relative gene expression units.

Figure 1

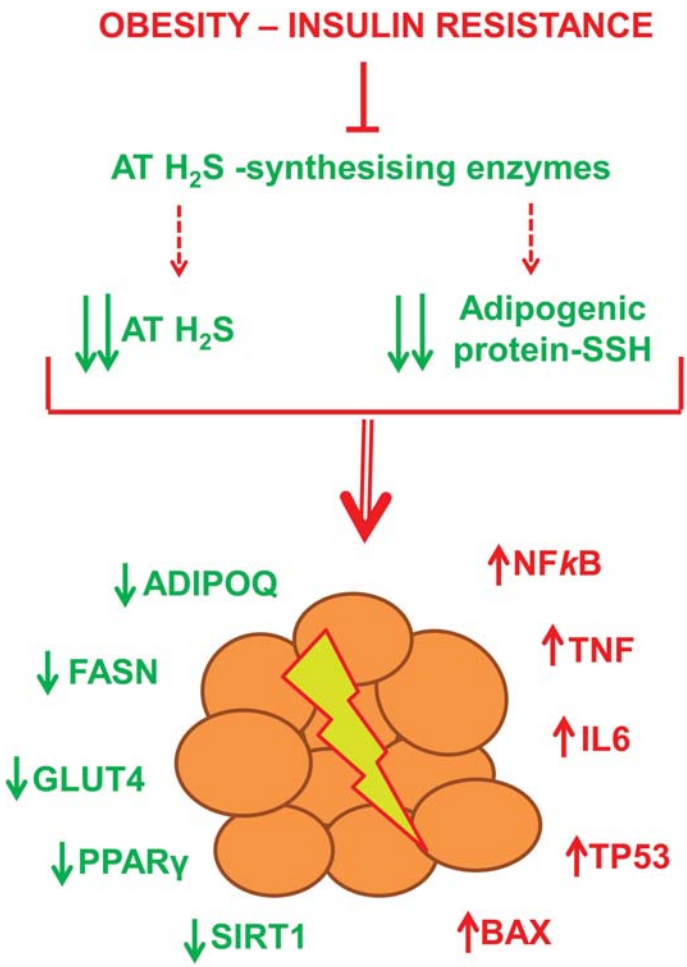
OBESITY – INSULIN RESISTANCE
AT H_2S -synthesising enzymes
AT H_2S
Adipogenic protein-SSH
↓ADIPOQ
↑NFkB
↓FASN
↑TNF
↑IL6
↓GLUT4
↓PPARγ
↑TP53
↓SIRT1
↑BAX

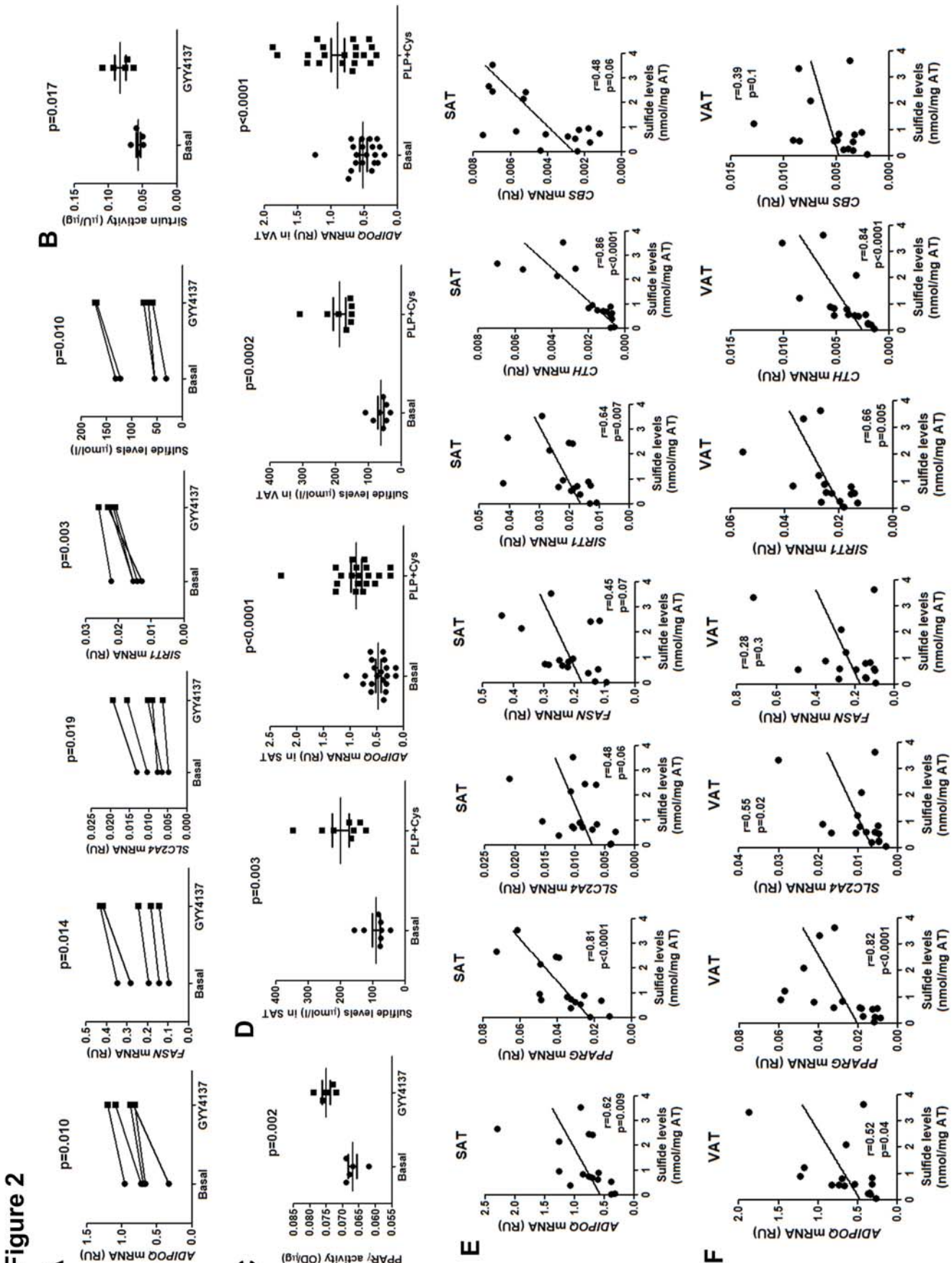
Figure 2
A
B
C
D
E
F
ADIPOQ mRNA (RU)
FASN mRNA (RU)
SLC2A4 mRNA (RU)
SIRT1 mRNA (RU)
PPARγ activity (OD/µg)
Sirtuin activity (µU/µg)
Sulfide levels (µmol/l)
ADIPOQ mRNA (RU) in SAT
ADIPOQ mRNA (RU) in VAT
Sulfide levels (µmol/l) in SAT
Sulfide levels (µmol/l) in VAT
PPARG mRNA (RU)
CTH mRNA (RU)
CBS mRNA (RU)
Basal
GYY4137
PLP+Cys
SAT
VAT
Sulfide levels (nmol/mg AT)
p=0.010
p=0.014
p=0.019
p=0.003
p=0.017
p=0.002
p<0.0001
p=0.0002
r=0.62 p=0.009
r=0.81 p<0.0001
r=0.48 p=0.06
r=0.45 p=0.07
r=0.64 p=0.007
r=0.86 p<0.0001
r=0.48 p=0.06
r=0.52 p=0.04
r=0.82 p<0.0001
r=0.55 p=0.02
r=0.28 p=0.3
r=0.66 p=0.005
r=0.84 p<0.0001
r=0.39 p=0.1

Figure 3

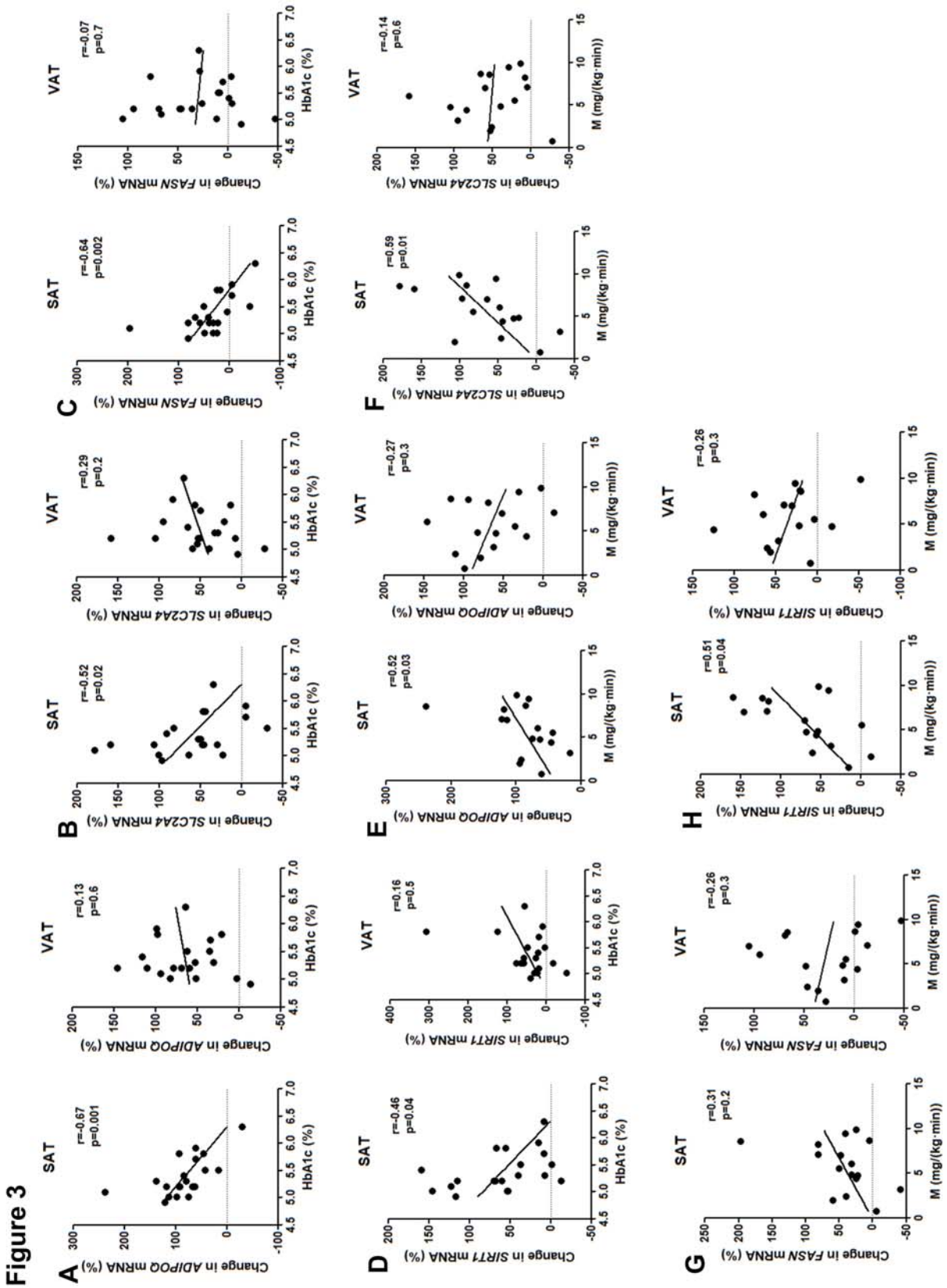
A
SAT
r=-0.67
p=0.001
Change in ADIPOQ mRNA (%)
HbA1c (%)
B
SAT
r=-0.52
p=0.02
Change in SLC2A4 mRNA (%)
HbA1c (%)
C
SAT
r=-0.64
p=0.002
Change in FASN mRNA (%)
HbA1c (%)
D
SAT
r=-0.46
p=0.04
Change in SIRT1 mRNA (%)
HbA1c (%)
E
SAT
r=0.52
p=0.03
Change in ADIPOQ mRNA (%)
M (mg/(kg·min))
F
SAT
r=0.59
p=0.01
Change in SLC2A4 mRNA (%)
M (mg/(kg·min))
G
SAT
r=0.31
p=0.2
Change in FASN mRNA (%)
M (mg/(kg·min))
H
SAT
r=0.51
p=0.04
Change in SIRT1 mRNA (%)
M (mg/(kg·min))
VAT
r=0.13
p=0.6
r=0.29
p=0.2
r=-0.07
p=0.7
r=0.16
p=0.5
r=-0.27
p=0.3
r=0.14
p=0.6
r=0.26
p=0.3
r=-0.26
p=0.3

Figure 4

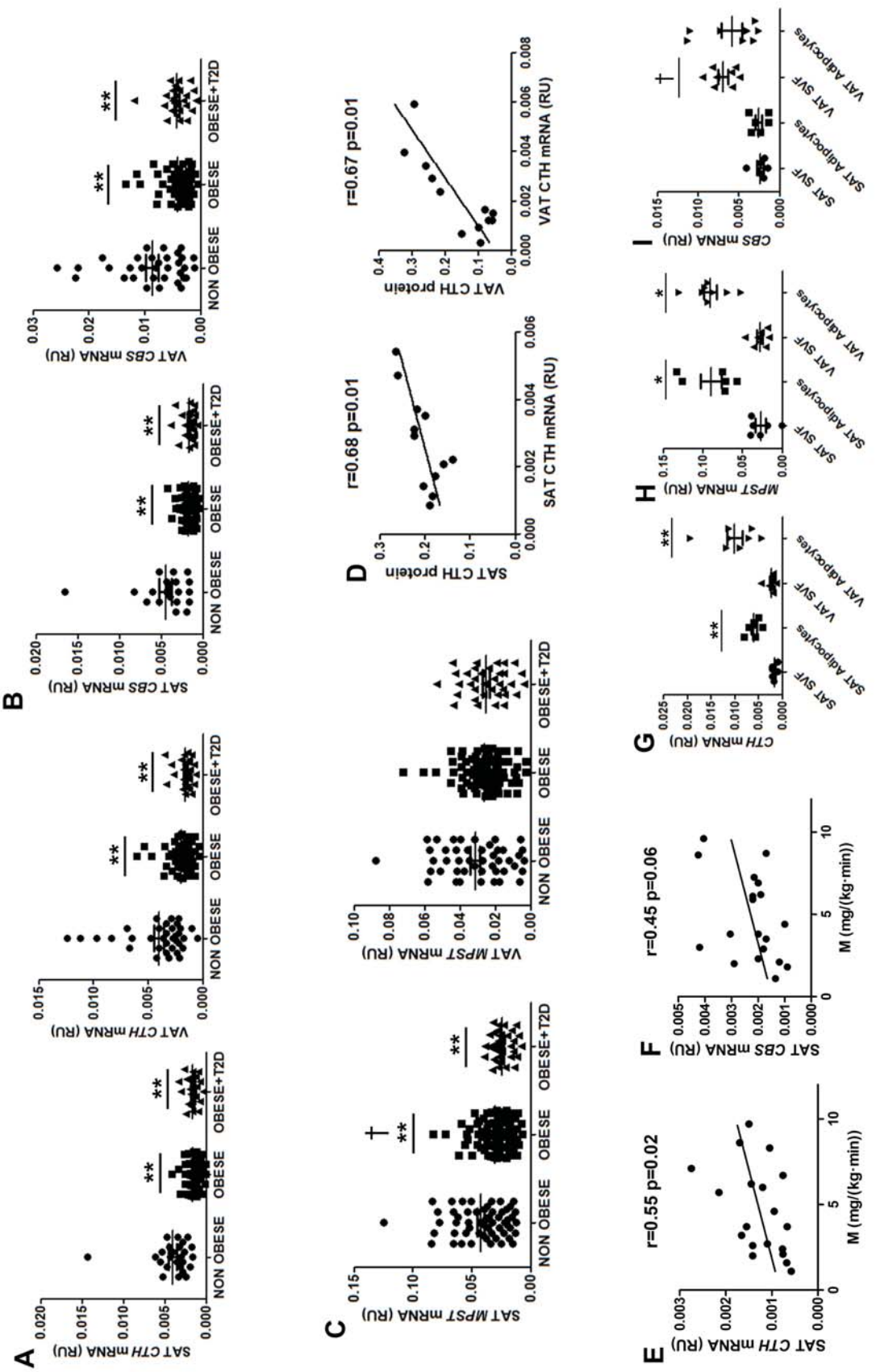
A
SAT CTH mRNA (RU)
NON OBESE
OBESE
OBESE+T2D
B
VAT CBS mRNA (RU)
SAT CBS mRNA (RU)
C
SAT MPST mRNA (RU)
VAT MPST mRNA (RU)
D
r=0.67 p=0.01
VAT CTH protein
VAT CTH mRNA (RU)
r=0.68 p=0.01
SAT CTH protein
SAT CTH mRNA (RU)
E
r=0.55 p=0.02
SAT CTH mRNA (RU)
M (mg/(kg·min))
F
r=0.45 p=0.06
SAT CBS mRNA (RU)
G
CTH mRNA (RU)
SAT SVF
SAT Adipocytes
VAT SVF
VAT Adipocytes
H
MPST mRNA (RU)
I
CBS mRNA (RU)

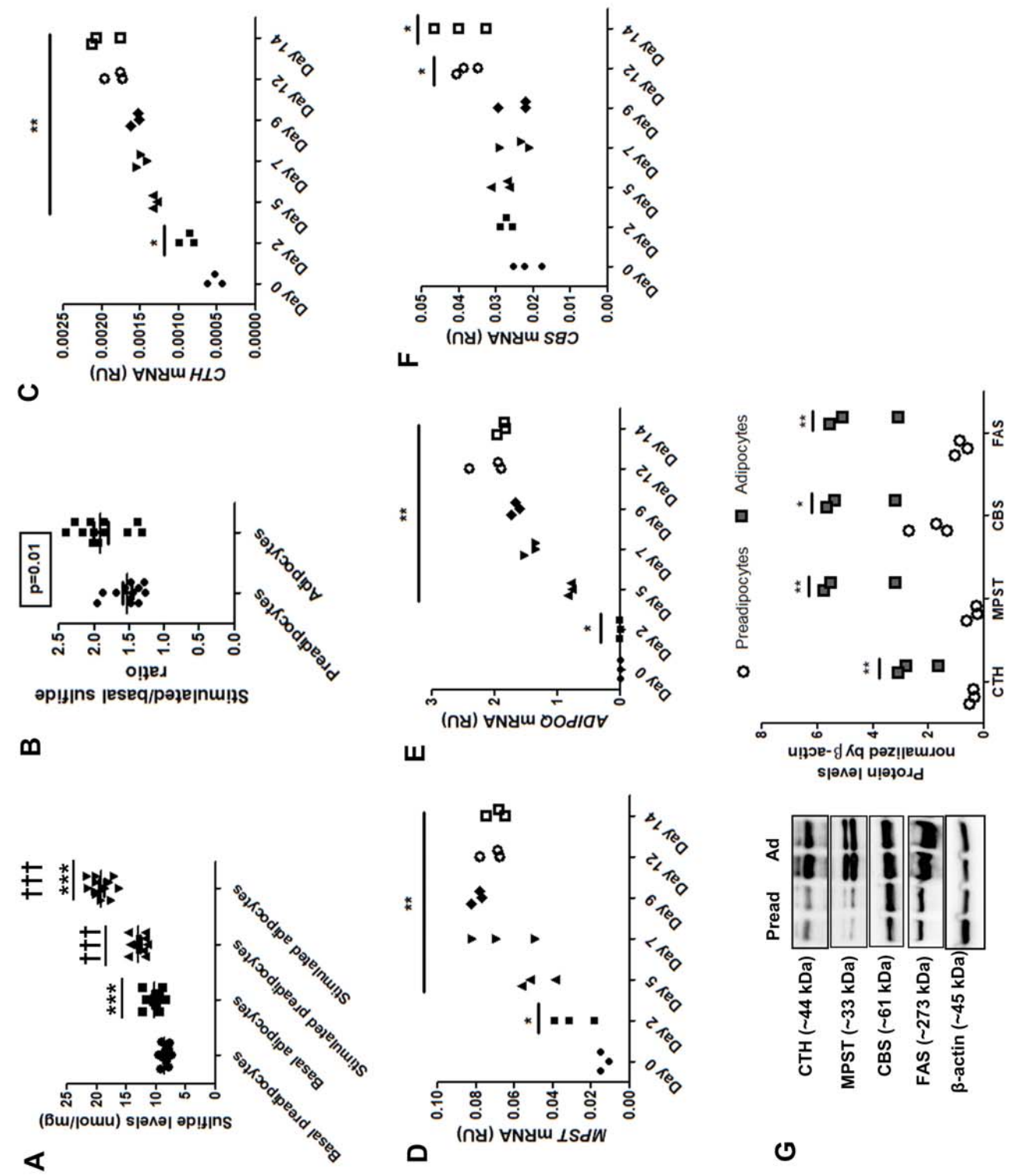
A
Sulfide levels (nmol/mg)
Basal preadipocytes
Basal adipocytes
Stimulated preadipocytes
Stimulated adipocytes
B
Stimulated/basal sulfide ratio
p=0.01
Preadipocytes
Adipocytes
C
CTH mRNA (RU)
Day 0
Day 2
Day 5
Day 7
Day 9
Day 12
Day 14
D
MPST mRNA (RU)
E
ADIPOQ mRNA (RU)
F
CBS mRNA (RU)
G
Preadipocytes
Adipocytes
Protein levels normalized by β-actin
CTH
MPST
CBS
FAS
Pread
Ad
CTH (~44 kDa)
MPST (~33 kDa)
CBS (~61 kDa)
FAS (~273 kDa)
β-actin (~45 kDa)

Figure 5

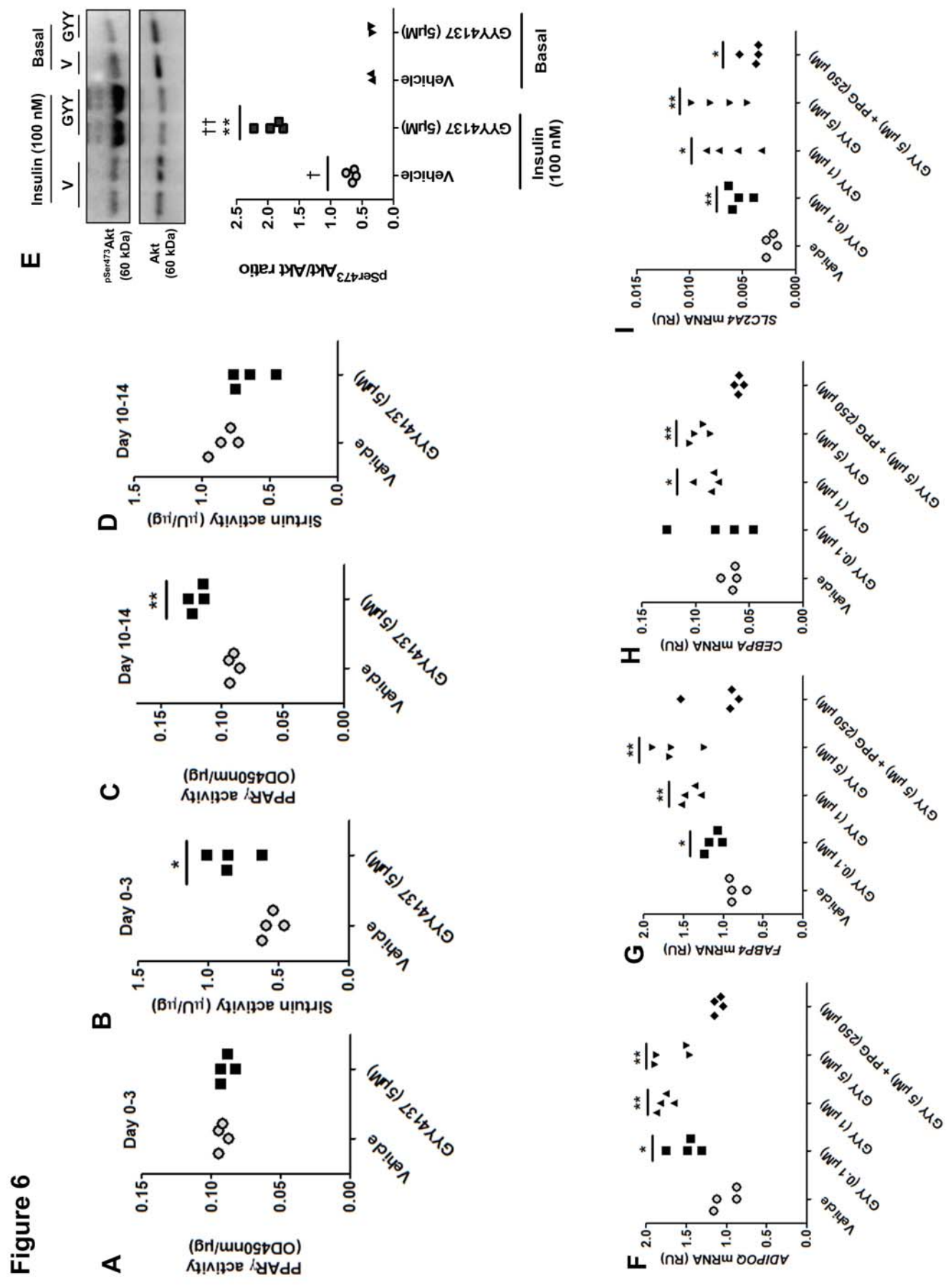
Figure 6
A
PPARγ activity (OD450nm/µg)
Day 0-3
Vehicle
GYY4137 (5µM)
B
Sirtuin activity (µU/µg)
Day 0-3
Vehicle
GYY4137 (5µM)
C
PPARγ activity (OD450nm/µg)
Day 10-14
Vehicle
GYY4137 (5µM)
D
Sirtuin activity (µU/µg)
Day 10-14
Vehicle
GYY4137 (5µM)
E
Insulin (100 nM)
V
GYY
Basal
V
GYY
pSer473Akt (60 kDa)
Akt (60 kDa)
pSer473Akt/Akt ratio
Vehicle
GYY4137 (5µM)
Insulin (100 nM)
Basal
F
ADIPOQ mRNA (RU)
G
FABP4 mRNA (RU)
H
CEBPA mRNA (RU)
I
SLC2A4 mRNA (RU)
Vehicle
GYY (0.1 µM)
GYY (1 µM)
GYY (5 µM)
GYY (5 µM) + PPG (250 µM)

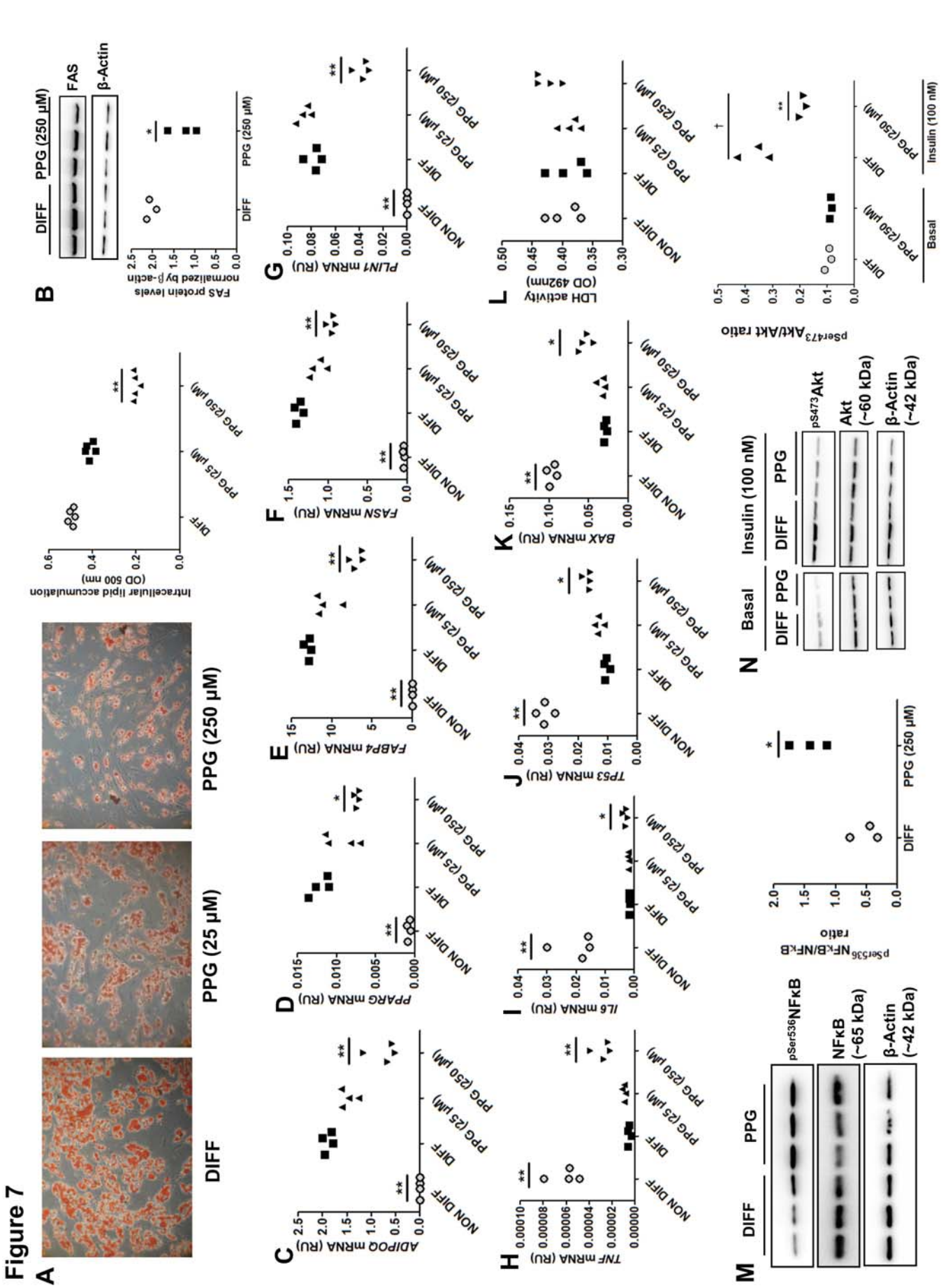
Figure 7
A
DIFF
PPG (25 µM)
PPG (250 µM)
Intracellular lipid accumulation (OD 500 nm)
DIFF
PPG (25 µM)
PPG (250 µM)
B
DIFF
PPG (250 µM)
FAS
β-Actin
FAS protein levels normalized by β-actin
C
ADIPOQ mRNA (RU)
D
PPARG mRNA (RU)
E
FABP4 mRNA (RU)
F
FASN mRNA (RU)
G
PLIN1 mRNA (RU)
H
TNF mRNA (RU)
I
IL6 mRNA (RU)
J
TP53 mRNA (RU)
K
BAX mRNA (RU)
L
LDH activity (OD 492nm)
NON DIFF
DIFF
PPG (25 µM)
PPG (250 µM)
M
DIFF
PPG
pSer536NFκB
NFκB (~65 kDa)
β-Actin (~42 kDa)
pSer536NFκB/NFκB ratio
N
Basal
Insulin (100 nM)
DIFF PPG
DIFF
PPG
pS473Akt
Akt (~60 kDa)
β-Actin (~42 kDa)
pSer473Akt/Akt ratio
Basal
Insulin (100 nM)

Figure 8

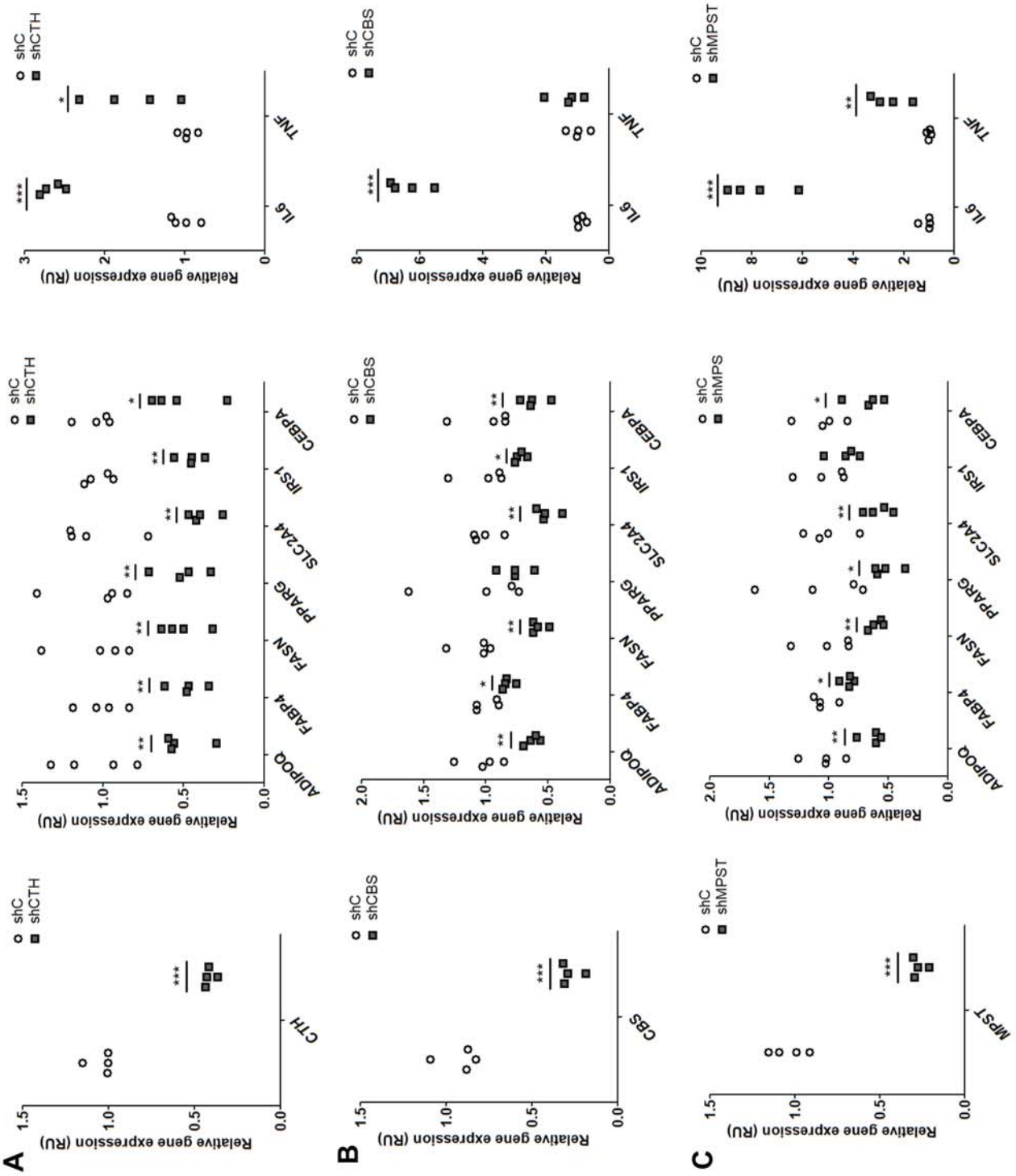
A
B
C
shC
shCTH
shCBS
shMPST
shMPS
Relative gene expression (RU)
CTH
CBS
MPST
ADIPOQ
FABP4
FASN
PPARG
SLC2A4
IRS1
CEBPA
IL6
TNF

Figure 9

A

Protein persulfidation-enriched biological processes in adipocytes (%)

#Term ID	Term description	%	FDR
GO:0006085	acetyl-CoA biosynthetic process	69.23	1.9E-10
GO:0033539	fatty acid beta-oxidation using acyl-CoA dehydrogenase	60.00	4.71E-10
GO:0006084	acetyl-CoA metabolic process	51.85	5.79E-15
GO:0006099	tricarboxylic acid cycle	50.00	6.83E-17
GO:0006101	citrate metabolic process	47.22	1.32E-17
GO:0072350	tricarboxylic acid metabolic process	45.00	2.58E-18
GO:0071616	acyl-CoA biosynthetic process	43.90	3.62E-18
GO:0006635	fatty acid beta-oxidation	41.07	1.53E-22
GO:0019395	fatty acid oxidation	32.00	1.56E-21
GO:0009060	aerobic respiration	30.99	1.34E-19
GO:0009062	fatty acid catabolic process	29.76	8.78E-22
GO:0006695	cholesterol biosynthetic process	29.27	1.71E-10
GO:0006637	acyl-CoA metabolic process	28.41	2.05E-21
GO:0043648	dicarboxylic acid metabolic process	25.77	1.22E-20
GO:0046364	monosaccharide biosynthetic process	25.45	1.53E-11
GO:0072329	monocarboxylic acid catabolic process	24.53	5.72E-21
GO:0006090	pyruvate metabolic process	24.24	6.84E-13
GO:0006119	oxidative phosphorylation	23.00	4.48E-18
GO:0045333	cellular respiration	22.88	2.24E-27
GO:0033875	ribonucleoside bisphosphate metabolic process	21.95	9.86E-21
GO:0034032	purine nucleoside bisphosphate metabolic process	21.95	9.86E-21
GO:0016999	antibiotic metabolic process	21.77	1.12E-20
GO:1990542	mitochondrial transmembrane transport	21.69	8.71E-14
GO:0046496	nicotinamide nucleotide metabolic process	21.50	1.54E-17
GO:0072524	pyridine-containing compound metabolic process	21.24	3.62E-18
GO:0044242	cellular lipid catabolic process	20.96	2.71E-26
GO:0042775	mitochondrial ATP synthesis coupled electron transport	20.51	6.18E-12

B

Protein persulfidation-enriched KEGG pathways in adipocytes (%)

#Term ID	Term description	%	FDR
hsa00020	Citrate cycle (TCA cycle)	63.33	8.75E-22
hsa00620	Pyruvate metabolism	56.41	2.91E-24
hsa00280	Valine, leucine and isoleucine degradation	50.00	2.02E-25
hsa00640	Propanoate metabolism	50.00	3.12E-17
hsa00071	Fatty acid degradation	47.73	4.7E-22
hsa01210	2-Oxocarboxylic acid metabolism	47.06	7.86E-09
hsa00061	Fatty acid biosynthesis	41.67	0.0000148
hsa01212	Fatty acid metabolism	39.58	7.19E-19
hsa00630	Glyoxylate and dicarboxylate metabolism	39.29	3.09E-11
hsa00380	Tryptophan metabolism	35.00	1.43E-13
hsa01200	Carbon metabolism	33.62	2.61E-36
hsa00410	beta-Alanine metabolism	32.26	1.29E-09
hsa00100	Steroid biosynthesis	31.58	0.00000567
hsa00062	Fatty acid elongation	28.00	0.00000152
hsa03320	PPAR signaling pathway	26.39	2.74E-16
hsa01040	Biosynthesis of unsaturated fatty acids	26.09	0.000014
hsa00650	Butanoate metabolism	25.00	0.00000281
hsa00220	Arginine biosynthesis	25.00	0.000096
hsa00030	Pentose phosphate pathway	23.33	0.00000404
hsa01230	Biosynthesis of amino acids	22.22	6.89E-13
hsa00010	Glycolysis / Gluconeogenesis	22.06	4.38E-12
hsa00310	Lysine degradation	22.03	1.48E-10
hsa00330	Arginine and proline metabolism	20.83	4.45E-08
hsa00190	Oxidative phosphorylation	17.56	2.74E-16
hsa00250	Alanine, aspartate and glutamate metabolism	17.14	0.0000949
hsa04714	Thermogenesis	13.60	7.19E-19
hsa04923	Regulation of lipolysis in adipocytes	13.21	0.0000912
hsa04146	Peroxisome	11.11	0.0000233
hsa04920	Adipocytokine signaling pathway	10.14	0.00035
hsa04922	Glucagon signaling pathway	9.00	0.000096
hsa04152	AMPK signaling pathway	8.33	0.0000682
hsa04910	Insulin signaling pathway	8.21	0.0000298

C

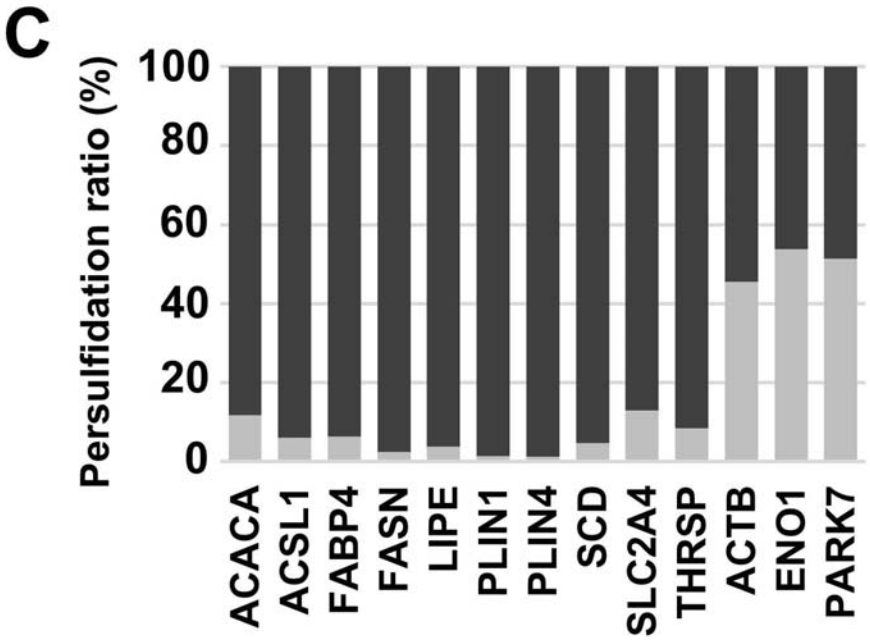

Figure legends

Figure 1. Graphic illustration summarizing how in patients with obesity and insulin resistance adipose tissue H_2S biosynthesis is attenuated, and this attenuation results in adipose tissue dysfunction, possibly promoted by decreased persulfidation in key adipogenic proteins. This summary suggests that the potentiation of adipose tissue H_2S biosynthesis might be a possible therapeutic approach to improve obesity-associated adipose tissue dysfunction.

Figure 2. A) Effect of GYY4137 (5 μM) administration for 16h on *ADIPOQ, FASN SLC2A4* and *SIRT1* mRNA levels and on tissue culture media sulfide levels in human adipose tissue explants (Cohort1). **B-C)** GYY4137 (200 μM) effects on Sirtuin deacetylase **(B)** and PPARγ transcriptional **(C)** activity (1 h, 37ºC) in adipose tissue lysates (Cohort1). **D)** Effect of L-cysteine (10 mM) and pyridoxal 5'-phosphate (2 mM) (PLP+ Cys) administration for 16h on sulfide concentration in media (N=8) and *ADIPOQ* gene expression (N=20) in human SAT and VAT explants (Cohort1). **E-F)** Bivariate correlation (Spearman r) between *ADIPOQ*, *PPARG*, *SLC2A4, FASN, SIRT1, CTH* and *CBS* and media sulfide levels in both SAT **(E)** and VAT **(F)** in cohort 1.

Figure 3. A-D) Bivariate correlation (Spearman r) between percent change in *ADIPOQ* **(A)**, *SLC2A4* **(B)**, *FASN* **(C)** and *SIRT1* **(D)** after PLP and Cys administration and HbA1c levels in both SAT and VAT (Cohort1). **E-H)** Bivariate correlation (Spearman r) between percent change in *ADIPOQ* **(E)**, *SLC2A4* **(F)**, *FASN* **(G)** and *SIRT1* **(H)** after PLP and Cys administration and insulin sensitivity (M value) (Cohort1).

Figure 4. A-C) SAT and VAT *CTH, CBS* and *MPST* gene expression according to obesity and type 2 diabetes (Cohort 2). **p<0.01 *vs* non-obese; †p<0.05 *vs* obese + T2D participants. **D)** Bivariate correlation (Spearman r) between CTH protein and *CTH*

mRNA levels in both SAT and VAT (Cohort 2). **E-F)** Bivariate correlation between insulin sensitivity and SAT *CTH* **(E)** and *CBS* **(F)** gene expression in cohort 3. **G-I)** *CTH*, *MPST* and *CBS* gene expression in SAT and VAT adipose tissue cell fractions [stromal vascular cell fraction (SVF) and adipocytes] in cohort 2. *p<0.05 and **p<0.01 *vs* SVF; †p<0.05 *vs* SAT cells.

Figure 5. A-B) Basal and stimulated [treated with L-cysteine 250 μM) and pyridoxal 5'-phosphate (50 μM)] H_2S production (A) and stimulated/basal H_2S ratio **(B)** in human preadipocytes and fully differentiated adipocytes. ***p<0.001 versus preadipocytes $^{+++}$p<0.001 versus basal. **C-F)** *CTH, MPST, ADIPOQ* and *CBS* gene expression during human preadipocyte differentiation into adipocytes. Time-course experiment included day 0, 2, 5, 7, 9, 12 and 14. *p<0.05 and **p<0.01 versus day 0 **(G)** CTH, MPST, CBS, and FASN protein levels in human preadipocytes and adipocytes. Protein levels were normalized by b-actin. Entire western blots are shown in Supplementary Fig. S3 and S4. *p<0.05 and **p<0.01 versus preadipocytes.

Figure 6. A-E) GYY4137 (5 μM) effects on PPARγ transcriptional and Sirtuin deacetylase activity in preadipocytes **(A, B)** and adipocytes **(C, D)**. **E)** GYY4137 (5 μM) effects on insulin-stimulated Akt phosphorylation at Ser473 in human differentiated adipocytes. Entire western blots are shown in Supplementary Fig. S5. *p<0.05 and **p<0.01 *vs* vehicle. †p<0.05 and ††p<0.01 *vs* basal. **F-I)** GYY4137 (0.1, 1, 5 μM) and GYY4137 (5 μM) + PPG (250 μM) on adipogenic [*ADIPOQ* **(F)**, *FABP4* **(G)**, *CEBPA* **(H)**, *SLC2A4* **(I)**] gene expression in human differentiated adipocytes. *p<0.05 and **p<0.01 *vs* vehicle.

Figure 7. A-M) Effects of DL-Propargylglycine (PPG, 25 and 250 μM) administration on intracellular lipid accumulation measured by Oil red staining (10X, OM) **(A)**, FAS protein levels **(B)**, adipogenic (*ADIPOQ, PPARG, FABP4, FASN, PLIN1*) gene

expression **(C-G)**, expression of inflammatory and cellular senescence gene markers (*TNF, IL6, BAX, TP53*) **(H-K)**, LDH activity **(L)** and ^{pSer536}NFκB / ^{pSer536}NFκB ratio measured using western blot band intensities **(M)** at day 14 of human sc adipocyte differentiation. **N)** Effects of DL-Propargylglycine (PPG 250 µM) administration on insulin-stimulated Akt phosphorylation at Ser473 in human differentiated adipocytes. *p<0.05 and **p<0.01 *vs* differentiated control cells (Diff); †<0.05 vs basal. Entire western blots were shown in Supplementary Fig S6, S7 and S8.

Figure 8. A-C) Effects of *CTH* **(A)**, *CBS* **(B)** and *MPST* **(C)** gene knockdown on H_2S-synthesising enzymes (*CTH, CBS, MPST*)-, adipogenic (*ADIPOQ, FABP4, FASN, PPARG, CEBPA*)-, insulin pathway (*SLC2A4, IRS1*)- and inflammatory (*IL6,* TNF)-related gene expression at day 14 of human subcutaneous adipocyte differentiation. *p<0.05, **p<0.01 and ***p<0.001 *vs* shC differentiated control cells.

Figure 9. A-B) Representation of protein persulfidation-enriched biological processes **(A)** and KEGG pathways **(B)** in human adipocytes. **C)** Persulfidation ratio of proteins involved in adipocyte lipid metabolism and control proteins (ACTB, ENO1, PARK7). Level of protein persulfidation in preadipocyte (clear grey boxes) compared to the level in adipocyte (dark grey boxes). ACACA, Acetyl-CoA carboxylase 1; ACSL1, Long-chain-fatty-acid--CoA ligase 1; FABP4, Fatty acid-binding protein; FASN, Fatty acid synthase; LIPE, Hormone-sensitive lipase; PLIN1, Perilipin-1; PLIN4, Perilipin-4; SLC2A4, Solute carrier family 2 member 4; THRSP, Thyroid hormone-inducible hepatic protein; ACTB, β-actin; ENO1, enolase 1; PARK7, Parkinsonism associated deglycase.

Supplementary figure legends

Suppl Figure 1. A-L) Effect of PPG (25 and 250 µM, 48h) administration on *ADIPOQ, FASN, DGAT1, PPARG, IRS1, PPARGC1A, SIRT1, BAX, TP53, IL6* and *TNF* gene expression, and on LDH activity in fully differentiated adipocytes.**p<0.01 and ***p<0.001 *vs* vehicle.

Suppl Figure 2. A-B) Protein persulfidation-enriched biological processes **(A)** and KEGG pathways **(B)** in human preadipocytes.

Suppl Figure 3. This figure includes entire blots of cropped Western blot band for CTH, MPST and CBS proteins shown in Figure 5G.

Suppl Figure 4. This figure includes entire blots of cropped Western blot band for FAS and β-actin proteins shown in Figure 5G.

Suppl Figure 5. This figure includes entire blots of cropped Western blot band for ^{pSer473}Akt and Akt proteins shown in Figure 6E.

Suppl Figure 6. This figure includes entire blots of cropped Western blot band for FAS and β-actin proteins shown in Figure 7B.

Suppl Figure 7. This figure includes entire blots of cropped Western blot band for ^{pSer536}NFκB, NFκB and β-actin proteins shown in Figure 7M.

Suppl Figure 8. This figure includes entire blots of cropped Western blot band for ^{pSer473}Akt, Akt and β-actin proteins shown in Figure 7N.

Suppl Figure 1

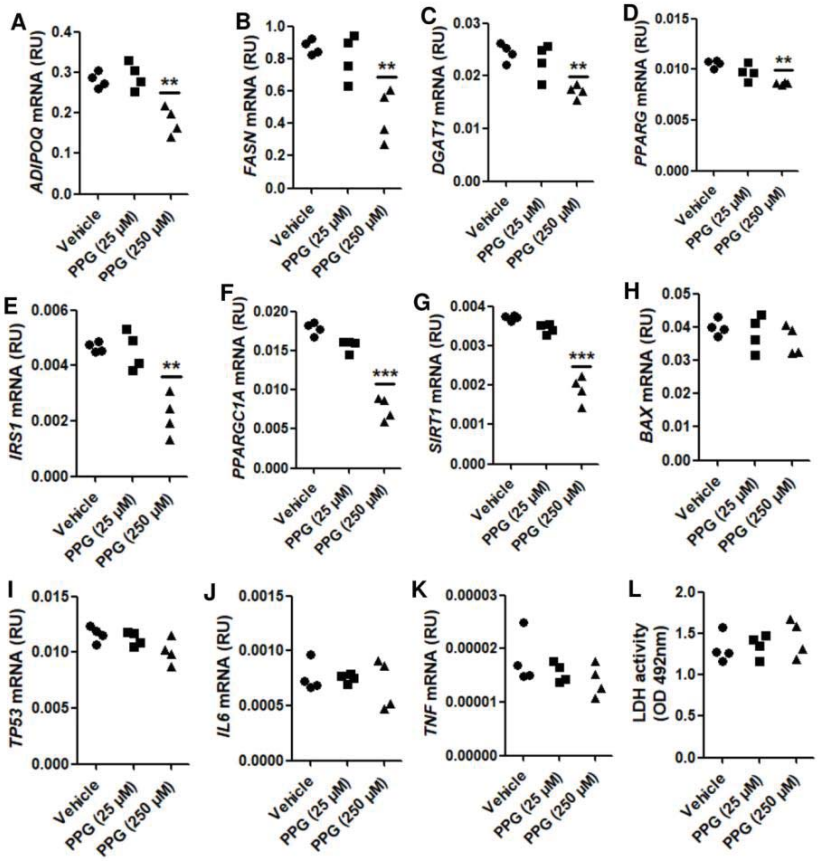

Suppl Figure 2

A

Protein persulfidation-enriched biological processes in preadipocytes (%)

#Term ID	Term description	%	FDR
GO:0002576	platelet degranulation	15.50	5.46E-11
GO:0002446	neutrophil mediated immunity	10.84	8.49E-24
GO:0043312	neutrophil degranulation	10.72	1.09E-22
GO:0002444	myeloid leukocyte mediated immunity	10.60	8.47E-24
GO:0036230	granulocyte activation	10.56	7.65E-23
GO:0043299	leukocyte degranulation	10.45	1.09E-22
GO:0045055	regulated exocytosis	10.42	5.97E-31
GO:0002275	myeloid cell activation involved in immune response	10.21	2.47E-22
GO:0002443	leukocyte mediated immunity	9.65	1.36E-24
GO:0002274	myeloid leukocyte activation	9.58	4.44E-22
GO:0006887	exocytosis	9.43	3.7E-29
GO:0002263	cell activation involved in immune response	8.87	1.16E-20
GO:0002366	leukocyte activation involved in immune response	8.77	4.82E-20
GO:0032940	secretion by cell	7.92	3.76E-26
GO:0097435	supramolecular fiber organization	7.83	8.64E-10
GO:0002252	immune effector process	7.77	3.17E-24
GO:0030036	actin cytoskeleton organization	7.66	3.59E-10
GO:0042060	wound healing	7.59	4.7E-11
GO:0006897	endocytosis	7.45	8.92E-12
GO:0046903	secretion	7.38	1.74E-25
GO:0045321	leukocyte activation	7.16	8.8E-20
GO:0009611	response to wounding	7.13	1.44E-11
GO:0030029	actin filament-based process	7.10	2.57E-10
GO:0016192	vesicle-mediated transport	7.06	3.78E-39
GO:0001775	cell activation	6.93	1.98E-21
GO:0098657	import into cell	6.90	4.81E-12
GO:0030334	regulation of cell migration	5.98	5.08E-11
GO:0051130	positive regulation of cellular component organization	5.85	3.4E-16
GO:0051270	regulation of cellular component movement	5.64	1.93E-11
GO:0022603	regulation of anatomical structure morphogenesis	5.62	2.55E-12
GO:0016477	cell migration	5.54	4.9E-10
GO:0048870	cell motility	5.25	5.29E-10
GO:0006955	immune response	5.06	2.58E-16
GO:0006928	movement of cell or subcellular component	5.02	1.35E-13

B

Protein persulfidation-enriched KEGG pathways in preadipocytes (%)

#Term ID	Term description	%	FDR
hsa00531	Glycosaminoglycan degradation	21.05	0.004
hsa00052	Galactose metabolism	16.13	0.0025
hsa04610	Complement and coagulation cascades	15.38	0.00000122
hsa05100	Bacterial invasion of epithelial cells	15.28	0.00000372
hsa04961	Endocrine and other factor-regulated calcium reabsorption	14.89	0.00052
hsa00520	Amino sugar and nucleotide sugar metabolism	14.58	0.00055
hsa05130	Pathogenic Escherichia coli infection	13.21	0.00073
hsa04142	Lysosome	13.01	6.43E-08
hsa04510	Focal adhesion	12.69	1.07E-11
hsa04721	Synaptic vesicle cycle	11.48	0.0013
hsa04520	Adherens junction	11.27	0.00069
hsa04810	Regulation of actin cytoskeleton	10.73	3.79E-09
hsa04145	Phagosome	10.34	0.0000025
hsa05205	Proteoglycans in cancer	10.26	3.18E-08
hsa04512	ECM-receptor interaction	9.88	0.0012
hsa04670	Leukocyte transendothelial migration	9.82	0.00014
hsa04210	Apoptosis	9.63	0.0000279
hsa05146	Amoebiasis	9.57	0.0007
hsa04144	Endocytosis	9.50	8.36E-09
hsa04540	Gap junction	9.20	0.0017
hsa04912	GnRH signaling pathway	9.09	0.0017
hsa04933	AGE-RAGE signaling pathway in diabetic complications	8.16	0.0031
hsa04611	Platelet activation	8.13	0.00085
hsa05206	MicroRNAs in cancer	8.05	0.0003
hsa04071	Sphingolipid signaling pathway	7.76	0.002
hsa04530	Tight junction	7.19	0.00069
hsa05203	Viral carcinogenesis	6.56	0.0011
hsa04015	Rap1 signaling pathway	5.42	0.0069

Suppl Figure 3

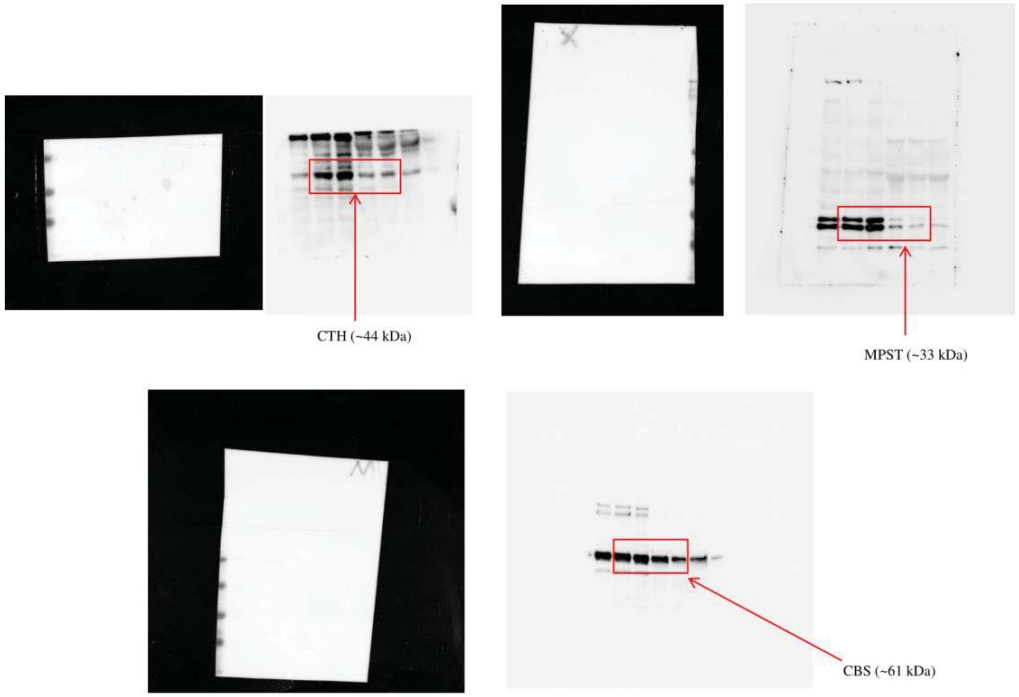

Suppl Figure 4

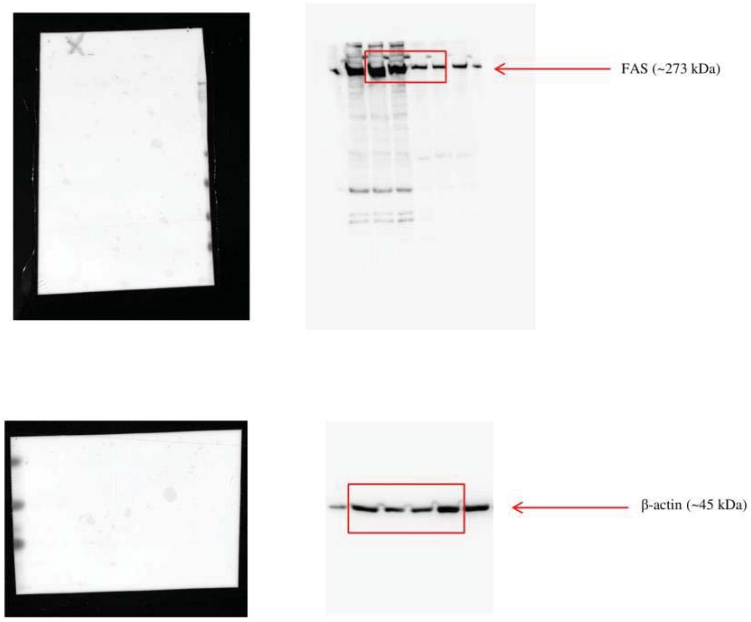

Suppl Figure 5

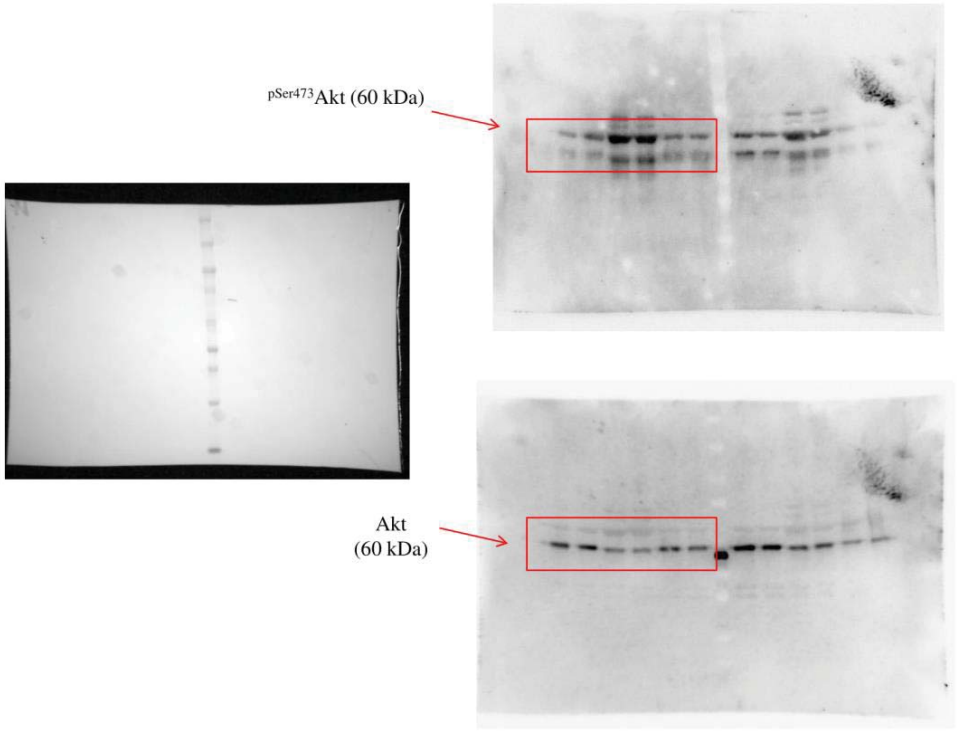

Suppl Figure 6

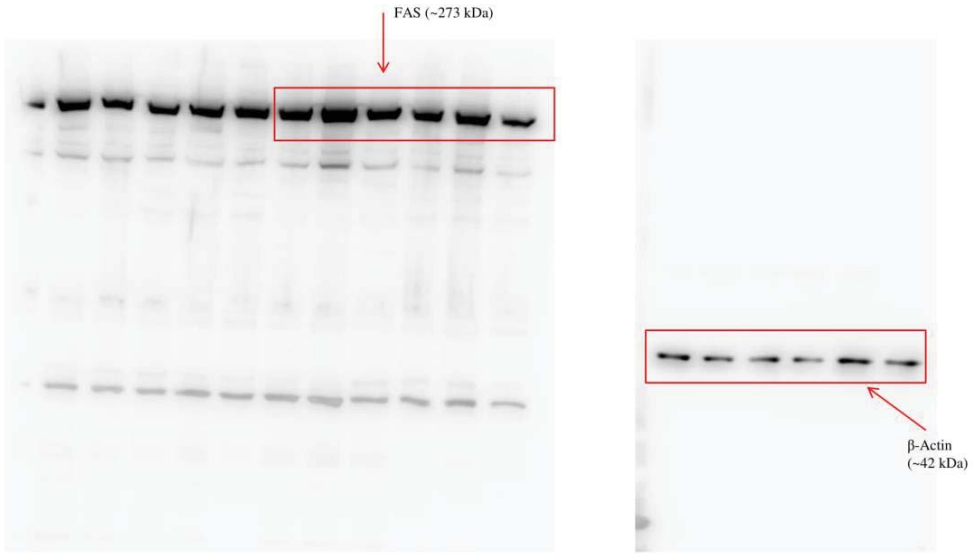

Suppl Figure 7

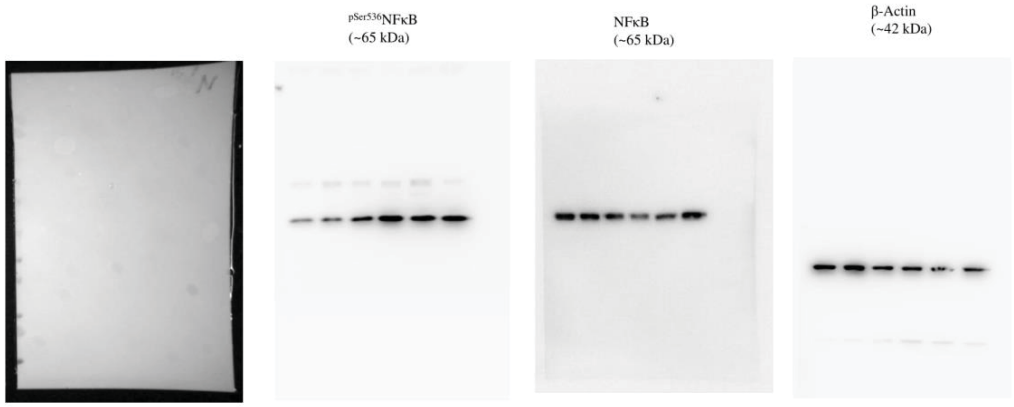

Suppl Figure 8

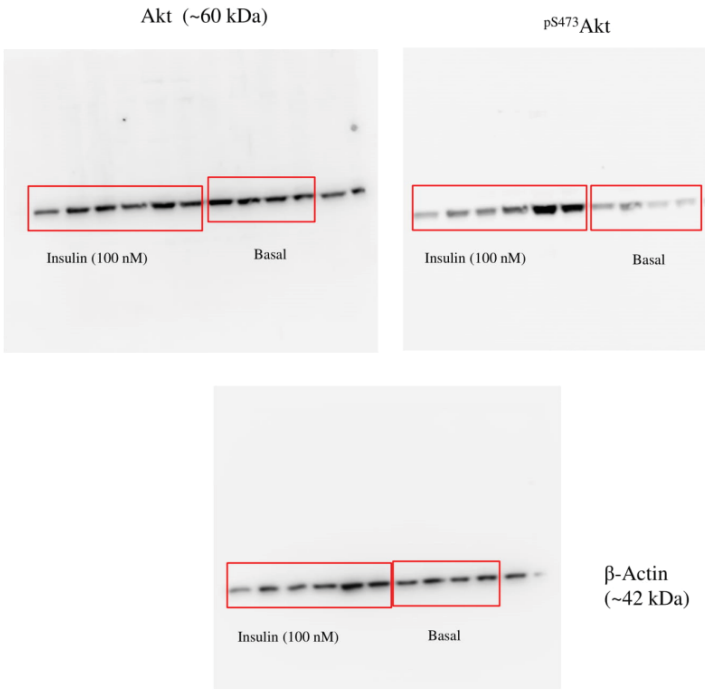

Suppl Table 1. Anthropometric and clinical characteristics of participants from *ex vivo* experiment in cohort 1.

	All participants
N	20
Age (years)	45.6 ± 9.7
BMI (kg/m^2)	44.9 ± 5.1
Waist circumference (cm)	123.9 ± 12.1
Fasting Glucose (mg/dL)	100.4 ± 13.2
HbA1c (%)	5.37 ± 0.36
M (mg/kg·min)[a]	5.73 (3.44-8.45)
Total Cholesterol (mg/dl)	181.7 ± 33.1
HDL Cholesterol (mg/dl)	50.4 ± 10.5
LDL Cholesterol (mg/dl)	111.1 ± 31.2
Fasting triglycerides (mg/dl)[a]	87 (58.2-146.2)

M, systemic insulin sensitivity measured by hyperinsulinemic-euglycemic clamp.
[a]median and interquartile range

Supp Table 2. Anthropometric and clinical characteristics in cohort 2.

	Non obese	Non obese + T2D	Obese	Obese + T2D	p-value
N	35	6	53	28	
Sex (male/female)	11/24	2/4	9/44	7/21	
Age (years)	51.1 ± 13.4	55.5 ± 13.2	45.9 ± 10.9	44.1 ± 10.4	**0.02**
BMI (kg/m^2)	25.8 ± 2.7	28.1 ± 1.3	45.1 ± 7.8$^{*\#}$	44.3 ± 5.3$^{*\#}$	**<0.0001**
Waist circumference (cm)	88.2 ± 11.1	97.6 ± 9.20	117.5 ± 20.8*	131.6 ± 14.4$^{*\#}$	**<0.0001**
Fat mass (%)	32.3 ± 5.8	36.3 ± 6.7	57.3 ± 10.1$^{*\#}$	55.2 ± 9.1$^{*\#}$	**<0.0001**
Fasting glucose (mg/dl)[a]	91 (81-98)	152.5 (99.7-210.7) *	92 (83.5-99.2) $^{\#}$	124 (92.5-167) $^{*+}$	**<0.0001**
Hb1Ac (%)	5.24 ± 0.5	8.18 ± 3.7*	4.9 ± 0.4$^{\#}$	6.1 ± 1.8$^{*\#+}$	**<0.0001**
HOMA-IR	2.3 ± 1.8	3.1 ± 0.2	2.5 ± 1.3	5.1 ± 3.1	0.1
Total Cholesterol (mg/dl)	210.7 ± 40.9	228.5 ± 47.9	189 ± 32.4	189 ± 32.4	**0.01**
HDL Cholesterol (mg/dl) [a]	57.5 (47.5-75.7)	47.5 (39-57.7)	52 (43.6-63)	51.6 (42.5-61.7)	0.5
LDL Cholesterol (mg/dl)	125.1 ± 31.4	152.5 ± 41.1	117.8 ± 29.9	106.5 ± 33.6$^{\#}$	**0.01**
Fasting triglycerides (mg/dl) [a]	98 (76.2-154.5)	160 (105-220)	98 (75.2-131.7)	125.5 (90.5-172)	0.1
VAT *CTH* (R.U.)	0.0041 ± 0.002	0.0026 ± 0.001	0.0021 ± 0.001*	0.0016 ± 0.0007*	**<0.0001**
SAT *CTH* (R.U.)	0.0040 ± 0.002	0.0026 ± 0.001	0.0016 ± 0.0008*	0.0017 ± 0.0007*	**<0.0001**
VAT *CBS* (R.U.)	0.0087 ± 0.006	0.0055 ± 0.003	0.0039 ± 0.002*	0.0046 ± 0.002*	**<0.0001**
SAT *CBS* (R.U.)	0.0045 ± 0.003	0.0021 ± 0.001*	0.0017 ± 0.0008*	0.0017 ± 0.0007*	**<0.0001**
VAT *MPST* (R.U.)	0.0315 ± 0.018	0.0222 ± 0.001	0.0265 ± 0.012	0.0252 ± 0.012	0.1
SAT *MPST* (R.U.)	0.0423 ± 0.023	0.0245 ± 0.016*	0.0301 ± 0.014*	0.0255 ± 0.009^{*+}	**<0.0001**

VAT, visceral adipose tissue; SAT, subcutaneous adipose tissue; T2D, Type 2 Diabetes; HOMA-IR, Homeostasis Model Assessment – Insulin Resistance Index; R.U., relative gene expression units.
[a]median and interquartile range
*p<0.05 compared to non obese participants after performing Bonferroni post hoc test.
# p<0.05 compared to non obese participants with type 2 diabetes after performing Bonferroni post hoc test.
+ p<0.05 compared to obese participants after performing Bonferroni post hoc test.

Suppl Table 3. Anthropometric and clinical characteristics in cohort 3.

	Obese	**Obese + T2D**	**p-value**
N	19	16	
Sex (male/female)	5/14	3/13	
Age (years)	47.2 ± 9.8	49.8 ± 8.1	0.4
BMI (kg/m^2)	42.9 ± 6.4	46.5 ± 6.5	0.1
WHR	0.89 (0.77-1.01)	0.88 (0.83-0.91)	0.3
M (mg/kg·min)	4.55 ± 2.5	3.11 ± 1.7	0.1
Fasting glucose (mg/dl)	94 (85.7 – 98.2)	113 (97.5-140)	**0.03**
Hb1Ac (%)	5.60 ± 0.4	7.02 ± 1.8	**0.01**
Total Cholesterol (mg/dl)	194.6 ± 36.8	175 ± 33.9	0.1
HDL Cholesterol (mg/dl)	46.3 ± 8.3	51.6 ± 18.3	0.2
LDL Cholesterol (mg/dl)	125.6 ± 29.3	96.6 ± 29.6	**0.008**
Fasting triglycerides (mg/dl)	113 ± 49.3	133.7 ± 66.2	0.2

5. GENERAL DISCUSSION

Hydrogen sulfide is one of the important biological mediators involved in physiological and pathological processes in mammals[163]. The physiological functions of H_2S are mediated through different molecular mechanisms, including scavenging of reactive oxygen species[136] and persulfidation[137], a highly prevalent post-translational modification known to modulate the structure and activity of molecular targets, such as different ion channels and signaling proteins[164]. A variety of diseases, such as cancer, diabetes, and metabolic disorders, are associated with altered endogenous levels of H_2S, endorsing the potential of H_2S as a therapeutical target[165]. Many new technologies have been developed to detect endogenous H_2S production, and novel H_2S-delivery compounds have been invented to aid therapeutic intervention of diseases related to abnormal H_2S metabolism. While acknowledging the challenges ahead, research on H_2S physiology and medicine is entering an exponential exploration era[164].

In this thesis, we provide first evidences linking H_2S to the physiology of human adipose tissue and circulating H_2S to obesity. The main findings were as follows:

- Serum sulfide concentrations were increased in subjects with morbid obesity in proportion to fat mass and inversely associated with circulating markers of heme degradation

- H_2S plays a pivotal role regulating adipogenesis under normal and pro-inflammatory conditions during the different stages of 3T3-L1 differentiation

- Permanent *CBS* gene KD in ASC52telo cells promotes a cellular senescence phenotype with a very increased adipogenic potential

- H_2S increased insulin action through the activation of PPARγ transcriptional activity in differentiated adipocytes

- H_2S induced sirtuin deacetylase activity preventing cellular senescence and inflammatory processes in human adipocytes

- Enhanced protein persulfidation of adipogenic-related proteins in human adipocytes was observed, possibly, preserving the adipogenic activity of these proteins.

5.1 CIRCULATING H_2S: A NEW MARKER FOR OBESITY?

The importance of hydrogen sulfide is increasingly recognized in the pathophysiology of obesity and type 2 diabetes in animal models. Very few studies have evaluated circulating sulfides in humans, with discrepant results. The novel results of this thesis show increased serum L1-sulfide levels in subjects with morbid obesity in parallel to fat mass accumulation. Cross-sectionally in both discovery (at baseline and follow-up) and validation cohort, multivariate regression and ROC analysis demonstrated the relevance of fat mass predicting serum sulfide levels. Longitudinally, changes in BMI and waist circumference were correlated to changes in serum sulfide, resulting in weight gain in increased and weight loss in reduced serum sulfide levels. Searching the possible source of serum sulfide, key enzymes in H_2S biosynthesis were investigated in whole blood, being *MPST* gene the most expressed. Supporting this finding, a previous study proposed that blood H_2S levels were produced via MPST in red blood cells[166]. However, in the current study, no significant associations between expression of MPST (and the other enzymes, *CTH* or *CBS*) and obesity (BMI or fat mass) or serum sulfide levels were found, indicating that additional endogenous H_2S sources might contribute to serum sulfide levels. Otherwise, H_2S-metabolizing enzymes (*SQR*, *TST* and *MPO*) mRNA levels were also not associated with obesity or correlated with serum L1-sulfide levels. Since mRNA are not always in proportion to protein levels, an important limitation of the current study was the absence of

protein data. Additional studies are required to investigate blood *CTH*, *CBS*, *MPST*, *SQR*, *TST* and *MPO* protein amount and enzymatic activity according to obesity status.

Another consistent finding of the current study was the negative association between L1- sulfide levels and circulating products of heme degradation, such as iron and bilirubin, suggesting a possible inhibitory activity of serum sulfide on heme degradation. Supporting this suggestion, Saravanan et al reported that administration of S- allylcysteine, a sulphur-containing amino acid, resulted in decreased iron, ferritin, bilirubin and heme oxygenase (a key enzyme in heme degradation) activity in diabetic rats[167]. Otherwise and also in line with current findings, increased heme oxygenase activity and carbon monoxide (CO, the third product of heme degradation) levels were associated with decreased H_2S levels[168]. Of note, this and other studies demonstrated that exogenous CO administration or increased endogenous CO levels reduced enzymatic H_2S production[168–170]. Current findings and these latter studies[167–169] suggest a bidirectional modulation between enzymatic H_2S production and heme degradation. The importance of heme biosynthesis on adipogenesis, adipocyte physiology[171,172] and fat mass accretion[173] has been well substantiated. Together with current findings, it could be proposed that increased fat mass accretion and heme biosynthesis result in decreased circulating iron, bilirubin and CO levels. The consequence would be raised enzymatic H_2S biosynthesis and serum L1-sulfide levels. Strengthening this hypothesis, we found that total bilirubin and serum iron were decreased in obese participants. In line with these findings, other studies have reported a negative association between bilirubin and obesity status. In fact, increased bilirubin production attenuated fat mass accretion, weight gain and liver fat accumulation[174–178]. Decreased serum iron levels in obesity have also been reported[179].

Current data also indicated a negative association between serum L1-sulfide levels and total and LDL cholesterol. In line with these associations, Mani et al. reported that plasma total cholesterol and LDL-cholesterol levels were significantly increased in CSE-KO compared to WT HFD-fed mice[180]. Interestingly, CSE-KO displayed decreased H_2S liver production, suggesting that H_2S was involved in liver cholesterol metabolism.

H_2S biosynthesis has been identified in a variety of mammalian tissues via enzymatic and non-enzymatic pathways, all contributing to the total amount of circulating H_2S[80,181]. Previous studies demonstrated that CBS and CTH enzymes are secreted into the bloodstream by the liver and vascular endothelial cells, circulating as components of plasma proteome and producing H_2S in human blood[182]. Supporting liver H_2S biosynthesis in obesity, mice fed with a high-fat diet for 5 weeks displayed increased expression of *CBS* and *CTH* genes and H_2S production in the liver[183]. Against this argument, other studies demonstrated that liver H_2S production was attenuated in high fat diet-induced obesity, but increased in conditions of dietary restriction[57,184]. In addition, Norris et al. reported that liver might have an important role in the regulation of H_2S levels in the circulation, as a consequence of its location and an enhanced capacity to clearance blood H_2S through H_2S oxidation[90]. Current data suggested that liver capacity to disposal blood H_2S might be attenuated in obesity. However, further studies are required to examine in depth this suggestion.

Otherwise, adipose tissue, which is proportional to fat mass, also might be considered an additional H_2S source in obese subjects[104]. Yang et al demonstrated that high-fat diet-induced fat mass accretion was associated with increased adipose tissue H_2S biosynthesis in mice and fruit flies[104]. However, the relative contribution of adipose tissue to serum sulfide levels has not been previously investigated and needs to be confirmed in further studies.

Opposite of enzymatic synthesis pathways, endogenous production of H_2S through non-enzymatic processes in mammalian tissues is not well understood or characterized. Yang et al. reported that apart from the liver and kidney, where the production of H_2S was mainly through the CTH enzyme, H_2S was non-enzymatically produced by iron and vitamin B6, and using cysteine as a substrate in other organs and at circulatory level[85]. However, taking into account the negative correlation between L1-sulfide and circulating iron-related parameters, this mechanism might be discarded.

It is important to note that increased levels of plasma cysteine predispose to obesity and its associated metabolic disturbances[185,186]. It is important to note that even though L1 probe azido group (R-N3) has been shown to be around 20-50 times more selective to H_2S, when compared to other thiols such as cysteine and glutathione[105], the higher amount of these interfering thiols in serum[187] might increase L1 fluorescence by non-specific reactions with cysteine-thiols. However, the following points indicated that current measurements could discriminate from cysteine-thiols: i) Bariatric surgery-induced weight loss did not change total cysteine levels[188], whereas a longitudinal reduction of serum L1-sulfide in association with fat mass and weight loss was observed in the current study. ii) Pretreatment with a reducing agent was not required in L1 measurements. Thus, it is less likely to pick up sulfur from disulphide bonded cysteine.

Another source of non-enzymatic H_2S is produced by the microbiota residing in the gastrointestinal tract belonging to the sulphate-reducing bacteria, such as *Desulfovibrio, Desulfomicrobium, Desulfobulbus, Desulfobacter, Desulfomonas, and Desulfotomaculum* genera[189]. Germ-free mice, which were resistant to high-fat diet induced obesity[190], were shown to have 50 to 80% less H_2S in their circulation and tissues[191], indicating that sulphate-reducing bacteria could be a significant contributor to H_2S concentration in obesity. Of note, metagenomic studies pointed to increased sulphate-reducing bacteria in obesogenic conditions[192,193]. Expansion of *Desulfovibrio* in detriment to *Clostridia* reduction enhanced lipid absorption and adiposity, and was associated to obesity in mice and humans with metabolic syndrome[193].

Another important finding from current study was that morbidly obese participants with impaired fasting glucose displayed decreased serum L1-sulfide levels similar to decreased insulin sensitivity or increased insulin resistance (HOMA-IR), suggesting that endogenous H_2S biosynthesis might contribute to maintain normal fasting glucose levels. Supporting this idea, exogenous H_2S administration led to improved glucose tolerance in high-fat diet fed mice[103,104] and decreased circulating sulfide levels were previously reported in men with poor glycemic control and type 2 diabetes[101,105]. Otherwise, other studies reported opposite effects in relation to

glucose metabolism[194,195], showing that H_2S decreased hepatocyte glucose uptake and increased hepatic gluconeogenesis[195], and inhibited insulin release from β-cells[194]. In fact, these findings go in the opposite direction from the correlations of serum sulfide with insulin sensitivity or insulin resistance observed in all participants, which were not maintained after adjusting by age, gender and fat mass.

A possible limitation of current study was that since it was designed to investigate changes in serum sulfide levels according to obesity in non-diabetic participants, the impact of H_2S on obesity-associated metainflammation disorders, such as type 2 diabetes and cardiovascular diseases cannot be examined in depth. However, these issues were previously investigated in humans[64,101,105,196] and rats[197,198]. Other study limitations were that distinct biological pools for H_2S, such as free gaseous, sulfane sulfur bound and acid-labile[62], were not analysed, and that only-one method was used to measure serum sulfide levels. To gain insight into the differences between serum L1-sulfide levels between lean and obese patients, the analysis of these three biological pools of serum H_2S and the validation of sulfide measurements using common alternative methods (such Monobromobimane derivatization/HPLC based method and assays to measure H_2S production) should be considered in future studies.

In conclusion, altogether these data demonstrated a potential link between serum sulfide concentration and obesity, being circulating sulfide increased in proportion to fat mass accumulation, and suggesting heme degradation as a negative regulator, and adipose tissue, plasma cysteine and gut microbiota as putative additional sources of serum sulfide levels.

5.2 HYDROGEN SULFIDE IMPACTS ON ADIPOGENEIS AND INFLAMMATION-INDUCED ADIPOCYTE DYSFUNCTION

Our previous data demonstrated a potential link between serum L1-sulfide concentration and obesity, being circulating L1-sulfide increased in parallel to fat mass accumulation, and suggesting heme degradation as a negative regulator, and adipose tissue, plasma cysteine and gut microbiota as putative additional sources of serum sulfide levels. Clinical data from this thesis and emerging *in vitro* studies are supporting the importance of H_2S in adipogenesis, offering new insight into their role in the pathogenesis of obesity.

H_2S has recently gained significant attention as an inflammation biological mediator, with antiinflamatory and proinflamatory effects reported in different tissues [56,127–129,132–135] and *in vitro*[130,131]. However, there are no studies in 3T3-L1 evaluating the role of H_2S in inflammation. We hypothesize that a possible role of H_2S in the modulation of adipocyte inflammation might underlie its adipogenic effects.

In this doctoral thesis, we study the role of H_2S in 3T3-L1 preadipocytes during stages of differentiation and in mature adipocytes under inflammatory conditions using different H_2S donors. Our data first revealed that H_2S biosynthesis was increased during adipocyte differentiation, and H_2S donor (GYY4137 and Na_2S) administration at different stages of adipocyte differentiation process resulted in enhanced adipogenesis, whereas treatments with a specific inhibitor of endogenous H_2S biosynthesis propargylglycine (PPG) impaired adipogenesis and increased inflammation. Even though, several studies reported H_2S concentration in human serum in a range of 10–200 μM[199–202] or higher[203], other studies[62,144,158,204] argue reduced H_2S levels in serum using sound arguments. In current study, to evaluate H_2S biosynthesis at different stages of adipocyte differentiation (day 0, 2 and 7), the 24 h cumulative H_2S concentration was measured, indicating cell capacity for H_2S production, but not its physiological levels. In line with these studies[62,144,158,204], when adipocyte conditioned medium with L1 probe was incubated for 1 h, H_2S concentration (physiological levels) were undetectable.

In addition, GYY4137 administration attenuated the negative effects of inflammation during adipogenesis[205,206], whereas Na_2S aggravates the negative effects of inflammation on mature inflamed adipocytes. These adipogenic and antiinflammatory activities of GYY4137 might be explained through the sulfhydration of PPARγ and NFκB cysteine residues[56,103]. Sulfhydrated PPARγ increased its nuclear accumulation, DNA binding activity and adipogenesis gene expression, thereby increasing glucose uptake and lipid storage[103], whereas sulfhydrated p65 subunit of NF-κB at cysteine-38 inhibited macrophage inflammation by suppressing NFκB pathway activation[56]. Supporting current data, Na_2S and GYY4137 administration was found to be associated positively with adipogenic and lipogenic gene expression in 3T3-L1 cells, whereas ZYJ1122 (a structural analog of GYY4137 lacking sulfur) had not any effects in these gene expression[111]. Furthermore, Lee and colleagues demonstrated that hydrogen sulfide donor, diallyl disulfide, promotes adipogenesis in 3T3-L1 cells[207]. On the other hand, other studies reported antiadipogenic effect of hydrogen sulfide donors derived from garlic[208,209]. Of note, daily administration of Na_2S during 3T3-L1 differentiation inhibited adipogenesis, suggesting that H_2S excess suppressed adipogenic differentiation. No significant effects of time expired Na_2S on adipogenic markers were found, indicating that H_2S from donors was the responsible of adipogenic effect. Donors used in current study released H_2S at different rates, Na_2S is a fast-releasing H_2S donor and GYY4137 is a slow-releasing H_2S donor, producing in consequence different concentrations of the H_2S at several times[210]. These differences in H_2S availability and concentration could explain why GYY4137 was more effective than Na_2S in promoting adipocyte differentiation and attenuating the negative effects of inflammation on adipogenesis. Inflammation in adipocytes is known to decrease adipogenesis in parallel to increased insulin resistance[211], so novel therapeutic strategies targeting adipose tissue to mitigate inflammation are emerging[212]. Current findings reveal that GYY4137 may represent an innovative therapeutic tool against obesity-related adipose tissue inflammation.

It is well known that GYY4137 release is slower than Na_2S[137,213]. A previous study demonstrated that the rate of H_2S release from GYY4137 (1 mM, pH 7.4, 37 °C) was 4.17 ± 0.5 nmol/25 min[142]. In agreement with these studies, GYY4137 (50 μM) administration did not result in a significant increase in H_2S levels in adipocyte conditioned media.

5.3 CYSTATHIONINE-B-SYNTHASE GENE KNOCKDOWN ENHANCED hAMSC ADIPOGENIC CAPACITY

The multipotent stem cell component of MSC isolates is able to differentiate into derivatives of the mesodermal lineage including adipocytes, osteocytes, chondrocytes, and myocytes[214]. The dysregulation of the adipo-osteogenic balance has been linked to several pathophysiologic processes, such as aging, obesity, osteopenia, osteopetrosis, and osteoporosis. Numerous i*n vitro* investigations have demonstrated that fat-induction factors inhibit osteogenesis, and, conversely, bone-induction factors hinder adipogenesis[215]. These factors trigger different signaling pathways and activate various transcription factors that guide MSCs to commit to either lineage. Increasing evidence implicates a tight regulation of these processes by reactive oxygen species. Thus, the regulation of MSC differentiation has increasingly attracted great attention in recent years[215].

Experimental studies in 3T3-L1 cell pointed to a relevant role of the transsulfuration pathway in adipogenesis[103,104,111,216], however, the importance of the transsulfuration pathway in hAMSC adipogenesis has not been yet examined. Even though, Tsai et al reported that both transsulfuration pathway enzymes [cystathionine β-synthase (CBS) and cystathionine γ-lyase (CTH or CSE)] were important in adipocyte differentiation[111], later studies demonstrated that only CTH exerted a relevant role in adipogenesis increasing PPARγ activity during adipocyte differentiation[103,104]. In fact, in our previous study, in which *Cth* and *Cbs* gene expression in 3T3-L1 cells was analysed and compared, we found that *Cth* was highly expressed in preadipocytes and increased during adipocyte differentiation, whereas expression of *Cbs* gene was almost

undetectable in preadipocytes and did not change during adipocyte differentiation, even tending to decrease in the first two days of the process[216].

This thesis demonstrated that, contrary to 3T3-L1 cell in which *CTH* levels were significantly increased but *CBS* was almost undetectable[216], ASC52telo cells showed an increased CBS/CTH ratio, characterized by increased *CBS*, but very low levels of *CTH* mRNA and protein. In line with these findings, previous studies also demonstrated increased *CBS* vs *CTH* mRNA and protein levels in human mesenchymal stem cells[217,218].

These data suggest a major role of CBS in intracellular H_2S biosynthesis compared to CTH in ASC52telo cells. In fact, *CBS* gene KD in ASC52telo cells resulted in a significant increased cellular inflammation and oxidative stress in parallel to a decreased capacity to produce endogenous H_2S. A large number of studies demonstrated anti-inflammatory and anti-oxidant effects of H_2S in mesenchymal stem cells[217,219] and other cells[220–222]. However, the pro-oxidant and pro-inflammatory effects of CBS depletion might be also explained by other causes, including:

i) Altered mitochondrial respiratory function, characterized by decreased proton leak and spare respiratory capacity, two functional measures of mitochondrial function[223,224]. Supporting these findings, a recent study demonstrated the importance of CBS on mitochondrial function in endothelial cells[225]. It is important to note that proton leak (uncoupled respiration), which was significantly decreased in *CBS* KD ASC52telo (shCBS-ASC52telo) cells, is a key mitochondrial process in the prevention of oxidative stress[226,227].

ii) Decreased expression of rejuvenation (*LC3* and *SIRT1*)-related genes. The protective effects of increased *SIRT1*[228–234] and *LC3*[235–238] mRNA levels in the prevention of cellular inflammation, oxidative stress and mitochondrial function are widely reported.

iii) Increased homocysteine/cysthationine ratio. CBS enzyme inhibition results in increased homocysteine in detrimental of cysthationine levels[239,240]. The pro-oxidant and pro-inflammatory effects of excess homocysteine have been demonstrated in *in vitro* and *in vivo* experiments[240–245]. Otherwise, similar to ASC52telo cells, breast tumor tissue displayed increased *CBS*, but very low *CTH* mRNA levels, resulting in increased intracellular levels of cysthationine, and in consequence preserving mitochondrial function and preventing oxidative and endoplasmic reticulum stress[246].

Another important finding of current study was that *CBS* gene knockdown in ASC52telo cells greatly enhanced their capacity to differentiate into adipocytes in detrimental to the ability to differentiate into osteogenic linage. It is well-stablished that increased oxidative stress (ROS levels) in adipose-derived mesenchymal stem cells promotes a cellular senescence and inflammation phenotype characterised by increased capacity for differentiate into adipocyte at the expense of decreased stemness capacity[247–249]. In fact, antioxidant treatment in mesenchymal stem cells prevented adipocyte differentiation[249]. In agreement with current data, the administration of diallyl disulfide, a slow H_2S donor[250], restored hAMSC stemness via inhibition of intracellular ROS levels[251]. The relevance of CBS on osteogenesis has been previously reported[252–254]. Interestingly, one of these studies demonstrated that exogenous homocysteine administration increased intracellular homocysteine levels, and resulted in increased ROS, altered mitochondrial function, reduced expression of *CBS* gene and intracellular H_2S level, and in consequence, inhibiting its capacity to differentiate into osteogenic linage[254]. Otherwise, to the best of our knowledge, the impact of CBS depletion enhancing hAMSC adipogenesis has not been previously shown. These findings could seem controversial with one previous study in 3T3-L1 cells, in which *CBS* gene knockdown decreased adipogenesis[111], whereas other studies demonstrated that CTH was the only enzyme of transsulfuration pathway with adipogenic properties[103,104,216]. In line with these studies, increased CTH/CBS ratio was associated with increased adipogenic potential in ASC52telo cells, which was characterised with very high expression of adipogenic genes (such

as *FABP4* and *SLC2A4*), even before adding the adipogenic media (at day 0). Moreover, supporting the cellular inflammation-associated adipogenic potential observed in shCBS-ASC52telo cells, two recent studies demonstrated that cellular inflammation promoted the generation of new adipocytes and adipose tissue expansion[255,256]. Otherwise, insulin receptor substrate 1 (IRS1) gene expression was significantly decreased in shCBS-ASC52telo cells at day 0 and during adipocyte differentiation. In line with this, even though IRS-1 is important for lipid storage in adipose tissue[257], a recent study reported that *IRS-1* knockdown in bone marrow mesenchymal stem cells increased their capacity to differentiate into adipocytes[258]. Current findings and these studies[253,254,256] suggest that cellular senescence and inflammation might promote a non-physiological increased adipocyte differentiation.

5.4 COMPREHENSIVE TRANSSULFURATION PATHWAY IN ADIPOSE TISSUE OF SUBJECTS WITH AND WITHOUT OBESITY

Translational studies in human adipose tissue supported adipose tissue H_2S biosynthesis linked to adipogenesis, cellular senescence and inflammation. H_2S is a signaling molecule that is actively synthesized in various tissues and plays diverse roles in metabolic and signaling pathways. Recently, it is recognized that H_2S persulfidation of protein, which modifies thiol groups, mediates most of H_2S activities in various cellular functions. We previously reported that disturbed H_2S metabolism plays a crucial role in the pathogenesis of obesity, and despite emerging observations in the 3T3-L1 mouse cell line and hAMSC, the role of endogenous H_2S and its impact on human adipose tissue physiology has been unknown. We postulated that H_2S may regulate adipose tissue physiology through inflammation, oxidative stress and senescence regulation. Considering that potential targets of persulfidation are proteins involved in adipogenic processes such as fatty acid and lipid metabolism, the modification of transsulfuration pathway might contribute to altered adipose tissue physiology.

Our study provides sound and novel evidences supporting the importance of H_2S biosynthesis in the physiology of human adipose tissue. Altogether current findings pointed to a crucial role of

H_2S and H_2S-synthetizing enzymes in human adipose tissue physiology at different cellular levels. Even though, the specific molecular mechanism to explain the possible effects of H_2S on human adipogenesis has not been fully resolved in this study, some mechanisms might be inferred from current findings. These putative mechanisms were as follows:

i) Preserving adipogenic-related proteins through protein persulfidation. Persulfidation often increases the reactivity of target proteins, modulating their biological activities, whereas other post-translational modifications, such as S-nitrosylation often decreases protein activity[140]. In fact, a recent study showed experimentally, for the first time, a higher chemical reactivity in proteins with persulfidated cysteines compared to proteins with cysteines with sulfur in the thiol state[259]. Even though, the most reported impact of persulfidation is to activate protein function, some studies demonstrated inhibitory effects in some important proteins[259].

Taking into account that we found increased persulfidation in FASN, SCD, ACACA, THRSP, PLIN4, LIPE, ACSL1, GLUT4 and FABP4, and that an appropriate functionality of these proteins is required for adipogenesis and adipocyte physiology[260–267], the current results suggest that endogenous H_2S biosynthesis might preserve the function of those proteins involved in adipogenesis. However, further experiments are required to confirm this suggestion.

Supporting the importance of H_2S in the physiology of adipose cells, *CTH*, *CBS* and *MPST* mRNA levels were detected at substantial levels in adipocytes, increasing during human adipocyte differentiation in parallel to *ADIPOQ*. The knockdown of *CTH*, *CBS* and *MPST* promoted the development of dysfunctional adipocytes during adipocyte differentiation, decreasing markers of adipogenesis and increasing the expression of proinflammatory cytokines in parallel to decreased H_2S biosynthesis. Of note, the most anti-adipogenic effect was observed in *CTH* gene KD. The chemical inhibition of CTH activity resulted in decreased adipogenesis during human adipocyte differentiation and in fully differentiated adipocytes. In fact, anti-adipogenic and inflammatory effects of high PPG dose (250 μM) during human adipocyte differentiation were comparable with the effects of *CTH* gene KD. In contrast, no significant effects of low PPG dose (25 μM) were found. This discrepancy could be explained by the previously reported low potency, low

selectivity and the limited cell-membrane permeability of PPG[268]. However, considering that inhibiting CBS, CTH and MPST may have effects independent of H_2S, such as perturbations in homocysteine metabolism, the results of PPG or gene knockdown experiments should be interpreted with caution. In addition, it should be considered that knockdown of one of these enzymes might be compensated by H_2S production by the remaining ones. Otherwise, the administration of GYY4137 in the last stage of the process resulted in a dose-dependent increased expression of adipogenic genes. Interestingly, when endogenous H_2S production was inhibited with PPG (250 μM), GYY4137 sustained adipogenic gene expression (Figure 6), preventing the reduction observed in Figure 7. Previous studies demonstrated that adipogenic[111] and anti-cancer[269] effects of GYY4137 were not observed when cells were treated with ZYJ1122, its structural analogue lacking sulfur, indicating that GYY4137 effects were dependent on H_2S moiety. *Ex vivo* experiments also demonstrated that the activation of H_2S-producing enzymes in adipose tissue increased expression of adipogenic genes in correlation to H_2S biosynthesis. Consistent with the suggested impact of H_2S on protein persulfidation in adipose cells (current study), a recent study demonstrated that persulfidation depends on intracellular H_2S levels, observing in those situations of decreased H_2S biosynthesis, such as aging, a significant decline in protein persulfidation, whereas conditions of enhanced H_2S production (such as dietary restriction) were associated with increased protein persulfidation[138].

ii) *Preventing inflammatory processes in human preadipocytes through the induction of sirtuin deacetylase activity*. Specifically, in human preadipocytes, exogenous H_2S (GYY4137) treatment enhanced sirtuin activity, whereas when endogenous H_2S biosynthesis was inhibited (using PPG or in *CTH, CBS* and *MPST* KD) markers of cellular senescence (*TP53*), apoptosis (*BAX*) and inflammation (*TNF, IL6*) increased. These findings suggest that the previously reported anti-senescence effects of H_2S[270–272] might contribute to improve the adipogenic function of preadipocytes, and preserve adipose tissue functionality[273]. In addition, increased *SIRT1* mRNA levels and sirtuin activity after transsulfuration pathway activation or GYY4137 administration in *ex vivo* experiment (adipose tissue explants) or the consistent association

between H_2S-producing enzymes and *SIRT1* gene expression in human adipose tissue reinforced this idea. Furthermore, both SAT and VAT *CTH* gene expression negatively correlated with markers of cellular senescence (*TP53*), inflammation (*TNF*) and apoptosis (*BAX*) in obese subjects, which were all associated to adipose tissue dysfunction and insulin resistance[274–277]. Even though, TP53, inflammatory cytokines (IL6 and TNF) or apoptosis markers has all been previously used to characterize senescence-associated adipose tissue dysfunction[274–277], a more accurate measurement of cellular senescence (such as β-galactosidase activity) should be considered to confirm current associations in further studies.

Strengthening current findings, increased SIRT1 activity led to enhanced adipose tissue rejuvenation (characterized by increased cellular stemness) and decreased inflammation [278–282] and H_2S administration resulted in enhanced Sirt1 expression and activity[270–272], preventing vascular aging[270] and cellular senescence in human fibroblasts[271]. In line with these findings, in immortalized human adipose-derived mesenchymal stem cells, which unlike human preadipocytes and adipocytes (current study) displayed a much higher expression of CBS than CTH gene[283], *CBS* gene knockdown promotes a cellular senescence phenotype characterized by increased inflammation and oxidative stress, and decreased H_2S production[283]. Of note, this cellular senescence phenotype resulted in adipocyte hypertrophy, when these cells differentiated into adipocytes, and attenuated their ability to differentiate into osteogenic linage[283].

iii) *Increasing insulin action through the activation of PPARγ transcriptional activity in differentiated adipocytes.* GYY4137 administration resulted in a significant increase of insulin-induced Akt phosphorylation at serine 473, whereas PPG administration had opposite effects. A fine regulation of insulin action is associated to adipogenesis and adipose tissue physiology[284,285]. *Ex vivo* experiments indicated that the adipogenic effect resulting from transsulfuration pathway activation was increased in association with insulin sensitivity, and negatively correlated with HbA1c levels, supporting the relationship between H_2S and adipose tissue insulin action. In addition, AT *CTH* gene expression was positively correlated to systemic insulin sensitivity in both cross-sectional studies (cohort 1 and cohort 2) and increased after bariatric surgery-induced

weight loss similar to insulin sensitivity. H_2S improved insulin action in mice[102,286–288]. GYY4137 administration improved high fat diet-induced insulin resistance through the activation of PPARγ in adipose tissue, whereas PPG exerted opposite effects[103]. Mechanistically, H_2S-induced PPARγ transactivation is mediated by enhanced PPARγ persulfidation in cysteine residues from DNA binding domain [103,104]. Since PPG administration also increased ^{pSer536}NFκB (p65)/NFκB ratio and proinflammatory cytokines (*IL6* and *TNF*), another potential mechanism to explain H_2S effects on insulin action was the inhibition of NFκB-induced inflammation[56].

In support of current findings, CBS deficiency is known to be associated with decreased fat mass in both mice and humans[289,290]. CTH is involved in adipogenesis in phylogenetically distant species from *Drosophila melanogaster* to mice[103,104,111] with *cth* knockout mice developing decreased fat mass under cysteine-limited diets[291].

Decreased levels of H_2S-synthetizing enzymes in morbidly obese subjects seem in contradiction with the relevance of these enzymes in adipogenesis and fat mass accretion. However, in conditions of obesity and insulin resistance, adipogenesis is attenuated[13–15], and size enlargement of pre-existing adipocytes acquires more relevance in fat mass sustaining[292]. The findings in human adipose tissue are in agreement with decreased adipose tissue H_2S production reported in *db/db* and high-fat diet-fed mice[109].

Even though, adipose tissue as a possible source of increased serum sulfide levels, recently described in morbidly obese subjects[293], cannot be discarded. Alternative hypothesis should be investigated: i) Expression of H2S-synthesizing enzymes could be higher in early phases of obesity but decrease in more advanced disease as a consequence of adipose tissue inflammation and insulin resistance. ii) In addition, H2S production depends not only by the expression/activity of synthesizing enzymes but also on its oxidation. Decreased oxidation may be the result of environmental hypoxia as that present in adipose tissue from subjects with obesity[294]. In this context, decreased oxidation could result in persistently higher serum sulfide levels.

Current data might anticipate clinical applications and also suggest that the modulation of adipose tissue H_2S biosynthesis may play a role in glucose metabolism. Dietary raw garlic homogenate (a complex mixture containing several H_2S precursors) administration restored plasma H_2S levels in

diabetic rats and led to increased insulin sensitivity[295]. Therapeutically, the potentiation of adipose tissue H_2S-synthetizing enzymes to improve adipose tissue physiology in patients with type 2 diabetes should be investigated in depth in further studies.

6. CONCLUSIONS

1- Serum sulfide concentrations were increased in subjects with morbid obesity, being circulating sulfide increased in proportion to fat mass accumulation.

2- Slow-releasing H_2S improved adipocyte differentiation in inflammatory conditions, and H_2S proadipogenic effects depend on dose, donor and exposure time.

3- Permanent *CBS* gene KD in ASC52telo cells promotes a cellular senescence phenotype, which resulted in a non-physiological enhanced adipocyte differentiation with excessive lipid storage.

4- Adipose tissue H_2S-synthetizing enzymes are important actors in human adipose tissue physiology and systemic insulin sensitivity, possibly, avoiding cellular senescence and inflammation, and in consequence preserving adipose tissue adipogenesis.

5- Increased adipogenic protein persulfidation in human adipocytes suggests a possible mechanism to understand the relevance of H_2S biosynthesis in the modulation of human adipocyte physiology, which consists in the preservation of the activity of adipogenic proteins.

7. REFERENCES

[1] Hruby A, Hu FB. The Epidemiology of Obesity: A Big Picture. *Pharmacoeconomics*. 2015;33:673–89. doi:10.1007/s40273-014-0243-x.

[2] Hotamisligil GS. Inflammation and metabolic disorders. *Nature*. 2006;444:860–7. doi:10.1038/nature05485.

[3] Purnell JQ. Definitions, Classification, and Epidemiology of Obesity. MDText.com, Inc.; 2000.

[4] Cypess AM, Kahn CR. The role and importance of brown adipose tissue in energy homeostasis. *Curr Opin Pediatr*. 2010;22:478–84. doi:10.1097/MOP.0b013e32833a8d6e.

[5] Trayhurn P, Beattie JH. Physiological role of adipose tissue: white adipose tissue as an endocrine and secretory organ. *Proc Nutr Soc*. 2001;60:329–39. doi:10.1079/pns200194.

[6] Scheja L, Heeren J. The endocrine function of adipose tissues in health and cardiometabolic disease. *Nat Rev Endocrinol*. 2019;15:507–24. doi:10.1038/s41574-019-0230-6.

[7] Rosenwald M, Wolfrum C. The origin and definition of brite versus white and classical brown adipocytes. *Adipocyte*. 2014;3:4–9. doi:10.4161/adip.26232.

[8] Betz MJ, Enerbäck S. Human brown adipose tissue: What we have learned so far. *Diabetes*. 2015;64:2352–60. doi:10.2337/db15-0146.

[9] Leitner BP, Huang S, Brychta RJ, Duckworth CJ, Baskin AS, McGehee S, et al. Mapping of human brown adipose tissue in lean and obese young men. *Proc Natl Acad Sci U S A*. 2017;114:8649–54. doi:10.1073/pnas.1705287114.

[10] Sharp LZ, Shinoda K, Ohno H, Scheel DW, Tomoda E, Ruiz L, et al. Human BAT Possesses Molecular Signatures That Resemble Beige/Brite Cells. *PLoS One*. 2012;7. doi:10.1371/journal.pone.0049452.

[11] Wu J, Boström P, Sparks LM, Ye L, Choi JH, Giang AH, et al. Beige adipocytes are a distinct type of thermogenic fat cell in mouse and human. *Cell*. 2012;150:366–76. doi:10.1016/j.cell.2012.05.016.

[12] de Ferranti S, Mozaffarian D. The Perfect Storm: Obesity, Adipocyte Dysfunction, and Metabolic Consequences. *Clin Chem*. 2008;54:945–55. doi:10.1373/clinchem.2007.100156.

[13] Kursawe R, Narayan D, Cali AMG, Shaw M, Pierpont B, Shulman GI, et al. Downregulation of ADIPOQ and PPARγ2 gene expression in subcutaneous adipose tissue of obese adolescents with hepatic steatosis. *Obesity*. 2010;18:1911–7. doi:10.1038/oby.2010.23.

[14] Moreno-Navarrete JM, Ortega F, Serrano M, Rodriguez-Hermosa JI, Ricart W, Mingrone G, et al. CIDEC/FSP27 and PLIN1 gene expression run in parallel to mitochondrial genes in human adipose tissue, both increasing after weight loss. *Int J Obes*. 2014;38:865–72. doi:10.1038/ijo.2013.171.

[15] Veilleux A, Blouin K, Rhéaume C, Daris M, Marette A, Tchernof A. Glucose transporter 4 and insulin receptor substrate-1 messenger RNA expression in omental and subcutaneous adipose tissue in women. *Metabolism*. 2009;58:624–31. doi:10.1016/j.metabol.2008.12.007.

[16] Hirsch J, Batchelor B. Adipose tissue cellularity in human obesity. *Clin Endocrinol Metab*. 1976;5:299–311. doi:10.1016/S0300-595X(76)80023-0.

[17] Stephens JM. The Fat Controller: Adipocyte Development. *PLoS Biol*. 2012;10:e1001436. doi:10.1371/journal.pbio.1001436.

[18] Grundy SM. Adipose tissue and metabolic syndrome: Too much, too little or neither. *Eur J Clin Invest*. 2015;45:1209–17. doi:10.1111/eci.12519.

[19] Sun K, Kusminski CM, Scherer PE. Adipose tissue remodeling and obesity. *J Clin Invest*. 2011;121:2094–101. doi:10.1172/JCI45887.

[20] Danforth E. J. Failure of adipocyte differentiation causes type II diabetes mellitus? [1]. *Nat Genet*. 2000;26:13. doi:10.1038/79111.

[21] Gustafson B, Hammarstedt A, Hedjazifar S, Smith U. Restricted adipogenesis in hypertrophic obesity: The role of WISP2, WNT, and BMP4. *Diabetes*. 2013;62:2997–3004. doi:10.2337/db13-0473.

[22] Heinonen S, Saarinen L, Naukkarinen J, Rodríguez A, Frühbeck G, Hakkarainen A, et al. Adipocyte morphology and implications for metabolic derangements in acquired obesity. *Int J Obes*. 2014;38:1423–31. doi:10.1038/ijo.2014.31.

[23] Hammarstedt A, Gogg S, Hedjazifar S, Nerstedt A, Smith U. Impaired adipogenesis and dysfunctional adipose tissue in human hypertrophic obesity. *Physiol Rev*. 2018;98:1911–41. doi:10.1152/physrev.00034.2017.

[24] Kim SM, Lun M, Wang M, Senyo SE, Guillermier C, Patwari P, et al. Loss of white adipose hyperplastic potential is associated with enhanced susceptibility to insulin resistance. *Cell Metab*. 2014;20:1049–58. doi:10.1016/j.cmet.2014.10.010.

[25] Skurk T, Alberti-Huber C, Herder C, Hauner H. Relationship between adipocyte size and adipokine expression and secretion. *J Clin Endocrinol Metab*. 2007;92:1023–33. doi:10.1210/jc.2006-1055.

[26] Cotillard A, Poitou C, Torcivia A, Bouillot JL, Dietrich A, Klöting N, et al. Adipocyte size threshold matters: Link with risk of type 2 diabetes and improved insulin resistance after gastric bypass. *J Clin Endocrinol Metab*. 2014;99. doi:10.1210/jc.2014-1074.

[27] Andrade-Oliveira V, Câmara NOS, Moraes-Vieira PM. Adipokines as drug targets in diabetes and underlying disturbances. *J Diabetes Res*. 2015;2015. doi:10.1155/2015/681612.

[28] Palmer AK, Xu M, Zhu Y, Pirtskhalava T, Weivoda MM, Hachfeld CM, et al. Targeting senescent cells alleviates obesity-induced metabolic dysfunction. *Aging Cell*. 2019;18. doi:10.1111/acel.12950.

[29] Ogrodnik M, Miwa S, Tchkonia T, Tiniakos D, Wilson CL, Lahat A, et al. Cellular senescence drives age-dependent hepatic steatosis. *Nat Commun*. 2017;8. doi:10.1038/ncomms15691.

[30] Ruiz-Ojeda FJ, Rupérez AI, Gomez-Llorente C, Gil A, Aguilera CM. Cell models and their application for studying adipogenic differentiation in relation to obesity: A review. *Int J Mol Sci*. 2016;17. doi:10.3390/ijms17071040.

[31] Wang QA, Scherer PE, Gupta RK. Improved methodologies for the study of adipose biology: Insights gained and opportunities ahead. *J Lipid Res*. 2014;55:605–24. doi:10.1194/jlr.R046441.

[32] Poulos SP, Dodson M V., Hausman GJ. Cell line models for differentiation: Preadipocytes and adipocytes. *Exp Biol Med*. 2010;235:1185–93.

doi:10.1258/ebm.2010.010063.

[33] Green H, Meuth M. An established pre-adipose cell line and its differentiation in culture. *Cell*. 1974;3:127–33. doi:10.1016/0092-8674(74)90116-0.

[34] Grégoire F, Todoroff G, Hauser N, Remacle C. The stroma-vascular fraction of rat inguinal and epididymal adipose tissue and the adipoconversion of fat cell precursors in primary culture. *Biol Cell*. 1990;69:215–22. doi:10.1016/0248-4900(90)90348-7.

[35] Hauner H, Entenmann G, Wabitsch M, Gaillard D, Ailhaud G, Negrel R, et al. Promoting effect of glucocorticoids on the differentiation of human adipocyte precursor cells cultured in a chemically defined medium. *J Clin Invest*. 1989;84:1663–70. doi:10.1172/JCI114345.

[36] Butterwith SC. Molecular events in adipocyte development. *Pharmacol Ther*. 1994;61:399–411. doi:10.1016/0163-7258(94)90018-3.

[37] Rosen ED, Spiegelman BM. What we talk about when we talk about fat. *Cell*. 2014;156:20–44. doi:10.1016/j.cell.2013.12.012.

[38] Bateman ME, Strong AL, McLachlan JA, Burow ME, Bunnell BA. The effects of endocrine disruptors on adipogenesis and osteogenesis in mesenchymal stem cells: A review. *Front Endocrinol (Lausanne)*. 2017;7:171. doi:10.3389/fendo.2016.00171.

[39] Galipeau J, Sensébé L. Mesenchymal Stromal Cells: Clinical Challenges and Therapeutic Opportunities. *Cell Stem Cell*. 2018;22:824–33. doi:10.1016/j.stem.2018.05.004.

[40] Fajas L, Landsberg RL, Huss-Garcia Y, Sardet C, Lees JA, Auwerx J. E2Fs regulate adipocyte differentiation. *Dev Cell*. 2002;3:39–49. doi:10.1016/S1534-5807(02)00190-9.

[41] Pairault J, Green H. A study of the adipose conversion of suspended 3T3 cells by using glycerophosphate dehydrogenase as differentiation marker. vol. 76. 1979.

[42] Entenmann G, Hauner H. Relationship between replication and differentiation in cultured human adipocyte precursor cells. *Am J Physiol - Cell Physiol*. 1996;270. doi:10.1152/ajpcell.1996.270.4.c1011.

[43] Lee B, Lee M, Lefevre M, Kim HR. Anthocyanins Inhibit Lipogenesis During Adipocyte Differentiation of 3T3-L1 Preadipocytes. *Plant Foods Hum Nutr*. 2014;69:137–41. doi:10.1007/s11130-014-0407-z.

[44] Darlington GJ, Ross SE, MacDougald OA. The role of C/EBP genes in adipocyte differentiation. *J Biol Chem*. 1998;273:30057–60. doi:10.1074/jbc.273.46.30057.

[45] Moseti D, Regassa A, Kim WK. Molecular regulation of adipogenesis and potential anti-adipogenic bioactive molecules. *Int J Mol Sci*. 2016;17. doi:10.3390/ijms17010124.

[46] Im SS, Kwon SK, Kang SY, Kim TH, Kim H Il, Hur MW, et al. Regulation of GLUT4 gene expression by SREBP-1c in adipocytes. *Biochem J*. 2006;399:131–9. doi:10.1042/BJ20060696.

[47] Lopez JM, Bennett MK, Sanchez HB, Rosenfeld JM, Osborne TF. Sterol regulation of acetyl coenzyme A carboxylase: A mechanism for coordinate control of cellular lipid. *Proc Natl Acad Sci U S A*. 1996;93:1049–53. doi:10.1073/pnas.93.3.1049.

[48] Griffin MJ, Wong RHF, Pandya N, Sul HS. Direct interaction between USF and SREBP-1c mediates synergistic activation of the fatty-acid synthase promoter. *J Biol Chem*. 2007;282:5453–67. doi:10.1074/jbc.M610566200.

[49] Kolluru GK, Shen X, Yuan S, Kevil CG. Gasotransmitter heterocellular signaling.

Antioxidants Redox Signal. 2017;26:936–60. doi:10.1089/ars.2016.6909.

[50] Wang R. The gasotransmitter role of hydrogen sulfide. *Antioxidants Redox Signal*. 2003;5:493–501. doi:10.1089/152308603768295249.

[51] Cirino G, Vellecco V, Bucci M. Nitric oxide and hydrogen sulfide: the gasotransmitter paradigm of the vascular system. *Br J Pharmacol*. 2017;174:4021–31. doi:10.1111/bph.13815.

[52] Yang G, Sener A, Ji Y, Pei Y, Pluth MD. Gasotransmitters in Biology and Medicine: Molecular Mechanisms and Drug Targets. *Oxid Med Cell Longev*. 2016;2016. doi:10.1155/2016/4627308.

[53] Mustafa AK, Gadalla MM, Snyder SH. Signaling by gasotransmitters. *Sci Signal*. 2009;2:re2. doi:10.1126/scisignal.268re2.

[54] Kimura H. Physiological role of hydrogen sulfide and polysulfide in the central nervous system. *Neurochem Int*. 2013;63:492–7. doi:10.1016/j.neuint.2013.09.003.

[55] Benavides GA, Squadrito GL, Mills RW, Patel HD, Isbell TS, Patel RP, et al. Hydrogen sulfide mediates the vasoactivity of garlic. *Proc Natl Acad Sci U S A*. 2007;104:17977–82. doi:10.1073/pnas.0705710104.

[56] Du J, Huang Y, Yan H, Zhang Q, Zhao M, Zhu M, et al. Hydrogen sulfide suppresses oxidized low-density lipoprotein (Ox-LDL)-stimulated monocyte chemoattractant protein 1 generation from macrophages via the nuclear factor κb (NF-κB) pathway. *J Biol Chem*. 2014;289:9741–53. doi:10.1074/jbc.M113.517995.

[57] Hine C, Harputlugil E, Zhang Y, Ruckenstuhl C, Lee BC, Brace L, et al. Endogenous hydrogen sulfide production is essential for dietary restriction benefits. *Cell*. 2015;160:132–44. doi:10.1016/j.cell.2014.11.048.

[58] Szab? C. Hydrogen sulphide and its therapeutic potential. *Nat Rev Drug Discov*. 2007;6:917–35. doi:10.1038/nrd2425.

[59] Yang G, Wu L, Jiang B, Yang W, Qi J, Cao K, et al. H2S as a physiologic vasorelaxant: Hypertension in mice with deletion of cystathionine γ-lyase. *Science (80-)*. 2008;322:587–90. doi:10.1126/science.1162667.

[60] Dombkowski RA, Russell MJ, Olson KR. Hydrogen sulfide as an endogenous regulator of vascular smooth muscle tone in trout. *Am J Physiol - Regul Integr Comp Physiol*. 2004;286. doi:10.1152/ajpregu.00419.2003.

[61] Ubuka T, Abe T, Kajikawa R, Morino K. Determination of hydrogen sulfide and acid-labile sulfur in animal tissues by gas chromatography and ion chromatography. *J Chromatogr B Biomed Sci Appl*. 2001;757:31–7. doi:10.1016/S0378-4347(01)00046-9.

[62] Shen X, Peter EA, Bir S, Wang R, Kevil CG. Analytical measurement of discrete hydrogen sulfide pools in biological specimens. *Free Radic Biol Med*. 2012;52:2276–83. doi:10.1016/j.freeradbiomed.2012.04.007.

[63] Ogasawara Y, Ishii K, Togawa T, Tanabe S. Determination of trace amounts of sulphide in human red blood cells by high-performance liquid chromatography with fluorimetric detection after derivatization with p-phenylenediamine and iron(III). *Analyst*. 1991;116:1359–63. doi:10.1039/AN9911601359.

[64] Rajpal S, Katikaneni P, Deshotels M, Pardue S, Glawe J, Shen X, et al. Total sulfane sulfur bioavailability reflects ethnic and gender disparities in cardiovascular disease. *Redox Biol*. 2018;15:480–9. doi:10.1016/j.redox.2018.01.007.

[65] Cuevasanta E, Möller MN, Alvarez B. Biological chemistry of hydrogen sulfide and

persulfides. *Arch Biochem Biophys*. 2017;617:9–25. doi:10.1016/j.abb.2016.09.018.

[66] Ondrias K, Stasko A, Cacanyiova S, Sulova Z, Krizanova O, Kristek F, et al. H2S and HS- donor NaHS releases nitric oxide from nitrosothiols, metal nitrosyl complex, brain homogenate and murine L1210 leukaemia cells. *Pflugers Arch Eur J Physiol*. 2008;457:271–9. doi:10.1007/s00424-008-0519-0.

[67] Giuffrè A, Vicente JB. Hydrogen sulfide biochemistry and interplay with other gaseous mediators in mammalian physiology. *Oxid Med Cell Longev*. 2018;2018. doi:10.1155/2018/6290931.

[68] Cao X, Ding L, Xie ZZ, Yang Y, Whiteman M, Moore PK, et al. A Review of Hydrogen Sulfide Synthesis, Metabolism, and Measurement: Is Modulation of Hydrogen Sulfide a Novel Therapeutic for Cancer? *Antioxidants Redox Signal*. 2019;31:1. doi:10.1089/ars.2017.7058.

[69] Jhee KH, Kruger WD. The role of cystathionine β-synthase in homocysteine metabolism. *Antioxidants Redox Signal*. 2005;7:813–22. doi:10.1089/ars.2005.7.813.

[70] Chiku T, Padovani D, Zhu W, Singh S, Vitvitsky V, Banerjee R. H2S biogenesis by human cystathionine γ-lyase leads to the novel sulfur metabolites lanthionine and homolanthionine and is responsive to the grade of hyperhomocysteinemia. *J Biol Chem*. 2009;284:11601–12. doi:10.1074/jbc.M808026200.

[71] Shibuya N, Tanaka M, Yoshida M, Ogasawara Y, Togawa T, Ishii K, et al. 3-Mercaptopyruvate sulfurtransferase produces hydrogen sulfide and bound sulfane sulfur in the brain. *Antioxidants Redox Signal*. 2009;11:703–14. doi:10.1089/ars.2008.2253.

[72] Sbodio JI, Snyder SH, Paul BD. Regulators of the transsulfuration pathway. *Br J Pharmacol*. 2019;176:583–93. doi:10.1111/bph.14446.

[73] Paul BD, Sbodio JI, Snyder SH. Cysteine Metabolism in Neuronal Redox Homeostasis. *Trends Pharmacol Sci*. 2018;39:513–24. doi:10.1016/j.tips.2018.02.007.

[74] McBean GJ, Aslan M, Griffiths HR, Torrão RC. Thiol redox homeostasis in neurodegenerative disease. *Redox Biol*. 2015;5:186–94. doi:10.1016/j.redox.2015.04.004.

[75] Mosharov E, Cranford MR, Banerjee R. The quantitatively important relationship between homocysteine metabolism and glutathione synthesis by the transsulfuration pathway and its regulation by redox changes. *Biochemistry*. 2000;39:13005–11. doi:10.1021/bi001088w.

[76] Banerjee R, Zou CG. Redox regulation and reaction mechanism of human cystathionine-β- synthase: A PLP-dependent hemesensor protein. *Arch Biochem Biophys*. 2005;433:144–56. doi:10.1016/j.abb.2004.08.037.

[77] Paul BD, Snyder SH. H 2S signalling through protein sulfhydration and beyond. *Nat Rev Mol Cell Biol*. 2012;13:499–507. doi:10.1038/nrm3391.

[78] Paul BD, Snyder SH. H2S: A Novel Gasotransmitter that Signals by Sulfhydration. *Trends Biochem Sci*. 2015;40:687–700. doi:10.1016/j.tibs.2015.08.007.

[79] Stipanuk MH, Ueki I. Dealing with methionine/homocysteine sulfur: Cysteine metabolism to taurine and inorganic sulfur. *J Inherit Metab Dis*. 2011;34:17–32. doi:10.1007/s10545-009-9006-9.

[80] Rose P, Moore PK, Zhu YZ. H2S biosynthesis and catabolism: new insights from molecular studies. *Cell Mol Life Sci*. 2017;74:1391–412. doi:10.1007/s00018-016-2406-8.

[81] Jurkowska H, Roman HB, Hirschberger LL, Sasakura K, Nagano T, Hanaoka K, et al. Primary hepatocytes from mice lacking cysteine dioxygenase show increased cysteine concentrations and higher rates of metabolism of cysteine to hydrogen sulfide and thiosulfate. *Amino Acids*. 2014;46:1353–65. doi:10.1007/s00726-014-1700-8.

[82] Schaffer S, Kim HW. Effects and mechanisms of taurine as a therapeutic agent. *Biomol Ther*. 2018;26:225–41. doi:10.4062/biomolther.2017.251.

[83] Shibuya N, Kimura H. Production of hydrogen sulfide from D-cysteine and its therapeutic potential. *Front Endocrinol (Lausanne)*. 2013;4. doi:10.3389/fendo.2013.00087.

[84] Shibuya N, Koike S, Tanaka M, Ishigami-Yuasa M, Kimura Y, Ogasawara Y, et al. A novel pathway for the production of hydrogen sulfide from D-cysteine in mammalian cells. *Nat Commun*. 2013;4. doi:10.1038/ncomms2371.

[85] Yang J, Minkler P, Grove D, Wang R, Willard B, Dweik R, et al. Non-enzymatic hydrogen sulfide production from cysteine in blood is catalyzed by iron and vitamin B6. *Commun Biol*. 2019;2:1–14. doi:10.1038/s42003-019-0431-5.

[86] Searcy DG, Lee SH. Sulfur reduction by human erythrocytes. *J Exp Zool*. 1998;282:310–22. doi:10.1002/(SICI)1097-010X(19981015)282:3<310::AID-JEZ4>3.0.CO;2-P.

[87] Olson KR, DeLeon ER, Gao Y, Hurley K, Sadauskas V, Batz C, et al. Thiosulfate: A readily accessible source of hydrogen sulfide in oxygen sensing. *Am J Physiol - Regul Integr Comp Physiol*. 2013;305. doi:10.1152/ajpregu.00421.2012.

[88] Wang Q, Liu HR, Mu Q, Rose P, Zhu YZ. S-propargyl-cysteine protects both adult rat hearts and neonatal cardiomyocytes from ischemia/hypoxia injury: The contribution of the hydrogen sulfide-mediated pathway. *J Cardiovasc Pharmacol*. 2009;54:139–46. doi:10.1097/FJC.0b013e3181ac8e12.

[89] Beauchamp RO, Bus JS, Popp JA, Boreiko CJ, Andjelkovich DA, Leber P. A critical review of the literature on hydrogen sulfide toxicity. *Crit Rev Toxicol*. 1984;13:25–97. doi:10.3109/10408448409029321.

[90] Norris EJ, Culberson CR, Narasimhan S, Clemens MG. The liver as a central regulator of hydrogen sulfide. *Shock*. 2011;36:242–50. doi:10.1097/SHK.0b013e3182252ee7.

[91] Libiad M, Yadav PK, Vitvitsky V, Martinov M, Banerjee R. Organization of the human mitochondrial hydrogen sulfide oxidation pathway. *J Biol Chem*. 2014;289:30901–10. doi:10.1074/jbc.M114.602664.

[92] Hildebrandt TM, Grieshaber MK. Three enzymatic activities catalyze the oxidation of sulfide to thiosulfate in mammalian and invertebrate mitochondria. *FEBS J*. 2008;275:3352–61. doi:10.1111/j.1742-4658.2008.06482.x.

[93] Kabil O, Banerjee R. Redox biochemistry of hydrogen sulfide. *J Biol Chem*. 2010;285:21903–7. doi:10.1074/jbc.R110.128363.

[94] Bartholomew TC, Powell. GM, Dodgson KS, Curtis CG. Oxidation of sodium sulphide by rat liver, lungs and kidney. *Biochem Pharmacol*. 1980;29:2431–7. doi:10.1016/0006-2952(80)90346-9.

[95] Brito JA, Sousa FL, Stelter M, Bandeiras TM, Vonrhein C, Teixeira M, et al. Structural and functional insights into sulfide:quinone oxidoreductase. *Biochemistry*. 2009;48:5613–22. doi:10.1021/bi9003827.

[96] Ríos-González BB, Román-Morales EM, Pietri R, López-Garriga J. Hydrogen sulfide

activation in hemeproteins: The sulfheme scenario. *J Inorg Biochem*. 2014;133:78–86. doi:10.1016/j.jinorgbio.2014.01.013.

[97] Pietri R, Román-Morales E, López-Garriga J. Hydrogen sulfide and hemeproteins: Knowledge and mysteries. *Antioxidants Redox Signal*. 2011;15:393–404. doi:10.1089/ars.2010.3698.

[98] Nagy P. Mechanistic chemical perspective of hydrogen sulfide signaling. Methods Enzymol., vol. 554, Academic Press Inc.; 2015, p. 3–29. doi:10.1016/bs.mie.2014.11.036.

[99] Bianco CL, Toscano JP, Fukuto JM. An Integrated View of the Chemical Biology of NO, CO, H2S, and O2. Nitric Oxide Biol. Pathobiol. Third Ed., Elsevier Inc.; 2017, p. 9–21. doi:10.1016/B978-0-12-804273-1.00002-8.

[100] Li Q, Lancaster JR. Chemical foundations of hydrogen sulfide biology. *Nitric Oxide - Biol Chem*. 2013;35:21–34. doi:10.1016/j.niox.2013.07.001.

[101] Whiteman M, Gooding KM, Whatmore JL, Ball CI, Mawson D, Skinner K, et al. Adiposity is a major determinant of plasma levels of the novel vasodilator hydrogen sulphide. *Diabetologia*. 2010;53:1722–6. doi:10.1007/s00125-010-1761-5.

[102] Geng B, Cai B, Liao F, Zheng Y, Zeng Q, Fan X, et al. Increase or Decrease Hydrogen Sulfide Exert Opposite Lipolysis, but Reduce Global Insulin Resistance in High Fatty Diet Induced Obese Mice. *PLoS One*. 2013;8:e73892–e73892. doi:10.1371/journal.pone.0073892.

[103] Cai J, Shi X, Wang H, Fan J, Feng Y, Lin X, et al. Cystathionine γ lyase-hydrogen sulfide increases peroxisome proliferator-activated receptor γ activity by sulfhydration at C139 site thereby promoting glucose uptake and lipid storage in adipocytes. *Biochim Biophys Acta - Mol Cell Biol Lipids*. 2016;1861:419–29. doi:10.1016/j.bbalip.2016.03.001.

[104] Yang G, Ju Y, Fu M, Zhang Y, Pei Y, Racine M, et al. Cystathionine gamma-lyase/hydrogen sulfide system is essential for adipogenesis and fat mass accumulation in mice. *Biochim Biophys Acta - Mol Cell Biol Lipids*. 2018;1863:165–76. doi:10.1016/j.bbalip.2017.11.008.

[105] Suzuki K, Sagara M, Aoki C, Tanaka S, Aso Y. Clinical implication of plasma hydrogen sulfide levels in Japanese patients with type 2 diabetes. *Intern Med*. 2017;56:17–21. doi:10.2169/internalmedicine.56.7403.

[106] Feng X, Chen Y, Zhao J, Tang C, Jiang Z, Geng B. Hydrogen sulfide from adipose tissue is a novel insulin resistance regulator. *Biochem Biophys Res Commun*. 2009;380:153–9. doi:10.1016/j.bbrc.2009.01.059.

[107] Fang L, Zhao J, Chen Y, Ma T, Xu G, Tang C, et al. Hydrogen sulfide derived from periadventitial adipose tissue is a vasodilator. *J Hypertens*. 2009;27:2174–85. doi:10.1097/HJH.0b013e328330a900.

[108] Bełtowski J. Endogenous hydrogen sulfide in perivascular adipose tissue: role in the regulation of vascular tone in physiology and pathology. *Can J Physiol Pharmacol*. 2013;91:889–98. doi:10.1139/cjpp-2013-0001.

[109] Katsouda A, Szabo C, Papapetropoulos A. Reduced adipose tissue H2S in obesity. *Pharmacol Res*. 2018;128:190–9. doi:10.1016/j.phrs.2017.09.023.

[110] Bełtowski J, Jamroz-Wiśniewska A. Hydrogen sulfide in the adipose tissue-physiology, pathology and a target for pharmacotherapy. *Molecules*. 2017;22. doi:10.3390/molecules22010063.

[111] Tsai CY, Peh MT, Feng W, Dymock BW, Moore PK. Hydrogen sulfide promotes adipogenesis in 3T3L1 cells. *PLoS One*. 2015;10:e0119511–e0119511. doi:10.1371/journal.pone.0119511.

[112] Pan Z, Wang H, Liu Y, Yu C, Zhang Y, Chen J, et al. Involvement of CSE/ H2S in high glucose induced aberrant secretion of adipokines in 3T3-L1 adipocytes. *Lipids Health Dis*. 2014;13:1–7. doi:10.1186/1476-511X-13-155.

[113] Lv H, Liu Q, Wen Z, Feng H, Deng X, Ci X. Xanthohumol ameliorates lipopolysaccharide (LPS)-induced acute lung injury via induction of AMPK/GSK3β-Nrf2 signal axis. *Redox Biol*. 2017;12:311–24. doi:10.1016/j.redox.2017.03.001.

[114] Kneeshaw S, Keyani R, Delorme-Hinoux V, Imrie L, Loake GJ, Le Bihan T, et al. Nucleoredoxin guards against oxidative stress by protecting antioxidant enzymes. *Proc Natl Acad Sci U S A*. 2017;114:8414–9. doi:10.1073/pnas.1703344114.

[115] Xiao Q, Ying J, Xiang L, Zhang C. The biologic effect of hydrogen sulfide and its function in various diseases. *Med (United States)*. 2018;97. doi:10.1097/MD.0000000000013065.

[116] Birben E, Sahiner UM, Sackesen C, Erzurum S, Kalayci O. Oxidative stress and antioxidant defense. *World Allergy Organ J*. 2012;5:9–19. doi:10.1097/WOX.0b013e3182439613.

[117] Corsello T, Komaravelli N, Casola A. Role of hydrogen sulfide in nrf2-and sirtuin-dependent maintenance of cellular redox balance. *Antioxidants*. 2018;7. doi:10.3390/antiox7100129.

[118] Lu SC. Regulation of glutathione synthesis. *Mol Aspects Med*. 2009;30:42–59. doi:10.1016/j.mam.2008.05.005.

[119] Kimura Y, Goto YI, Kimura H. Hydrogen sulfide increases glutathione production and suppresses oxidative stress in mitochondria. *Antioxidants Redox Signal*. 2010;12:1–13. doi:10.1089/ars.2008.2282.

[120] Li W, Kong AN. Molecular mechanisms of Nrf2-mediated antioxidant response. *Mol Carcinog*. 2009;48:91–104. doi:10.1002/mc.20465.

[121] Yang G, Zhao K, Ju Y, Mani S, Cao Q, Puukila S, et al. Hydrogen sulfide protects against cellular senescence via s-sulfhydration of keap1 and activation of Nrf2. *Antioxidants Redox Signal*. 2013;18:1906–19. doi:10.1089/ars.2012.4645.

[122] Hourihan JM, Kenna JG, Hayes JD. The gasotransmitter hydrogen sulfide induces Nrf2-target genes by inactivating the keap1 ubiquitin ligase substrate adaptor through formation of a disulfide bond between Cys-226 and Cys-613. *Antioxidants Redox Signal*. 2013;19:465–81. doi:10.1089/ars.2012.4944.

[123] Singh CK, Chhabra G, Ndiaye MA, Garcia-Peterson LM, MacK NJ, Ahmad N. The Role of Sirtuins in Antioxidant and Redox Signaling. *Antioxidants Redox Signal*. 2018;28:643–61. doi:10.1089/ars.2017.7290.

[124] Santos L, Escande C, Denicola A. Potential modulation of sirtuins by oxidative stress. *Oxid Med Cell Longev*. 2016;2016. doi:10.1155/2016/9831825.

[125] Caito S, Rajendrasozhan S, Cook S, Chung S, Yao H, Friedman AE, et al. SIRT1 is a redox-sensitive deacetylase that is post-translationally modified by oxidants and carbonyl stress. *FASEB J*. 2010;24:3145–59. doi:10.1096/fj.09-151308.

[126] Meng G, Liu J, Liu S, Song Q, Liu L, Xie L, et al. Hydrogen sulfide pretreatment improves mitochondrial function in myocardial hypertrophy via a SIRT3-dependent

manner. *Br J Pharmacol*. 2018;175:1126–45. doi:10.1111/bph.13861.

[127] Tokuda K, Kida K, Marutani E, Crimi E, Bougaki M, Khatri A, et al. Inhaled hydrogen sulfide prevents endotoxin-induced systemic inflammation and improves survival by altering sulfide metabolism in mice. *Antioxidants Redox Signal*. 2012;17:11–21. doi:10.1089/ars.2011.4363.

[128] Chen YH, Wu R, Geng B, Qi YF, Wang PP, Yao WZ, et al. Endogenous hydrogen sulfide reduces airway inflammation and remodeling in a rat model of asthma. *Cytokine*. 2009;45:117–23. doi:10.1016/j.cyto.2008.11.009.

[129] Chen X, Xu W, Wang Y, Luo H, Quan S, Zhou J, et al. Hydrogen sulfide reduces kidney injury due to urinary-derived sepsis by inhibiting NF-κB expression, decreasing TNF-α levels and increasing IL-10 levels. *Exp Ther Med*. 2014;8:464–70. doi:10.3892/etm.2014.1781.

[130] Yang C, Ling H, Zhang M, Yang Z, Wang X, Zeng F, et al. Oxidative stress mediates chemical hypoxia-induced injury and inflammation by activating NF-κb-COX-2 pathway in HaCaT cells. *Mol Cells*. 2011;31:531–8. doi:10.1007/s10059-011-1025-3.

[131] Velmurugan G V., Huang H, Sun H, Candela J, Jaiswal MK, Beaman KD, et al. Depletion of H2S during obesity enhances store-operated Ca2+ entry in adipose tissue macrophages to increase cytokine production. *Sci Signal*. 2015;8. doi:10.1126/scisignal.aac7135.

[132] Badiei A, Chambers ST, Gaddam RR, Bhatia M. Cystathionine-γ-lyase gene silencing with siRNA in monocytes/macrophages attenuates inflammation in cecal ligation and puncture-induced sepsis in the mouse. *J Biosci*. 2016;41:87–95. doi:10.1007/s12038-016-9598-9.

[133] Collin M, Anuar FBM, Murch O, Bhatia M, Moore PK, Thiemermann C. Inhibition of endogenous hydrogen sulfide formation reduces the organ injury caused by endotoxemia. *Br J Pharmacol*. 2005;146:498–505. doi:10.1038/sj.bjp.0706367.

[134] Yan Y, chen C, Zhou H, Gao H, Chen L, Chen L, et al. Endogenous hydrogen sulfide formation mediates the liver damage in endotoxemic rats. *Res Vet Sci*. 2013;94:590–5. doi:10.1016/j.rvsc.2012.10.009.

[135] Zhang H, Zhi L, Moochhala S, Moore PK, Bhatia M. Hydrogen sulfide acts as an inflammatory mediator in cecal ligation and puncture-induced sepsis in mice by upregulating the production of cytokines and chemokines via NF-κB. *Am J Physiol - Lung Cell Mol Physiol*. 2007;292. doi:10.1152/ajplung.00388.2006.

[136] Spassov SG, Donus R, Ihle PM, Engelstaedter H, Hoetzel A, Faller S. Hydrogen Sulfide Prevents Formation of Reactive Oxygen Species through PI3K/Akt Signaling and Limits Ventilator-Induced Lung Injury 2017. doi:10.1155/2017/3715037.

[137] Powell CR, Dillon KM, Matson JB. A review of hydrogen sulfide (H2S) donors: Chemistry and potential therapeutic applications. *Biochem Pharmacol*. 2018;149:110–23. doi:10.1016/j.bcp.2017.11.014.

[138] Zivanovic J, Kouroussis E, Kohl JB, Adhikari B, Bursac B, Schott-Roux S, et al. Selective Persulfide Detection Reveals Evolutionarily Conserved Antiaging Effects of S-Sulfhydration. *Cell Metab*. 2019;30:1152–1170.e13. doi:10.1016/j.cmet.2019.10.007.

[139] Dóka, Ida T, Dagnell M, Abiko Y, Luong NC, Balog N, et al. Control of protein function through oxidation and reduction of persulfidated states. *Sci Adv*. 2020;6:eaax8358. doi:10.1126/sciadv.aax8358.

[140] Filipovic MR. Persulfidation (S-sulfhydration) and H2S. *Handb Exp Pharmacol*.

2015;230:29–59. doi:10.1007/978-3-319-18144-8_2.

[141] Zhao Y, Biggs TD, Xian M. Hydrogen sulfide (H2S) releasing agents: Chemistry and biological applications. *Chem Commun*. 2014;50:11788–805. doi:10.1039/c4cc00968a.

[142] Li L, Whiteman M, Guan YY, Neo KL, Cheng Y, Lee SW, et al. Characterization of a novel, water-soluble hydrogen sulfide-releasing molecule (GYY4137): New insights into the biology of hydrogen sulfide. *Circulation*. 2008;117:2351–60. doi:10.1161/CIRCULATIONAHA.107.753467.

[143] Levitt MD, Abdel-Rehim MS, Furne J. Free and acid-labile hydrogen sulfide concentrations in mouse tissues: Anomalously high free hydrogen sulfide in aortic tissue. *Antioxidants Redox Signal*. 2011;15:373–8. doi:10.1089/ars.2010.3525.

[144] Furne J, Saeed A, Levitt MD. Whole tissue hydrogen sulfide concentrations are orders of magnitude lower than presently accepted values. *Am J Physiol - Regul Integr Comp Physiol*. 2008;295. doi:10.1152/ajpregu.90566.2008.

[145] Shen X, Pattillo CB, Pardue S, Bir SC, Wang R, Kevil CG. Measurement of plasma hydrogen sulfide in vivo and in vitro. *Free Radic Biol Med*. 2011;50:1021–31. doi:10.1016/j.freeradbiomed.2011.01.025.

[146] Wintner EA, Deckwerth TL, Langston W, Bengtsson A, Leviten D, Hill P, et al. A monobromobimane-based assay to measure the pharmacokinetic profile of reactive sulphide species in blood. *Br J Pharmacol*. 2010;160:941–57. doi:10.1111/j.1476-5381.2010.00704.x.

[147] Nishida M, Sawa T, Kitajima N, Ono K, Inoue H, Ihara H, et al. Hydrogen sulfide anion regulates redox signaling via electrophile sulfhydration. *Nat Chem Biol*. 2012;8:714–24. doi:10.1038/nchembio.1018.

[148] Shen X, Kolluru GK, Yuan S, Kevil CG. Measurement of H2S in vivo and in vitro by the monobromobimane method. Methods Enzymol., vol. 554, Academic Press Inc.; 2015, p. 31–45. doi:10.1016/bs.mie.2014.11.039.

[149] Yang Z, Feng L, Jun-Bao D, Chao-Shu T, Guo-Heng X, Bin G. Modified methylene blue method for measurement of hydrogen sulfide level in plasma. vol. 64. 2012.

[150] Moest RR. Hydrogen Sulfide Determination by the Methylene Blue Method. *Anal Chem*. 1975;47:1204–5. doi:10.1021/ac60357a008.

[151] Yu F, Han X, Chen L. Fluorescent probes for hydrogen sulfide detection and bioimaging. *Chem Commun*. 2014;50:12234–49. doi:10.1039/c4cc03312d.

[152] Hu X, Mutus B. Electrochemical detection of sulfide. *Rev Anal Chem*. 2013;32:247–56. doi:10.1515/revac-2013-0008.

[153] Doeller JE, Isbell TS, Benavides G, Koenitzer J, Patel H, Patel RP, et al. Polarographic measurement of hydrogen sulfide production and consumption by mammalian tissues. *Anal Biochem*. 2005;341:40–51. doi:10.1016/j.ab.2005.03.024.

[154] Kolluru GK, Shen X, Bir SC, Kevil CG. Hydrogen sulfide chemical biology: Pathophysiological roles and detection. *Nitric Oxide - Biol Chem*. 2013;35:5–20. doi:10.1016/j.niox.2013.07.002.

[155] Olson KR. A practical look at the chemistry and biology of hydrogen sulfide. *Antioxidants Redox Signal*. 2012;17:32–44. doi:10.1089/ars.2011.4401.

[156] Lin VS, Chen W, Xian M, Chang CJ. Chemical probes for molecular imaging and detection of hydrogen sulfide and reactive sulfur species in biological systems. *Chem Soc Rev*. 2015;44:4596–618. doi:10.1039/c4cs00298a.

[157] Xu T, Scafa N, Xu L-P, Zhou S, Abdullah Al-Ghanem K, Mahboob S, et al. Electrochemical hydrogen sulfide biosensors. *Analyst*. 2016;141:1185. doi:10.1039/c5an02208h.

[158] Whitfield NL, Kreimier EL, Verdial FC, Skovgaard N, Olson KR. Reappraisal of H2S/sulfide concentration in vertebrate blood and its potential significance in ischemic preconditioning and vascular signaling. *Am J Physiol - Regul Integr Comp Physiol*. 2008;294. doi:10.1152/ajpregu.00025.2008.

[159] Jaffrey SR, Erdjument-Bromage H, Ferris CD, Tempst P, Snyder SH. Protein S-nitrosylation: A physiological signal for neuronal nitric oxide. *Nat Cell Biol*. 2001;3:193–7. doi:10.1038/35055104.

[160] Kouroussis E, Adhikari B, Zivanovic J, Filipovic MR. Measurement of protein persulfidation: Improved tag-switch method. Methods Mol. Biol., vol. 2007, Humana Press Inc.; 2019, p. 37–50. doi:10.1007/978-1-4939-9528-8_4.

[161] Aroca Á, Serna A, Gotor C, Romero LC. S-sulfhydration: A cysteine posttranslational modification in plant systems. *Plant Physiol*. 2015;168:334–42. doi:10.1104/pp.15.00009.

[162] Zhang D, MacInkovic I, Devarie-Baez NO, Pan J, Park CM, Carroll KS, et al. Detection of protein S-sulfhydration by a tag-switch technique. *Angew Chemie - Int Ed*. 2014;53:575–81. doi:10.1002/anie.201305876.

[163] Zaorska E, Tomasova L, Koszelewski D, Ostaszewski R, Ufnal M. Hydrogen sulfide in pharmacotherapy, beyond the hydrogen sulfide-donors. *Biomolecules*. 2020;10:323. doi:10.3390/biom10020323.

[164] Wang R. Physiological implications of hydrogen sulfide: A whiff exploration that blossomed. *Physiol Rev*. 2012;92:791–896. doi:10.1152/physrev.00017.2011.

[165] Yang CT, Chen L, Xu S, Day JJ, Li X, Xian M. Recent development of hydrogen sulfide releasing/stimulating reagents and their potential applications in cancer and glycometabolic disorders. *Front Pharmacol*. 2017;8. doi:10.3389/fphar.2017.00664.

[166] Vitvitsky V, Yadav PK, Kurthen A, Banerjee R. Sulfide oxidation by a noncanonical pathway in red blood cells generates thiosulfate and polysulfides. *J Biol Chem*. 2015;290:8310–20. doi:10.1074/jbc.M115.639831.

[167] Saravanan G, Ponmurugan P, Begum MS. Effect of S-allylcysteine, a sulphur containing amino acid on iron metabolism in streptozotocin induced diabetic rats. *J Trace Elem Med Biol*. 2013;27:143–7. doi:10.1016/j.jtemb.2012.07.009.

[168] Yu S, Yan Z, Che N, Zhang X, Ge R. Impact of Carbon Monoxide/Heme Oxygenase on Hydrogen Sulfide/Cystathionine-γ-lyase Pathway in the Pathogenesis of Allergic Rhinitis in Guinea Pigs. *Otolaryngol Neck Surg*. 2015;152:470–6. doi:10.1177/0194599814567112.

[169] Hishiki T, Yamamoto T, Morikawa T, Kubo A, Kajimura M, Suematsu M. Carbon monoxide: Impact on remethylation/transsulfuration metabolism and its pathophysiologic implications. *J Mol Med*. 2012;90:245–54. doi:10.1007/s00109-012-0875-2.

[170] Guo S Bin, Duan ZJ, Wang QM, Zhou Q, Li Q, Sun XY. Endogenous carbon monoxide downregulates hepatic cystathionine-γ-lyase in rats with liver cirrhosis. *Exp Ther Med*. 2015;10:2039–46. doi:10.3892/etm.2015.2823.

[171] Galmozzi A, Kok BP, Kim AS, Montenegro-Burke JR, Lee JY, Spreafico R, et al. PGRMC2 is an intracellular haem chaperone critical for adipocyte function. *Nature*.

2019;576:138–42. doi:10.1038/s41586-019-1774-2.

[172] Moreno-Navarrete JM, Rodríguez A, Ortega F, Becerril S, Girones J, Sabater-Masdeu M, et al. Heme Biosynthetic Pathway is Functionally Linked to Adipogenesis via Mitochondrial Respiratory Activity. *Obesity*. 2017;25:1723–33. doi:10.1002/oby.21956.

[173] V N-S, NM D-J, MA E-S, VP F-N, FA M, N A, et al. 3-Amino-1,2,4-Triazole Induces Quick and Strong Fat Loss in Mice with High Fat-Induced Metabolic Syndrome. *Oxid Med Cell Longev*. 2020;2020. doi:10.1155/2020/3025361.

[174] Takei R, Inoue T, Sonoda N, Kohjima M, Okamoto M, Sakamoto R, et al. Bilirubin reduces visceral obesity and insulin resistance by suppression of inflammatory cytokines. *PLoS One*. 2019;14. doi:10.1371/journal.pone.0223302.

[175] Stec DE, John K, Trabbic CJ, Luniwal A, Hankins MW, Baum J, et al. Bilirubin Binding to PPARα Inhibits Lipid Accumulation. *PLoS One*. 2016;11. doi:10.1371/journal.pone.0153427.

[176] Gordon DM, Neifer KL, Hamoud A-RA, Hawk CF, Nestor-Kalinoski AL, Miruzzi SA, et al. Bilirubin remodels murine white adipose tissue by reshaping mitochondrial activity and the coregulator profile of peroxisome proliferator-activated receptor α. *J Biol Chem*. 2020;295:jbc.RA120.013700. doi:10.1074/jbc.ra120.013700.

[177] Cimini FA, Arena A, Barchetta I, Tramutola A, Ceccarelli V, Lanzillotta C, et al. Reduced biliverdin reductase-A levels are associated with early alterations of insulin signaling in obesity. *Biochim Biophys Acta - Mol Basis Dis*. 2019;1865:1490–501. doi:10.1016/j.bbadis.2019.02.021.

[178] Gordon DM, Adeosun SO, Ngwudike SI, Anderson CD, Hall JE, Hinds TD, et al. CRISPR Cas9-mediated deletion of biliverdin reductase A (BVRA) in mouse liver cells induces oxidative stress and lipid accumulation. *Arch Biochem Biophys*. 2019;672. doi:10.1016/j.abb.2019.108072.

[179] Zhao L, Zhang X, Shen Y, Fang X, Wang Y, Wang F. Obesity and iron deficiency: A quantitative meta-analysis. *Obes Rev*. 2015;16:1081–93. doi:10.1111/obr.12323.

[180] Mani S, Li H, Untereiner A, Wu L, Yang G, Austin RC, et al. Decreased endogenous production of hydrogen sulfide accelerates atherosclerosis. *Circulation*. 2013;127:2523–34. doi:10.1161/CIRCULATIONAHA.113.002208.

[181] Szijártó IA, Markó L, Filipovic MR, Miljkovic JL, Tabeling C, Tsvetkov D, et al. Cystathionine γ-lyase-produced hydrogen sulfide controls endothelial no bioavailability and blood pressure. *Hypertension*. 2018;71:1210–7. doi:10.1161/HYPERTENSIONAHA.117.10562.

[182] Bearden SE, Beard RS, Pfau JC. Extracellular transsulfuration generates hydrogen sulfide from homocysteine and protects endothelium from redox stress. *Am J Physiol - Hear Circ Physiol*. 2010;299:H1568-76. doi:10.1152/ajpheart.00555.2010.

[183] Hwang SY, Sarna LK, Siow YL, Karmin O. High-fat diet stimulates hepatic cystathionine β-synthase and cystathionine γ-lyase expression. *Can J Physiol Pharmacol*. 2013;91:913–9. doi:10.1139/cjpp-2013-0106.

[184] Yang Y, Wang Y, Sun J, Zhang J, Guo H, Shi Y, et al. Dietary methionine restriction reduces hepatic steatosis and oxidative stress in high-fat-fed mice by promoting H 2 S production. *Food Funct*. 2019;10:61–77. doi:10.1039/c8fo01629a.

[185] Carter RN, Morton NM. Cysteine and hydrogen sulphide in the regulation of metabolism: Insights from genetics and pharmacology. *J Pathol*. 2016;238:321–32. doi:10.1002/path.4659.

[186] Elshorbagy AK, KoziC.H. V, David Smith A, Refsum H. Cysteine and obesity: Consistency of the evidence across epidemiologic, animal and cellular studies. *Curr Opin Clin Nutr Metab Care*. 2012;15:49–57. doi:10.1097/MCO.0b013e32834d199f.

[187] Giustarini D, Dalle-Donne I, Lorenzini S, Milzani A, Rossi R. Age-related influence on thiol, disulfide, and protein-mixed disulfide levels in human plasma. - Abstract - Europe PMC n.d. https://europepmc.org/article/med/17077195 (accessed July 29, 2020).

[188] Aasheim ET, Elshorbagy AK, My Diep L, Søvik TT, Mala T, Valdivia-Garcia M, et al. Effect of bariatric surgery on sulphur amino acids and glutamate. *Br J Nutr*. 2011;106:432–40. doi:10.1017/S0007114511000201.

[189] Rey FE, Gonzalez MD, Cheng J, Wu M, Ahern PP, Gordon JI. Metabolic niche of a prominent sulfate-reducing human gut bacterium. *Proc Natl Acad Sci U S A*. 2013;110:13582–7. doi:10.1073/pnas.1312524110.

[190] Bäckhed F, Manchester JK, Semenkovich CF, Gordon JI. Mechanisms underlying the resistance to diet-induced obesity in germ-free mice. *Proc Natl Acad Sci U S A*. 2007;104:979–84. doi:10.1073/pnas.0605374104.

[191] Shen X, Carlström M, Borniquel S, Jädert C, Kevil CG, Lundberg JO. Microbial regulation of host hydrogen sulfide bioavailability and metabolism. *Free Radic Biol Med*. 2013;60:195–200. doi:10.1016/j.freeradbiomed.2013.02.024.

[192] Hildebrandt MA, Hoffmann C, Sherrill-Mix SA, Keilbaugh SA, Hamady M, Chen YY, et al. High-Fat Diet Determines the Composition of the Murine Gut Microbiome Independently of Obesity. *Gastroenterology*. 2009;137:1716. doi:10.1053/j.gastro.2009.08.042.

[193] Petersen C, Bell R, Klag KA, Lee S-H, Soto R, Ghazaryan A, et al. T cell–mediated regulation of the microbiota protects against obesity. *Science (80-)*. 2019;365:eaat9351. doi:10.1126/science.aat9351.

[194] Kaneko Y, Kimura Y, Kimura H, Niki I. L-cysteine inhibits insulin release from the pancreatic β-cell: Possible involvement of metabolic production of hydrogen sulfide, a novel gasotransmitter. *Diabetes*. 2006;55:1391–7. doi:10.2337/db05-1082.

[195] Zhang L, Yang G, Untereiner A, Ju Y, Wu L, Wang R. Hydrogen sulfide impairs glucose utilization and increases gluconeogenesis in hepatocytes. *Endocrinology*. 2013;154:114–26. doi:10.1210/en.2012-1658.

[196] Guo R, Wu Z, Jiang J, Liu C, Wu B, Li X, et al. New mechanism of lipotoxicity in diabetic cardiomyopathy: Deficiency of Endogenous H2S Production and ER stress. *Mech Ageing Dev*. 2017;162:46–52. doi:10.1016/j.mad.2016.11.005.

[197] Gomez CB, de la Cruz SH, Medina-Terol GJ, Beltran-Ornelas JH, Sánchez-López A, Silva-Velasco DL, et al. Chronic administration of NaHS and L-Cysteine restores cardiovascular changes induced by high-fat diet in rats. *Eur J Pharmacol*. 2019;863. doi:10.1016/j.ejphar.2019.172707.

[198] Jeddi S, Gheibi S, Kashfi K, Carlström M, Ghasemi A. Protective effect of intermediate doses of hydrogen sulfide against myocardial ischemia-reperfusion injury in obese type 2 diabetic rats. *Life Sci*. 2020;256. doi:10.1016/j.lfs.2020.117855.

[199] Karunya R, Jayaprakash KS, Gaikwad R, Sajeesh P, Ramshad K, Muraleedharan KM, et al. Rapid measurement of hydrogen sulphide in human blood plasma using a microfluidic method. *Sci Rep*. 2019;9:1–11. doi:10.1038/s41598-019-39389-7.

[200] Chen YH, Yao WZ, Geng B, Ding YL, Lu M, Zhao MW, et al. Endogenous hydrogen sulfide in patients with COPD. *Chest*. 2005;128:3205–11. doi:10.1378/chest.128.5.3205.

[201] Li L, Bhatia M, Zhu YZ, Zhu YC, Ramnath RD, Wang ZJ, et al. Hydrogen sulfide is a novel mediator of lipopolysaccharide-induced inflammation in the mouse. *FASEB J*. 2005;19:1196–8. doi:10.1096/fj.04-3583fje.

[202] Peng H, Cheng Y, Dai C, King AL, Predmore BL, Lefer DJ, et al. A Fluorescent Probe for Fast and Quantitative Detection of Hydrogen Sulfide in Blood. *Angew Chemie*. 2011;123:9846–9. doi:10.1002/ange.201104236.

[203] Hamidi Shishavan M, Henning RH, Van Buiten A, Goris M, Deelman LE, Buikema H. Metformin Improves Endothelial Function and Reduces Blood Pressure in Diabetic Spontaneously Hypertensive Rats Independent from Glycemia Control: Comparison to Vildagliptin. *Sci Rep*. 2017;7. doi:10.1038/s41598-017-11430-7.

[204] Olson KR. Is hydrogen sulfide a circulating "gasotransmitter" in vertebrate blood? *Biochim Biophys Acta - Bioenerg*. 2009;1787:856–63. doi:10.1016/j.bbabio.2009.03.019.

[205] Yarmo MN, Gagnon A, Sorisky A. The anti-adipogenic effect of macrophage-conditioned medium requires the IKKβ/NF-κB pathway. *Horm Metab Res*. 2010;42:831–6. doi:10.1055/s-0030-1263124.

[206] Constant VA, Gagnon AM, Yarmo M, Sorisky A. The antiadipogenic effect of macrophage-conditioned medium depends on ERK1/2 activation. *Metabolism*. 2008;57:465–72. doi:10.1016/j.metabol.2007.11.005.

[207] Lee JH, Kim KA, Kwon KB, Kim EK, Lee YR, Song MY, et al. Diallyl disulfide accelerates adipogenesis in 3T3-L1 cells. *Int J Mol Med*. 2007;20:59–64. doi:10.3892/ijmm.20.1.59.

[208] Kim EJ, Lee DH, Kim HJ, Lee SJ, Ban JO, Cho MC, et al. Thiacremonone, a sulfur compound isolated from garlic, attenuates lipid accumulation partially mediated via AMPK activation in 3T3-L1 adipocytes. *J Nutr Biochem*. 2012;23:1552–8. doi:10.1016/j.jnutbio.2011.10.008.

[209] Lii CK, Huang CY, Chen HW, Chow MY, Lin YR, Huang CS, et al. Diallyl trisulfide suppresses the adipogenesis of 3T3-L1 preadipocytes through ERK activation. *Food Chem Toxicol*. 2012;50:478–84. doi:10.1016/j.fct.2011.11.020.

[210] Whiteman M, Li L, Rose P, Tan CH, Parkinson DB, Moore PK. The effect of hydrogen sulfide donors on lipopolysaccharide-induced formation of inflammatory mediators in macrophages. *Antioxidants Redox Signal*. 2010;12:1147–54. doi:10.1089/ars.2009.2899.

[211] Gustafson B, Smith U. Cytokines promote Wnt signaling and inflammation and impair the normal differentiation and lipid accumulation in 3T3-L1 preadipocytes. *J Biol Chem*. 2006;281:9507–16. doi:10.1074/jbc.M512077200.

[212] Kusminski CM, Bickel PE, Scherer PE. Targeting adipose tissue in the treatment of obesity-associated diabetes. *Nat Rev Drug Discov*. 2016;15:639–60. doi:10.1038/nrd.2016.75.

[213] Rose P, Dymock BW, Moore PK. GYY4137, a novel water-soluble, H2S-releasing molecule. Methods Enzymol., vol. 554, Academic Press Inc.; 2015, p. 143–67. doi:10.1016/bs.mie.2014.11.014.

[214] Atashi F, Modarressi A, Pepper MS. The role of reactive oxygen species in mesenchymal stem cell adipogenic and osteogenic differentiation: A review. *Stem Cells Dev*. 2015;24:1150–63. doi:10.1089/scd.2014.0484.

[215] Chen Q, Shou P, Zheng C, Jiang M, Cao G, Yang Q, et al. Fate decision of mesenchymal stem cells: Adipocytes or osteoblasts? *Cell Death Differ*. 2016;23:1128–39.

doi:10.1038/cdd.2015.168.

[216] Comas F, Latorre J, Cussó O, Ortega F, Lluch A, Sabater M, et al. Hydrogen sulfide impacts on inflammation-induced adipocyte dysfunction. *Food Chem Toxicol*. 2019;131:110543. doi:10.1016/j.fct.2019.05.051.

[217] Fox B, Schantz JT, Haigh R, Wood ME, Moore PK, Viner N, et al. Inducible hydrogen sulfide synthesis in chondrocytes and mesenchymal progenitor cells: Is H2S a novel cytoprotective mediator in the inflamed joint? *J Cell Mol Med*. 2012;16:896–910. doi:10.1111/j.1582-4934.2011.01357.x.

[218] Markel TA, Drucker NA, Jensen AR, Olson KR. Human Mesenchymal Stem Cell Hydrogen Sulfide Production Critically Impacts the Release of Other Paracrine Mediators After Injury. *J Surg Res*. 2020;254:75–82. doi:10.1016/j.jss.2020.04.014.

[219] Cacciotti I, Ciocci M, Di Giovanni E, Nanni F, Melino S. Hydrogen sulfide-releasing fibrous membranes: Potential patches for stimulating human stem cells proliferation and viability under oxidative stress. *Int J Mol Sci*. 2018;19. doi:10.3390/ijms19082368.

[220] Li J, Teng X, Jin S, Dong J, Guo Q, Tian D, et al. Hydrogen sulfide improves endothelial dysfunction by inhibiting the vicious cycle of NLRP3 inflammasome and oxidative stress in spontaneously hypertensive rats. *J Hypertens*. 2019;37:1633–43. doi:10.1097/HJH.0000000000002101.

[221] Lin Z, Altaf N, Li C, Chen M, Pan L, Wang D, et al. Hydrogen sulfide attenuates oxidative stress-induced NLRP3 inflammasome activation via S-sulfhydrating c-Jun at Cys269 in macrophages. *Biochim Biophys Acta - Mol Basis Dis*. 2018;1864:2890–900. doi:10.1016/j.bbadis.2018.05.023.

[222] P W, F C, W W, XD Z. Hydrogen Sulfide Attenuates High Glucose-Induced Human Retinal Pigment Epithelial Cell Inflammation by Inhibiting ROS Formation and NLRP3 Inflammasome Activation. *Mediators Inflamm*. 2019;2019. doi:10.1155/2019/8908960.

[223] Xiao YX, Lanza IR, Swain JM, Sarr MG, Nair KS, Jensen MD. Adipocyte mitochondrial function is reduced in human obesity independent of fat cell size. *J Clin Endocrinol Metab*. 2014;99. doi:10.1210/jc.2013-3042.

[224] Moreno-Navarrete JM, Ortega F, Rodríguez A, Latorre J, Becerril S, Sabater-Masdeu M, et al. HMOX1 as a marker of iron excess-induced adipose tissue dysfunction, affecting glucose uptake and respiratory capacity in human adipocytes. *Diabetologia*. 2017;60:915–26. doi:10.1007/s00125-017-4228-0.

[225] Rao G, Murphy B, Dey A, Dwivedi SKD, Zhang Y, Roy RV, et al. Cystathionine beta synthase regulates mitochondrial dynamics and function in endothelial cells. *FASEB J*. 2020. doi:10.1096/fj.202000173R.

[226] Cadenas S. Mitochondrial uncoupling, ROS generation and cardioprotection. vol. 1859. Elsevier B.V.; 2018. doi:10.1016/j.bbabio.2018.05.019.

[227] Brookes PS. Mitochondrial H + leak and ROS generation: An odd couple. *Free Radic Biol Med*. 2005;38:12–23. doi:10.1016/j.freeradbiomed.2004.10.016.

[228] Zhang G-Z, Deng Y-J, Xie Q-Q, Ren E-H, Ma Z-J, He X-G, et al. Sirtuins and intervertebral disc degeneration: Roles in inflammation, oxidative stress, and mitochondrial function. *Clin Chim Acta*. 2020;508:33–42. doi:10.1016/j.cca.2020.04.016.

[229] S L, SH B, YJ K, JH P, B DL, WB J, et al. MHY2233 Attenuates Replicative Cellular Senescence in Human Endothelial Progenitor Cells via SIRT1 Signaling. *Oxid Med Cell Longev*. 2019;2019:6492029–6492029. doi:10.1155/2019/6492029.

[230] Baker JR, Vuppusetty C, Colley T, Hassibi S, Fenwick PS, Donnelly LE, et al. MicroRNA-570 is a novel regulator of cellular senescence and inflammaging. *FASEB J*. 2019;33:1605–16. doi:10.1096/fj.201800965R.

[231] Wang P, Lv C, Zhang T, Liu J, Yang J, Guan F, et al. FOXQ1 regulates senescence-associated inflammation via activation of SIRT1 expression. *Cell Death Dis*. 2017;8:e2946. doi:10.1038/cddis.2017.340.

[232] Guo Y, Li P, Gao L, Zhang J, Yang Z, Bledsoe G, et al. Kallistatin reduces vascular senescence and aging by regulating microRNA-34a-SIRT1 pathway. *Aging Cell*. 2017;16:837–46. doi:10.1111/acel.12615.

[233] Yuan Y, Cruzat VF, Newsholme P, Cheng J, Chen Y, Lu Y. Regulation of SIRT1 in aging: Roles in mitochondrial function and biogenesis. *Mech Ageing Dev*. 2016;155:10–21. doi:10.1016/j.mad.2016.02.003.

[234] Hwang JW, Yao H, Caito S, Sundar IK, Rahman I. Redox regulation of SIRT1 in inflammation and cellular senescence. *Free Radic Biol Med*. 2013;61:95–110. doi:10.1016/j.freeradbiomed.2013.03.015.

[235] D'Adamo S, Cetrullo S, Guidotti S, Silvestri Y, Minguzzi M, Santi S, et al. Spermidine rescues the deregulated autophagic response to oxidative stress of osteoarthritic chondrocytes. *Free Radic Biol Med*. 2020;153:159–72. doi:10.1016/j.freeradbiomed.2020.03.029.

[236] W J, P Z, X Z. Apelin Promotes ECM Synthesis by Enhancing Autophagy Flux via TFEB in Human Degenerative NP Cells under Oxidative Stress. *Biomed Res Int*. 2020;2020:4897170–4897170. doi:10.1155/2020/4897170.

[237] Bhansali S, Bhansali A, Dutta P, Walia R, Dhawan V. Metformin upregulates mitophagy in patients with T2DM: A randomized placebo-controlled study. *J Cell Mol Med*. 2020;24:2832–46. doi:10.1111/jcmm.14834.

[238] Li R, Shang J, Zhou W, Jiang L, Xie D, Tu G. Overexpression of HIPK2 attenuates spinal cord injury in rats by modulating apoptosis, oxidative stress, and inflammation. *Biomed Pharmacother*. 2018;103:127–34. doi:10.1016/j.biopha.2018.03.117.

[239] Zuhra K, Augsburger F, Majtan T, Szabo C. Cystathionine-β-synthase: Molecular regulation and pharmacological inhibition. *Biomolecules*. 2020;10. doi:10.3390/biom10050697.

[240] Robert K, Nehmé J, Bourdon E, Pivert G, Friguet B, Delcayre C, et al. Cystathionine β Synthase Deficiency Promotes Oxidative Stress, Fibrosis, and Steatosis in Mice Liver. *Gastroenterology*. 2005;128:1405–15. doi:10.1053/j.gastro.2005.02.034.

[241] AnandBabu K, Sen P, Angayarkanni N. Oxidized LDL, homocysteine, homocysteine thiolactone and advanced glycation end products act as pro-oxidant metabolites inducing cytokine release, macrophage infiltration and pro-angiogenic effect in ARPE-19 cells. *PLoS One*. 2019;14:e0216899–e0216899. doi:10.1371/journal.pone.0216899.

[242] Wu X, Zhang L, Miao Y, Yang J, Wang X, Wang C chen, et al. Homocysteine causes vascular endothelial dysfunction by disrupting endoplasmic reticulum redox homeostasis. *Redox Biol*. 2019;20:46–59. doi:10.1016/j.redox.2018.09.021.

[243] Longoni A, Bellaver B, Bobermin LD, Santos CL, Nonose Y, Kolling J, et al. Homocysteine Induces Glial Reactivity in Adult Rat Astrocyte Cultures. *Mol Neurobiol*. 2018;55:1966–76. doi:10.1007/s12035-017-0463-0.

[244] Zhang D, Fang P, Jiang X, Nelson J, Moore JK, Kruger WD, et al. Severe hyperhomocysteinemia promotes bone marrow-derived and resident inflammatory

monocyte differentiation and atherosclerosis in LDLr/CBS-deficient mice. *Circ Res*. 2012;111:37–49. doi:10.1161/CIRCRESAHA.112.269472.

[245] Papatheodorou L, Weiss N. Vascular Oxidant Stress and Inflammation in Hyperhomocysteinemia. *Antioxid Redox Signal*. 2007;9:1941–58. doi:10.1089/ars.2007.1750.

[246] Sen S, Kawahara B, Mahata SK, Tsai R, Yoon A, Hwang L, et al. Cystathionine: A novel oncometabolite in human breast cancer. *Arch Biochem Biophys*. 2016;604:95–102. doi:10.1016/j.abb.2016.06.010.

[247] Lin CH, Li NT, Cheng HS, Yen ML. Oxidative stress induces imbalance of adipogenic/osteoblastic lineage commitment in mesenchymal stem cells through decreasing SIRT1 functions. *J Cell Mol Med*. 2018;22:786–96. doi:10.1111/jcmm.13356.

[248] K M, KA T, K K, BM H, S W, J T, et al. Metformin Decreases Reactive Oxygen Species, Enhances Osteogenic Properties of Adipose-Derived Multipotent Mesenchymal Stem Cells In Vitro, and Increases Bone Density In Vivo. *Oxid Med Cell Longev*. 2016;2016. doi:10.1155/2016/9785890.

[249] de Villiers D, Potgieter M, Ambele MA, Adam L, Durandt C, Pepper MS. The role of reactive oxygen species in adipogenic differentiation. Adv. Exp. Med. Biol., vol. 1083, Springer New York LLC; 2018, p. 125–44. doi:10.1007/5584_2017_119.

[250] Liang D, Wu H, Wong MW, Huang D. Diallyl Trisulfide Is a Fast H2S Donor, but Diallyl Disulfide Is a Slow One: The Reaction Pathways and Intermediates of Glutathione with Polysulfides. *Org Lett*. 2015;17:4196–9. doi:10.1021/acs.orglett.5b01962.

[251] Bahrampour Juybari K, Kamarul T, Najafi M, Jafari D, Sharifi AM. Restoring the IL-1β/NF-κB-induced impaired chondrogenesis by diallyl disulfide in human adipose-derived mesenchymal stem cells via attenuation of reactive oxygen species and elevation of antioxidant enzymes. *Cell Tissue Res*. 2018;373:407–19. doi:10.1007/s00441-018-2825-y.

[252] Liu Y, Yang R, Liu X, Zhou Y, Qu C, Kikuiri T, et al. Hydrogen sulfide maintains mesenchymal stem cell function and bone homeostasis via regulation of Ca2+ channel sulfhydration. *Cell Stem Cell*. 2014;15:66–78. doi:10.1016/j.stem.2014.03.005.

[253] Gambari L, Lisignoli G, Gabusi E, Manferdini C, Paolella F, Piacentini A, et al. Distinctive expression pattern of cystathionine-β-synthase and cystathionine-γ-lyase identifies mesenchymal stromal cells transition to mineralizing osteoblasts. *J Cell Physiol*. 2017;232:3574–85. doi:10.1002/jcp.25825.

[254] Zhai Y, Behera J, Tyagi SC, Tyagi N. Hydrogen sulfide attenuates homocysteine-induced osteoblast dysfunction by inhibiting mitochondrial toxicity. *J Cell Physiol*. 2019;234:18602–14. doi:10.1002/jcp.28498.

[255] Wernstedt Asterholm I, Tao C, Morley TS, Wang QA, Delgado-Lopez F, Wang Z V., et al. Adipocyte inflammation is essential for healthy adipose tissue expansion and remodeling. *Cell Metab*. 2014;20:103–18. doi:10.1016/j.cmet.2014.05.005.

[256] Zhu Q, An YA, Kim M, Zhang Z, Zhao S, Zhu Y, et al. Suppressing Adipocyte Inflammation Promotes Insulin Resistance in Mice. *Mol Metab*. 2020;39:101010. doi:10.1016/j.molmet.2020.101010.

[257] Tseng YH, Butte AJ, Kokkotou E, Yechoor VK, Taniguchi CM, Kriauciunas KM, et al. Prediction of preadipocyte differentiation by gene expression reveals role of insulin receptor substrates and necdin. *Nat Cell Biol*. 2005;7:601–11. doi:10.1038/ncb1259.

[258] Wang N, Li Y, Li Z, Ma J, Wu X, Pan R, et al. IRS-1 targets TAZ to inhibit adipogenesis of rat bone marrow mesenchymal stem cells through PI3K-Akt and MEK-ERK pathways. *Eur J Pharmacol*. 2019;849:11–21. doi:10.1016/j.ejphar.2019.01.064.

[259] Fu L, Liu K, He J, Tian C, Yu X, Yang J. Direct Proteomic Mapping of Cysteine Persulfidation. *Antioxidants Redox Signal*. 2020;33:1061–76. doi:10.1089/ars.2019.7777.

[260] Cui Y, Liu Z, Sun X, Hou X, Qu B, Zhao F, et al. Thyroid hormone responsive protein spot 14 enhances lipogenesis in bovine mammary epithelial cells. *Vitr Cell Dev Biol - Anim*. 2015;51:586–94. doi:10.1007/s11626-014-9865-8.

[261] Schmid B, Rippmann JF, Tadayyon M, Hamilton BS. Inhibition of fatty acid synthase prevents preadipocyte differentiation. *Biochem Biophys Res Commun*. 2005;328:1073–82. doi:10.1016/j.bbrc.2005.01.067.

[262] Levert KL, Waldrop GL, Stephens JM. A biotin analog inhibits acetyl-CoA carboxylase activity and adipogenesis. *J Biol Chem*. 2002;277:16347–50. doi:10.1074/jbc.C200113200.

[263] Lyu Y, Su X, Deng J, Liu S, Zou L, Zhao X, et al. Defective differentiation of adipose precursor cells from lipodystrophic mice lacking perilipin 1. *PLoS One*. 2015;10. doi:10.1371/journal.pone.0117536.

[264] Cheng X, Xi QY, Wei S, Wu D, Ye RS, Chen T, et al. Critical role of miR-125b in lipogenesis by targeting stearoyl-CoA desaturase-1 (SCD-1). *J Anim Sci*. 2016;94:65–76. doi:10.2527/jas.2015-9456.

[265] Albert JS, Yerges-Armstrong LM, Horenstein RB, Pollin TI, Sreenivasan UT, Chai S, et al. Null Mutation in Hormone-Sensitive Lipase Gene and Risk of Type 2 Diabetes. *N Engl J Med*. 2014;370:2307–15. doi:10.1056/nejmoa1315496.

[266] Zhan T, Poppelreuther M, Ehehalt R, Füllekrug J. Overexpressed FATP1, ACSVL4/FATP4 and ACSL1 Increase the Cellular Fatty Acid Uptake of 3T3-L1 Adipocytes but Are Localized on Intracellular Membranes. *PLoS One*. 2012;7. doi:10.1371/journal.pone.0045087.

[267] Gustafson B, Hedjazifar S, Gogg S, Hammarstedt A, Smith U. Insulin resistance and impaired adipogenesis. *Trends Endocrinol Metab*. 2015;26:193–200. doi:10.1016/j.tem.2015.01.006.

[268] Asimakopoulou A, Panopoulos P, Chasapis CT, Coletta C, Zhou Z, Cirino G, et al. Selectivity of commonly used pharmacological inhibitors for cystathionine β synthase (CBS) and cystathionine γ lyase (CSE). *Br J Pharmacol*. 2013;169:922–32. doi:10.1111/bph.12171.

[269] Lee ZW, Zhou J, Chen CS, Zhao Y, Tan CH, Li L, et al. The slow-releasing Hydrogen Sulfide donor, GYY4137, exhibits novel anti-cancer effects in vitro and in vivo. *PLoS One*. 2011;6. doi:10.1371/journal.pone.0021077.

[270] Das A, Huang GX, Bonkowski MS, Longchamp A, Li C, Schultz MB, et al. Impairment of an Endothelial NAD+-H2S Signaling Network Is a Reversible Cause of Vascular Aging. *Cell*. 2018;173:74–89.e20. doi:10.1016/j.cell.2018.02.008.

[271] Sanokawa-Akakura R, Akakura S, Tabibzadeh S. Replicative senescence in human fibroblasts is delayed by hydrogen sulfide in a NAMPT/SIRT1 dependent manner. *PLoS One*. 2016;11:e0164710–e0164710. doi:10.1371/journal.pone.0164710.

[272] Miller DL, Roth MB. Hydrogen sulfide increases thermotolerance and lifespan in Caenorhabditis elegans. *Proc Natl Acad Sci U S A*. 2007;104:20618–22.

doi:10.1073/pnas.0710191104.

[273] Arner E, Westermark PO, Spalding KL, Britton T, Rydén M, Frisén J, et al. Adipocyte turnover: Relevance to human adipose tissue morphology. *Diabetes*. 2010;59:105–9. doi:10.2337/db09-0942.

[274] Krstic J, Reinisch I, Schupp M, Schulz TJ, Prokesch A. P53 functions in adipose tissue metabolism and homeostasis. *Int J Mol Sci*. 2018;19. doi:10.3390/ijms19092622.

[275] Minamino T, Orimo M, Shimizu I, Kunieda T, Yokoyama M, Ito T, et al. A crucial role for adipose tissue p53 in the regulation of insulin resistance. *Nat Med*. 2009;15:1082–7. doi:10.1038/nm.2014.

[276] Khanahmadi M, Manafi B, Tayebinia H, Karimi J, Khodadadi I. Downregulation of sirt1 is correlated to upregulation of p53 and increased apoptosis in epicardial adipose tissue of patients with coronary artery disease. *EXCLI J*. 2020;19:1387–98. doi:10.17179/excli2020-2423.

[277] Tinahones FJ, Araguez LCI, Murri M, Olivera WO, Torres MDM, Barbarroja N, et al. Caspase induction and BCL2 inhibition in human adipose tissue. *Diabetes Care*. 2013;36:513–21. doi:10.2337/dc12-0194.

[278] Rappou E, Jukarainen S, Rinnankoski-Tuikka R, Kaye S, Heinonen S, Hakkarainen A, et al. Weight Loss Is Associated With Increased NAD {<}sup{>}+{<}/sup{>} /SIRT1 Expression But Reduced PARP Activity in White Adipose Tissue. *J Clin Endocrinol {&} Metab*. 2016;101:1263–73. doi:10.1210/jc.2015-3054.

[279] Chalkiadaki A, Guarente L. High-fat diet triggers inflammation-induced cleavage of SIRT1 in adipose tissue to promote metabolic dysfunction. *Cell Metab*. 2012;16:180–8. doi:10.1016/j.cmet.2012.07.003.

[280] Gillum MP, Kotas ME, Erion DM, Kursawe R, Chatterjee P, Nead KT, et al. SirT1 regulates adipose tissue inflammation. *Diabetes*. 2011;60:3235–45. doi:10.2337/db11-0616.

[281] Liu T, Ma X, Ouyang T, Chen H, Lin J, Liu J, et al. SIRT1 reverses senescence via enhancing autophagy and attenuates oxidative stress-induced apoptosis through promoting p53 degradation. *Int J Biol Macromol*. 2018;117:225–34. doi:10.1016/j.ijbiomac.2018.05.174.

[282] Xu C, Cai Y, Fan P, Bai B, Chen J, Deng HB, et al. Calorie restriction prevents metabolic aging caused by abnormal sirt1 function in adipose tissues. *Diabetes*. 2015;64:1576–90. doi:10.2337/db14-1180.

[283] Comas F, Latorre J, Ortega F, Oliveras-Cañellas N, Lluch A, Ricart W, et al. Permanent cystathionine-β-Synthase gene knockdown promotes inflammation and oxidative stress in immortalized human adipose-derived mesenchymal stem cells, enhancing their adipogenic capacity. *Redox Biol*. 2020:101668. doi:10.1016/j.redox.2020.101668.

[284] Shearin AL, Monks BR, Seale P, Birnbaum MJ. Lack of AKT in adipocytes causes severe lipodystrophy. *Mol Metab*. 2016;5:472–9. doi:10.1016/j.molmet.2016.05.006.

[285] Morley TS, Xia JY, Scherer PE. Selective enhancement of insulin sensitivity in the mature adipocyte is sufficient for systemic metabolic improvements. *Nat Commun*. 2015;6:7906. doi:10.1038/ncomms8906.

[286] Manna P, Jain SK. Hydrogen sulfide and L-cysteine increase phosphatidylinositol 3,4,5-trisphosphate (PIP3) and glucose utilization by inhibiting phosphatase and tensin homolog (PTEN) protein and activating phosphoinositide 3-kinase (PI3K)/serine/threonine protein kinase (A. *J Biol Chem*. 2011;286:39848–59.

doi:10.1074/jbc.M111.270884.

[287] Manna P, Jain SK. Vitamin D up-regulates glucose transporter 4 (GLUT4) translocation and glucose utilization mediated by cystathionine-γ-lyase (CSE) activation and H2S formation in 3T3L1 adipocytes. *J Biol Chem*. 2012;287:42324–32. doi:10.1074/jbc.M112.407833.

[288] Xue R, Hao DD, Sun JP, Li WW, Zhao MM, Li XH, et al. Hydrogen sulfide treatment promotes glucose uptake by increasing insulin receptor sensitivity and ameliorates kidney lesions in type 2 diabetes. *Antioxidants Redox Signal*. 2013;19:5–23. doi:10.1089/ars.2012.5024.

[289] Gupta S, Kruger WD. Cystathionine beta-synthase deficiency causes fat loss in mice. *PLoS One*. 2011;6:e27598–e27598. doi:10.1371/journal.pone.0027598.

[290] Kruger WD. Cystathionine β-synthase deficiency: Of mice and men. *Mol Genet Metab*. 2017;121:199–205. doi:10.1016/j.ymgme.2017.05.011.

[291] Mani S, Yang G, Wang R. A critical life-supporting role for cystathionine γ-lyase in the absence of dietary cysteine supply. *Free Radic Biol Med*. 2011;50:1280–7. doi:10.1016/j.freeradbiomed.2011.01.038.

[292] Longo M, Zatterale F, Naderi J, Parrillo L, Formisano P, Raciti GA, et al. Adipose tissue dysfunction as determinant of obesity-associated metabolic complications. *Int J Mol Sci*. 2019;20. doi:10.3390/ijms20092358.

[293] Comas F, Latorre J, Ortega F, Arnoriaga Rodríguez M, Lluch A, Sabater M, et al. Morbidly obese subjects show increased serum sulfide in proportion to fat mass. *Int J Obes*. 2020. doi:10.1038/s41366-020-00696-z.

[294] Trayhurn P. Hypoxia and adipose tissue function and dysfunction in obesity. *Physiol Rev*. 2013;93:1–21. doi:10.1152/physrev.00017.2012.

[295] Padiya R, Khatua TN, Bagul PK, Kuncha M, Banerjee SK. Garlic improves insulin sensitivity and associated metabolic syndromes in fructose fed rats. *Nutr Metab*. 2011;8:53. doi:10.1186/1743-7075-8-53.

[296] Moreno-Navarrete JM, Escoté X, Ortega F, Serino M, Campbell M, Michalski M-CC, et al. A role for adipocyte-derived lipopolysaccharide-binding protein in inflammation- and obesity-associated adipose tissue dysfunction. *Diabetologia*. 2013;56:2524–37. doi:10.1007/s00125-013-3015-9.

[297] Choi SA, Park CS, Kwon OS, Giong HK, Lee JS, Ha TH, et al. Structural effects of naphthalimide-based fluorescent sensor for hydrogen sulfide and imaging in live zebrafish. *Sci Rep*. 2016;6:305–806. doi:10.1038/srep26203.

[298] Murphy B, Bhattacharya R, Mukherjee P. Hydrogen sulfide signaling in mitochondria and disease. *FASEB J*. 2019;33:13098–125. doi:10.1096/fj.201901304R.

8. APPENDIX

8.1 *EX VIVO* EXPERIMENTS IN ADIPOSE TISSUE EXPLANTS

Paired SAT and VAT were obtained from 20 obese participants undergoing open abdominal surgery (gastrointestinal bypass) under general anesthesia after an overnight fast. Anthropometric and clinical parameters were detailed in Suppl Table 2. The study had the approval of the ethical committee, and all patients gave informed written consent.

These experiments were performed as previously described [296]. In brief, samples of adipose tissue were immediately transported to the laboratory (5–10 min). The handling of tissue was carried out under strictly aseptic conditions. The tissue was cut with scissors into small pieces (5–10 mg) and incubated in buffer plus albumin (3 ml/g of tissue) for 30 min. After incubation, the tissue explants were centrifuged for 30 s at 400 g. Then ~100 mg of minced tissue was placed into 1 ml M199 (Life Technologies, Invitrogen) containing 10% fetal bovine serum (Hyclone, Thermo Fisher Scientific), 100 unit/ml penicillin (Life Technologies, Invitrogen), and 100 µg/ml streptomycin (Life Technologies, Invitrogen) and incubated for 16 h in suspension culture under aseptic conditions. The following treatments were performed: i) Vehicle and ii) L-cysteine (10 mM) and pyridoxal 5'-phosphate (2 mM), as an inductor of the transsulfuration pathway (H_2S-synthesising enzymes) (**Figure 9)**.

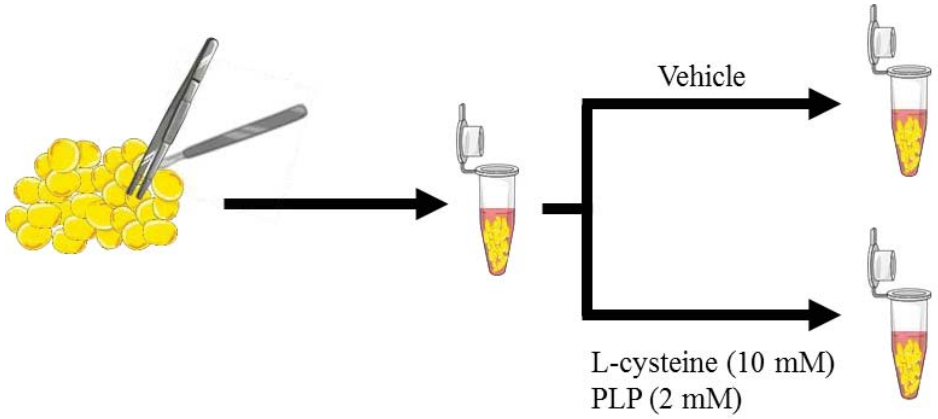

Figure 9. Schematic overview of adipose tissue explants methods. In this method, tissue was cut into small pieces, and placed in control or stimulus (L-cysteine (10 mM) and PLP (2 mM)) eppendorfs.

8.2 H_2S QUANTIFICATION

8.2.1 *In vitro* and AT explants measurements

In cell cultured medium H_2S concentration was assessed using a highly water-soluble naphthalimide-based fluorescent sensor 6-Azido-2-[2-[2-(2hydroxyethoxy) ethoxy]ethyl]benzo[de]isoquinoline-1,3-dione (L1) (**Figure 10)**, which was chemically synthesized in Institute of Computational Chemistry and Catalysis (Chemistry Department, University of Girona) as described previously[297].

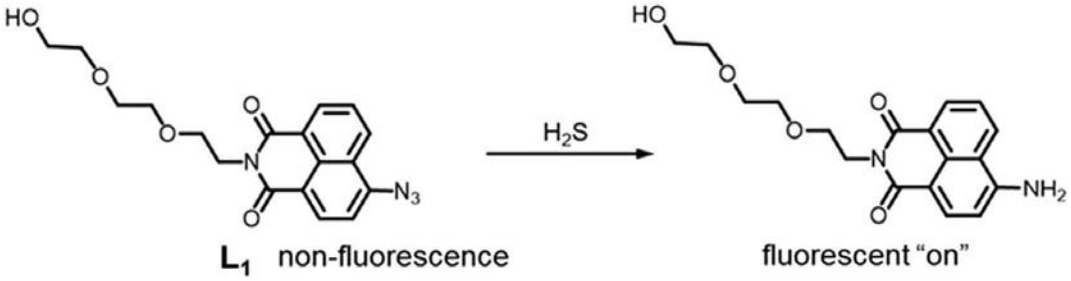

Figure 10. Fluorescent L1 probe. L1 fluorescent probe for hydrogen sulfide detection. *Figure taken from Choi S.A. (2016)*[297].

L1 probe (5 μM) was included and incubated in adipose tissue (16 h) or *in vitro* cell media (24 h). In each experiment, a negative control that consisted in the incubation of cell culture media plus L1 probe (5 μM) without adipose tissue explants or adipocytes was also performed. This negative control was used to subtract spontaneous H_2S production. After incubation, media was transferred to new eppendorf tubes to be homogenized, and were kept at –80ºC in the dark, until the read. Fluorescence was read in a Biotek Cytation 5 reader at λ ex = 435 nm and λ em = 550nm in duplicate and quantified with a Na_2S standard curve (0, 7.8, 15.6, 31.25, 62.5, 125, 250 and 500 μM).

8.2.2 Serum H_2S measurements

H_2S concentration in serum was assessed using a naphthalimide-based fluorescent sensor 6-Azido-2-(2-(2-(2-hydroxyethoxy) ethoxy)ethyl)-1H-benzo[de]isoquinoline-1,3 (2H)-dione (L1), as described previously[297]. To measure H_2S levels, serum and standard curve were incubated 70 minutes at 37ºC in the dark with 5 µmol/l of L1 probe. The standard curve was generated from a 10 mM stock solution of sodium sulfide (Na_2S) in phosphate-buffered saline (PBS) containing 5 µmol/l of L1 at various concentrations (0, 3.8, 7.8, 15.6, 31.25, 62.5, 125 and 250 µmol/l Na_2S). After incubation, fluorescence was read in a BiotekCytation 5 reader at λ ex = 435 ± 20 nm and λ em = 550 ± 20 nm. Blank control of serum samples was performed in the same incubation conditions without L1 probe. Intra- and inter-assay coefficients of variation for these determinations were between 9.7% and 10.5% respectively (**Figure 11)**.

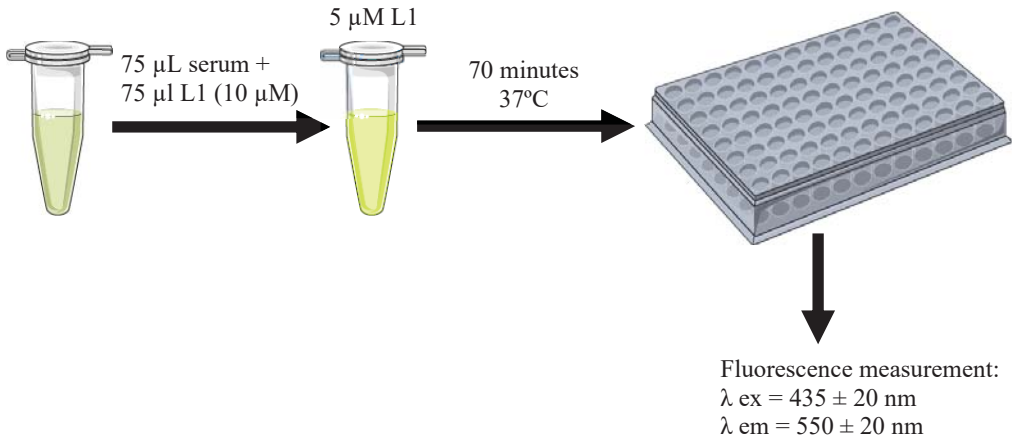

Figure 11. Serum H_2S fluorescent probe quantification workflow.